

**Some pages of this thesis may have been removed for copyright restrictions.**

If you have discovered material in AURA which is unlawful e.g. breaches copyright, (either yours or that of a third party) or any other law, including but not limited to those relating to patent, trademark, confidentiality, data protection, obscenity, defamation, libel, then please read our [Takedown Policy](#) and [contact the service](#) immediately

# LIPOSOMES AS CARRIERS FOR POLYMYXINS IN THE TREATMENT OF CYSTIC FIBROSIS LUNG INFECTIONS

STEPHEN MARK McALLISTER

Doctor of Philosophy

THE UNIVERSITY OF ASTON IN BIRMINGHAM

October 1995

This copy of the thesis has been supplied on condition that anyone who consults it is understood to recognise that its copyright rests with its author and that no quotation from the thesis and no information derived from it may be published without proper acknowledgement.

THE UNIVERSITY OF ASTON IN BIRMINGHAM

LIPOSOMES AS CARRIERS FOR POLYMYXINS IN THE TREATMENT OF  
CYSTIC FIBROSIS LUNG INFECTIONS

by

Stephen Mark McAllister

Doctor of Philosophy

1995

SUMMARY

Cystic fibrosis (CF) is the most common autosomal recessive disorder affecting Caucasian populations. The pathophysiology of this disorder predisposes the lungs of affected patients to chronic infection, typically by *Pseudomonas aeruginosa*, which is the main cause of morbidity and mortality. The management of CF lung infections relies upon aggressive antimicrobial regimens which commonly include the frequent administration of aerosolised antibiotics. Recently, attention has focused on aerosolised polymyxins, which are given prophylactically in an effort to limit infection and subsequent lung damage. This class of antimicrobial compounds is highly active against *P. aeruginosa* and possess the advantage that resistance rarely develops. However, the rapid lung clearance of antibiotics is a well documented phenomenon and it was postulated that polymyxin treatment could be further improved by liposomal encapsulation. As part of the development of liposomal polymyxin B, analytical methodology (radiolabelling, HPLC and protein assay) applicable to liposomal formulations was established. Liposomes were prepared by the dehydration-rehydration method and encapsulation efficiencies were determined for a number of phospholipid compositions. Vesicles were characterised with respect to size, zeta potential, morphology and release characteristics. The surface hydrophobicity of vesicles was quantified by hydrophobic interaction chromatography and it was found that this method produced comparable results to techniques conventionally used to assess this property. *In vivo* testing of liposomal polymyxins demonstrated that encapsulation successfully prevented the rapid pulmonary clearance of PXB. Antimicrobial activity of liposomal formulations was quantified and found to be dependent on both the vesicle surface characteristics and their release profile. Investigation of the interaction of PXB with lipopolysaccharide was undertaken and results demonstrated that PXB caused significant structural distortion of the lipid A region. This may be sufficient to abrogate the potentiating action of LPS in the inflammatory cascade.

**Keywords:** Liposomes; Cystic fibrosis; Pulmonary delivery; Polymyxin B.

## ACKNOWLEDGEMENTS

I am grateful to my supervisor Dr H.O. Alpar for her enthusiasm, support and guidance throughout the course of this project. I would also like to thank my associate supervisor Professor M.R.W. Brown for useful discussions and advice during this project.

I wish to acknowledge the Medical Research Council for financial support during my three years of study.

Technical assistance throughout the course of the project was provided by Mrs Dorothy Townley and Mr Roy Tilling. I would like to express my gratitude to Roy and Dorothy as without their help, my project would have been a much harder task. I would like to thank Ms. Bernadette Baretto for performing the antimicrobial assays, Dr. E. Poyner for her assistance with *in vivo* studies and Dr Peter Lambert for advice and useful discussions. I also would like to thank Mel Gamble for his enthusiastic assistance with the *in vivo* studies.

My thanks also go to my mother and father for their support and encouragement during my three years at Aston.

Finally, my thanks go to Roz for her encouragement and patience which have helped me inestimably over the last three years.

## CONTENTS

	<b>Page</b>
Title	1
Thesis summary	2
Acknowledgements	3
Contents	4
List of figures	10
List of tables	15
Abbreviations	18
<b>1.0. Introduction</b>	<b>19</b>
1.1. Cystic Fibrosis	20
1.1.1. General Background	21
1.1.2. Clinical Features	21
1.1.3. Discovery of the CF gene	22
1.1.4. Structure and function of CFTR	23
1.1.5. Role of CFTR in CF pathophysiology	24
1.1.6. Pathogenesis of lung disease in CF	25
1.1.7. Initial colonisation events	26
1.1.8. Antimicrobial treatment of CF lung infections	31
1.1.9. New approaches to the management of CF lung disease	33
1.1.9.1. Anti-inflammatory treatments	34
1.1.9.2. Immunomodulation	34
1.1.9.3. Transplantation	35
1.1.9.4. Development of gene therapy for CF	35
1.2. The polymyxin group of antibiotics	36
1.2.1. Microbiological characteristics	38
1.2.2. Mode of action	39
1.2.3. Biodistribution and pharmacokinetics of the polymyxins	40
1.2.4. Side-effects/adverse reactions associated with polymyxins	41
1.2.5. Clinical use of the polymyxins	42
1.2.6. The use of polymyxins for the treatment of cystic fibrosis lung infections	43
1.2.7. Rationale for the development of a liposomal polymyxin formulation	46
1.3. Therapeutic advantages of drug delivery systems	47

1.3.1.	Liposome structure and assembly	48
1.3.2.	Liposome composition and structural properties	50
1.3.3.	Liposome classification and production technologies	53
1.3.4.	Methods of liposome preparation	55
1.3.5.	Factors affecting the behaviour of liposomes <i>in vivo</i>	62
1.3.6.	Clinical applications of liposomes as drug carriers	66
1.3.7.	Liposomes as carriers of antimicrobial agents	70
1.3.8.	Aerosolisation of liposomal drug delivery systems	74
<b>2.0.</b>	<b>Development of analytical methodology for polymyxin B</b>	<b>78</b>
2.1.	Introduction	79
2.2.	Materials	79
2.2.1.	Polymyxin B	79
2.2.2.	Phospholipids	80
2.2.3.	Chemicals	80
2.2.4.	General instrumentation	80
2.3.	Methods	80
2.3.1.	Bioassay for polymyxin B	80
2.3.2.	Bicinchoninic acid protein assay	83
2.3.2.1.	The standard assay protocol	84
2.3.2.2.	The micro-assay protocol	85
2.3.3.	High performance liquid chromatography (HPLC) determination of polymyxin B	87
2.3.3.1.	HPLC theory	87
2.3.3.2.	Methodology	87
2.3.4.	Radiolabelling and scintillation counting of polymyxin B	91
2.3.4.1.	Theory	91
2.3.4.2.	Radiolabelled PXB and sample preparation	92
2.3.4.3.	Evaluation of scintillation counting for the detection of PXB	93
2.4.	Summary of assay development	96
<b>3.0.</b>	<b>Formulation Development of Liposomal Polymyxin B (LPXB)</b>	<b>98</b>
3.1.	Introduction	99
3.2.	Materials	100
3.2.1.	Polymyxin B	100
3.2.2.	Phospholipids	100
3.2.3.	Chemicals	100

3.3.	Methods	100
3.3.1.	Dehydration-rehydration vesicle (DRV) technique	100
3.3.2.	Thin-film hydration	103
3.3.3.	Analysis of PXB entrapment	103
3.3.4.	Phospholipid assay	103
3.3.5.	Laser diffraction particle size analysis	105
3.3.6.	Photon correlation spectroscopy (PCS)	107
3.3.7.	Zeta potential analysis	109
3.3.8.	Light Microscopy	111
3.3.9.	Transmission electron microscopy (TEM)	112
3.3.10.	Thin layer chromatography	112
3.3.11.	Gel exclusion chromatography (GEC)	113
3.3.12.	Ultrafiltration separation of non-entrapped PXB from LPXB preparations	113
3.3.13.	Reduction of liposome size by extrusion	114
3.3.14.	Differential scanning calorimetry (DSC)	114
3.4.	Results and Discussion	116
3.4.1.	Preparation of PXB DRV formulations: identification of compatible phospholipids	116
3.4.2.	Encapsulation efficiencies of PXB DRVs: effect of initial drug loading	121
3.4.3.	Effect of charged phospholipids on encapsulation efficiencies	126
3.4.4.	Inclusion of stealth lipids	127
3.4.5.	Differential scanning calorimetry (DSC) of the interaction between PXB and DSPC bilayers	129
3.4.6.	Membrane interaction of PXB: adsorption of PXB to preformed EPC vesicles	133
3.4.7.	Membrane interaction of PXB: zeta potential of LPXB formulations	136
3.4.8.	Size characterisation of LPXB formulations	142
3.4.8.1.	Laser diffraction sizing	142
3.4.8.2.	Photon correlation spectroscopy (PCS)	147
3.4.9.	Transmission electron microscopy of LPXB formulations	152
3.4.10.	Light microscopy assessment of LPXB formulations	157
3.4.11.	Phospholipid measurement of LPXB DRV	161
3.4.12.	Drug release from LPXB formulations	163
3.4.12.1.	Release of PXB from LPXB formulations stored at 4°C	

	in PBS pH 7.4	164
3.4.12.2.	Release of PXB from LPXB formulations stored at 37°C in PBS pH 7.4	168
3.4.12.3.	Release of PXB from LPXB formulations in 20% FCS in PBS pH 7.4	175
<b>4.0.</b>	<b>In vivo testing of LPXB formulations</b>	<b>180</b>
4.1.	Introduction	181
4.2.	Materials	182
4.2.1.	Polymyxin B	182
4.2.2.	Phospholipids	182
4.2.3.	Chemicals	182
4.3.	Methods	183
4.3.1.	Preparation of LPXB for intratracheal instillation	183
4.3.2.	Intracheal instillation of LPXB	183
4.3.3.	Intravenous administration of free and LPXB	184
4.3.4.	Preparation of EPC:CH:PEG extruded DRV for intravenous (i.v.) administration	184
4.3.5.	Ion-exchange separation of 100nm extruded EPC:CH:PEG vesicles from non-entrapped PXB - preparation and activity of Dowex-50WX4 cation exchange resin	185
4.3.6.	Intravenous administration of non-encapsulated PXB and LPXB	187
4.3.7.	Preparation of LPXB for macrophage uptake assay	187
4.3.8.	Macrophage uptake assay for LPXB	188
4.4.	Results and Discussion	188
4.4.1.	Characterisation of LPXB formulations used for intratracheal (i.t.) instillation	188
4.4.2.	Pulmonary retention of non-encapsulated PXB after intratracheal administration	190
4.4.3.	Pulmonary retention of LPXB after intratracheal administration	193
4.4.4.	Biodistribution of PXB and LPXB after intratracheal administration	198
4.4.5.	Characterisation of EPC:CH:PEG 100nm extruded vesicles used for i.v. injection	203
4.4.6.	Biodistribution of non-entrapped PXB after i.v.	



	administration	206
4.4.7.	Biodistribution of PXB after i.v. administration of EPC:CH:PEG 100nm vesicles	210
4.4.8.	Characterisation of LPXB preparations used for macrophage uptake studies	216
4.4.9.	Macrophage uptake of extruded LPXB formulations	218
<b>5.0.</b>	<b>Surface characterisation of liposomes by hydrophobic interaction chromatography (HIC)</b>	<b>225</b>
5.1.	Materials	227
5.1.1.	Phospholipids	227
5.1.2.	Chemicals	227
5.1.2.	Chemicals	227
5.2.	Methods	227
5.2.1.	Preparation of MLV by thin-film hydration	227
5.2.2.	Preparation of DRV	227
5.2.3.	Extrusion of MLV and DRV	227
5.2.4.	Laser Diffraction Sizing	228
5.2.5.	Zeta potential analysis	228
5.2.6.	HIC	228
5.2.7.	Statistical analysis	229
5.3.	Results and Discussion	229
5.3.1.	Effect of Molarity on elution of liposomes from HIC columns	229
5.3.2.	Effect of liposome extrusion on vesicle elution from HIC columns	230
5.3.3.	Influence of phospholipid composition on elution profiles from HIC columns	233
5.3.3.1.	Effect of surface charge	233
5.3.3.2.	Effect of cholesterol	235
5.3.3.3.	Effect of acyl chain	236
5.3.3.4.	Effect of pegylated lipids	237
5.3.3.5.	HIC characterisation of drug-loaded vesicles	239
5.4.	Conclusions	240
<b>6.0.</b>	<b>Antimicrobial and anti-endotoxin properties of PXB</b>	<b>242</b>
6.1.	Materials	244
6.1.1.	Polymyxin B	244

6.1.2.	Phospholipids	244
6.1.3.	Chemicals	244
6.1.4.	Organism and culture maintenance	244
6.1.5.	Chemically defined medium (CDM12)	244
6.2.	Methods	245
6.2.1.	Preparation of LPXB for antimicrobial bactericidal assay and MIC studies	245
6.2.2.	Zeta potential analysis of LPXB formulations	245
6.2.3.	Laser diffraction sizing of LPXB formulations	245
6.2.4.	Antimicrobial bactericidal assay	246
6.2.5.	Determination of the minimal inhibitory concentrations of PXB and LPXB	246
6.2.6.	Extraction and purification of <i>P. aeruginosa</i> LPS	247
6.2.7.	Gel electrophoresis of LPS	248
6.2.8.	Silver stain of LPS	250
6.2.9.	Immunoblotting of LPS	251
6.2.10.	Investigation of the PXB/LPS interaction using SDS-PAGE and immunoblotting techniques	252
6.4.	Results and Discussion	253
6.4.1.	Characterisation of DRV used in antimicrobial bactericidal assays and MIC studies	253
6.4.2.	Antimicrobial bactericidal testing of PXB and LPXB	255
6.4.3.	MIC studies with PXB and LPXB	259
6.4.4.	Investigation of the structural distortion of LPS by PXB using SDS-PAGE/immunoblotting techniques	261
7.0.	Concluding remarks	265
8.0.	References	267

## LIST OF FIGURES

Figure	Page
1.1. Interactions between <i>Pseudomonas aeruginosa</i> and the host responses in the lung	30
1.2. Chemical structure of PXB	37
1.3. Amino acid variation in the polymyxin group of antibiotics	38
1.4. Diagram depicting the arrangement of phospholipid molecules around an aqueous core to form a unilamellar liposome	49
1.5. Structure of phospholipids commonly used to prepare liposomes	52
1.6. Schematic diagram depicting the compartmental site of drugs following encapsulation	55
2.1. Calibration plot for bioassay demonstrating linearity over 2-200 $\mu$ g/ml (each point represents the mean $\pm$ sd, n=3)	82
2.2. Appearance of a multiwell bioassay tray containing PXB calibration standards after 24 hr incubation at 37°C	83
2.3. Calibration plot of PXB for standard BCA assay protocol (each point represents the mean $\pm$ sd, n=4)	85
2.4. Calibration plot of PXB for the BCA microassay protocol (Each point represents the mean $\pm$ sd, n=8)	86
2.5. Typical calibration plot for HPLC assay of PXB. Each point represents the response factor (peak area ratio of PXB1/PHBA) after a single injection	89
2.6. Specimen chromatogram of a polymyxin B sample (200 $\mu$ g/ml)	90
2.7. Quench curve for [ <sup>3</sup> H] PXB	93
3.1. Schematic flow diagram of the main steps in the DRV process	102
3.2. Calibration plot for egg phosphatidylcholine (EPC) using the Stewart colorimetric assay. (Each point represents the mean $\pm$ sd, n=3)	105
3.3. Encapsulation of PXB within EPC based DRVs as a function of cholesterol concentration and initial PXB loading. Each point represents the percentage mean $\pm$ sd, n=3	123
3.4. Encapsulation efficiencies of DRVs as a function of cholesterol concentration and initial PXB loading. (Each point represents the mean $\pm$ sd, n=3)	123
3.5. Changes in the main transition of DSPC by entrapped PXB	132
3.6. Adsorption of PXB to preformed EPC 0.8 $\mu$ m vesicles:	

	separation of vesicles and drug by gel exclusion chromatography	134
3.7.	Laser diffraction size distribution (Malvern Mastersizer E) of DSPC vesicles after 10 extrusions through a 0.8 $\mu$ m filter	135
3.8.	Representative size distributions of LPXB DRV formulations as determined by laser diffraction sizing	147
3.9.	Intensity weighted size distribution of empty EPC DRV determined using PCS. Hydrodynamic mean diameter 1776 $\pm$ 444nm	150
3.10.	Intensity weighted size distribution of loaded EPC DRV determined using PCS.	150
3.11.	Intensity weighted size distribution of empty EPC:CH 1:1 DRV determined using PCS.	151
3.12.	Intensity weighted size distribution of loaded EPC:CH 1:1 DRV determined using PCS.	151
3.13.	Negative stain TEM of EPC:CH (2:1) loaded DRVs. Magnification 57K.	154
3.14.	Negative stain TEM of EPC:CH (2:1) loaded DRVs. Magnification 100K.	154
3.15.	Negative stain TEM of EPC:CH:PEG (2:1:0.2) loaded DRVs. Magnification 25K.	155
3.16.	Negative stain TEM of EPC:CH:PEG (2:1:0.2) loaded DRVs. Magnification 120K.	155
3.17.	Negative stain TEM of DSPC:CH (1:1) loaded DRV. Magnification 150K.	156
3.18.	Negative stain TEM of DSPC loaded DRVs. Magnification 60K.	156
3.19.	Phase contrast micrograph of EPC:CH (2:1) empty DRV (x40 objective).	160
3.20.	Phase contrast micrograph of EPC:CH (2:1) loaded DRV (x40 objective).	160
3.21.	Release of PXB from EPC based DRV at 4 $^{\circ}$ C in PBS pH 7.4. Each point represents the mean $\pm$ sd, n=3	167
3.22.	Release of PXB from DSPC based DRV at 4 $^{\circ}$ C in PBS pH 7.4. Each point represents the mean $\pm$ sd, n=3	167
3.23.	Percentage released against square root of time for EPC, EPC:CH (2:1) and (1:1) LPXB formulations. Each point represents the mean, n=3	173
3.24.	Percentage released against square root of time for EPC:SA (9:1) and EPC:CH:SA (6:3:1) LPXB formulations. Each point represents	

	the mean, n=3	173
3.25.	Percentage released against square root of time for EPC:CH:GM <sub>1</sub> (2:1:0.2) and EPC:CH:PEG (2:1:0.2) LPXB formulations. Each point represents the mean, n=3	174
3.26.	Percentage released against square root of time for DSPC based LPXB formulations. Each point represents the mean, n=3	174
3.27.	FCS induced-release of PXB from DSPC-based DRV expressed as a percentage of that originally entrapped. Each point represents the mean±sd, n=3	179
3.28.	FCS induced-release of PXB from EPC-based DRV expressed as a percentage of that originally entrapped. Each point represents the mean±sd, n=3	179
4.1.	Adsorption of PXB (5mg) by Dowex 50WX-4. Each point represents the mean of duplicate samples	186
4.2.	Serum levels of [ <sup>3</sup> H]-PXB after i.t. instillation of free drug in male rats. Each point represents the percentage of the administered dose expressed as the mean±sd, n=3	200
4.3.	Size distributions of EPC:CH:PEG vesicles extruded 10 times through a 0.1µm filter, before and after Dowex treatment	203
4.4.	Gel exclusion chromatograms of extruded EPC:CH:PEG vesicles before and after Dowex resin treatment	204
4.5.	TEM of EPC:CH:PEG vesicles before 10 extrusions through a 100nm filter. Magnification 120k	205
4.6.	TEM of EPC:CH:PEG vesicles after 10 extrusions through a 100nm filter. Magnification 100k	205
4.7.	Serum levels of PXB after i.v. administration of a 0.8mg/kg dose to five adult male rats. Each time-point represents the mean±sd of three samples for each individual animal	206
4.8.	Serum levels of PXB after i.v. administration of a 2.5mg/kg dose to five adult male rats. Each time-point represents the mean±sd of three samples for each individual animal	207
4.9.	Tissue distribution of PXB after i.v. injection of 0.8mg/kg (n=5) and 2.5mg/kg (n=4) doses. Each point represents the % administered dose expressed as the mean±sd	208
4.10.	Serum levels of PXB determined by scintillation counting of [ <sup>3</sup> H]-PXB in untreated (free and liposomal drug) and Dowex treated (liposomal drug only) samples, expressed as a percentage of the total [ <sup>3</sup> H]-PXB dose administered. Each point represents the mean±sd, n=5	210

4.11.	Serum levels of liposomal [ <sup>3</sup> H]-PXB and [ <sup>14</sup> C]-cholesteryl oleate determined by scintillation counting of Dowex treated (liposomal drug only) samples, expressed as a percentage of the total [ <sup>3</sup> H]/[ <sup>14</sup> C] dose administered. Each point represents the mean±sd, n=5	212
4.12.	Serum levels of [ <sup>14</sup> C]-cholesteryl oleate determined by scintillation counting of untreated and Dowex treated samples, expressed as a percentage of the total [ <sup>14</sup> C]-cholesteryl oleate dose administered. Each point represents the mean±sd, n=5	212
4.13.	Tissue distribution of [ <sup>3</sup> H]-PXB and [ <sup>14</sup> C]-cholesteryl oleate 24hr after administration of EPC:CH:PEG vesicles. The recovery of each label is expressed as a percentage of the originally administered dose. Each point represents the mean±sd, n=5	214
4.14.	Encapsulation efficiencies (µM PXB/µM lipid) of LPXB formulations before and after 10 extrusions through a 0.2µm filter	217
4.15.	PCS Size distribution of EPC:SA vesicles after 10 extrusion through a 0.2µm filter	217
4.16.	Gel exclusion chromatogram of EPC:SA 200nm extruded vesicles	218
4.17.	J774.1 macrophage with ingested fluorescent latex particles after 3hr incubation at 37°C without FCS	219
4.18.	Binding of LPXB to J774.1 cells after 3hr incubation at 4°C. Each point represents the mean±sd of three experiments	220
4.19.	Uptake of LPXB to J774.1 cells after 3hr incubation at 37°C. Each point represents the mean±sd of three experiments	221
4.20.	HIC of EPC, EPC:SA and EPC:CH:PEG vesicles using hexyl and octyl stationary phases. Retention values are the mean±sd, n=3	222
5.1.	Schematic of Pasteur pipette columns used for HIC	228
5.2.	Influence of saline ionic strength on the retention of 0.8µm extruded EPC liposomes (each point represents the mean±sd, n=3)	230
5.3.	Influence of extrusion on the retention of EPC liposomes in agarose and octyl-agarose phases. Eluting medium 0.2M NaCl, (each point represents the mean±sd, n=3)	232
5.4.	Particle size distribution determined by laser diffraction of non-extruded and 0.8µm extruded EPC liposomes in 0.2M NaCl	232
5.5.	Influence of charged phospholipids on hydrophobicity of surfaces of EPC based liposomes (each point represents the mean±sd, n=3)	234
5.6.	Influence of cholesterol on retention of EPC based liposomes (each point represents the mean±sd, n=3)	236
5.7.	Influence of acyl chain saturation on retention of liposomes	

	(each point represents the mean $\pm$ sd, n=3)	237
5.8.	Influence of DSPE-PEG <sub>1900</sub> on retention of liposomes (each point represents the mean $\pm$ sd, n=3)	238
5.9.	Influence of drug-loading on retention of EPC:DCP liposomes (each point represents the mean $\pm$ sd, n=3)	239
6.1.	Entrapment of PXB within DRV. Entrapment values expressed as a percentage of the initial drug loading (9mg PXB/66 $\mu$ M total lipid). Each point represents the mean $\pm$ sd, n=3	254
6.2.	Zeta potential of loaded and unloaded DRV in 0.02M diphosphate buffer pH 7.4. Each point represents the mean $\pm$ sd, n=5	254
6.3.	Bactericidal activity of PXB and LPXB (0.3 $\mu$ g/ml dose) against <i>P. aeruginosa</i> after 1hr incubation at 37°C. Each point represents the mean $\pm$ sd, n=3	256
6.4.	Bactericidal activity of PXB and LPXB (0.1 $\mu$ g/ml dose) against <i>P. aeruginosa</i> after 1hr incubation at 37°C. Each point represents the mean $\pm$ sd, n=3	256
6.5.	Schematic diagram of LPS illustrating main structural features	263
6.6.	Structural distortion of LPS by PXB as visualised by SDS-PAGE. Concentrations of PXB used were 5000 (lane 1), 10000 (lane 2), 25000 (lane 3), 50000 (lane 4), 75000 (lane 5), 100000 (lane 6), 0 (lane 7), units/ml	264
6.7.	Structural distortion of LPS by PXB as visualised by immunoblotting. Concentrations of PXB used were 5000 (lane 1), 10000 (lane 2), 25000 (lane 3), 50000 (lane 4), 75000 (lane 5), 100000 (lane 6), 0 (lane 7), units/ml	264

## LIST OF TABLES

Table	Page
1.1. Summary of capture volumes and size distributions of liposomes made by various methods (adapted from Perkins <i>et al.</i> , 1993)	61
1.2. Review of the studies using liposomes with encapsulated antibiotics for the treatment of experimental infections <i>in vivo</i> (adapted from Couvreur <i>et al.</i> , 1991)	72
2.1. Potentiation of PXB bioassay activity by 1% triton-X 100. Each zone of inhibition represents the mean $\pm$ sd of three samples	82
2.2. Interference of phospholipids and 1% (v/v) Triton-X 100 in the standard BCA assay protocol. Absorbances represent the mean $\pm$ sd of four samples	85
2.3. Encapsulation of PXB by EPC liposomes (66 $\mu$ M lipid/18mg PXB): discrepancies between encapsulation results (values are the mean $\pm$ standard deviation of three replicate measurements)	94
2.4. Analysis of [ <sup>3</sup> H] and unlabelled PXB before and after freeze-drying cycles	94
2.5. Encapsulation of PXB by EPC liposomes using the DRV method (66 $\mu$ M lipid/9mg PXB) determined using different assay techniques. Values are the mean $\pm$ sd of three determinations	95
3.1. Transition temperature of phospholipids commonly used to prepare liposomes (adapted from Szoka & Papahadjopoulos, 1980)	102
3.2. Parameters used in zeta potential measurements	110
3.3. Compatibility of phospholipids for the preparation of PXB DRVs	116
3.4. Encapsulation of PXB within liposomes of varying composition prepared by the DRV method. Drug loading 9mg/66 $\mu$ M lipid. Each encapsulation represents the mean $\pm$ standard deviation of at least three preparations	129
3.5. Encapsulation efficiencies of DSPC DRV loaded with high PXB levels. Values determined directly from liposomal pellet by scintillation counting of [ <sup>3</sup> H]-PXB (each point represents the mean $\pm$ sd, n=3)	130
3.6. Changes induced in DSPC peak gel-liquid crystalline phase transition temperature by entrapped PXB (each point represents the mean $\pm$ sd of six determinations)	131
3.7. Zeta potential values of unloaded and loaded LPXB DRV formulations. All loaded values relate to washed vesicles after a standard initial	



	loading of 9mg PXB/66 $\mu$ M lipid. Zeta potentials are the mean of those determined from five measurements for at least three preparations	138
3.8.	Representative size distributions of LPXB DRV formulations as determined by laser diffraction sizing. Loading refers to a standard initial loading of 9mg PXB/66 $\mu$ M total lipid	146
3.9.	Geometric mean diameters and dispersions of LPXB formulations determined by PCS using a 90° scattering angle. Loading refers to a standard loading of 9mg PXB/66 $\mu$ M total lipid	149
3.10.	Gross morphology of LPXB formulations observed using phase contrast light microscopy with x40 magnification	159
3.11.	Phospholipid determination for a number of LPXB DRVs. Phospholipid retained is expressed as a percentage of the starting quantity and represents the mean $\pm$ sd of three samples	162
3.12.	Release of PXB from EPC based DRV incubated in PBS pH 7.4 at 37°C. Each value represents the mean $\pm$ sd of three independent preparations	169
3.13.	Release of PXB from DSPC based DRV preparation incubated in PBS pH 7.4 at 37°C. Each value represents the mean $\pm$ sd of three independent preparations	170
3.14.	Slopes of linear regression plots for PXB release from LPXB preparations in PBS pH 7.4 at 37°C	172
4.1.	Characterisation of DRV used for i.t. administration. Each encapsulation is the mean $\pm$ sd of three determinations for a single preparation. Zeta potentials are the mean of five individual measurements in each buffer system	190
4.2.	Lung levels of [ <sup>14</sup> C]-CHOL in DRV, 4 and 24hr, after i.t. administration. Each point represents the percent of the original quantity of [ <sup>14</sup> C]-CHOL administered (average $\pm$ s.d., n=3)	195
4.3.	Biodistribution of i.t. instilled PXB and LPXB in male rats at a dose of 0.4mg kg <sup>-1</sup> PXB. Each point represents the percent of the original dose of [ <sup>3</sup> H]-PXB administered (average $\pm$ s.d., n=3). ND denotes that [ <sup>3</sup> H] levels were not detectable above background	202
5.1.	Zeta potentials, determined by laser doppler velocimetry, of liposome formulations used for HIC experiments. Each value represents the mean of five determinations for a single preparation	235
6.1.	Components of CDM12	245
6.2.	Composition of running gel, stacking gel and sample buffer for SDS-PAGE of LPS	250

6.3. Entrapment and MIC values for LPXB formulations compared to free drug after 18hr incubation at 37°C. Entrapment is expressed as the percentage of drug initially loaded (initial loading 9mg PXB/66µM total lipid). Release was determined as detailed in text and used to calculate effective free drug concentration

261

## ABBREVIATIONS

BCA	bicinchoninic acid
cAMP	cyclic adenylate monophosphate
CF	cystic fibrosis
CFTR	cystic fibrosis transmembrane regulator protein
CH	cholesterol
DCP	dicetylphosphate
DMPC	dimyristoylphosphatidylcholine
DPPC	dipalmitoylphosphatidylcholine
DRV	dehydration-rehydration vesicles
DSC	differential scanning calorimetry
DSPC	distearoylphosphatidylcholine
DSPE	distearoylphosphatidylethanolamine
EDTA	ethylenediaminetetraacetate
EPC	egg phosphatidylcholine
FCS	foetal calf serum
GEC	gel exclusion chromatography
GM <sub>1</sub>	monosialoganglioside GM <sub>1</sub>
HIC	hydrophobic interaction chromatography
HPLC	high performance liquid chromatography
i.m.	intramuscular
i.p.	intraperitoneal
i.t.	intratracheal
i.v.	intravenous
LPS	lipopolysaccharide
LPXB	liposomal polymyxin B
LUV	large unilamellar vesicles
MIC	minimum inhibitory concentration
MLV	multilamellar vesicles
MPS	mononuclear phagocyte system
Mwt	molecular weight
OD	optical density
PA	phosphatidic acid
PBS	phosphate buffered saline
PCS	photon correlation spectroscopy
PE	phosphatidylethanolamine

PEG	polyethylene-glycol
PG	phosphatidylglycerol
PI	phosphatidylinositol
PS	phosphatidylserine
PXB	polymyxin B sulphate
RES	reticuloendothelial system
REV	reverse-evaporation vesicles
SA	stearylamine
sd	standard deviation
SDS	sodium dodecyl sulphate
SDS-PAGE	sodium dodecyl sulphate - polyacrylamide gel electrophoresis
SEM	scanning electron microscopy
SUV	single unilamellar vesicles
T <sub>m</sub>	transition temperature
TEM	transmission electron microscopy
v/v	volume <i>per</i> volume
w/v	weight <i>per</i> volume
w/w	weight <i>per</i> weight

# Chapter 1

## Introduction

---

### ABSTRACT

Cystic fibrosis (CF) is the most common serious genetic disease among Caucasian populations. This disease is characterised by chronic pulmonary infection which is the main cause of morbidity and mortality. This chapter reviews the pathophysiology and treatment of CF and in particular, reviews the role of polymyxins in the management of CF lung infections. It is proposed that current therapy with polymyxins may be optimised through a drug-delivery approach. The advantages of liposomal encapsulation in improving the therapeutic efficacy of a number of agents is reviewed and the potential of this approach to the lung delivery of polymyxin B to infected CF lungs evaluated.

---

## 1.1. Cystic Fibrosis

### 1.1.1. General Background

Cystic fibrosis (CF) is the most common serious autosomal recessive genetic disease amongst Caucasian populations affecting between 1 in 2000 and 1 in 4500 live births (Koch & Høiby, 1993). In the UK there are 2 million carriers of the disease and approximately 6000 CF patients. Originally described as a gastrointestinal disease (Anderson, 1938), CF is a multisystem disorder arising from epithelial dysfunction with respiratory complications accounting for 98% of deaths from CF in adults. Until relatively recently CF was exclusively a childhood disorder but aggressive treatment regimens in children have resulted in prolonged survival and increased quality of life (Shale, 1991). In the UK 50% of patients now survive in excess of 30 years and this figure is expected to improve up to and beyond the year 2000. This improvement in median survival age has been achieved through a therapeutic approach which prevents or treats the symptoms but does not yet treat the primary cause of the disease.

### 1.1.2 Clinical Features

The main clinical symptoms of increased salt loss in sweat, exocrine pancreatic insufficiency, male infertility and bacterial colonisation and infection of the respiratory tract are the result of defects in the regulation of transepithelial ion movements across affected epithelia (Fiel, 1993). Defective chloride ion transport results in an accumulation of dehydrated mucus which blocks the exocrine glands of the body's major organ systems. Gastrointestinal symptoms include *meconium ileus*, or bowel obstruction in the new-born with inspissated meconium. Obstruction can also occur in the adult bowel due to incomplete digestion. Pancreatic insufficiency is present in most CF patients from birth, although 10-15% of patients retain some pancreatic function (Kubesch *et al.*, 1993). Malabsorption, steatorrhoea,

*diabetes mellitus* and a general failure to thrive are among the consequences of a lack of pancreatic digestive enzymes. Epithelial irregularities also reduce the reproductive potential of male CF patients. Wolfian duct structure is altered in 95% of patients with *vas deferens*, epididymus and seminal vesicles being atrophic, fibrotic or absent (Taussig *et al.*, 1972). Female CF patients are much less affected although thickened cervical mucus and general ill-health may delay conception (Cohen *et al.*, 1980). However the overriding clinical feature of CF is the cycle of bacterial colonisation and infection of the lower airways which progressively damages the respiratory epithelium. The majority of CF patients eventually die a pulmonary death due to purulent bronchitis, bronchiectasis, bronchiolitis and pneumonia, leading to hypercapnoea and respiratory failure (Stableforth, 1994).

### 1.1.3 Discovery of the CF gene

The CF gene was localised to the long arm of chromosome 7 by linkage studies in 1985 (White *et al.*, 1985). Further research culminated in the identification of the CF gene in 1989 (Riordan *et al.*, 1989; Rommens *et al.*, 1989). Mutant forms of the gene, which spans 250,000 base pairs, were shown to be present in CF patients but absent from normal individuals (Riordan *et al.*, 1989). The first mutation described was a deletion of three adjacent base pairs leading to the absence of a phenylalanine residue at position 508 ( $\Delta F508$  mutation). The frequency of the  $\Delta F508$  mutation differs significantly between ethnic groups. The overall frequency is approximately 70% but the relative frequency varies from 30% in Israeli patients to 88% in Danish patients. Over 200 mutations have now been described although many of the more rare defects have been reported in only individual patients. These can include missense, nonsense, frame-shift and splice-site mutations. The clinical severity of the disease widely varies among patients reflecting the mutational diversity and differing environmental factors affecting patients such as the frequency of viral infection and nutritional status. The relationship between genotype and phenotype is controversial. The most important correlation is that the  $\Delta F508$  mutation is related to pancreatic insufficiency,

while patients with other mutations often have near normal pancreatic function. However, pulmonary pathophysiology is not as closely related to phenotype (Koch & Høiby, 1993).

Cloning of the CF gene enabled the primary amino acid sequence to be predicted together with a proposal for a potential structure and function of the gene product. The protein coded for by the gene has been designated chloride channel transmembrane regulator protein (CFTR) and its role in CF pathophysiology has been significantly clarified in the last few years.

#### 1.1.4. Structure and function of CFTR

The collective pathophysiology of CF has now been attributed to a defect in the cystic fibrosis transmembrane regulator protein (CFTR). This 1480 amino acid protein consists of two symmetrical motifs each possessing six membrane-spanning domains and a hydrophilic nucleotide binding domain (NBD) (Cuthbert, 1994). These two motifs are joined by a highly charged cytoplasmic regulatory domain (R) which has multiple phosphorylation sites for protein kinases A and C. The transmembrane domain and the NBDs share sequence homology with the ABC superfamily of protein transporters (which includes *p*-glycoprotein, involved in multi-drug resistance) whilst the R domain is unique to CFTR (Santis & Geddes, 1994). The transition of CFTR from open to closed state is mediated by a cAMP dependent protein kinase that can phosphorylate one of the many phosphorylation sites on the R domain. ATP can interact with one of the NBDs and ADP may exert opposite effects by interaction with the second NBD (Anderson & Welsh, 1992).

After initial controversy, CFTR has now been shown to function as a chloride channel although it may have other functions. CFTR has been localised to the apical membranes of a number of epithelia involved in CF pathophysiology (Cuthbert, 1994; Cuthbert, 1991). Further evidence to support a chloride channel function for CFTR comes from transfection



studies using CF cells (Rich *et al.*, 1990). Insertion with the cDNA for CFTR conferred a cAMP sensitive chloride channel conductance upon the cells. Mouse fibroblast and HeLa cells which do not ordinarily possess CFTR demonstrated cAMP dependent chloride conductance after transfection with CFTR. Reconstitution of CFTR into liposomes resulted in chloride channel activity. This evidence suggests that CFTR is a cAMP sensitive low conductance chloride channel located in the apical membrane of transporting cells and is consistent with the clinical manifestations observed with mutated CFTR (Bear *et al.*, 1992).

Whilst accumulated evidence demonstrates the chloride channel activity of CFTR, localisation of mutated CFTR in sweat ducts from  $\Delta F508$  homozygous patients showed its absence from apical membranes but it was detected in smaller amounts in cytoplasmic granules. In cells expressing  $\Delta F508$  mutated CFTR the protein has a mass of  $\sim 145$ kDa while true CFTR has a value of  $\sim 165$ kDa. This difference is clearly not the result of a phenylalanine deletion and can be explained by the failure of glycosylation of mutated CFTR. Therefore it appears that the protein both malfunctions and is mislocated. *In vitro* evidence in cell lines has shown that membrane insertion of over expressed  $\Delta F508$  CFTR can confer a cAMP dependent chloride conductance upon these cells. If  $\Delta F508$  CFTR is similarly mislocated in the respiratory tract, strategies to increase apical cell membrane delivery may be useful in the treatment of this disease.

### 1.1.5. Role of CFTR in CF pathophysiology

Much of the knowledge of the function of CFTR comes from studies on the sweat gland abnormality in CF patients. Early observations of increased sodium and chloride ion concentrations in sweat (Di Sant' Agnese *et al.*, 1953), had implied a defect in ion transport in CF epithelial cells. This was later shown to be due to the low permeability of sweat glands to chloride ions resulting in much reduced reabsorption of both sodium and chloride ions (Quinton, 1990). However the aetiology of bronchopulmonary disease in the CF patient is

more complex. The surface of the tracheo-bronchial tree is composed of a secretory ciliated epithelium that prevents particles and microorganisms reaching the lower respiratory tract. This protection from invasive challenge depends upon an upward directional flow of a mucus (gel) layer positioned on the tips of cilia that move freely in a periciliary liquid (sol) layer. In normal healthy patients, CFTR contributes to chloride secretion through the apical cell membrane of airway epithelial cells and the balance of secretion and reabsorption of water and electrolytes is maintained. However, in CF patients, the reduction in chloride secretion (and sodium to maintain electroneutrality and water to maintain isotonicity) and increased absorption of sodium (with similar changes in the flow of chloride and water) leads to a dehydration of pulmonary secretions. The viscous mucus blanket lining the pulmonary epithelium decreases mucociliary clearance and is the critical pathogenic mechanism leading to chronic infection and colonisation of the lower respiratory tract.

#### **1.1.6. Pathogenesis of lung disease in CF**

The dehydrated mucus layer lining the CF respiratory mucosa presents a different environment to potential pathogenic organisms from that in non-CF patients (Govan & Glass, 1990). Reduced fluid secretion and dehydration of the mucus and periciliary layers reduces mucociliary clearance and contributes to the persistence of microorganisms within the lung. The volume and viscosity of bronchial mucus is further enhanced by DNA derived from bacteria and inflammatory immune cells and by increased concentrations of electrolytes such as  $\text{Na}^+$  and  $\text{Ca}^+$  (Govan & Glass, 1990). The respiratory epithelium secretes defence mechanisms such as mucins, lysozyme, transferrin, secretory IgA, cytokines and bronchial secretory leukoprotease inhibitor (a small molecular weight inhibitor of serine proteases such as granulocyte elastase) (Suter, 1994). However, in spite of these defences, the sum of CF pathophysiological changes is an environment which facilitates initial bacterial colonisation.

### 1.1.7. Initial colonisation events

In general the spectrum of bacteria, viruses and fungi associated with respiratory infections in CF patients is relatively small. Susceptibility of CF patients to particular pathogens is usually age-related and follows a common sequence. The primary event is usually colonisation with *Staphylococcus aureus* in infants, followed by *Haemophilus influenzae* before *Pseudomonas aeruginosa* takes hold as the dominant pathogen in the adolescent years. *Burkholderia cepacia* (formerly *Pseudomonas cepacia*) is an emerging problem in some adult CF clinics (Fiel, 1993; Govan & Glass, 1990). *Pseudomonas* infection of the respiratory tree is seen only when the bronchial mucosa is diseased or injured e.g. endotracheal intubation (Niederman *et al.*, 1984), bronchiectasis (Rivera & Nicotra, 1982), and in the ciliary dyskinesia syndromes (Pederson & Stafanger, 1983), *i.e.*, situations where there is some abnormality of the mucosal surface. The predominance of *P. aeruginosa* as the principle pathogen in CF patients has prompted investigators to study the possible role of trophic factors in the colonisation process. Several conflicting studies have been published in this controversial area. It was found that *P. aeruginosa* did not display preferential binding to mucins from CF patients compared to mucins from healthy individuals (Gupta & Jentoft, 1992; Sajjan *et al.*, 1992). However Saiman *et al.* (1992) have shown an increased binding of *P. aeruginosa* to CF epithelial cells compared with normal human respiratory epithelium cultured *in vitro*. Plotowski *et al.* (1993) did not show such a difference and it was suggested that adherence of *P. aeruginosa* is promoted by the dehydration of mucus and the exposition of receptors for microbial adhesion through the action of granulocyte elastase. Such damage may follow inflammatory reactions provoked by viruses or by bacteria and this initial damage may predispose the respiratory epithelium to later pseudomonal colonisation. Binding of *P. aeruginosa* to injured cells is mediated by a specific receptor adhesin mechanism. In the case of the mucoid strains, the mucoid exopolysaccharide (alginic acid like exopolysaccharide) mediated adherence to the cells. Pili or fimbriae mediated the adherence of the non-mucoid strains. Tracheobronchial mucins, high molecular weight glycoproteins composed of peptides linked to a large variety of sugar chains, normally serve a defensive function to protect

respiratory cells from colonisation by binding bacteria which are then removed by ciliary action. However in CF the bacteria bound by mucins persist in stagnant mucus due to defective mucociliary clearance and results in a state of chronic colonisation.

The bacterial response to colonisation is characterised by the expression of the mucoid phenotype of *P. aeruginosa*, which produces copious quantities of alginate, as extracellular polysaccharide. In contrast to acute pulmonary infections in non-CF patients in which *P. aeruginosa* are observed, by microscopy, to be dispersed throughout the sputum, the mucoid *P. aeruginosa* present in CF sputum are often observed as microcolonies or biofilm adhering to the bronchial mucosa and posing formidable targets to phagocytic cells. Those mechanisms in the host-bacterium interaction, responsible for the non-mucoid to mucoid transformation, have as yet not been fully elucidated, but the  $\text{Fe}^{2+}/\text{Fe}^{3+}$  ratio present in the CF airway (Brown *et al.*, 1984) might be a crucial factor (Fick, 1989). Alginate forms a wall around the bacteria, thereby protecting the bacterium against the patient's mechanical, cellular and biochemical defences. The volume of such an alginate-protected microcolony not only prevents macrophages and neutrophils from ingesting the bacteria, but also reduces the mechanical efficacy of mucociliary clearance (Baltimore & Mitchell, 1980; Lam *et al.*, 1980).

Bacterial extracellular virulence factors contribute to tissue damage and impair several aspects of host immunity and mechanical defences. In the early stages of lung infection, proteases of *P. aeruginosa* may contribute to the persistence of the organism by combating the defence response through cleavage of immunoglobulins and complement components in addition to inactivation of neutrophils by inhibition of chemotaxis and chemiluminescence (Döring *et al.*, 1985). Once colonisation has become established, bacterial virulence factors are effectively neutralised by the production of serum-derived IgG and IgA antibodies of the local secretory immune system. However the high levels of immune complexes in endobronchial mucus only serves to stimulate a damaging inflammatory response from neutrophils.

Neutrophils are thought to release lysozyme-derived proteases as they attempt to engulf microcolonies of *P. aeruginosa*. In addition to the release of proteolytic enzymes, neutrophils also generate oxidants. The serine protease, neutrophil elastase, is capable of hydrolysing all the major connective proteins that constitute the lung matrix. Alpha<sub>1</sub>-antiprotease ( $\alpha_1$ -AP) is the major antiprotease of the lower respiratory tract and inactivates neutrophil elastase under normal physiological conditions. However high levels of neutrophil elastase have been observed in sputa from CF patients with correspondingly low levels of  $\alpha_1$ -AP. Circulating blood levels of neutrophil elastase/ $\alpha_1$ -AP complex have been used as an inflammatory marker for the disease (Meyer *et al.*, 1991). Further imbalance to elastase homeostatic mechanisms is caused by pseudomonas elastase destruction of  $\alpha_1$ -AP and bronchial mucus inhibitor, the main antiprotease inhibitor of the upper airway (Fick, 1989). The hydrolysis of  $\alpha_1$ -AP by pseudomonas elastase frees low molecular weight polypeptides which act to increase the elastolytic ability of neutrophil elastase. These polypeptides function as chemotaxins for neutrophils and monocytic macrophages, and the attracted cells further augment the proteolytic and oxidative damage to the CF lung. The net result of such changes is reflected by the abnormal white cell differential observed in the CF lung. Bronchoalveolar lavage fluids from healthy normal volunteers generally contain approximately 90% pulmonary macrophages, up to 12% lymphocytes and less than 3% neutrophils. By contrast, bronchoalveolar lavage fluids from CF airways reveal that the predominant cell is the neutrophil (30 to 90%, depending on the clinical state of the patient) with a greatly decreased percentage of pulmonary macrophages and few lymphocytes (Fick, 1989)

The elastase-antielastase imbalance has been viewed as a potential target for therapeutic intervention. A clinical trial of intravenously-administered human plasma  $\alpha_1$ -AP succeeded in re-establishing the epithelial  $\alpha_1$ -AP activity and was tolerated without side-effects. Higher efficacy was observed with aerosol delivery. However, replacement therapy is limited by the oxidative inactivation of  $\alpha_1$ -AP and strategies such as recombinant oxidant resistant  $\alpha_1$ -AP have yet to be clinically evaluated (Zach, 1991).

In summary, the bacterial pathogens supply the antigens for an immune complex disease, that, *via* complement activation and generation of chemotactic products, attracts large numbers of polymorphonuclear neutrophils to the airways; these hyperstimulated neutrophils release lysosomal enzymes and oxygen radicals during successful or frustrated phagocytosis, thereby subjecting the airway to high concentrations of host derived, cytotoxic and proteolytic agents (Zach, 1991). The contributing factors to lung damage are represented in figure 1.1.

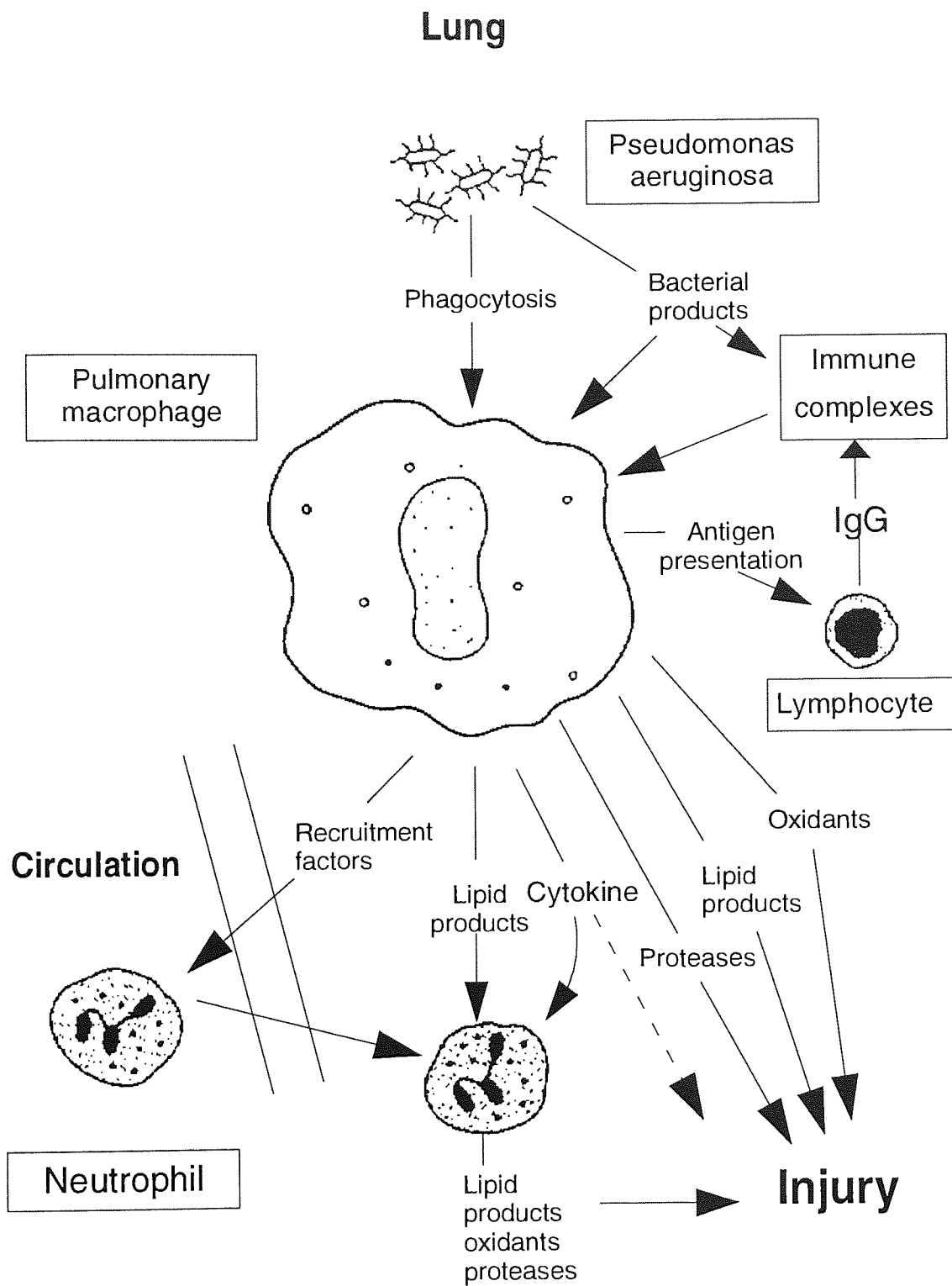


Figure 1.1. Interactions between *Pseudomonas aeruginosa* and the host responses in the lung (adapted from Elborn & Shale, 1990)

### 1.1.8. Antimicrobial treatment of CF lung infections

The classical aim of antimicrobial therapy is to resolve clearly defined clinical symptoms of infections by elimination of the pathogen with the minimal risk of toxic side-effects or of developing antibiotic resistance. These ideals are difficult and probably unattainable in CF patients and have to be modified to include clinical benefits which include maintenance of weight and lung function (Geddes, 1988). The aggressive use of antibiotic therapy, together with improved nutritional management, have been largely responsible for the increased life-span of CF patients. Although, as yet, chronic *P. aeruginosa* infection cannot be eradicated, intensive treatment with antibiotics can maintain near normal lung function for many years. Effective antimicrobial chemoprophylaxis may be achieved by a regimen of inhaled antibiotics administered on a long-term basis. Systemically administered antimicrobials penetrate endobronchial secretions poorly and large intravenous doses are needed to attain therapeutic concentrations at the infection site. Such high doses carry a significant risk of side-effects (Ramsey *et al.*, 1993). Direct delivery by aerosol produces high concentrations of the antibiotic at the infection site and reduces systemic side-effects due to an altered absorption profile from the lung to the systemic vasculature. One study has shown that nebulised carbenicillin and gentamicin produced subjective improvement in the respiratory systems of patients and objective improvement in lung function (Hodson *et al.*, 1981). Aerosolised ceftazidime was shown to have equivalent activity to the combination of gentamicin and carbenicillin (Stead *et al.*, 1987). The short-term administration of a high dose of tobramycin in patients with clinically stable CF was shown to be efficacious and safe (Ramsey *et al.*, 1993). A recent approach has been the use of nebulised colistin for early *pseudomonas* colonisation. This treatment has been shown to reduce the number of *pseudomonas* organisms isolated and also the frequency of isolation from respiratory tract cultures of treated patients (Littlewood *et al.*, 1985). Inhaled colistin, given over a six month period maintained lung function in symptomatic patients colonised with *P. aeruginosa*, when compared with inhaled saline (Day *et al.*, 1988). In a controlled study by Valerius *et al.* (1991) it was found that the institution of 3-week courses of anti-pseudomonal



chemotherapy (oral ciprofloxacin and colistin aerosol twice daily) prevented or delayed the development of chronic lung infection. It was demonstrated in a small uncontrolled study that early treatment with oral ciprofloxacin plus aerosolised colistin and tobramycin may delay the onset of chronic bronchial *P. aeruginosa* infection in CF (Vazquez *et al.*, 1993). The theoretical risk of the emergence of resistant strains was not observed during these studies and selection of *P. cepacia* or *P. maltophilia* strains was not observed. However, longer-term studies are required to confirm these findings. The cost incurred with aerosol therapy is less than alternative systemic administration and the development of improved nebulisers will further reduce this cost.

The selection of antimicrobial agents for the treatment of acute lung infections in CF patients remains a much discussed subject. As with prophylactic regimens there is widespread centre-to-centre variation. However the basis of therapy is usually an aminoglycoside given in combination with one of the newer  $\beta$ -lactams with anti-pseudomonal activity (such as ceftazidime) to obtain synergistic activity (Højby *et al.*, 1982). Probenecid is commonly given orally to all patients receiving  $\beta$ -lactam antibiotics eliminated by renal tubular excretion to achieve higher concentrations for prolonged periods of time (Højby & Koch, 1990). There is little agreement on the indications for optimum time of treatment, the choice of antibiotic, dosage schedules or the duration of treatment. Newer agents such as third generation cephalosporins, monobactams and 4-quinolones have allowed the possibility of monotherapy as opposed to traditionally favoured combination therapy. Despite the clinical efficacy of monotherapy and little clear evidence in favour of combined therapy, there remains a tendency to combine two anti-pseudomonal agents based on a theoretical rationale that combined therapy will reduce the emergence of multi-resistant strains. In practice, antibiotic resistance in *P. aeruginosa* is often temporary and reverts in most instances within weeks or months after treatment is stopped. Eventually, however, after the repeated courses of antibiotic treatment which are a feature of CF therapy, there is a gradual decrease in bacterial susceptibility at least on the basis of *in vitro* tests. Such resistant strains usually grow very slowly, produce small colonies and lose the ability to produce virulence factors such as

elastase (Govan, 1988). In addition to the above considerations, the dose of antimicrobial frequently requires adjustment in the CF patient (Lindsay & Bosso, 1993). Many antibiotics have altered pharmacokinetics in CF patients and the dose of agents such as tobramycin, which exhibits increased clearance in CF, may exceed that recommended in other patient groups (Høiby & Koch, 1990).

### 1.1.9. New approaches to the management of CF lung disease

Amiloride inhibits sodium reabsorption by renal tubular cells and is thought to act in the lung by blocking excess sodium reabsorption by the respiratory epithelium. The administration of nebulised amiloride was shown to enhance mucus clearance. No toxic effects were observed and a potential clinical benefit was suggested (Knowles *et al.*, 1990). The evidence in subsequent studies for such an improvement is conflicting. The first clinical trial (App *et al.*, 1990) showed a benefit when all other respiratory treatment had been withdrawn, whilst a later study (Graham *et al.*, 1993) failed to demonstrate efficacy when nebulised amiloride was administered as an additional treatment. Further studies are needed in larger patient groups before nebulised amiloride can be confirmed to be a useful therapeutic option. A potential *in vivo* anti-inflammatory action for amiloride has been suggested following *in vitro* reduction of cytokine production by alveolar macrophages (Davis *et al.*, 1992).

Delivery of extracellular nucleotides to respiratory epithelia has been suggested as a potential means of modifying CF airway secretions. Adenosine and uridine triphosphate stimulate chloride channel secretion independent of the defective cAMP/CFTR pathway at the apical surface of airway epithelia. However the potential of these agents has yet to be confirmed in a clinical setting (Stableforth, 1994).

One of the main factors contributing to the high viscosity of bronchial secretions is the large concentration of neutrophil-derived DNA (Santis & Geddes, 1994). Recombinant human

deoxyribonuclease I (rhDNase) reduces the viscosity of CF sputum (Shak *et al.*, 1990) and clinical studies have shown an improvement in clinical well-being (Hubbard *et al.*, 1992). No serious side-effects were reported and it appears that rhDNase (marketed as Pulmozyme<sup>®</sup>, Hoffman La Roche) is a valuable addition to the clinician's armamentarium.

### 1.1.9.1. Anti-inflammatory treatments

Analysis of bronchoalveolar lavage fluids from CF patients with stable clinically mild lung disease found significant on-going infection and inflammation (Konstan *et al.*, 1994). Strategies to reduce lung inflammation may improve lung function. Alternate-day prednisolone treatment reduced morbidity and improved pulmonary function in children with CF (Auerbach *et al.*, 1985). A large multi-centre study of steroid treatment in the USA has yet to be published, although the high steroid dosage arm of the trial had to be stopped due to the development of glucose intolerance in treated patients (Stableforth, 1994). A short-term study of ibuprofen in children has shown no adverse side-effects (Konstan *et al.*, 1991). A preliminary study of patients receiving oral piroxicam reported a trend towards improvement in respiratory function compared to control groups (Sordelli *et al.*, 1994).

### 1.1.9.2. Immunomodulation

Anti-pseudomonas immunotherapy, utilising intravenously administered hyperimmune  $\gamma$ -globulin, containing IgG antibodies against *P. aeruginosa* lipopolysaccharide, was shown to enhance opsonisation and bacterial killing, improve clinical scores, and improve lung function status (Van Wye *et al.*, 1990). Long-term induction of anti-pseudomonas immunity by early vaccination would be desirable but clinical trials to date have been disappointing (Holder, 1988). An alternative approach utilising cyclosporin, azathioprine and prednisolone as routine post-graft rejection suppression treatment, reduced specific anti-*P. aeruginosa* antibodies and improved lung function in a young CF renal transplant patient (Koch *et al.*, 1993). Further studies are now in progress.

### 1.1.9.3. Transplantation

Encouraging results have been obtained with CF patients who have received double lung transplants (Madden *et al.*, 1992). However in spite of a favourable long-term prognosis (Santis & Geddes, 1994), limited donor organ availability prevents transplantation being the general solution for advanced CF lung disease (Zach, 1991).

### 1.1.9.4. Development of gene therapy for CF

Many cell types have been transfected *in vitro* with the CFTR sequence with its subsequent expression conferring a cAMP sensitive chloride channel conductance. The aim of gene therapy is to repeat this success *in vivo* but several major obstacles must first be surmounted before gene therapy can be regarded as a cure for CF. Due to the physicochemical nature of genetic material, vector systems are required to introduce DNA to the cell interior. Two gene vector systems, viruses and liposomes, are currently in clinical trial for CF. Adenoviruses have the advantage of a high transfer efficiency but have the potential for adverse immunological and inflammatory responses. Liposome-based systems have not shown overt toxicological properties but their transfection efficiency is lower than that of viral vectors (Cuthbert, 1994). Trials in the US, using an adenovirus vector, have been performed on six CF patients over the last 12 months (Crystal, 1994). Gene transfer was evident in all patients and no chronic adverse effects were noted although one patient experienced a mild inflammatory reaction. A UK phase I trial of a liposome vector has shown that liposome mediated gene transfer was safe and some correction of ion transport was observed (Caplen *et al.*, 1995). The development of transgenic CF mice by a number of centres will allow the optimisation of gene delivery systems and dosage schedules, and further the studies of clinical pathology (Higgins & Trezise, 1992; Wilson & Collins, 1992).

Gene therapy is potentially an enormous step forward in the treatment of CF (Stableforth, 1994). Development of vector systems will facilitate the treatment becoming a realistic

prospect for patients although the correction of the lung CFTR defect represents an easier challenge than other sites, notably the pancreas and the gastrointestinal tract (Cuthbert, 1994).

## 1.2. The polymyxin group of antibiotics

The polymyxins are a group of basic polypeptide antibiotics, which were first isolated in 1947 from a spore-bearing soil bacillus (*Bacillus polymyxa*). Five major and chemically distinct polymyxins were recognised and designated alphabetically as polymyxins A, B, C, D and E. Their general structure comprises a cyclic heptapeptide moiety attached to a tripeptide side chain which terminates with a fatty acyl residue, (figure 1.2) (Elverdam *et al.*, 1981). They have a molecular weight in the range of 1200 and they characteristically contain a high percentage of  $\alpha$ ,  $\gamma$ -diaminobutyric acid (Storm *et al.*, 1977). They differ from each other in amino acid composition and in the fatty acyl residue of the tripeptide side chain. The variation in amino acid composition is shown in figure 1.3. Each individual polymyxin is a mixture of several closely related polypeptides which are named by numerical suffix according to the constituent fatty acid residue. Polymyxin (1) denotes a methyloctanoic acid residue, polymyxin (2) an isooctanoyl residue, polymyxin (3) an octanoyl residue and polymyxin (4) a heptanoyl residue (Elverdam *et al.*, 1981).

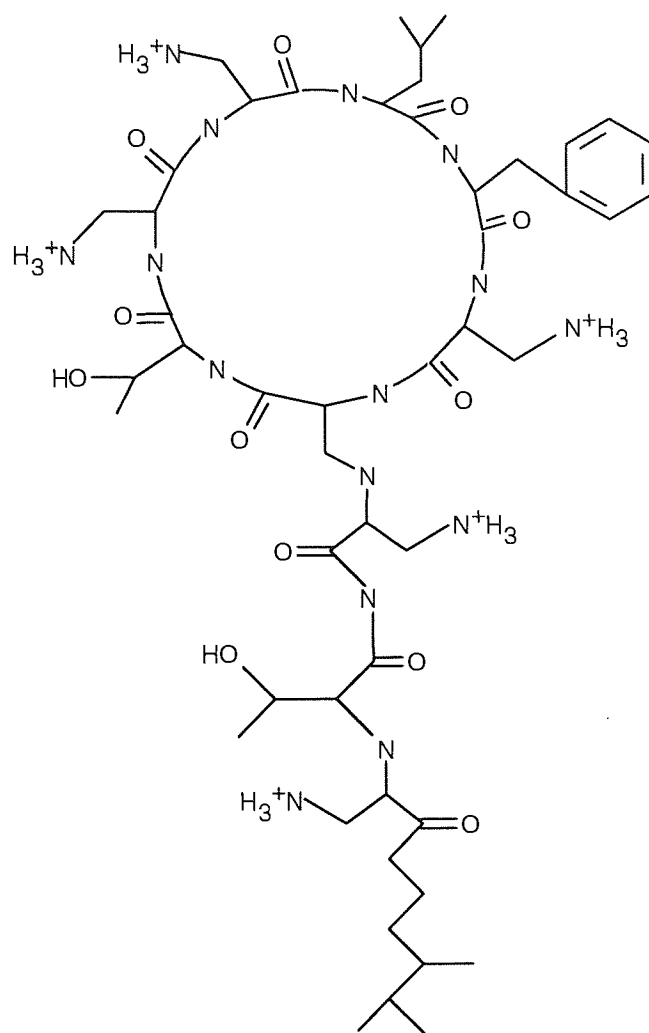
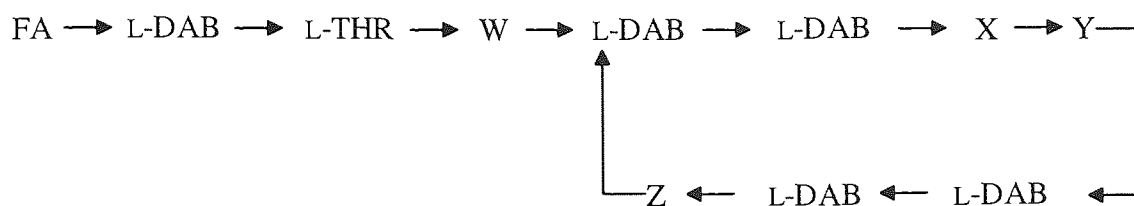


Figure 1.2. Chemical structure of PXB.

Initially only polymyxin B (Aerosporin<sup>®</sup>), mainly composed of polymyxin B<sub>1</sub> and B<sub>2</sub>, in the form of its sulphate was commercially available. Polymyxin E (also known as colistin), mainly composed of polymyxin E<sub>1</sub> and E<sub>2</sub>, became available for clinical use in 1959 in the methane sulphonate form. It was represented as a better drug than polymyxin B on the grounds of reduced toxicity. However the sulphates have been shown to have eight times more activity than the methane sulphonates against *P. aeruginosa* (Eickhoff & Finland, 1965). As activity of these derivatives was found to be directly related to their toxicity they offered no clinical advantage to the physician. The other polymyxins (A, C and D) are too toxic for clinical use.



Compound	W	X	Y	Z
Polymyxin A (or M)	L-Dab	D-Leu	L-Thr	L-Thr
Polymyxin B	L-Dab	D-Phe	L-Leu	L-Thr
Polymyxin C (or P)	Dab	Phe	Thr	Thr
Polymyxin D	D-Ser	D-Leu	L-Thr	L-Thr
Polymyxin E	L-Dab	D-Leu	L-Leu	L-Thr

Figure 1.3. Amino acid variation in the polymyxin group of antibiotics. L-Dab= L- $\alpha$ ,  $\gamma$ -diaminobutyric acid, D-Leu/L-Leu= D/L-leucine, L-Thr= L-threonine, D-Phe= D-phenylalanine, D-Ser= D-serine, FA= fatty acid moiety, as discussed in text.

### 1.2.1. Microbiological characteristics

All the polymyxins have a similar antibacterial spectrum, although quantitative differences in activity exist. The spectrum of sensitive organisms includes Gram-negative enteric bacilli such as *E. coli*, *Enterobacter* and *Klebsiella* spp. and also *P. aeruginosa*. All *Proteus* spp. are resistant and *Serratia marcescens* is also usually resistant. Other Gram-negative bacteria which are sensitive include *H. influenzae*, *B. pertussis*, the *Salmonellae* and the *Shigellae* (Kucers & Bennett, 1987). Gram-positive bacteria are generally less sensitive to polymyxins than Gram-negative bacteria. However, there are polymyxin-sensitive strains of *Staphylococcus*, *Bacillus*, *Streptococcus pyogenes* and *Corynebacterium* (Storm *et al.*, 1977).

An important property of the polymyxins is that the bacteria usually sensitive to these drugs do not readily acquire resistance. Occasionally resistant *P. aeruginosa* strains are encountered, and these show complete cross-resistance between polymyxin B and colistin. Some *P. aeruginosa* strains, while developing resistance to polymyxins, have increased sensitivity to antibiotics, such as chloramphenicol and in particular tetracycline, to which these organisms are normally insensitive (Brown *et al.*, 1972).

### 1.2.2. Mode of action

The amphipathic nature of the polymyxins suggests that their disruptive influence on cytoplasmic membranes can be attributed to a cationic detergent-like action. On contact with bacteria, polymyxin molecules site themselves between the protein and phospholipid layers of the cell membrane. This membrane immediately becomes porous and releases intracellular material of low molecular weight (phosphates, amino acids, purines and pyrimidines). Rapid cell death follows. However, the biocidal activity of polymyxins is seen at concentrations much lower than that required for detergent activity suggesting that the interaction between polymyxins and bacterial membranes involves a degree of specificity (Storm *et al.*, 1977). The cationic and amphipathic nature of the polymyxins promotes interaction with lipopolysaccharides and acidic phospholipids situated in the outer membrane of Gram-negative bacteria. Schindler & Osborn (1979) reported that polymyxin acts by binding to the acidic groups of the lipid A portion of LPS and so displaces the divalent cations which play a crucial role in the cross-linking of LPS. The binding of polymyxins to LPS with subsequent displacement of  $Mg^{2+}$  and disruption of the stabilising effect afforded by the  $Mg^{2+}$  cross-bridging of adjacent LPS molecules in the outer membrane results in a permeability increase (Moore *et al.*, 1986). Morphological studies have shown the formation of blebs after polymyxin treatment on the outer membrane which is followed by subsequent disruption of the cytoplasmic membrane (Koike *et al.*, 1969). The aggregation of lipopolysaccharide and acidic phospholipids at the bleb site could lead to removal of these molecules from the



membrane lattice (Schindler & Teuber, 1975). The permeabilised membrane allows uptake of polycationic antibiotics such as polymyxins and aminoglycosides. This effect may explain the synergy observed between polymyxins and aminoglycosides (Joris & van Saene, 1985). The bactericidal activity of the polymyxins is primarily physiochemical as opposed to the biochemical action of other antibiotics and is therefore exerted whether or not the cell is growing. The relative lack of resistance to polymyxins may be explained by this mode of action (Storm *et al.*, 1977).

### 1.2.3. Biodistribution and pharmacokinetics of the polymyxins

The large polypeptide structure of the polymyxins results in absorption from the gastrointestinal tract being very poor (Brownlee *et al.*, 1952). When administered by the intramuscular route, peak serum levels are usually attained within 2-3 hours and demonstrable levels persist for at least 8 hours. The peak serum level is subject to considerable individual variation, and it may be as high as 8 $\mu$ g/ml or as low as 1-2 $\mu$ g/ml. The half-life of polymyxin B sulphate in serum is about 6 hours. Some accumulation of the drug occurs and repeated administration yields higher serum levels. A modified dosage schedule coupled with serum level monitoring is necessary in patients with renal failure (Kucers & Bennett, 1987). After intravenous injection much lower levels of either polymyxin B or E are observed than would be expected. The polymyxins do not accumulate in red blood cells (Brownlee *et al.*, 1952) and they exhibit a low degree of protein binding (Kunin, 1967). Animal studies have shown that polymyxins become bound to and persist in various body tissues such as the liver, kidney, brain, heart, muscle and lung (Kunin & Bugg, 1971). The detection of high levels of polymyxin B in the brain was unexpected as a previous study had concluded that polymyxins do not cross the blood-brain barrier (Brownlee *et al.*, 1952). Polymyxins persist in these tissues for up to 72 hours after single injections and for up to 5 days after a course of treatment.

The polymyxins are mainly excreted by glomerular filtration in the kidney. However, a delay in excretion after the initial dose is observed with only about 0.1% of polymyxin B sulphate recovered from urine during the first 12 hours after administration. Colistin methane sulphonate is more rapidly excreted *via* the kidney with about 40% recovered in the urine after 8 hours. The polymyxins are not excreted *via* the biliary route (Kucers & Bennett, 1987). The fraction of drug which remains bound in the tissues is probably slowly enzymatically inactivated (Brownlee *et al.*, 1952).

When given by aerosol, transpulmonary absorption has been reported and appears to be influenced by aerosol particle size. In one study (Halliday, 1967) 1 million units administered to normal subjects *via* a Wright's nebuliser giving droplets 5-8 microns in diameter did not produce detectable blood levels; the Collision inhaler (3-5 microns) and the Croupette atomiser (1-6 microns) both produced levels of between 1.28 and 6.6 $\mu$ g/ml. These levels are significant as considering the serum levels which can be anticipated after intramuscular administration of normal therapeutic doses (Technical information, Pharmax, Kent).

#### 1.2.4. Side-effects/adverse reactions associated with polymyxins

The polymyxins, even when administered in the recommended doses, frequently cause side-effects. This has curtailed the usefulness of these drugs as antimicrobial agents. The antibacterial activity of these compounds is proportional to their toxicity so that for a certain degree of antimicrobial activity, the toxicity is the same regardless of which derivative (sulphate or the methane sulphonate) is used (Kucers & Bennett, 1987). Nephrotoxicity is the most serious toxic effect, occurring in 20.2% of patients (Koch-Weser *et al.*, 1970). Acute tubular necrosis may result and renal impairment may sometimes continue to progress for 1 or 2 weeks after the drug has been stopped. Neurotoxicity is another serious side-effect of the polymyxins and presents as giddiness, disturbances of sensation, nausea and vomiting, muscle weakness and peripheral neuropathy. Another serious neurotoxic effect is reversible

neuromuscular blockade which may result in respiratory paralysis. Most reported cases have involved potentiating factors such as sedatives, neuromuscular blocking agents and renal disease. Renal and neural tissue, the major sites of expression of toxicity, share binding affinity for polymyxins with a number of other tissues. This perhaps suggests that these tissues have an increased sensitivity to polymyxins (Kunin & Bugg, 1971). Other observed adverse reactions include hypersensitivity reactions such as rashes, pruritus and fever (Koch-Weser *et al.*, 1970).

### 1.2.5. Clinical use of the polymyxins

The toxicity profile of the polymyxins has meant that their clinical use has changed from that of the 1960s when they were the only anti-pseudomonal agents available. Today use of polymyxins has been curtailed due to the advent of newer cephalosporins, aminoglycosides and improved  $\beta$ -lactams, which are now the agents of choice in the treatment of Gram-negative systemic infections. Polymyxins still play a role in the treatment of superficial infections and are available as ear-drops, topical powders and solutions. Other areas of clinical use which still exist include the use of polymyxins in selective decontamination of the digestive tract (SDD), a procedure which is indicated in granulocytopenic patients. Polymyxins are one of several drugs, which, when given orally, produce selective decontamination of the digestive tract. Amphotericin and an aminoglycoside, commonly tobramycin, are often used in this regime. SDD involves selective decontamination of potentially pathogenic aerobic micro-organisms and yeasts from the throat and intestine using orally administered antibiotics which do not affect the beneficial anaerobic flora. The antibiotics used must be non-absorbable and have a narrow-spectrum of activity (or a 'directed spectrum' *i.e.* Gram-negative pathogens). The antibiotics must be bactericidal with low minimal bactericidal concentrations and be minimally inactivated by food or faeces. Polymyxins fulfill these requirements and when used in combination with tobramycin are synergistic against most aerobic Gram-negative organisms (Joris & van Saene, 1985).

FRACON therapy, a combination of framycetin, colistin and nystatin together with antiseptic treatment has been used in the prevention of infection in patients with acute myeloid leukaemia (Trexler *et al.*, 1975).

The high affinity of polymyxins for lipopolysaccharide (Vaara, 1983) has been utilised for the treatment of Gram-negative septic shock syndrome. In animals with experimental endotoxaemia, polymyxin B reduced levels of mortality and endotoxin levels (Endo *et al.*, 1994). However, the widespread clinical use is precluded by its nephrotoxicity and neurotoxicity (Prins *et al.*, 1994). An alternative approach has been to couple polymyxin B to a resin packing for use in endotoxin removal by dialysis (Talmadge & Siebert, 1989). A similar material has been used clinically to treat septic shock patients (Aoki *et al.*, 1992). Endotoxin blood levels decreased significantly after haemoperfusion through polystyrene fibres with immobilised polymyxin B. Haemoperfusion utilising polymyxin B packings appears to be a promising treatment for septic shock.

There has recently been a resurgence of interest in the polymyxins for the treatment of CF lung infections. Polymyxin E is commonly administered by aerosol for prophylactic treatment (section 1.2.6). Intravenous administration has also regained favour for the treatment of resistant *P. aeruginosa*. A surprising lack of side-effects were noted despite the administration of high doses (Stableforth, 1994).

### **1.2.6. The use of polymyxins for the treatment of cystic fibrosis lung infections**

Colistin is the polymyxin of choice in the treatment of CF lung infections. It differs from polymyxin B by a single amino-acid residue, possessing l-leucine instead of d-phenylalanine. The spectrum of activity remains the same. It is most commonly administered as a nebulised solution of Colomycin<sup>®</sup> (colistin sulphomethate sodium), manufactured by Pharmax, UK. At Birmingham childrens' hospital, colistin therapy is initiated on first isolation of *P. aeruginosa*.

The patient undergoes physiotherapy twice daily which is followed by aerosol administration of colistin in a dose of 1 or 2 mega units, depending on age. Treatment is continued and is terminated only if adverse effects make it necessary (personal communication, Dr. Weller, Birmingham childrens' hospital).

The rationale for colistin therapy is twofold. Firstly, parenteral anti-pseudomonal chemotherapy is the mainstay of modern treatment, but it is rarely possible to eradicate the pathogen from the lower airways (Høiby *et al.*, 1982). However, it offers symptomatic relief (Cerny *et al.*, 1984) and halts the progressive deterioration of pulmonary function that would otherwise occur (Szaff *et al.*, 1983). Between courses of anti-pseudomonal treatment lung function parameters decline and signs and symptoms of infection may develop (Høiby *et al.*, 1982). Additional therapy administered at home would therefore be desirable in order to prevent such deterioration. Therapy with aerosolised colistin constitutes such treatment. Colistin is particularly suitable for this indication as it has high activity against *P. aeruginosa*, even against multi-resistant strains, and colistin resistance is seldom seen among *P. aeruginosa* (Sabath, 1984). A number of studies (section 1.2.6) have demonstrated a clinical benefit from polymyxin aerosol therapy either administered with or without concomitant anti-pseudomonal chemotherapy. In a double-blind placebo-controlled study of colistin inhalation by Jensen *et al.* (1987), it was shown that treatment reduced deterioration in wellbeing and pulmonary function, and also reduced the inflammatory response that otherwise occurs after completion of a course of intravenous anti-pseudomonal therapy. The treatment was safe and systemic absorption of colistin was not detected, although this may have been due to the high MIC of the assay organism used (*P. maltophilia*, lower detection limit 2.5mg/L). Superinfection with colistin-resistant micro-organisms was not seen, although *P. cepacia*, an established pathogen in CF, is colistin resistant and may pose a problem in such treatment. However, an outbreak of nosocomial *Flavobacterium meningosepticum* respiratory infection associated with the use of aerosolised polymyxin B has been reported by Brown *et al.* (1989). Colistin sulphomethate sodium did not cause bronchospasm which is an adverse effect often observed following inhalation of polymyxin B (Dickie & De Groot, 1973). It

would appear, however, that colistin shares this side-effect as a recent study indicated that a significant number of CF adults (32%) were intolerant of colistin because of chest tightness. It may be possible to continue therapy in this patient group by reducing the dose and concentration of the nebulised drug (Maddison, 1994). Nebulised colistin has also been used for AIDS-associated *P. aeruginosa* pneumonia (Green *et al.*, 1992).

Jensen *et al.* (1987) suggested that the reduction in the degree of pulmonary inflammation by colistin inhalation may reduce the lung damage caused by *P. aeruginosa* infection. This proposed anti-inflammatory activity forms part of the rationale for its use in inhalation therapy. Bacterial lipopolysaccharide (LPS) has a major role in the aetiology of lung damage in CF. An antibody response to pseudomonal LPS generates the formation of immune-complexes both within the lung and in the circulation. These complexes can maintain the inflammatory response by direct stimulation of inflammatory cells (Elborn & Shale, 1990). LPS is also capable of regulating chemotactic and chemiluminescent responses from human neutrophils, the predominant cells of the alveolar space in CF patients with chronic pseudomonal infection (Kharazmi *et al.*, 1991). Polymyxins have a high affinity for LPS and a number of studies (David *et al.*, 1992; Morrison & Jacobs, 1976; Peterson *et al.*, 1985) have demonstrated that polymyxin B forms stable molecular complexes with the lipid A region of LPS and the binding involves both electrostatic and hydrophobic interactions. *In vitro*, PXB blocks several biological effects induced by LPS including the release of lysosomal enzymes by neutrophils, the neutrophil respiratory burst, LPS-enhanced tumor cell killing by macrophages and LPS-induced release of TNF- $\alpha$  from alveolar macrophages (Prins *et al.*, 1994). The structural integrity of the lipid A region is essential for specific binding of LPS to macrophages and the structure also plays a critical role for LPS-promoted cell activation (Kirikae *et al.*, 1994). The structure of LPS may also play a role in binding of LPS to neutrophils through an interaction with endotoxin receptors at the cell surface. Preliminary studies indicate that neutrophil receptors are lipid-like, which is consistent with a role for the hydrophobic lipid A region in binding (Wilson, 1985). It is possible that the therapeutic benefit observed in CF patients, following polymyxin aerosol therapy, is due not only to the

antimicrobial activity of polymyxins, but also to their interaction with LPS. It has been known that polymyxin B has a neutralising effect on LPS (Applemelk *et al.*, 1988). Rifkind (1967) showed that incubation of LPS with polymyxin B resulted in a 20-fold increase in LD<sub>50</sub> of LPS in mice. Polymyxin B has also been shown to block the enhanced release of toxic oxygen radicals induced by LPS in human neutrophils (Danner *et al.*, 1989). Therefore, it would appear reasonable to speculate that improvement in patients' symptomology may be due to structural distortion of LPS by polymyxin.

### 1.2.7. Rationale for the development of a liposomal polymyxin formulation

Although the aerosol administration of polymyxins, particularly colistin, is viewed as an effective treatment for the management of chronic infection in CF patients, the pharmacokinetics of the preparation are far from ideal. Høiby (1991) has suggested that aerosolised colistin should ideally be administered six times a day instead of the twice daily regimen which is currently used. Such a rigorous dosing schedule is unacceptable from a patient viewpoint and other ways of improving the pharmacokinetic profile of aerosolised polymyxins are required. The absorption of polymyxins from the lung mucosae is similar to that observed with a number of other antimicrobial compounds (Burton & Schanker, 1974). A review of drug needs in cystic fibrosis highlighted the need for a means of retaining compounds on the airway surfaces (Boucher & Beall, 1989). Liposomes were proposed as a candidate delivery system due to accumulated research data which illustrate the potential of liposomes to improve drug delivery to the lung (Schreier, 1992; Schreier *et al.*, 1993; Taylor & Newton, 1992). Liposomes provide a means of prolonging local therapeutic drug levels and minimising local and systemic toxicity of aerosolised agents. They have been shown to be relatively non-toxic and they are suitable for aerosol administration (Schreier *et al.*, 1993). Therefore the development of a liposomal formulation of polymyxins represents a potential means of improving the pharmacokinetics and efficacy of this drug in the treatment of CF lung infections.

### 1.3. Therapeutic advantages of drug delivery systems

Most modern drugs are highly potent molecules which are efficacious at doses which minimise side-effects. However, certain drug groups, principally cytotoxic agents, possess a narrow therapeutic index as they illicit undesirable effects in normal tissues at doses required for a pharmacological effect in the target tissue. Although rational drug design is a relatively recent attempt to rectify such problems at the initial discovery stage, such an approach has inherent limitations. An alternative solution is to modify the characteristics of the drug molecule by combining it with a carrier system. The goal of this approach is to deliver the drug to the affected tissue in high concentration and divert the drug from normal tissues. Drug targeting was first proposed almost a century ago by Paul Ehrlich, who suggested the 'magic bullet' concept (Torchillin, 1985).

Several experimental strategies have been developed, in which the agent of interest is combined with a moiety which alters its pharmacokinetics and biodistribution (Gupta, 1990). Macromolecules, such as polymers and polysaccharides, have been used whilst specific targeting to tissues may be achieved through the linkage of a bioactive agent with a site-specific monoclonal antibody. Controlled release systems utilise the characteristics of biodegradable polymers/matrices to release drugs in a pulsatile or sustained fashion. Such delivery systems can alter the pharmacokinetic properties of a drug but they cannot target an active agent to non-local sites. Colloidal carrier systems have proved the most successful approach to drug targeting. Microcapsules, nanoparticles, microspheres and liposomes are examples of colloidal carriers which are capable of altering the pharmacokinetics of bioactive agents and delivering them to specific tissues. Colloidal carriers are an attractive concept for drug delivery in that particles can be prepared reproducibly with a wide range of physicochemical characteristics (Bakker-Woudenberg *et al.*, 1991). Whilst particulate systems share general *in vivo* characteristics, liposomes have the advantages of relatively low toxicity and a flexibility in structure which allows manipulation of their *in vivo* properties. The



structure and composition of liposomes also makes them versatile carriers, suitable for a wide variety of drug molecules (Gregoriadis, 1993).

### 1.3.1. Liposome structure and assembly

Liposomes were first described in 1965 by Sir Alec Bangham who described structures with similarities to biological membranes which he termed 'smectic mesospheres' (Bangham *et al.*, 1965). They were formed when an aqueous solution was added to a dried lipid film and they were shown to be closed membrane structures which exhibited semipermeability and osmotic properties. This led to the first application of liposome technology soon afterwards with their use in model membrane studies (Bangham, 1993). The ability of liposomes to entrap and release ions led to the pioneering work of Gregoriadis and Ryman in the early 1970's in which they utilised liposomes as drug delivery vehicles (Gregoriadis & Ryman, 1972). Research in this area has culminated in liposomes making the transition from the bench to the marketplace with the marketing of the first commercial liposomal formulation, Ambisome®, in 1991 (Gregoriadis & Florence, 1993b).

The spontaneous assembly process of phospholipids into liposomes occurs when these relatively insoluble components arrange themselves as stable, concentric bilayers, around an internal aqueous compartment (see figure 1.4) (Fielding, 1991). The central aqueous core can range in diameter from 20nm to several micrometers and liposomes can contain from one to tens of concentric bilayers each creating its own aqueous compartment. The bimolecular leaflet is arranged with the polar headgroups of individual phospholipids in contact with water molecules on either side of the structure, while apolar hydrocarbon tails form a thin hydrophobic phase sandwiched in between.

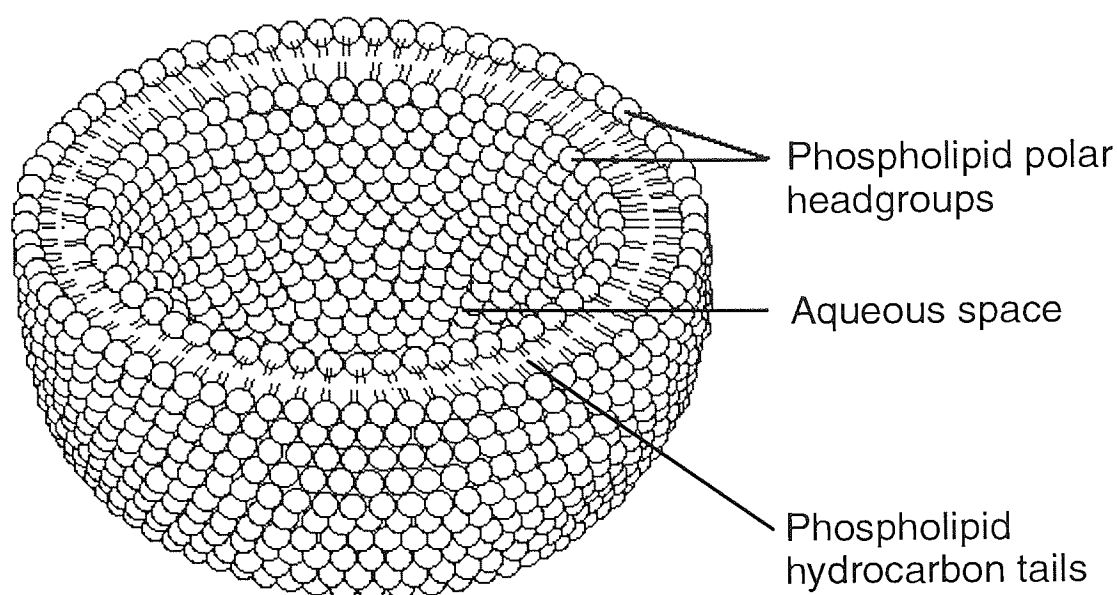


Figure 1.4. Diagram depicting the arrangement of phospholipid molecules around an aqueous core to form a unilamellar liposome

Covalent bonds are not formed during the assembly process, but the summation of hydrophobic interactions between the hydrocarbon chains of the membrane interior leads to high stability (Martin, 1990). The hydrophobic effect is a consequence of the large free energy change between water and hydrophobic environments, and is the driving force behind the bilayer assembly process (Cevc, 1993b). Lipids aggregate to form bilayers which exclude as much water as possible from the hydrocarbon core in order to achieve the lowest free energy level and therefore the highest stability state for the aggregate. The extremely low critical micelle concentration ( $4.6 \times 10^{-10}\text{M}$ ) of phosphatidylcholines is further evidence of the preference of these molecules for the hydrophobic environment of a micelle or bilayer core (Riaz *et al.*, 1989).

The type of aggregate formed, *i.e.* bilayer, micelle or other structure, depends upon the interaction with water and most importantly, the hydrated surface area of the polar phospholipid headgroup relative to the surface area of the hydrophobic chains. Phosphatidylcholine, phosphatidylinositol, and phosphatidylglycerol form bilayer structures. Lysolecithin (the degradation product of phosphatidylcholine) forms micelles, whereas

phosphatidylethanolamine (and negatively charged phospholipids at low pH or in the presence of divalent cations) form hexagonal structures. It is however, possible to incorporate these components in a bilayer leaflet by mixing them with relatively large amounts of bilayer forming phospholipids (Riaz *et al.*, 1989).

### 1.3.2. Liposome composition and structural properties

Glycerol containing phospholipids are the most commonly used component of liposome formulations and also represent more than 50% of lipid present in biological membranes (Riaz *et al.*, 1989). The 1- and 2- positions of glycerol in natural phospholipids are both esterified with fatty acids and phosphate is attached to the 3- position of the molecule (Eibl, 1981). Most naturally occurring phospholipids contain two different fatty acids *per* phospholipid molecule and are termed mixed acid phospholipids. The phosphate headgroup may be further esterified to a wide range of organic alcohols, including glycerol, choline, ethanolamine, serine and inositol. The structures of phospholipids commonly used in liposome formulation are shown in figure 1.5 (Riaz *et al.*, 1989). Other important membrane lipids include the sphingolipids, such as sphingomyelin, which contain sphingosine or a related base as their structural backbone. Sphingomyelin possesses similar physical properties to its glycerolphospholipid counterpart, phosphatidylcholine (both are esterified through the phosphate group with a choline headgroup), in that it is zwitterionic at physiological pH and readily forms bilayers upon hydration. The bulk of liposomal constituents have no net charge at physiological pH (phosphatidylcholine and cholesterol, for example) and negatively charged phospholipids such as phosphatidylglycerol, phosphatidylserine and phosphatidic acid, or positively charged agents such as stearylamine, are frequently employed to reduce the tendency of uncharged liposomes to aggregate in aqueous suspension. The structural diversity of naturally occurring phospholipids is a result of varying fatty acid content which can differ in the number of carbon atoms and the degree of unsaturation. The presence of unsaturated fatty acids can lead to chemical instability through oxidation processes (Eibl,

1981). These problems can be overcome by the use of synthetic phospholipids of well defined structure and controlled, if any, unsaturation. The large scale synthesis of such phospholipids has enabled liposomes for clinical use, to be prepared reproducibly in large scale quantities to criteria which satisfy the regulatory authorities (Isele *et al.*, 1994).

The composition of the lipid bilayer is critically important in determining the biological and physicochemical properties of liposomes, mainly through influences on membrane fluidity, permeability, and surface properties. Membrane fluidity refers to the existence of thermal phase transitions in phospholipid aggregates. As temperature increases these lipids move from a relatively ordered gel state to a more disordered, fluid-like liquid crystalline state. In the gel state, liposomal membranes are more stable, less permeable to solutes and less likely to interact with destabilising macromolecules than in the liquid crystalline state. A number of intermediate phases also exist, for example phosphatidylcholine has been proposed to exist in more than a dozen different phases (Cevc, 1993b). Maximum bilayer permeability occurs at the phase transition temperature ( $T_m$ ). At a temperature below the phase transition temperature the phospholipids are considered to be 'solid', at a temperature higher than the transition temperature the phospholipids are considered to be 'fluid' (Bakker-Woudenberg & Lokerse, 1991). Cholesterol, an important component of many cell membranes, is often included in liposome formulations because it reduces the permeability and increases the stability of phospholipid bilayers in the liquid crystalline state (Senior, 1987). Cholesterol has relatively little effect on the position of the phase transition, but it is able to abolish completely the heat of transition. As the concentration of cholesterol reaches equimolar proportions with phospholipid, the freedom of molecular motion above the phase transition is decreased, while below the phase transition mobility is increased. Therefore cholesterol can exert effects on permeability which are dependent both on molar concentration and the  $T_m$  of the bulk phospholipid (New, 1990).



### 1.3.3 Liposome classification and production technologies

The liposomes first described by Bangham are now referred to as multilamellar vesicles (MLV) and they range in size from  $0.2\mu\text{m}$  to  $>10\mu\text{m}$  (Ostro & Cullis, 1989). Sonication of MLV results in size reduction of these liposomes to vesicles containing only a single bilayer with diameters ranging from 25-50nm. These structures are referred to as small unilamellar vesicles (SUV). Single bilayer vesicles which exhibit a size range of 100-500nm in diameter are referred to as large unilamellar vesicles (LUV) (Riaz *et al.*, 1989). The encapsulation properties of these classes of liposomes are quite different. LUV have the highest ratio of encapsulated volume to lipid mass and are therefore most efficient at encapsulating water soluble agents. SUV have extremely inefficient solute trapping and a typical SUV preparation has ~10% the capture volume of an equimolar LUV preparation (Karlowsky & Zhanel, 1992). MLV have the highest lipid mass to volume ratio and are more efficient carriers of hydrophobic membrane-bound drugs (Talsma & Crommelin, 1992).

The liposomal compartment in which a drug may be entrapped is dependent upon the physicochemical characteristics of the drug. Highly polar, water-soluble drugs are entrapped within the aqueous space of the liposome. Lipophilic compounds can be incorporated into the interior of the bilayer, while amphiphilic drugs can adsorb or partition across the membrane-aqueous phase interface. This is illustrated in figure 1.6. Drugs with intermediate partition coefficients tend to diffuse across the bilayer and show less retention than very hydrophobic or very hydrophilic drugs (Karlowsky & Zhanel, 1992). For a given production process, the aqueous space captured by bilayers is directly proportional to the lipid mass. Liposomes containing charged phospholipids entrap an increased aqueous volume due to repulsion between like-charged bilayers increasing interlamellar distances (Szoka & Papahadjopoulos, 1980).

The encapsulation efficiency of hydrophilic, non-bilayer interacting drugs, depends solely on the entrapped volume and therefore, on the particle size, number of bilayers and the lipid

concentration utilised. The entrapment of charged drug molecules may be increased by the incorporation of an oppositely charged phospholipid within the bilayer. Electrostatic interaction leads to sequestration or attraction of the drug to the bilayer surface (Ostro & Cullis, 1989). For hydrophobic, bilayer-bound drugs, the efficiency depends on the total lipid used and the fluidity of the bilayer. Fluidity may also determine the leakage rate of encapsulated drugs. Liposomes composed of unsaturated lipids such as PC, which is in the relatively disordered liquid crystalline state at room temperature, tend to have greater release rates than liposomes composed of saturated lipids such as DSPC, which are in the ordered gel state at room temperature (Kulkarni *et al.*, 1995). The encapsulation of amphiphiles is determined by the mechanism of interaction with the bilayer. If the drug-liposome interaction is based on electrostatic forces, the density of charged phospholipids and the ionic strength and pH of the aqueous medium play a role. Hydrophobic interaction may also occur and the choice of lipid phase transition properties or phospholipid acyl chain length will be important factors governing the extent of interaction (Talsma & Crommelin, 1992). Cholesterol also increases the encapsulation of hydrophobic drugs although this is dependent on the specific interaction characteristics of the drug with bilayer phospholipids (Kulkarni *et al.*, 1995).

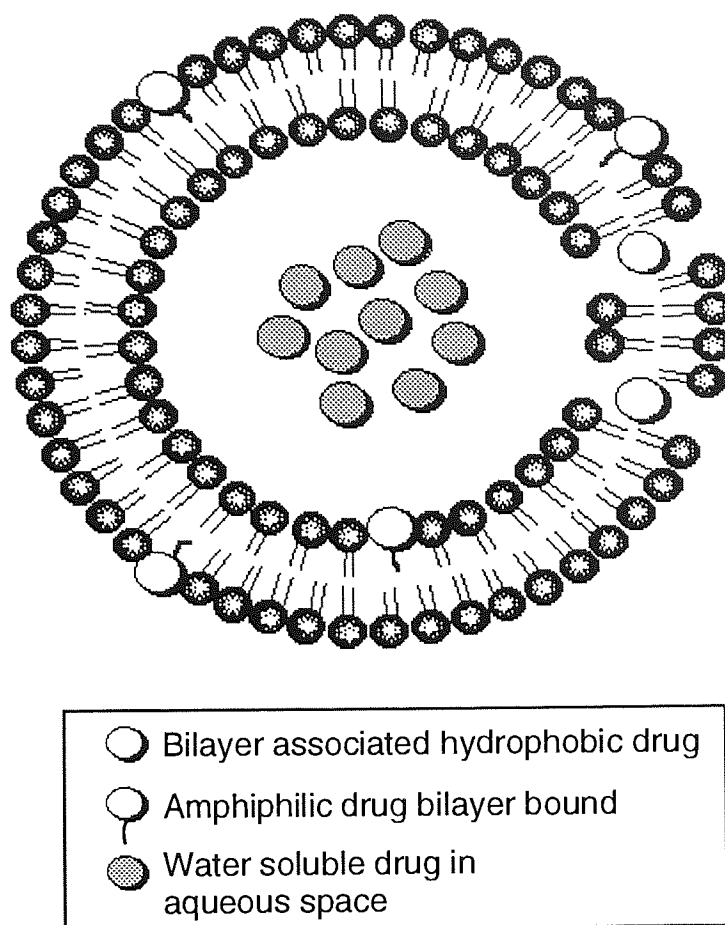


Figure 1.6. Schematic diagram depicting the compartmental site of drugs following encapsulation

#### 1.3.4. Methods of liposome preparation

Multilamellar vesicles (MLV) were the first liposome preparation to be described in detail (Bangham *et al.*, 1965) and are exceptionally simple to prepare. Phospholipids are deposited from organic solvents in a thin film on the wall of a round bottom flask by rotary evaporation under reduced pressure. Aqueous buffer is added and the phospholipids are hydrated at a temperature above the phase transition temperature ( $T_m$ ) of the phospholipid or above the  $T_m$  of the highest melting component in the mixture. The hydration time is important for obtaining maximal encapsulation along with the method of resuspension. The wide size range of MLV can be reduced by sonication or extrusion through polycarbonate membranes (Olson



*et al.*, 1979). The main drawback of MLV is low entrapment efficiencies, typically 5-15% (% entrapment/mg lipid) (Riaz *et al.*, 1989). Entrapment efficiencies of water-soluble drugs may be improved by applying a number of freeze and thaw (FAT) cycles to the preparation which increase the entrapped volume for a given lipid concentration (Nayar *et al.*, 1989).

Small unilamellar vesicles (SUV) can be prepared from MLV by sonicating a suspension at a temperature above the  $T_m$  of the highest melting lipid in the mixture and allowing the vesicles to anneal at a temperature above the  $T_m$  for at least 30 minutes. The principal drawbacks of SUV are the low encapsulation efficiency of the aqueous space, usually 0.1-1.0%, depending on the lipid composition and the low ratio of captured volume *per* mole of lipid (Szoka & Papahadjopoulos, 1980).

An alternative method for the preparation of SUV that avoids sonication is the ethanol injection technique described by Batzri & Korn (1973). Lipids dissolved in ethanol are rapidly injected into a buffer solution where they spontaneously form SUV. This procedure is simple, rapid and gentle. The major drawback of this technique is the relatively dilute preparation of liposomes obtained which decreases the encapsulation efficiency of the aqueous phase (Szoka & Papahadjopoulos, 1980).

Dispersion of MLV can be reduced in size by extrusion at high pressures through a French press. After multiple extrusion the resulting vesicles are somewhat larger than SUV prepared by sonication and the technique is applicable to a wide variety of lipid compositions. It is a simple, reproducible and non-destructive technique that makes it possible to prepare large volumes of vesicles at high lipid concentrations with minimal dilution (Szoka & Papahadjopoulos, 1980).

Large unilamellar vesicles (LUV) can be prepared from water-in-oil emulsions of phospholipids and buffer in an excess organic phase, followed by removal of the organic phase under reduced pressure (Szoka & Papahadjopoulos, 1978). Vesicles formed by this

technique, which are referred to as reverse-phase evaporation vesicles (REV), have a high aqueous space to lipid ratio and encapsulate a high percentage of the initial aqueous phase (20-68%). The phospholipids are dissolved first in organic solvents such as diethylether, isopropylether, or mixtures of organic solvents such as isopropylether and chloroform (1:1). The aqueous material is added directly to this phospholipid-solvent mixture. The preparation is then sonicated for a brief period to form a homogenous emulsion. The organic solvents are removed under reduced pressure, resulting in the formation of a viscous gel-like intermediate phase, which spontaneously forms a liposome dispersion when residual solvent is removed by continued rotary evaporation under reduced pressure. The size range of the resulting vesicles is sensitive to the percentage of cholesterol included in the lipid mixture. Vesicles composed from phospholipid mixtures lacking cholesterol have a size range of 0.08 to 0.24 $\mu\text{m}$ , compared to 0.16 to 0.9 $\mu\text{m}$  for cholesterol containing mixtures. The principal disadvantage of this method is the exposure of the material to be encapsulated to organic solvents and to short periods of sonication — conditions that may damage sensitive proteins and DNA. An alternative method of LUV production is detergent dialysis which depends upon the removal of detergents from phospholipid-detergent mixtures to form unilamellar vesicles (Szoka & Papahadjopoulos, 1980). Removal of all detergent residues is an important consideration which may limit the usefulness of this method particularly for large-scale pharmaceutical production (Talsma & Crommelin, 1992). However, it has been reported that toxic effects are not expected after systemic administration of liposomes prepared by bile salt removal due to physiologically compatible concentrations of bile salt residues (Lasch & Schubert, 1993).

Stable-plurilamellar vesicles (SPLV) are formed by first depositing a thin film of phospholipids from chloroform on a round-bottomed flask by rotary evaporation under reduced pressure. The lipid film is then dissolved in ethylether. The aqueous phase is then added to the ether-lipid solution and the two phase mixture emulsified in a bath sonicator (at a temperature higher than the  $T_m$  of the phospholipid with the highest melting point) during which time a gentle stream of nitrogen is passed over the mixture to evaporate the ether. The resulting cake is resuspended with buffer and washed and pelleted as for MLV. Although

SPLV appear similar to MLV in the electron microscope, the two types of vesicle differ as determined by stability, entrapment efficiency, electron spin resonance, NMR and X-ray diffraction techniques (Gruner *et al.*, 1985). The two types of vesicle possess similar gross physical structures but the intravesicular distribution of solute differs. SPLV have solute distributed evenly throughout the different compartments while MLV have solutes unevenly distributed with the outer compartments being solute depleted. The even distribution of solutes in SPLV results in higher entrapment percentages (typically 30%) than obtainable with MLV (New, 1990).

The dehydration-rehydration vesicle (DRV) method is capable of encapsulating a wide variety of materials, with high efficiency and using mild conditions, into liposomes of variable lipid composition. The procedure, based on the use of dehydration and controlled rehydration to induce fusion of preformed liposomes, is simple to use and importantly, from a pharmaceutical point of view, scaling up is straightforward. Briefly, MLV are formed by suspending a lipid film and then sonicating the resulting suspension to clarity to form SUV. The SUV are frozen after mixing with an equal volume of an aqueous drug solution. The preparation is then freeze-dried and the lyophilised plug rehydrated in a controlled manner (*i.e.* initially using minimal quantities of water). In this method all of the lipid can be brought into contact with all of the solute in the anhydrous state. Reduced hydrophobic forces during dehydration will result in loss of vesicle stability and fusion may then occur, with the formation of larger vesicles during rehydration. The high entrapment efficiency obtained with DRV is a result of lipids being dried down in a highly organised state (SUV) which, on addition of buffer, readily reform. As intimate contact between solute and phospholipids is achieved during the freeze-drying stage, a small volume of water can successfully rehydrate large lipid concentrations with a high solute entrapment (New, 1990). DRV are mainly oligo- and multilamellar and tend to be heterogenous in size. If necessary, DRV can be converted to a more homogenous preparation of defined size-frequency distribution by extrusion through polycarbonate membrane filters. The simplicity of the DRV method makes it particularly suitable to scaling up to commercial scales. It is possible to interrupt the process after the

dehydration stage, in which form, with appropriate precautions, it may be possible to store the material for long periods (Kirby & Gregoriadis, 1984). Vesicles produced by the DRV method range have a predominantly sub-micron size distribution. If required, downsizing of vesicles can be efficiently performed using microfluidization (Gregoriadis & Florence, 1993a).

Currently, the most direct methods for producing liposomes are based on high pressure homogenization (Talsma & Crommelin, 1992). Vesicles produced by this method have a narrow size distribution (typically from 30nm to 200nm) and may be formed in one step. The method is suitable for scaling up to larger batch sizes but suffers from poor entrapment volumes (Brandl *et al.*, 1993).

Recent developments in liposome production technology include the 'bubble method' in which liposomes are prepared under mild shear conditions in the absence of detergents or organic solvents (Talsma *et al.*, 1994). Interdigitation-fusion vesicles (IFV) are formed from an interdigitation-induced fusion of SUVs. High concentrations of ethanol were used to cause interdigitation of MLVs comprised of saturated chain lipids such as dipalmitoylphosphatidylcholine and distearoylphosphatidylcholine (Perkins *et al.*, 1993). The unique fusion process results in vesicles with an extremely high capture volume (see table 1.1). The large captured volume of IFVs makes them ideally suited as carriers of water soluble drugs requiring high drug/lipid ratios. *In vivo* testing of these vesicles has been performed using encapsulated iodinated contrast agents (Janoff *et al.*, 1991).

An important consideration in liposome production is the need to achieve high entrapment efficiencies. One of the most successful approaches to this problem has been the development of pH-gradient/remote loading methods. This technique relies on the ability of liposomes to sequester certain classes of drug molecules (anionic and cationic amphiphiles) in response to a transmembrane ion gradient. Weak acids and bases can be loaded into preformed liposomes by the application of ionic gradients across the liposome bilayer (Hope *et al.*, 1993). This

results in high entrapment efficiencies and drug/lipid ratios that are independent of the phospholipid composition used. The success of this method is highlighted by the entrapment of doxorubicin in concentrations which exceed its aqueous solubility and results in the formation of drug gel phases in the liposome interior (Lasic *et al.*, 1992).

In summary, a wide range of production methods have been developed since the initial description of liposomes formed after simple lipid hydration. Vesicles can now be prepared with a defined size range, high entrapment efficiencies and pharmaceutically acceptable stability profiles. The characteristics of vesicles produced by a number of methods is shown in table 1.1. The success of these production methods is an important step in the development of liposomes for clinical use.

Liposome Type	Description	Size distribution ( $\mu\text{m}$ )	Captured volume ( $\mu\text{l}/\mu\text{mol}$ )
MLV	Rehydration of dried film	1-10	0.5-2.3
SUV	Extensive sonication	Heterogenous 0.02-0.03	0.3
	French Press	0.03-0.06	0.3
	Microfluidizer	0.03-0.05	0.7-1.0
Detergent dialysis vesicles	Removal of octylglucoside/ deoxycholate <i>via</i> dialysis	0.23-0.5	3-8
REV	Reverse phase evaporation	0.1-1.0	8-16
Ethanol injection vesicles	Lipid in ethanol injected into buffer	~0.03	0.5
DRV	Dehydration-rehydration of SUV	0.1-0.5	1-4
LUVET	Egg PC MLV passed through a: 50nm filter 100nm filter 400nm filter	0.06	0.9
		0.1	0.9
		0.2-0.3	1.2
	Egg PC FATMLV passed through a: 50nm filter 100nm filter 400nm filter	as above	1
			1.5
			3.5
FATMLV	Egg PC frozen-thawed five times	1-5 Heterogenous	5-7
SPLV	Plurilamellar vesicles with wide interbilayer spacing	0.1-0.3	3-4
IFV	DPPC SUV, 3M ethanol added and removed	0.5-5	15-25
	DSPC SUV, 3M ethanol added and removed		14-23
Bubble method	Hydrogenated soy PC:DCP (10:1)	0.2-0.5	2-3

Table 1.1. Summary of capture volumes and size distributions of liposomes made by various methods  
(adapted from Perkins *et al.*, 1993)

### 1.3.5. Factors affecting the behaviour of liposomes *in vivo*

Many applications of liposomes as drug carriers have utilised the intravenous (i.v.) route of administration. The relatively large size of liposomes prevents their passage from the circulation to tissues, except where capillaries are lined with discontinuous endothelium (*i.e.* liver, spleen, and to a lesser extent the bone marrow and lymphoid organs) (Karlowsky & Zhanel, 1992). However capillary integrity may be compromised at inflamed sites and liposomes may leave the circulation and accumulate in these areas (Bakker-Woudenberg *et al.*, 1993). Extravasation of liposomes may also occur at certain tumour sites due to an increased permeability of the tumour vasculature (Allen, 1994a). The extent of uptake by these tissues is determined by the stability of liposomes in the circulation. Immediately upon injection into the blood compartment liposomes encounter high concentrations of plasma proteins which are responsible for the destabilising effects of serum (Gregoriadis, 1988). These effects are mediated by several groups of plasma proteins. Surface adsorbed opsonins promote endocytosis by the mononuclear phagocyte system (MPS; formerly known as the reticuloendothelial system or RES) and circulating monocytes. Uptake is prevalent in the Kupffer cells of the liver and macrophages of the spleen. High density lipoproteins (HDL) cause vesicle disintegration through the removal of phospholipids from the bilayer resulting in the release of encapsulated solutes (Gregoriadis & Florence, 1993b). Other plasma components including albumin, immunoglobulins, complement, fibronectin and clotting factors can interact with the bilayer surface and exert destabilising or opsonic effects (Bonté & Juliano, 1986). It is possible to influence the *in vivo* behaviour of liposomes by varying phospholipid composition and physical properties. Parameters affecting the blood clearance rate and tissue distribution include size, composition, dose and surface characteristics (charge, hydrophobicity and targeting ligands) (Senior, 1987).

Early studies on liposomal systems indicated the importance of vesicle size on clearance rates from the circulation (Gregoriadis & Allison, 1974; Juliano & Stamp, 1975). It was commonly observed that small unilamellar vesicles were cleared less rapidly than large multilamellar

vesicles. A clear relationship between vesicle diameter and circulation half-life was established by Senior *et al.* (1985). Vesicles of identical composition were produced to have diameters of 30-50nm (SUV), 0.2 $\mu$ m (REV) and 0.4 $\mu$ m (REV). The half-lives ranged from 0.2 hours (0.4 $\mu$ m REV), to 1.5 hours (0.2 $\mu$ m REV) with SUV demonstrating a half-life of 7.5 hours. SUV with diameters less than 100nm are able to extravasate through the fenestrations of liver sinusoids and interact with liver parenchymal cells, possibly through endocytosis. This may be the mechanism by which SUV partially avoid the efficient degradative mechanisms of Kupffer cells. Larger vesicles are taken up only by Kupffer cells and are degraded three times faster than SUV (Bakker-Woudenberg *et al.*, 1993). Biodistribution of liposomes may be directed towards the lung by utilising the physical trapping of large liposomes (>1 $\mu$ m) in capillary beds (Abra *et al.*, 1984).

The phospholipid composition of liposomes determines the fluidity of the bilayer which in turn affects the interaction with serum components. Relatively loosely packed bilayers composed of egg phosphatidylcholine can be rigidified with the incorporation of cholesterol in 33-50% molar ratios. Alternatively phospholipids with long chain saturated fatty acids (*e.g.* DSPC), with a  $T_m$  above 37°C, can be chosen to form vesicles with stable gel-state bilayers. Both strategies result in a decreased interaction with HDL and the leakage of entrapped solutes is much reduced (Gregoriadis & Florence, 1993b). In general the most stable vesicle composition is that which contains phospholipids with a high transition temperature and have a high molar ratio of cholesterol. A number of alternative approaches to promote vesicle stability have been developed. Novel phospholipid analogues containing polymerizable groups in their fatty acid chains exhibit increased mechanical stability and increased resistance to leakage (Bonté *et al.*, 1987). Fluorinated phospholipid-based liposomes have greater membrane stability and display increased circulation times than conventional phospholipid liposomes (Frezard *et al.*, 1994).

The inclusion of charged amphiphiles within the liposome bilayer changes the affinity of the surface for serum proteins. This is reflected in the clearance rates of charged vesicles (Ostro



& Cullis, 1989). Negatively charged liposomes exhibit shorter circulation times than neutral and positively charged liposomes of similar size (Juliano & Stamp, 1975). On contact with serum, neutral and positively charged liposomes acquire a net negative charge through the adsorption of plasma components, principally  $\alpha_2$ -macroglobulin, a recognized phagocytosis factor. Negatively charged liposomes retain the same charge in the presence of serum (Senior, 1987). Surface negative charges are thought to function as binding sites for blood opsonins and they may also be involved in direct binding to macrophages (Allen & Paphadjopoulos, 1993). The liver uptake of negatively charged vesicles is particularly rapid. Other biodistribution variations include a greater accumulation of positively or negatively charged vesicles in the lungs than neutral liposomes of a similar size. Greatest uptake of negatively charged liposomes was seen when phosphatidylserine (PS) was used as the charged amphiphile. The use of stearylamine in positively charged liposomes is limited by its *in vivo* toxicity (Sato & Sunamoto, 1992).

Widely varying half-lives of liposome preparations were described by various groups during the initial phase of liposome research. This was due to the use of liposomes, albeit with similar composition, but which exhibited heterogeneity in vesicle size and were administered in different doses (Gregoriadis, 1988). The clearance of liposomes is a dose-dependent phenomenon. The half-life of a 100nm PC:CHOL preparation increased from 20 minutes to 3 hours when the lipid dose was increased from 0.4 to 40mg/kg (Ostro & Cullis, 1989). This effect is related to the saturation of the MPS at higher doses (Senior, 1987). Oja *et al.* (1994) have suggested that there is a limited population of blood proteins which can associate with liposomes of a given composition. As a consequence higher doses have lower protein binding values and longer circulation times.

It has been proposed that opsonisation may increase the hydrophobicity of the liposomal surface and promote uptake by the MPS. The importance of surface hydrophilicity was first illustrated by the reduced uptake of hydrophilic coated colloidal particles by liver and peritoneal macrophages (Illum *et al.*, 1986). This approach has now been extended to

liposomes with increased hydrophilicity postulated to reduce opsonisation of liposomes plasma proteins. A liposome surface can be rendered hydrophilic by the inclusion of a so-called 'Stealth<sup>®</sup>' (trademark of Liposome Technology Incorporated, USA) lipids. Such lipids include ganglioside GM<sub>1</sub>, hydrogenated phosphatidylinositol, and the synthetic derivative polyethylene-glycol-distearoylphosphatidylethanolamine (PEG-DSPE). These lipids share the common property of a negatively-charged headgroup which is sterically shielded by the presence of bulky groups. The incorporation of 5-10% molar quantity of PEG-DSPE (PEG 1900 derivative) prolongs the circulation half-life of small 100nm liposomes and is independent of bilayer fluidity and dose effects. Other stealth-like compounds include polyglycerol phospholipid derivatives which also exhibit prolonged circulation times (Maruyama *et al.*, 1994) and polysialic acids which may have applications in this area (Gregoriadis *et al.*, 1993). Stealth or sterically stabilised liposomes appear to have overcome the long-standing problem of MPS uptake and have opened up new clinical applications particularly in the treatment of extracellular infections and tumour targeting (Allen, 1994b; Woodle, 1993; Woodle & Lasic, 1992).

The surface modification of liposomes with ligands such as saccharides, glycoproteins, glycolipids, lectins and antibodies, has been studied as a means of producing tissue/cell specific or vectorised liposomes (Jones, 1994; Sato & Sunamoto, 1992). The majority of studies have not translated *in vitro* success to *in vivo* activity as the recognition of ligands by the MPS tissues leads to the rapid removal of vectorised liposomes before they can reach their target tissues. The development of long-circulating liposomes has allowed the potential therapeutic applications of vectorised liposomes to be explored. Ligand attachment methods which optimise antibody/polymer ratios have resulted in liposomes which possess acceptable pharmacokinetic and cell binding properties (Allen, 1994a). The recent modification of the PEG-DSPE conjugate to produce a cationic derivative may facilitate the attachment of small ligands to the terminal of the PEG polymer (Zalipsky *et al.*, 1994).

### 1.3.6. Clinical applications of liposomes as drug carriers

The ability of liposomes to contain, transport and release therapeutic agents has led to a remarkable array of clinical applications. The commercial application of this technology has been accelerated by the setting up of several dedicated, USA based, liposome companies (Vestar, The Liposome Company, and Liposome Technology Incorporated). The simplest use of liposomes is as a non-toxic carrier for insoluble drugs (Lidgate *et al.*, 1988). More sophisticated applications include the use of liposomes as prolonged release reservoirs, or for localisation of drug within the body to avoid or target specific tissues or subcellular sites (Fielding, 1991). Passive targeting of liposomes to cells of the MPS exploits their rapid uptake by such tissues after i.v. administration. Liposomes have been used target drugs to activate macrophages against tumoricidal cells. One of the most successful examples of this application has been the development of liposomal MTP-PE (muramyl tripeptide phosphatidylethanolamine), the lipophilic analogue of MDP (muramyl dipeptide), the minimal subunit of the cell wall of Mycobacteria with immune-potentiating activity. The systemic administration of liposomes containing MTP-PE has been shown to eradicate spontaneous metastases in several animal tumour models. The enhanced efficacy and reduced adverse effects of liposomal MTP-PE compared with free drug were attributed to site-specific delivery of the immunomodulator directly to macrophages (Gay *et al.*, 1993; Sone, 1989). The use of non-MPS directed stealth liposomes as a controlled delivery system for the cytokine interleukin-2 also demonstrated improved immunomodulatory and antitumour activity *in vivo* (Kedar *et al.*, 1994). Passively targeted liposomes have been used to treat intracellular infections of the MPS. The most advanced example of this class is the first commercial liposome formulation, Ambisome<sup>®</sup>, (Vestar Inc., USA). This liposomal formulation of amphotericin has reduced systemic toxicity and has proved extremely successful in the treatment of refractory fungal infections of the MPS (de Marie *et al.*, 1994). This product has now to compete against two other lipid based products; ABLC<sup>®</sup> (amphotericin B lipid complex. The Liposome Company, USA) and ABCD<sup>®</sup> (amphotericin

B colloid dispersion, or Amphocil<sup>®</sup>, Liposome Technology Incorporated, USA). Further studies of liposomal antimicrobials are discussed in section 1.3.7.

One of the main applications of liposomes in clinical therapeutics is in the treatment of neoplastic disorders. Of the many cytotoxic agents encapsulated in liposomes, the drug which has been the subject of the most intensive investigation is doxorubicin. Doxorubicin has activity against solid tumours and leukaemias but is limited by adverse effects, particularly chronic cumulative cardiotoxicity. Liposomal encapsulation of doxorubicin changes the observed pharmacokinetics and biodistribution. Liposomal doxorubicin is well tolerated with a reduced incidence of side-effects compared to free drug, whilst antitumour activity is retained. Encapsulation of doxorubicin in stealth liposomes as opposed to conventional formulations has increased the efficacy of this treatment in a number of animal carcinoma models. Clinical applications include the use of stealth doxorubicin in the treatment of human Kaposi's sarcoma and other solid tumours (Allen, 1994a). Studies with liposomal formulations of daunomycin demonstrated increased delivery to an *in vivo* tumour site (Forssen, 1988). The use of liposomes as carriers of insoluble drugs is highlighted with the development of liposomal NDDP (neodecanoate diaminocyclohexane platinum), an analogue of cisplatin insoluble in biocompatible excipients. Animal studies have demonstrated that liposomal NDDP does not possess the nephrotoxicity associated with cisplatin and is active against cisplatin resistant tumours (Perez-Soler *et al.*, 1988). Despite evidence of accumulation and enhanced extravasation of liposomes at tumour sites, the greatest advantage of liposomal encapsulation of cytotoxic agents is the reduction in side-effects commonly observed with such therapy (Gregoriadis & Florence, 1993b). Current developments in stealth technology and ligand/antibody attachment may lead to increased targeting to specific tumour sites or the eradication of migrating micro-metastases (Allen, 1994a).

The development of synthetic small peptide and subunit vaccines, which are usually only weakly immunogenic, has highlighted the need for improved adjuvants. Liposomes appear to

be a safe and versatile adjuvant capable of augmenting the immune response to a wide variety of antigens including bacterial, viral and protozoal antigens (Buiting *et al.*, 1992; Gregoriadis, 1990). The mechanisms of liposome adjuvanticity are not fully understood although the uptake of liposomes by antigen presenting cells and the spatial arrangement of antigen and lipid bilayer may play a role in the increased immune response commonly observed.

Liposomes have been proposed as carriers of enzymes for enzyme replacement and enzyme therapy. Liposomal encapsulation enhanced the *in vivo* retention of tyrosine phenol-lyase in plasma, a compound used in the treatment of malignant melanomas (Meadows & Pierson, 1988). Liposomes have also been used to mask the toxicity of L-asparaginase and protect the enzyme from circulating antibodies (Gregoriadis & Allison, 1974). Liposomal enzymes have been used to treat storage diseases notably liposomal  $\alpha$ -glucosidase for Pompe's disease and  $\beta$ -glucosidase for Gaucher's disease (Belchetz *et al.*, 1977).

Liposomes loaded with contrast agents have been used for tumour effective imaging. This is appropriate for the visualisation of liver and spleen sites and a number of studies have shown enhanced imaging with liposomal formulations (Karlik *et al.*, 1991; Schwendener *et al.*, 1990; Seltzer *et al.*, 1988). The increased accumulation of liposomes in tumours and inflammatory sites may allow more effective imaging of these lesions. Long-circulating immunoliposomes carrying a heavy metal based imaging agent were modified with a monoclonal antibody capable of specific accumulation in myocardial infarct areas, with a resultant increase in imaging efficiency observed when used in a rabbit infarct model. Similar liposomes modified with dextrans showed better lymph node accumulation, an effect attributed to increased receptor mediated endocytosis (Torchilin *et al.*, 1994).

The challenge of introducing highly polar genetic material to the cell interior has necessitated the use of vector systems. DNA-polymer conjugates and viral vectors are the subject of ongoing studies. However cationic liposomes have been shown to be a successful means of

achieving some of the goals of gene therapy (Afione *et al.*, 1995). The use of a liposome vector in the phase I UK trial of CF gene therapy indicates the potential applications of this new technology (Caplen *et al.*, 1995). The efficiency of liposomal vectors needs to be improved and the systemic administration of cationic liposomes, used to complex polynucleotides, is problematic due to their instability in physiological saline. Recent developments in stealth lipid chemistry have seen the synthesis of amino functionalised PEG which endows the liposome surface with a cationic charge, yet retains a biodistribution profile similar to non-derivatised PEG containing vesicles (Zalipsky *et al.*, 1994).

The topical administration of liposomal drugs has been studied as a means of prolonging the retention of drugs in the applied area and reducing systemic absorption of the active compound. This property of liposomes has been exploited for the delivery of moisturising agents to the skin by cosmetic firms and whilst these products are not of clinical relevance they demonstrate the therapeutic concept of liposome formulations and the feasibility of large scale liposome production (Gregoriadis, 1994). Liposome formulations of triamcinolone showed increased accumulation in the dermis and epidermis with reduced systemic absorption compared to free drug. Clinical investigation of liposomal progesterone illustrated the efficacy of this formulation in idiopathic hirsutism. Sustained release of methotrexate into the epidermis may be achieved with liposomal formulations (Mezei, 1988). Current research with ultraflexible liposome-like carriers (Transferosomes<sup>®</sup>) has shown that these vesicles can penetrate and transport material through the permeability barriers of the skin. However, the efficiency and mechanism of transferosomes remains controversial (Cevc, 1993c).

The ocular administration of liposomal formulations is a means of prolonging the ocular retention of therapeutic agents. Liposomal fluorouracil produced significantly higher concentrations of drug in the vitreous humor after intravitreal injection in rabbits and to a lesser extent after sub-conjunctival injection when compared to free drug (Fishman *et al.*, 1989). The encapsulation of antimicrobial agents should offer improved therapy in the treatment of ocular infections. The administration of tobramycin in MLV, as a single

subconjunctival injection, was significantly more effective than the single administration administration of free drug and almost as effective as 24 doses of hourly topical drug in a model of pseudomonal keratitis (Assil *et al.*, 1991). However the advantages of liposomal encapsulation for delivery to the ocular surface is less clear with a number of studies showing little or no therapeutic benefit compared to free drug (Gregoriadis & Florence, 1993b).

### 1.3.7. Liposomes as carriers of antimicrobial agents

The biological and pharmacological attributes of liposomes have been exploited by several researchers for the delivery of antimicrobial agents as shown in table 1.2. The usefulness of liposomes in this area was first demonstrated in the treatment of leishmaniasis in mice with liposome-encapsulated antimonial drugs. Alving *et al.* (1978 & 1980) showed that liposome-encapsulated drugs were far superior to free drugs against this parasite. Leishmanias are intracellular parasites of phagocytic cells of the reticuloendothelial system (RES) and therefore offer a natural target for liposomal delivery due to the high uptake of liposomes by cells of the RES after intravenous administration. Similar results were found with primaquine in experimental malaria (Pirson *et al.*, 1980). Most antimicrobial drugs are relatively ineffective against intracellular infections due to poor penetration inside the cells or decreased activity intracellularly. Therefore liposomal encapsulation affords an excellent means of increasing therapeutic efficacy and reducing toxicity of antimicrobials for use in the treatment of intracellular pathogens. *Mycobacterium avium intracellulare* (MAI) complex infections typify the problems associated in the therapy of intracellular infections and are frequently present in patients with acquired immunodeficiency syndrome (AIDS). Numerous *in vitro* and *in vivo* studies have demonstrated the advantages of liposomal encapsulation of the agents commonly used in the treatment of this infection. *In vitro* studies of the activity of rifapentine and amikacin showed increased killing of MAI complex in human macrophages (Bermudez *et al.*, 1987). *In vivo* studies with liposomal streptomycin in mice infected with *Mycobacterium tuberculosis* led to prolonged survival and a significant inhibition in bacterial

growth in the spleen (Vladimirsky & Ladigina, 1982). Liposomal streptomycin also gave a several-fold increase in therapeutic efficacy in experimental MAI complex infections in beige mice (Gangadharam *et al.*, 1991). Rifampin-loaded liposomes containing the macrophage activator, tuftsin, showed increased antitubercular activity in mice (Agarwal *et al.*, 1994). Liposomal amikacin was found to be 100 times more efficacious against MAI than an equivalent concentration of free amikacin (Wichert *et al.*, 1992). A liposomal amikacin formulation, currently in development by Vestar Inc., was more effective in delivering amikacin to affected tissues than free drug and was more efficacious in clearing MAI complex from the liver and spleen of infected mice (Proffitt *et al.*, 1993). Liposomal kanamycin has also shown enhanced activity against MAI complex (Tomioka *et al.*, 1991). This approach has now been applied in the clinic with liposome encapsulated gentamicin showing beneficial effects in a phase I/II study for the treatment of MAI complex bacteraemia in AIDS patients (Nightingale *et al.*, 1993). Similarly successful results against other intracellular pathogens have been obtained with liposomal sisomicin for the treatment of *Legionella pneumophila* in guinea pigs (Sunamoto *et al.*, 1984), liposomal cephalothin in *Salmonella typhimurium* infected mice (Desiderio & Campbell, 1983) and liposomal ampicillin in *Listeria monocytogenes* infected mice (Bakker-Woudenberg *et al.*, 1985). Clearly the treatment of intracellular bacterial infections, is one of the solid indications for the use of liposomal formulations.



Antibiotic	Bacteria	Animal model	Reference
Amikacin	<i>Mycobacterium avium</i> <i>Mycobacterium intracellulare</i>	Beige mice	Duzgunes <i>et al.</i> , 1988
Streptomycin Oxytetracycline	<i>Brucella abortus</i>	Pig	Milward <i>et al.</i> , 1984
Ampicillin	<i>Listeria monocytogenes</i>	Normal mice	Bakker-Woudenberg <i>et al.</i> , 1985
Cephalothin	<i>Salmonella typhimurium</i>	ICR mice	Desiderio & Campbell, 1983
Streptomycin	<i>Salmonella enteridis</i>	Black mice	Tadakuma <i>et al.</i> , 1985
Sisomicin	<i>Legionella pneumophila</i>	Guinea pig	Sunamoto <i>et al.</i> , 1983
Gentamicin Kanamycin Dihydrostreptomycin Streptomycin	<i>Brucella canis</i>	Swiss mice	Fountain <i>et al.</i> , 1985
Kanamycin	<i>Mycobacterium avium intracellulare</i>	Balb/c mice	Tomioka <i>et al.</i> , 1991
Rifampin	<i>Mycobacterium tuberculosis</i>	Normal mice	Agarwal <i>et al.</i> , 1994
Cefoxitin	Intrabdominal sepsis	Rats	Kresta & Shek, (1994)

Table 1.2. - Review of the studies using liposomes with encapsulated antibiotics for the treatment of experimental infections *in vivo*

Liposomes may also be of use for the delivery of antimicrobial agents to the extracellular sites of infection. This objective is hampered by the removal of circulating liposomes by the MPS tissues of the liver, spleen, lungs and bone-marrow. However circulating phagocytic cells have been shown to phagocytose liposomes and may serve as a transport system for antibiotic-loaded liposomes to infection sites (Bakker-Woudenberg & Lokerse, 1991). Liposomes may be targeted to the lungs by manipulation of vesicle size. In a study by Debs *et al.* (1987), pentamidine levels in the lung were found to be 34 times greater when the liposomal dosage form was given by intravenous injection compared to an equivalent dose of free drug. However, reduction of liposome diameter greatly reduced lung uptake. Surface

modification with palmitoylopectin results in greater levels of drug being recovered in the lungs (Sunamoto *et al.*, 1984). Liposomal gentamicin has been tested in the treatment of *Klebsiella pneumoniae* and thigh infections, both extravascular sites (Ginsberg *et al.*, 1989). The liposomal treatment had enhanced efficacy in both cases, although the reason for this is not clear. The pharmacokinetics of gentamicin are radically altered after encapsulation and the difference in pharmacokinetic profile may benefit the treatment of extracellular infections (Ginsberg *et al.*, 1989). There has been an increasing awareness of the importance of pharmacokinetic and pharmacodynamic parameters in the successful therapy of extracellular bacterial infections (Drusano, 1988). The altered pharmacokinetic profile (increased  $t_{1/2}$  and AUC; decreased  $V_d$  and  $C_{pmax}$ ) shifts drug accumulation from the kidney to other organs, potentially reducing nephrotoxicity. However, there is insufficient data to support a reduction in ototoxicity for liposomal aminoglycosides. Although the use of liposomal aminoglycosides in the treatment of extracellular infections is based on limited *in vitro* and *in vivo* data, it appears reasonable that a reduction in nephrotoxicity is the very least that may be achieved. Speculation that sustained release will promote antimicrobial resistance is so far unsupported by *in vivo* data (Karlowsky & Zhanel, 1992). Liposomal encapsulation of antibiotics has been reported to potentiate activity against normally resistant strains. Naccucchio *et al.* (1988) showed increased efficacy of piperacillin and gentamicin when encapsulated against *P. aeruginosa* and *E. coli* strains normally resistant to these antibiotics. In a similar set of *in vitro* experiments, Lagacé *et al.* (1991) reported ticarcillin and tobramycin resistant strains of *P. aeruginosa* to have a markedly increased sensitivity to antibiotics enclosed in liposomes. Alpar *et al.* (1992) showed that sub-MIC concentrations of encapsulated tobramycin gave greater growth inhibition of *P. aeruginosa* compared to free drug, although the effect was less at higher concentrations. The increased activity was attributed to an increase in outer membrane permeability although the exact mechanism remains unknown. Jones & Osborn (1977) demonstrated that phospholipids can be transferred from vesicles to intact bacterial cells. Fusion of liposomes and bacteria may be a mechanism through which liposomes could specifically deliver their entrapped drug into target cells. The liposome may also afford protection from exogenous enzymes such as  $\beta$ -lactamase (Naccucchio *et al.*, 1985).

Encapsulated drug may also be released at a site of high bacterial density through the action of bacterial derived phospholipases, resulting in disruption of the bilayer structure. A new development in the treatment of extracellular infections with liposomal antimicrobials has been achieved through the application of stealth technology. Bakker-Woudenberg *et al* (1992) originally reported enhanced localisation of liposomes, containing the stealth lipid hydrogenated phosphatidylinositol, in *Klebsiella pneumonia* infected lung tissue in rats. This success was repeated with vesicles containing PEG-DSPE<sub>1900</sub> with the extent of localisation dependent upon lipid dose and intensity of infection. Up to 9% of the administered dose reached the lungs of severely infected animals (Bakker-Woudenberg *et al.*, 1993). A therapeutic effect, in the same animal model, was seen with a single dose of encapsulated gentamicin proving more efficacious than multi-dose treatment with free drug (Bakker-Woudenberg, 1995). This clearly has implications for the treatment of CF lung infections by systemic therapy, as the CF lung is chronically inflamed and therefore would represent an ideal target for liposomes with stealth properties.

In summary, liposomal encapsulation of antimicrobials offers targeting to specific cellular and subcellular sites, sustained release of drug, lower toxicity and an altered pharmacokinetic profile with enhanced therapeutic efficacy.

### 1.3.8. Aerosolisation of liposomal drug delivery systems

Local delivery to the lung may be achieved by inhalation of liposome aerosols. Inhalation of antibiotics is part of the management of CF lung infections and this would be the preferred first-line route of administration of a liposomal polymyxin formulation. The rationale for such a formulation has been discussed in section 1.2.7. The physical characteristics of liposomes during aerosolisation by jet nebulisers, have been extensively investigated. Drug retention is greatly dependent on formulation with liposomes composed of rigid bilayer forming lipids retaining more aqueous phase marker than those composed of unsaturated lipids. Drug

retention is also affected by the size of liposomes nebulised. Small extruded (0.2 $\mu$ m) vesicles lost ten-fold less marker than unextruded MLV. This is a result of liposomal downsizing occurring in response to air-flow pressure generated shear pressures within the nebulising chamber. Extent of drug loss increased when air-pressure was increased. Cholesterol (in a 30% molar ratio) reduced aqueous entrapped solute loss (Niven & Schreier, 1990). Maintenance of bilayer integrity during nebulisation may be less important if a bilayer associated hydrophobic drug is to be delivered to the lung (Taylor & Farr, 1993). The solubilising property of liposomes has been used to generate aerosols of insoluble drugs such as cyclosporin and beclomethasone (Waldrep *et al.*, 1994). Other approaches currently in development for liposome delivery to the lung include pressurised aerosol (MDI-like) formulations and dry powder type inhalers loaded with lyophilised vesicles which are reconstituted in situ on contact with the lung mucosal surface (Schreier *et al.*, 1994b). However both approaches may be limited by the quantity of drug which can be delivered in an acceptable number of doses (Taylor & Farr, 1993).

Once delivered to the lung, liposomes are cleared mainly through uptake by pulmonary alveolar macrophages. Processing and recycling of liposomal phospholipid in the surfactant phospholipid pool is performed by alveolar type II cells. Liposomes may also be cleared in the bronchial regions by the mucociliary escalator (Schreier *et al.*, 1993). Bronchoalveolar lavage fluid has been shown to destabilize liposomes and the interaction with bronchoalveolar protein components, similar to those in serum, may determine the pattern of liposomal drug release (Jurima-Romet *et al.*, 1992).

Liposomes seem particularly appropriate carriers for the delivery of drugs to the lungs as they can be prepared from materials endogenous to the lung as components of lung surfactant. Lung surfactant is a complex mixture, of which about 85% is phospholipid, mostly dipalmitoylphosphatidylcholine, with phosphatidylglycerol as the next most prevalent phospholipid (Taylor & Newton, 1992). The compositional similarity endows liposomes with a good toxicological profile in the lung. The *in vitro* toxicity of liposomes was investigated

by monitoring functional and morphological changes of rat alveolar macrophages. It was found that *in vitro* exposure of alveolar macrophages to large concentrations of liposomes did not result in any functional, morphological or toxicological changes (Gonzalez-Rothi *et al.*, 1991). The *in vitro* findings were validated in an *in vivo* study which showed that alveolar macrophage function and ultrastructure were unaffected. No lung histologic changes were observed and no adverse effects on the general health of the animals were noticed (Myers *et al.*, 1993). The pulmonary delivery of amikacin loaded liposomes in sheep found that liposomes were innocuous and non-irritating to the lung (Schreier *et al.*, 1992). A study of the acute effects of liposome inhalation by healthy volunteers indicated that small soya phosphatidylcholine liposomes were well tolerated, with no apparent changes in pulmonary function (Thomas *et al.*, 1991).

The intratracheal administration of a large number of liposomal compounds has demonstrated increased lung retention of the liposomal form over free drug (Meisner, 1993). Fielding & Abra (1992) have shown that by manipulation of liposome size, cholesterol content, and phospholipid composition, the half-life of liposome encapsulated terbutaline in the lungs after intratracheal instillation could be varied from 1.4 hours to 18 hours. Liposomal encapsulation of atropine resulted in higher sustained levels in the lung after intratracheal instillation compared with free drug (Meisner *et al.*, 1989). Absorption of drug into the systemic circulation was less when administered in encapsulation form. Prolonged retention of encapsulated glutathione was shown by Jurima-Romet *et al.* (1990). In a study by Taylor *et al.* (1989) in healthy volunteers, liposomal sodium cromoglycate produced peak plasma levels seven-fold less than free drug and gave sustained release over a 24 hour period. Antimicrobial agents which have been encapsulated and aerosolised include liposomal amphotericin B (Gilbert *et al.*, 1992), enviroxime for use in rhinovirus infections (Six *et al.*, 1989) and amikacin for *Mycobacterium avium-intracellulare* infection (Wichert *et al.*, 1992). The intratracheal instillation of liposomal tobramycin, in rats with a chronic pseudomonal infection model, showed increased lung residence times compared to free tobramycin, despite an increased lung permeability arising from infection derived

inflammation (Omri *et al.*, 1994). It is one of the main objectives of this project to produce a liposomal polymyxin formulation which may be administered as an aerosol to treat *P. aeruginosa* lung infections.

## Chapter 2

### Analytical methodology for liposomal polymyxin B

---

#### ABSTRACT

The analytical methods relevant to the development of liposomal polymyxin B are discussed. The range of assays included the bicinchoninic acid protein assay, a microbiological bioassay, HPLC and radiolabelling. In order to successfully determine the encapsulation efficiencies of liposomal preparations, it was necessary to measure both the intra and extraliposomal concentrations of polymyxin B. The above methods were evaluated and it was found that scintillation counting of tritiated polymyxin B allowed accurate, reproducible and convenient quantification of both non-entrapped and encapsulated drug.

---

## 2.0. Development of analytical methodology for polymyxin B

### 2.1. Introduction

Polymyxin B (PXB) was the model polymyxin chosen for the development of a liposomal formulation.. Although used less for aerosol delivery than colistin, or polymyxin E, its interaction with phospholipids has been extensively studied (Hartmann *et al.*, 1978). Polymyxin B differs from colistin by the substitution of phenylalanine in the heptapeptide ring in place of d-leucine (figure 1.2). The sulphate derivative of PXB was the preferred compound throughout the course of this study. In order to calculate encapsulation efficiencies accurately and reproducibly it was necessary to develop an analytical method that was applicable to the assay of liposomal formulations *i.e.*, unaffected by interference from phospholipids or agents used to lyse liposomes. The accurate quantitative determination of PXB entrapments is a prerequisite to further liposomal characterisation and testing. The suitability of several methods is discussed in the following sections.

### 2.2 Materials

#### 2.2.1 Polymyxin B

Polymyxin B sulphate was purchased from Sigma Chemical Company (Poole, UK). The activity was 7730 international units per milligram.

#### 2.2.2 Phospholipids

Phospholipids were purchased from Lipid Products, S.Nutfield, Surrey, UK. All phospholipids were stored in chloroform/methanol at -20°C.



### 2.2.3. Chemicals

All chemicals and reagents not specified in the text were supplied by BDH Chemicals Ltd. (Poole, UK), Sigma Chemical Company (Poole, UK) and Fisons (Loughborough, UK) and were of Analar grade or equivalent. Double distilled water was used in all experimental procedures unless otherwise specified.

### 2.2.4. General instrumentation

All pH measurements were undertaken using a Corning model 140 digital pH meter equipped with a Gallenkamp combination glass electrode, appropriately calibrated with buffer solutions of pH 4 and pH7 (BDH, Poole, Dorset). Sartorius three place and four place digital analytical balances were used for all weighing operations.

## 2.3. Methods

### 2.3.1. Bioassay for polymyxin B

This assay is a modification of the zone of inhibition bioassay described in the technical reference sheet supplied by Pharmax (Kent, UK). *Bordetella bronchiseptica* ATCC 4617 (PHLS Collingdale) was used as the test organism. Linearity was demonstrated over the test range (2-200 $\mu$ g/ml), with a correlation coefficient of >0.99. The minimum detection limit was 2 $\mu$ g/ml.

The inoculum was prepared by sloping 250ml of drug sensitivity testing agar (Oxoid) in a 500ml bottle. All procedures were carried out using aseptic technique. The surface of the slope was flooded with 7.5ml of a stationary phase nutrient broth culture of the test organism. After incubation at 37°C for 18hr, the resultant growth was washed off the slope using sterile 1:4 Ringer's solution. The resulting suspension was then centrifuged and resuspended in 100ml sterile Ringer's solution and adjusted to contain  $20 \times 10^8$  viable cells/ml *i.e.*, to an  $O.D_{470nm} \sim 2$ . This suspension is viable for four weeks if stored at 4°C.

To prepare the test medium, 150ml of drug sensitivity testing agar was autoclaved and cooled to 45-50°C. After equilibration at this temperature, 1.2ml of test organism suspension was added and the flask gently swirled to evenly distribute the inoculum. The seeded medium was then poured into a bioassay tray (243 x 243 x 18mm, Nunc, Denmark) and allowed to set on a level surface. Wells were created by removing plugs of agar with a no.6 (10mm) cork borer. Test sample or standard (100µl), in PBS (0.14M NaCl, 2.7mM KCl, 1.5mM KH<sub>2</sub>PO<sub>4</sub>, 8.1mM Na<sub>2</sub>HPO<sub>4</sub>) pH 7.4, was added to each well. The plate was then left at room temperature for 3hrs to allow diffusion of the drug solution into the agar prior to incubation. The plate was then incubated at 37°C overnight and the resulting zones of inhibition determined by placing the assay tray on an overhead projector and measuring the projected zones of inhibition. It was found that this increased the ease of use and accuracy of measurement. Figure 2.1 shows a typical calibration plot demonstrating linearity over the test range 2-200µg/ml of PXB. Figure 2.2 shows the appearance of a bioassay calibration tray after overnight incubation.

This method allowed quantification of polymyxin in supernatant washes of liposomes but difficulty was encountered when liposome preparations were lysed by Triton-X 100, in a final concentration of 1% (v/v). Potentiation of PXB activity was observed when co-incubated with this concentration of surfactant (table 2.1). A 1% (v/v) concentration is the minimum concentration of Triton-X 100 required to lyse liposome preparations. Indeed, for formulations containing high molar ratios of cholesterol, higher surfactant levels are required. Formulations comprising of saturated lipids such as distearoylphosphatidylcholine (DSPC) required methanol for successful lysis which is obviously incompatible with the bioassay technique. It was found that PBS pH 7.4 and 1% (v/v) Triton-X 100 in PBS pH 7.4 exhibited no antimicrobial activity. A 50µg/ml standard of PXB in PBS gave a zone diameter of 8.12±0.08cm. However the same standard in the presence of 1% (v/v) surfactant yielded a much larger zone of 9.3±0.09cm. This effect was not adequately accounted for by the inclusion of assay standards containing Triton-X 100. The increased activity is predictable given the surfactant activity of Triton-X 100. It may be that at the concentrations used, the

surfactant activity of Triton-X 100 permeabilises the bacterial outer membrane and potentiates the action of PXB. Agar diffusion of PXB may be changed in the presence of surfactant. Synergistic activity of Triton-X 100 and PXB limits the usefulness of the bioassay for direct determination of encapsulation from liposome lysates. The presence of phospholipids in these samples may further complicate analysis as lecithin is a component of broth used to inactivate PXB in MIC assays. Attempted analysis of liposomal contents gave varying results which conflicted with those determined from supernatant washes. Therefore liposome encapsulations determined by this method are calculated by mass balance of the drug recovered in the supernatant washes and the activity of the solution used to load the liposome preparations.

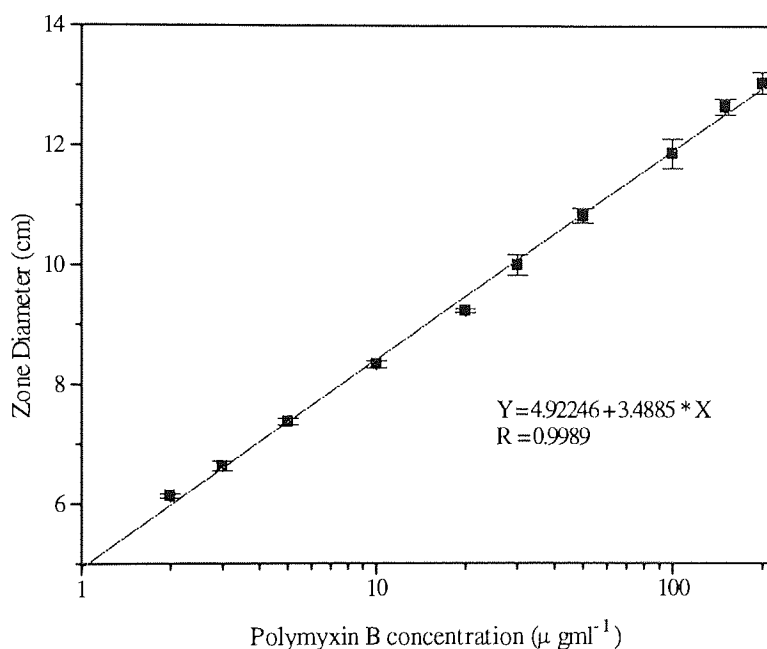


Figure 2.1. Calibration plot for bioassay demonstrating linearity over 2-200 $\mu\text{g/ml}$  (each point represents the mean  $\pm$  standard deviation of three replicates)

Test Sample	Zone Size (cm)
PBS pH 7.4	0
1% (v/v) Triton-X 100 in PBS pH 7.4	0
50 $\mu\text{g/ml}$ PXB in PBS pH 7.4	8.12 $\pm$ 0.08
50 $\mu\text{g/ml}$ PXB/1% Triton-X 100 in PBS pH 7.4	9.3 $\pm$ 0.09

Table 2.1. Potentiation of PXB bioassay activity by 1% Triton-X 100. Each zone of inhibition represents the mean $\pm$ sd of three samples.

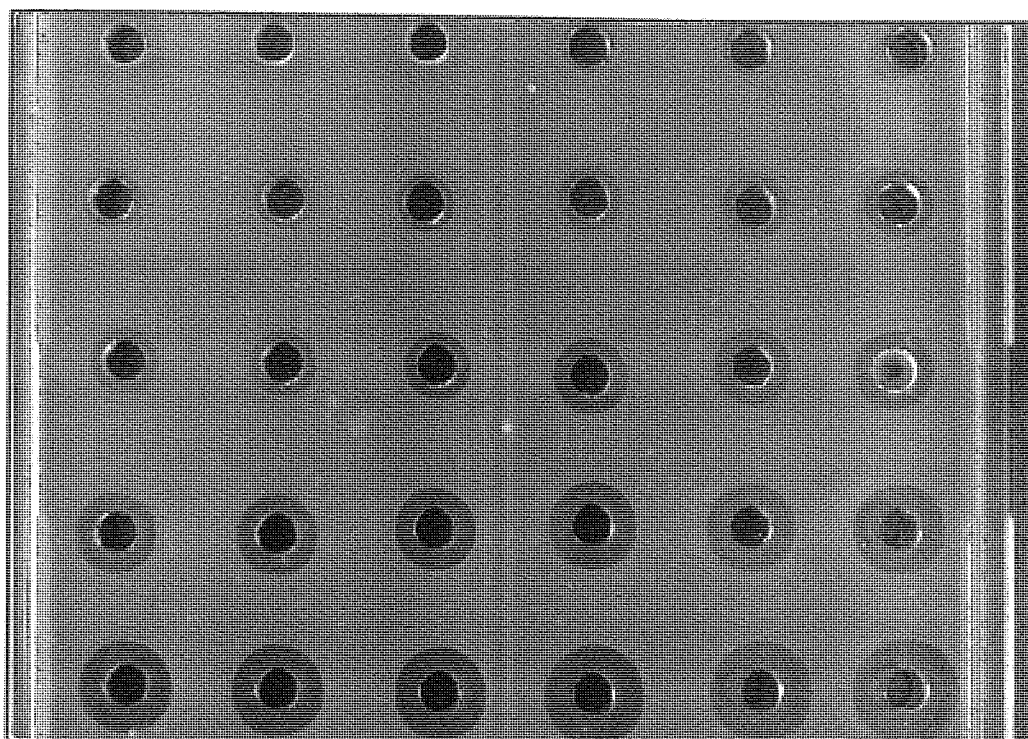


Figure 2.2. Appearance of a multiwell bioassay tray containing PXB calibration standards after 24 hr incubation at 37°C

### 2.3.2. Bicinchoninic acid protein assay

The amino acid composition of PXB lends it to assay by protein assay methodology. The bicinchoninic acid (BCA) assay is a sensitive and reproducible assay, particularly suitable for working with small sample volumes (Smith *et al.*, 1985). The BCA assay utilises the formation of a protein-copper complex, similar in principle, to the classic Lowry protein assay (Lowry *et al.*, 1951). Proteins, and PXB, react with copper (II) to produce copper (I). The 4, 4'-dicarboxy-2,2'-biquinolone (bicinchoninic acid, or BCA), the key component of this assay (Smith *et al.*, 1985) forms water soluble alkali metal salts. The purple reaction product is also water soluble enabling the spectrophotometric measurement of an aqueous protein solution. It is subject to less interferences than the Lowry assay and is also more sensitive (10 µg/ml protein/peptide). Sample volume can be reduced to 10µl by performing the assay in a microtitre plate (flat bottom microtitre trays, LIP equipment and Services Ltd, West Yorkshire, UK).

### 2.3.2.1. The standard assay protocol

The scaled down microtitre version of the BCA assay involves mixing one volume (10 $\mu$ l) of sample or standard (10 to 100 $\mu$ g/ml) with twenty volumes (200 $\mu$ l) of freshly prepared protein reagent. Colour development proceeded at 60°C for 1hr and plates were allowed to cool at room temperature before the absorbance was measured at 550nm (Anthos reader 2001, Anthos Labtec Instruments, Austria). A minimum of four samples of each test solution were used.

The BCA protein reagent is prepared by mixing 50 volumes of reagent A with 1 volume of reagent B. This solution should be freshly prepared. Reagent A consists of an aqueous solution of 1% (w/v) bicinchoninic acid (disodium salt), 2% (w/v) Na<sub>2</sub>CO<sub>3</sub>·H<sub>2</sub>O, 0.16% (w/v) disodium tartrate, 0.4% (w/v) NaOH and 0.95% (w/v) NaHCO<sub>3</sub>. This reagent was adjusted to pH 11.25 with NaOH (50% w/v) or solid NaHCO<sub>3</sub>. Reagent B consists of 4% (w/v) CuSO<sub>4</sub>·5H<sub>2</sub>O in double distilled water. Reagents A and B are stable indefinitely at room temperature.

Figure 2.3 shows that the assay using PXB is linear over the range 20-800 $\mu$ g/ml. Liposome encapsulation may be determined from the PXB content of supernatant washes, as for the bioassay protocol. However, it was found that the combination of Triton-X 100 and phospholipids in lysis samples resulted in interference, which was not adequately accounted for by the inclusion of assay standards containing suitable quantities of surfactant and phospholipid. Increased absorbance was seen when Triton-X 100 was present in the incubation mixture. Table 2.2 illustrates the changes in absorbance obtained with such samples.

Test Sample	Absorbance (550nm)
PBS pH 7.4	$0.156 \pm 6.2 \times 10^{-3}$
1% (v/v) Triton-X 100 in PBS pH 7.4	$0.521 \pm 0.127$
1% Triton-X 100 and liposomal phospholipid (0.5 $\mu$ M/ml) in PBS pH 7.4	$0.391 \pm 0.09$

Table 2.2. Interference of phospholipids and 1% (v/v) Triton-X 100 in the standard BCA assay protocol. Absorbances represent the mean  $\pm$  sd of four samples.

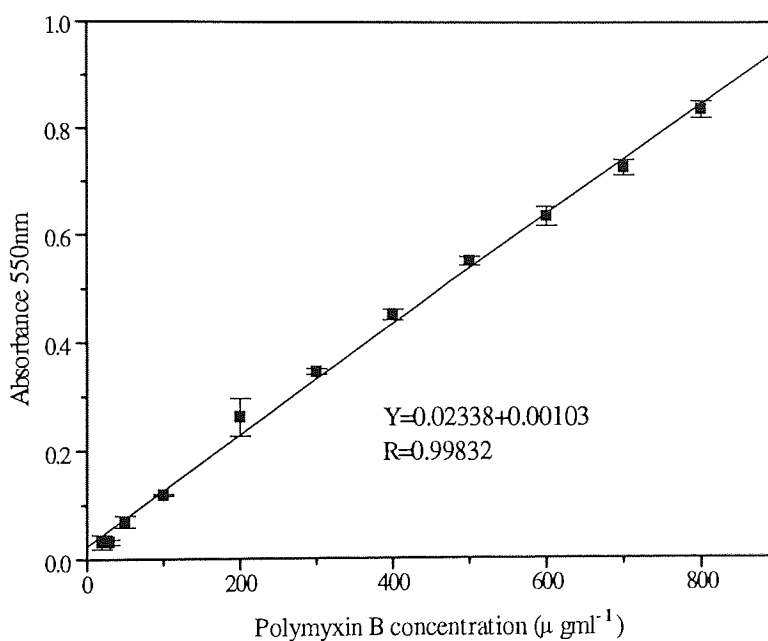


Figure 2.3. Calibration plot of PXB for standard BCA assay protocol (each point represents the mean  $\pm$  the standard deviation of four replicates)

### 2.3.2.2. The micro-assay protocol

Dilute protein solutions (0.5-10  $\mu$ g/ml) can be assayed with a modified BCA protocol which utilises a more concentrated reagent formulation. Micro-reagent A (MA) consists of an aqueous solution of 8% (w/v)  $\text{Na}_2\text{CO}_3 \cdot \text{H}_2\text{O}$ , 1.6% (w/v) NaOH, 1.6% (w/v) disodium tartrate, adjusted to pH 11.25 with  $\text{NaHCO}_3$ . Micro-reagent B (MB) consists of 4% (w/v) bicinchoninic acid (disodium salt) in double-distilled water. Micro-reagent C (MC) consists

of 4% (w/v) aqueous  $\text{CuSO}_4 \cdot 5\text{H}_2\text{O}$  plus 100 volumes of MB. Micro-working reagent (M-WR) consists of 1 volume of MC plus 1 volume of MA. MC and M-WR should be freshly prepared but MA and MB are stable indefinitely at room temperature. Samples and standards (100  $\mu\text{l}$ , 1-20  $\mu\text{g}/\text{ml}$ ) were mixed in a microtitre plate with an equal volume of M-WR and incubated at 60°C for 1hr. Plates were allowed to cool at room temperature before absorbance was measured at 550nm. A total of eight samples of each test solution were assayed and the average used to determine protein concentration by reference to a calibration curve (figure 2.4). The linear range of the calibration plot (2-18  $\mu\text{g}/\text{ml}$ ) was found to be suitable for the range of concentrations not covered by the standard protocol. There was a larger variation in this assay as evidenced by the lower correlation coefficient obtained ( $R=0.977$ ). This may reflect non-linear response with the lower concentrations of standards. Lysis samples were not assayed by this protocol as similar interferences could be expected due to the similarity of the reagents employed.

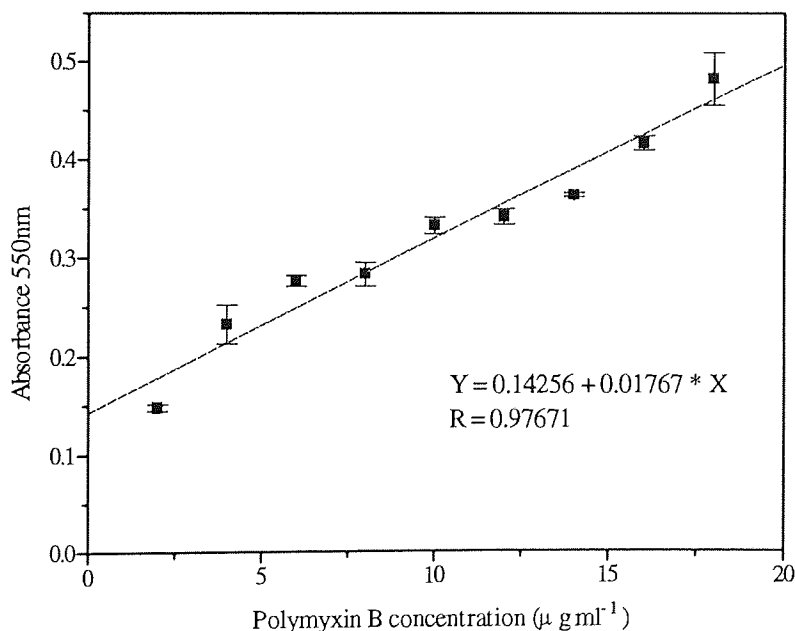


Figure 2.4. Calibration plot of PXB for the BCA microassay protocol. Each point represents the mean  $\pm$ sd for eight samples.

### 2.3.3. High performance liquid chromatography (HPLC) determination of PXB

#### 2.3.3.1. HPLC theory

HPLC is the most commonly used analytical method for the detection of drugs in dosage forms and biological fluids. Its attributes include the ability to efficiently separate and detect a wide range of molecules with varying molecular weights, polarities and thermal labilities. The technique is especially valuable in the analytical separation of groups of closely related compounds such as naturally occurring products (e.g., the polymyxins), enantiomers, degradation products, metabolites and structural analogues. The simplicity, high specificity and wide range of sensitivity make HPLC an ideal analytical method. Comprehensive accounts of the theoretical principles and practical aspects of HPLC may be found in several texts (Fifield & Kealey, 1983; Lindsay, 1987). Very simply, the system involves the delivery of a mobile phase through an injection valve onto a solid-phase chromatographic column. A combination of partitioning and adsorption of the analyte(s) between the solid stationary phase and the liquid mobile phase, which is determined by the physicochemical characteristics of the system, results in separation and elution of the analyte(s) into a detection device where they may be quantified. Analyte concentrations may be determined by interpolation from calibration plots which are validated in terms of their linearity.

#### 2.3.3.2. Methodology

HPLC has been previously used to separate individual species of polymyxins within a major class. The method described below is based on that of Whall *et al.* (1981). Complete separation of the three major PXB components, PB<sub>1</sub>, PB<sub>2</sub> and PB<sub>3</sub>, was achieved using reverse-phase chromatography with isocratic elution. The mobile phase comprised a phosphate buffer/acetonitrile solvent system (15.6g sodium dihydrogen orthophosphate, 700ml HPLC grade water, 230ml far UV acetonitrile, adjusted to pH 3.2 with phosphoric acid and filtered through a 0.45µm filter before use). As dissolved gases can cause



deterioration in chromatography by out-gassing in detection flow-cells, the mobile phase was degassed by placing in an ultrasonic bath for 15min. During use, solvent reservoirs were sparged with nitrogen at a flow-rate of 15ml/min. The chromatographic equipment used consisted of a Waters 600 multisolvent delivery system and Cecil CE292 variable wavelength digital UV spectrophotometer equipped with a flow-cell. A stainless steel chromatographic column (20cm x 0.5cm internal diameter) packed with Hypersil-ODS (C18, particle size 5 $\mu$ m, Shandon, UK) was used as the stationary phase. Mobile phase was pumped through the column at a flow-rate of 1.4ml/min. Samples were injected onto the column via a rheodyne loop (100 $\mu$ l) and a Chromjet integrator (Spectra Physics, UK) was used for integration of peak areas. UV detection was performed at 205nm.

In order to minimise errors due to fluctuations in injection volume, an internal standard was included with calibration and test samples. Before injection, samples were mixed with the internal standard, p-hydroxybenzoic acid (PHBA), in a 9:1 ratio (sample:internal standard). The retention time ( $29.02 \pm 3.46$  min,  $n=10$ ) and elution profile of PXB were unaffected by dilution with PHBA (retention time  $2.34 \pm 0.20$  min,  $n=10$ ). PXB was separated into a number of peaks reflecting its multicomponent nature. The three major components, PB2, PB3 and PB1, in increasing order of elution, were well resolved. This is consistent with elution patterns previously described (Taylor *et al.*, 1994; Whall, 1981) and is a function of the increasing hydrophobicity of the respective fatty acid residues. A typical chromatogram is shown in figure 2.6. The ratio of PB1 peak height and that of the internal standard was used to calculate a response factor which was plotted against total PXB concentration. There is a linear relationship between the peak heights of any of the major components and total PXB concentration (Taylor *et al.*, 1994). PB1 was chosen as it is the dominant component and therefore allows increased sensitivity of detection. The ratio of major components varies between sources of the drug but should remain constant for a given batch of PXB.

Quantification of sample peak responses was achieved by calibration measurements. These were performed during each assay procedure under the conditions of that particular

experiment and in an appropriate concentration range. The validity of this technique was assessed by examining the linearity of the calibration plots of peak area ratios. A typical calibration plot is shown in figure 2.5. It was found that the calibration plot was linear over the range tested (45-720 $\mu\text{g/ml}$ ). Due to the long retention time, determinations of PXB content of liposome samples were made from lysis samples rather than indirect determination from the two supernatant washes. After a single injection of a lysed liposomal preparation, retention time and elution profile of PXB and PHBA were unaffected by the presence of phospholipids and triton-X 100 in the lysate samples. A broader peak at the solvent front indicated early elution of some of these components. A sharp peak at  $\sim 5\text{min}$  was observed with all lysate samples. The origin of this peak was not elucidated, although it was present when lysed EPC vesicles devoid of cholesterol were analysed, indicating that it was due to elution of either triton-X 100 or EPC. A wide peak was obtained after multiple injections, presumably due to elution of surfactant/phospholipid components from the column. This effect was not seen after multiple injections of simple PXB solution. Washing of the column with mobile phase was sufficient to allow successful elution of subsequent samples.

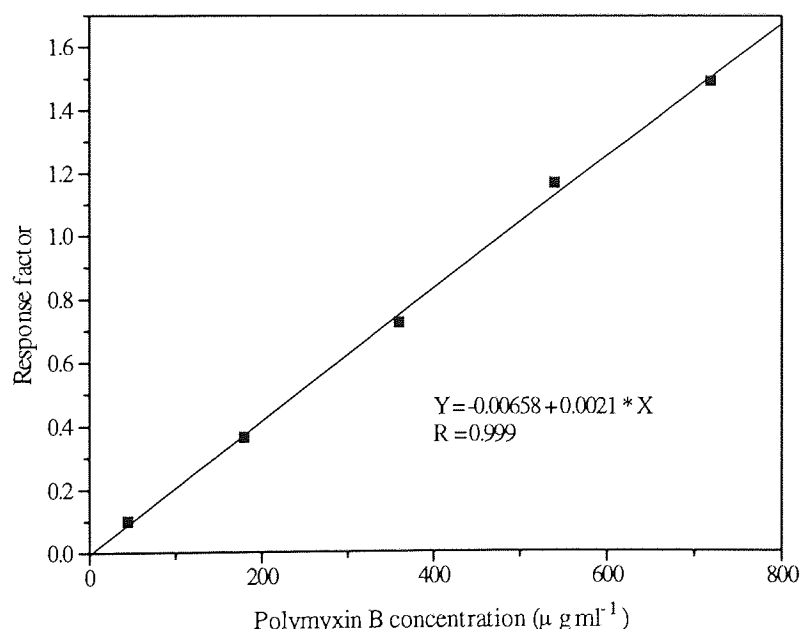


Figure 2.5. Typical calibration plot for HPLC assay of PXB. Each point represents the response factor (peak area ratio of PXB1/PHBA) after a single injection.

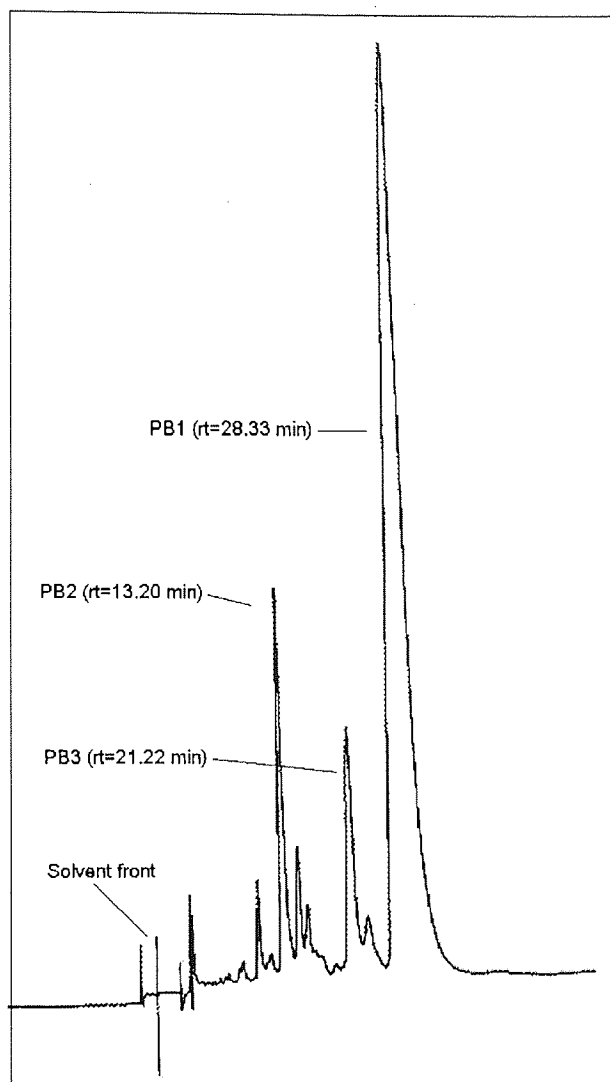


Figure 2.6. Specimen chromatogram of a polymyxin B sample (200 $\mu$ g/ml). Peak identification as illustrated.

### 2.3.4. Radiolabelling and scintillation counting of polymyxin B

#### 2.3.4.1. Theory

Radioactive isotopes such as tritium [ $^3\text{H}$ ] and carbon-14 [ $^{14}\text{C}$ ] interact with matter in two ways causing ionisation, which forms the basis of Geiger-Müller counting, and excitation. The latter effect leads to the emission of photons by the excited compound (or fluor). This fluorescence can be detected and quantified. This process is known as scintillation and when the light is detected by a photomultiplier tube, forms the basis of scintillation counting. With liquid (or internal) scintillation counting the sample is mixed with a scintillation cocktail containing a solvent and one or more fluors. The electric pulse which results from the conversion of photons to electric energy in the photomultiplier is directly proportional to the energy of the original radioactive event. Therefore two or more isotopes (*i.e.* [ $^3\text{H}$ ] and [ $^{14}\text{C}$ ]) can be separately detected and measured in the same sample provided they have sufficiently different emission spectra. Low energy  $\beta$ -emitters such as [ $^3\text{H}$ ] can be routinely measured with greater than 50% efficiency (Wilson & Goulding, 1986). However, quenching (optical, colour or chemical) can interfere with the energy transfer process and reduce the efficiency of counting. Samples can be corrected for quench by monitoring the extent of quenching agent present in the sample and expressing the activity in absolute units of disintegrations *per* minute (DPM). This requires the determination of the counting efficiency and the conversion of counts *per* minute (CPM) to DPM as shown in the equation:

$$\text{Counting efficiency} = \frac{\text{CPM} - \text{background counts}}{\text{DPM}} \times 100\%$$

The samples channel ratio (SCR) method may be used to correct quench. In this method two regions of the samples liquid scintillation (LS) spectrum are monitored in two channels and a ratio of the count rate determined. The assumption in this type of quench monitoring is that the entire LS spectrum will change in its distribution and shift downward due to quenching,

which lowers the pulse height of many energetic decays. To obtain the DPM of samples by this method, a quench curve is required. A quench curve is a mathematical curve relating the counting efficiency of standards (whose activity is known) to the SCR (*i.e.* the extent of quench). Practically, this may be achieved by counting of samples in the presence of increasing quantities of a quenching agent such as chloroform. The DPM can then be calculated from the measured CPM and counting efficiency of the sample.

#### 2.3.4.2. Radiolabelled PXB and sample preparation

Tritiated PXB was prepared by NEN products (Canada) by catalytic exchange with tritium gas in aqueous solution at room temperature, followed by the removal of labile tritium with ethanol. This method is particularly suitable for the tritium labelling of compounds which contain benzylic protons, such as PXB (Vaara & Viljanen, 1985). HPLC analysis of radiolabelled PXB (100 $\mu$ g/ml) showed the same peak pattern as unlabelled drug, indicating no degradative changes had occurred. The specific activity of PXB was 39.59MBq/ml (1.07 mCi/mg). For preparing labelled solutions of PXB, a quantity of diluted label was added to a cold PXB solution to provide a sufficient number of counts for subsequent analysis. This was typically a 0.1-1.0% ratio of hot to cold drug. It was assumed that the behaviour of labelled drug was entirely representative of that of the excess cold drug present.

PXB was quantified by scintillation counting of aqueous PXB in scintillation fluid. Samples were prepared by pipetting 10-50 $\mu$ l of tritiated sample into a scintillation vial and mixing with 3-10ml of scintillant (Optiphase Hisafe 2, LKB scintillation products, UK). The volume of scintillant used did not affect the DPM obtained but it was necessary to use larger volumes to incorporate increased aqueous volumes. Vials were counted for 5 minutes (Canberra Packard 1300TR scintillation counter, Berkshire, UK) and DPM derived from CPM by reference to a quench curve. Counts were corrected for quench effects using an external set of quench standards. This was prepared by adding increasing amounts of chloroform (0-5000

$\mu\text{l}$ ) to a set activity of  $[^3\text{H}]$  PXB. Vials were counted for three cycles of 10 minutes and a quench curve established. Maximum efficiency of counting of  $[^3\text{H}]$  PXB was found to be 64.99% (figure 2.7).

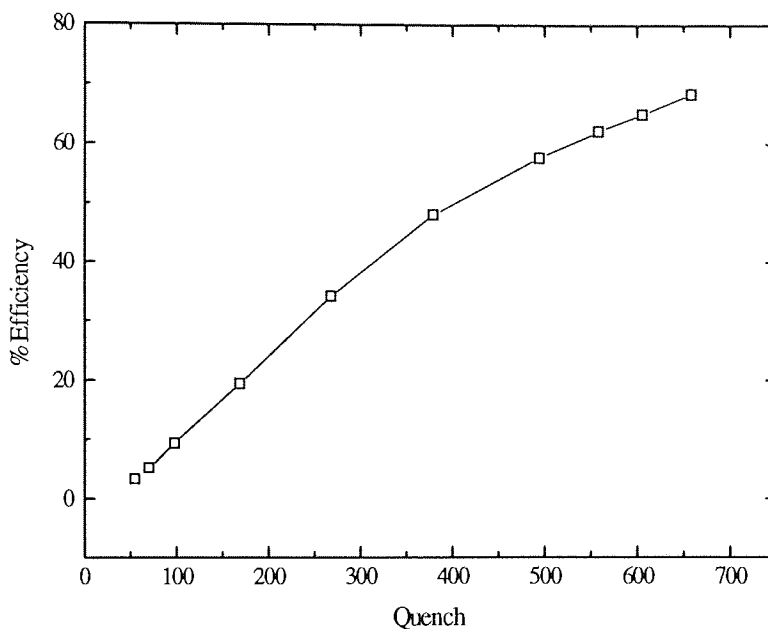


Figure 2.7. Quench curve for  $[^3\text{H}]$  PXB.

#### 2.3.4.3. Evaluation of scintillation counting for the detection of PXB

Radiolabelling was used to determine encapsulation efficiencies by measuring  $[^3\text{H}]$  PXB counts in supernatant washes and those in the final liposome preparation. It was found that it was unnecessary to lyse liposomes before addition to scintillation fluid as similar counts were obtained by direct addition as after lysis using methanol or triton-X 100. This is predictable given the high concentrations of surfactant present in the scintillation cocktail to aid incorporation of aqueous samples.

Initially discrepancies were noted for encapsulations determined by indirect and direct means, for liposomes produced by the dehydration-rehydration vesicle method (see section 3.3.1). This was not seen with simple vortex mixed MLV. These results are summarised in table 2.3.

Formulation	Encapsulation determined indirectly from supernatant [ <sup>3</sup> H] PXB	Encapsulation determined directly from liposomal [ <sup>3</sup> H] PXB
EPC MLV	4.64±1.96%	6.80±0.33%
EPC DRV	63.91%±0.96%	30.37±0.54%

Table 2.3. Encapsulation of PXB by EPC liposomes (66µM lipid/18mg PXB): discrepancies between encapsulation results (values are the mean±standard deviation of three replicate measurements)

Values determined by counting of [<sup>3</sup>H] PXB in the supernatant washes of EPC liposomes were approximately 30% greater than those determined directly from the counts of washed liposome samples. The cause of this discrepancy was found to be the freeze-drying step of the DRV process. Free solutions of PXB lost ~35% of [<sup>3</sup>H] after one freeze-drying cycle (table 2.4). A smaller decrease was noted after a second cycle. Analysis by HPLC and BCA protocols showed no change in PXB concentration indicating that a physical loss of drug was not occurring. Loss of tritium was presumably due to exchange processes with the buffer. Removal of PXB during freeze-drying was reasonably reproducible (39.12±4.91%, n=16).

	Before freeze-drying	After 1 freeze-drying cycle	After 2 freeze-drying cycles
% [ <sup>3</sup> H] PXB activity (n=3)	100±1.44	45.28±0.53	40.02±0.98
% PXB concentration (BCA assay, n=4)	100±1.90	97.73±0.54	ND
% PXB concentration (HPLC assay, n=1)	100	96.95	ND

Table 2.4. Analysis of [<sup>3</sup>H] and unlabelled PXB before and after freeze-drying cycles. ND denotes not value not determined.

The differential in observed encapsulation values can be explained by considering the equations used to calculate the encapsulation percentages:

$$\text{indirect encapsulation \%} = \left( \frac{(\text{DPM of initial loading solution} - \text{supernatant DPM})}{\text{DPM of initial loading solution}} \right) \times 100$$

$$\text{direct encapsulation \%} = \left( \frac{\text{DPM of washed liposomes}}{\text{DPM of initial loading solution}} \right) \times 100$$

As there is a loss of [<sup>3</sup>H] activity during freeze-drying, values of encapsulation determined indirectly will give an overestimate of encapsulation. Conversely values determined directly will be underestimates. This problem was resolved by freeze-drying an aliquot of loading solution and using this to determine the total [<sup>3</sup>H] counts remaining after freeze-drying. Encapsulation values calculated in this manner showed good agreement between indirect and direct values. This was also confirmed by BCA assay of the liposome preparations also indicating that the behaviour of radiolabelled PXB is representative of the bulk unlabelled drug. The encapsulation values are shown in table 2.5. Single determinations by HPLC of lysis samples gave encapsulation values in agreement with those determined by scintillation counting. However, the less time-consuming BCA assay facilitates multiple determinations and is a more useful routine method to verify encapsulation values calculated from scintillation counts.

Assay method	% Encapsulation
[ <sup>3</sup> H] PXB counts of washed liposomes (direct method)	43.98±2.38
[ <sup>3</sup> H] PXB counts of supernatant washes (indirect method)	39.93±5.81
BCA assay of supernatant washes (indirect method)	45.38±4.11

Table 2.5. Encapsulation of PXB by EPC liposomes using the DRV method (66µM lipid/9mg PXB) determined using different assay techniques. Values are the mean±sd of three determinations.



#### 2.4. Summary of assay development

The bioassay has good sensitivity (2-200 $\mu$ g/ml) but the procedure is time-consuming and the method of measurement is operator dependent. This method has been used in the analysis of PXB tissue levels although an extraction process was necessary to separate PXB from acidic phospholipids (Kunin & Bugg, 1971). These disadvantages combined with interference effects encountered with lysis samples restrict the usefulness of this assay for determination of liposomal PXB encapsulation.

The BCA assay proved a successful technique for quantifying PXB in aqueous solutions. Although subject to interference from lysis samples, this assay offered advantages over the bioassay such as a wider range (20-800 $\mu$ g/ml) and less time consuming preparation and processing of samples. Lower PXB concentrations could be assayed using the micro-protocol.

HPLC assay of PXB enabled separation of the parent polymyxin into its minor components. This assay was accurate and reproducible but its usefulness was hindered by the long retention time of PB1 (~29mins). Recently a solvent system has been described which reduces the retention time of PB1 to 7 minutes (Taylor *et al.*, 1994). It was also found that the retention times of PXB components were very sensitive to changes in acetonitrile concentration. In acid solution (pH 3), a change in acetonitrile concentration from 20 to 24% (v/v) reduced the retention time of PB2 from 37 to 7.8min. Decreased pH also decreased retention times. Limits of detection were not established in this study. Triton-X and/or phospholipids from lysis samples appeared to accumulate on the column and were eluted periodically through sample runs. It may be possible to prevent this by using methanol to lyse liposome preparations and extracting PXB from the resulting phospholipid solution using a modified Bligh-Dyer extraction procedure (New, 1990). However, the low sensitivity (50 $\mu$ g/ml) may restrict the usefulness of the HPLC assay when working with very dilute PXB solutions. Further development and modification of this assay (including sample delivery *via*

an autosampler) would make this assay the most suitable for further pharmaceutical development of liposomal PXB.

Radiolabelling of PXB with tritium proved to be the most successful assay method in terms of sensitivity and ease of use. Assay of PXB in aqueous solutions by [<sup>3</sup>H] scintillation counting was initially verified using BCA and HPLC assays for cold PXB. Accounting for tritium losses encountered during freeze-drying resulted in a very useful method capable of determining liposome encapsulation by direct and indirect methods. The superior sensitivity of this assay (~50ng/ml) made it useful for the detection of low PXB concentrations in tissue and release samples.

## Chapter 3

### Formulation Development of Liposomal Polymyxin B

---

#### ABSTRACT

The work presented in this chapter covers the formulation methodology of liposomal polymyxin B and the role of phospholipid composition in determination encapsulation efficiencies, release characteristics in a number of media and physical characteristics of the vesicles produced (size, surface charge and morphology).

---

### 3.0. Formulation Development of Liposomal Polymyxin B (LPXB)

#### 3.1. Introduction

The interaction of PXB and phospholipids has been the subject of numerous studies which have investigated the interaction using lipid monolayers or exogenously applied PXB with empty liposomes (Beurer *et al.*, 1988; Colomé *et al.*, 1993; Imai *et al.*, 1975; Schroder *et al.*, 1992). Although the entrapment of PXB within liposomes has not been previously reported, such studies provide useful information when considering formulation approaches for the development of LPXB. Some general principles apply to liposome formulation, but it is accepted that a specific formulation needs to be optimised for the particular drug in question (Fielding, 1991). The method of liposome formulation is a major determinant of liposomal properties and the phospholipids employed can affect the encapsulation efficiency and physical properties of the vesicles. The DRV method (see section 3.3.1) was the preferred method of liposome preparation due to the high encapsulation efficiencies which may be obtained and the mild conditions used. Antibiotics which have been successfully encapsulated using this technique include piperacillin and gentamicin, (Nacucchio *et al.*, 1988) tobramycin and ticarcillin (Lagacé *et al.*, 1991), chloramphenicol (Onur *et al.*, 1992) and amikacin (Wichert *et al.*, 1992). The initial aims of this study were to identify which phospholipids could be used, the effect of lipid and drug ratios on entrapment, and to show which factors affected stability and release profiles of the vesicles. Characterisation was performed using light microscopy, transmission electron microscopy (TEM), laser light diffraction sizing, photon correlation spectroscopy (PCS) and laser Doppler velocimetry (zeta potential measurements). The overall objective was to formulate LPXB to give a preparation with high, reproducible entrapments, with a suitable size distribution and surface charge, and which possessed the desired release properties.

## 3.2 Materials

### 3.2.1 Polymyxin B

As section 2.2.1

### 3.2.2 Phospholipids

As section 2.2.2.

### 3.2.3. Chemicals

All chemicals and reagents not specified in the text were supplied by BDH Chemicals Ltd. (Poole, UK), Sigma Chemical Company (Poole, UK) and Fisons (Loughborough, UK) and were of Analar grade or equivalent.

## 3.3. Methods

### 3.3.1. Dehydration-rehydration vesicle (DRV) technique

DRV composed of varying phospholipid/cholesterol ratios were prepared as described by Kirby and Gregoriadis (1984). The process is outlined in figure 3.1. Lipids were added to a round-bottomed flask (Quickfit, 100ml) and sufficient chloroform added (typically 5ml) to obtain a thin-film. The lipid mixture was dried by rotary evaporation (Rotavapor, Büchi, Germany) under reduced pressure above the transition temperatures ( $T_m$ ) of the phospholipids used. Solvent traces were removed by drying under a nitrogen stream. The resulting thin-film was redispersed with PBS pH 7.4 by gentle agitation for 30min in a water bath at a temperature greater than the transition temperature of the phospholipids used. Table 3.1 lists the transition temperatures ( $T_m$ ) of the phospholipids commonly used. The mixture was briefly sonicated (Bath sonicator, England) to fully disperse the dried film. After a 30 minute incubation period at the required temperature, the milky-white liposome MLV suspension was sonicated to clarity using a probe sonicator (probe diameter 14mm,

amplitude 18000, Soniprep 150, MSE, UK) for 10 cycles of 60 seconds on/30 seconds off. Preparations composed of unsaturated phospholipids (such as EPC) were placed in a bath of iced water during sonication to disperse heat generated during sonication. Saturated phospholipids were cooled using only a water bath. The resulting suspension of SUV was centrifuged (Beckmann JII, Beckmann Instruments Ltd., Bucks., UK) at 400 x g for 10 min to remove large lipid aggregates and titanium particles. An aliquot of SUV was then mixed with an aliquot of PXB solution at the desired concentration and the mixture frozen at -70°C. After freezing (~3hr) the preparation was freeze-dried for 18hr (Edwards Modulyo Freeze-drier, Edwards High Vacuum Ltd., Sussex, UK). The preparation was then rehydrated with a volume of distilled water equivalent to one tenth of the total volume of SUV used, at a temperature greater than the temperature of the phospholipids used. Rehydration was aided by vortex mixing (30sec) and incubation with shaking at the required temperature for 30mins. The rehydration procedure was repeated using 1.8ml and 4.0ml of PBS pH 7.4.

Liposomes were separated from non-entrapped drug by centrifugation (18000 x g for 30mins, Beckman JII, UK). The supernatant was retained and a further 20ml of buffer was used to resuspend the pellet and centrifugation was repeated. The final pellet was resuspended by vortexing with 1ml of PBS and making up to 5ml with buffer. Liposomes were stored at 4°C until required. The two supernatant samples retained during liposome preparation were used to indirectly estimate the percentage liposomal entrapment of drug using an appropriate assay method. Liposomes suspensions were also assayed directly (either by lysis or addition of radiolabelled preparations to scintillation fluid, see section 2.3.4) to estimate entrapment efficiencies.

Phospholipid	Transition temperature (T <sub>m</sub> )
Egg phosphatidylcholine (EPC)	-15 to -7°C
Dimyristoylphosphatidylcholine (DMPC)	23°C
Dipalmitoylphosphatidylcholine (DPPC)	41°C
Distearoylphosphatidylcholine (DSPC)	55°C

Table 3.1. Transition temperature of phospholipids commonly used to prepare liposomes (adapted from Szoka & Papahadjopoulos, 1980)

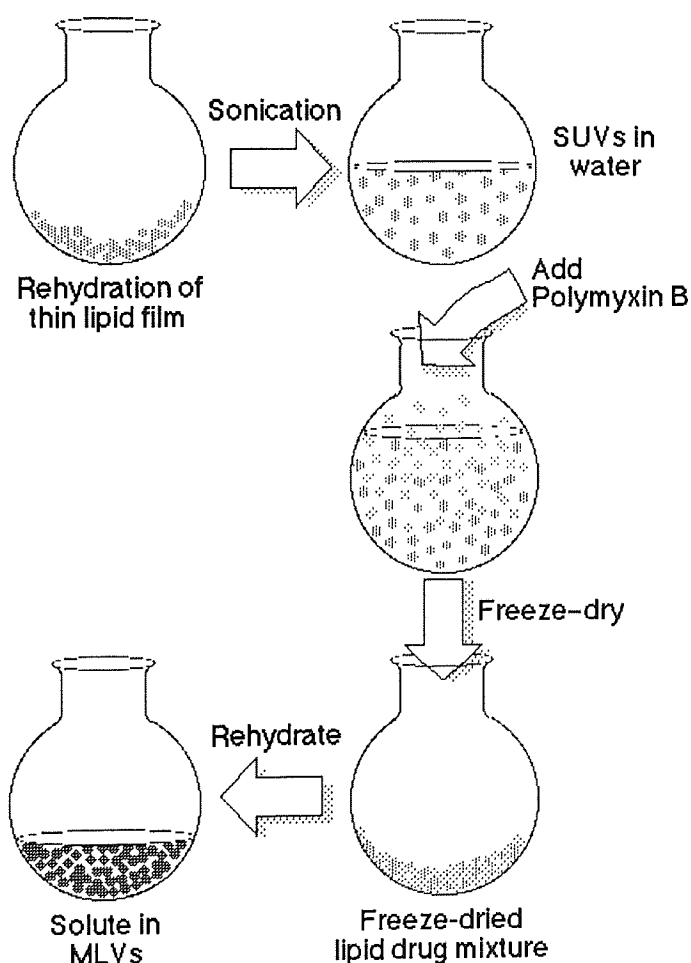


Figure 3.1. Schematic flow diagram of the main steps in the DRV process

### 3.3.2 Thin-film hydration

Thin-film hydration was used to prepare MLV composed of varying phospholipid/cholesterol ratios. Lipids were added to a round-bottomed flask (100ml) and sufficient chloroform added (typically 5ml) to obtain a thin-film. The lipid mixture was evaporated under reduced pressure at 40°C to dryness. Solvent traces were removed by drying under nitrogen (20min). The resulting thin-film was redispersed with PBS pH 7.4, containing the required concentration of PXB, by gentle agitation in a water bath at a temperature greater than the transition temperature of the phospholipids used. The mixture was briefly sonicated (Bath sonicator, England) to fully disperse the dried film. After a 1hr incubation period at the required temperature, the MLV suspension was separated from non-entrapped drug by centrifugation and encapsulation efficiencies determined as for liposomes prepared by the DRV method (section 3.3.1.).

### 3.3.3. Analysis of PXB entrapment

The methods used to assess entrapment of PXB were as described in sections 2.1-2.6.

### 3.3.4. Phospholipid assay

Phospholipid concentrations were determined by the colorimetric method of Stewart (1980). This method is based on complex formation between ammonium ferrothiocyanate and phospholipids in the range 0.01-0.1mg. The red inorganic compound ammonium ferrothiocyanate is insoluble in chloroform, but forms a coloured complex with phospholipid solutions in chloroform. The coloured complex ( $\lambda_{\max}$  488nm) is freely soluble in chloroform and therefore partitions in this phase.



This rapid and simple method avoids the need for acid digestion and colour development which are drawbacks of the methods described by Bartlett (1959) and Raheja (1973), respectively.

Ammonium ferrothiocyanate solution (N/10) was prepared by dissolving 27.03g of ferric chloride hexahydrate ( $\text{FeCl}_3 \cdot 6\text{H}_2\text{O}$ ) and 30.4g ammonium thiocyanate ( $\text{NH}_4\text{SCN}$ ) in deionised distilled water and making up to 1L. This solution is stable for months at room temperature.

A stock solution of 10mg phosphatidylcholine in 100ml chloroform was prepared. Triplicate volumes of this between 0.1ml and 1.0ml were then pipetted off, added to 2.0ml ammonium ferrothiocyanate solution, and enough chloroform was added to make 2.0ml. The biphasic system was then vigorously mixed on a vortex mixer for 1 min. A calibration graph was prepared by measuring the optical density of increasing phospholipid concentrations in the chloroform phase at  $\lambda_{488\text{nm}}$ . Figure 3.2 is the plot obtained for concentrations of phosphatidylcholine up to 0.1mg in 2ml of chloroform and is linear up to 0.4 O.D. units. Beyond this point Beer-Lambert's law is not obeyed, and there is progressive deviation of the plot from linearity.

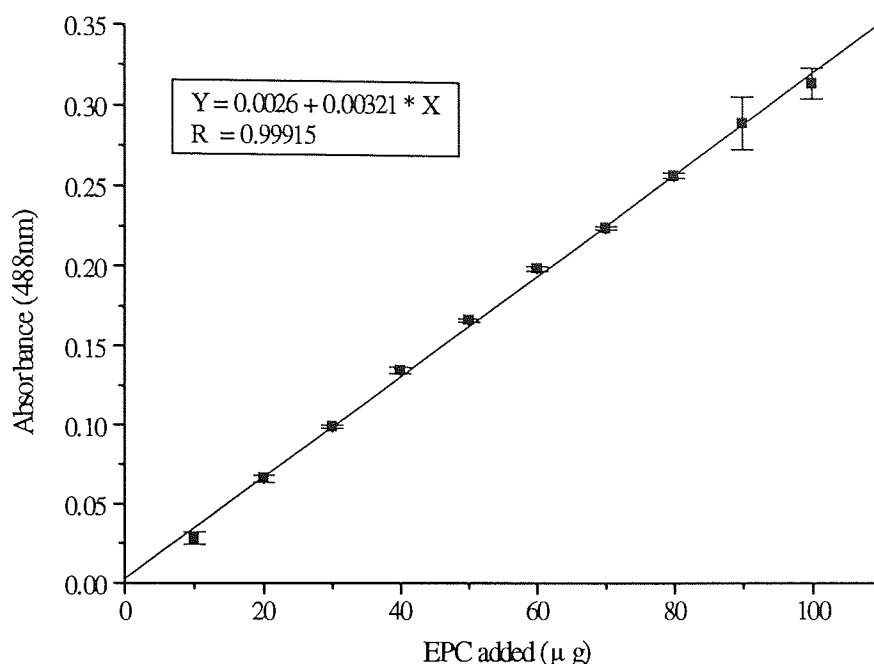


Figure 3.2. Calibration plot for egg phosphatidylcholine (EPC) using the Stewart (1980) colorimetric assay. Each point represent the mean $\pm$ sd of three triplicates.

### 3.3.5 Laser diffraction particle size analysis

Laser light diffraction may be used to determine the size distribution of liposome preparations. Particles pass through a laser beam and the light scattered by them is collected over a range of angles in the forward direction. The angular intensity distribution of the scattered light varies strongly with particle size over a wide size range. The particles pass through an expanded and collimated laser beam (source, Helium-Neon gas laser with a wavelength of  $0.633\mu\text{m}$ ) in front of a lens in whose focal plane is positioned a photosensitive detector consisting of a series of concentric annular rings. The unscattered portion of the laser beam is brought to focus in the detector plane and is usually allowed to pass through an aperture at the detector centre and effectively pass out of the system. The annular rings centred around the axis of the incident laser beam record the intensity of the light scattered over a range of angles and the distribution of scattered intensity is analysed by computer to

yield the particle size distribution. For a polydisperse sample of particles, the detector measures the integral angular scattering across the complete size distribution. Several thousand particles may be illuminated at any one time and the diffraction pattern will change in time as the number distribution of particles in each size class varies with particles entering and leaving the beam. This temporal variation is usually integrated to give an average for a truly representative sample of the particles present. The Malvern Mastersizer E (Malvern Instruments, England) uses reverse fourier optics to enable size distribution to be measured in the sub-micron range. Mie theory analysis of the distribution of scattered intensity is also needed to calculate the size distribution of particles in the sub-micron range. Analysis of small particles is not possible using the simpler and more widely used Fraunhofer scattering theory as it requires particles to be large compared with the laser wavelength. Fraunhofer theory also fails to recognise that light can pass through the particles. Mie theory predicts all paths of light around and through the particle and copes with partially absorbing particles including those which are totally opaque or clear. Therefore it may be applied over the whole range of particle types and sizes to predict scattering at any angle from forward diffraction to back scatter. The combination of reverse fourier optics with Mie theory analysis allows the Malvern Mastersizer E to measure liposome size distributions over the range 0.1-80  $\mu\text{m}$ . The volume mean reproducibility of the system is given as  $\pm 0.5\%$  for a stable sample under recirculating conditions in liquid suspension.

The Malvern laser diffraction technique generates a volume distribution for the analysed light energy data. Although the volume distribution can be mathematically transformed to generate a number distribution, care is required in the interpretation of such data. The amount of light scattered by a particle is proportional to the sixth power of the diameter. Therefore in the 0.1 to 1.0  $\mu\text{m}$  range the ratio of scattered intensities is  $10^6$ . The data may be heavily skewed by a small number of large particles or aggregates. For this reason values are reported as the equivalent volume mean (D[4,3]) plus or minus the standard deviation.

A quantity (200 $\mu$ l or sufficient to give the required obscuration) of liposome dispersion was vortex mixed with 10ml of filtered buffer (0.22 $\mu$ m polycarbonate filter, Millipore, UK) and sized using the Mastersizer E. Liposome diameters are given as those determined from both the volume and number size distributions.

### 3.3.6. Photon correlation spectroscopy (PCS)

PCS (also referred to as quasi-electric light scattering or dynamic light scattering) may be used to measure the size distribution of vesicles in the sub-micron range. Colloidal particles in a liquid undergo random motion due to multiple collision with the thermally driven molecules of the liquid (Brownian motion). Light scattered by these particles will fluctuate in time, the characteristic dependence describable in terms of the diffusion coefficient of the particle, which can be related to the particle size. Small particles diffuse more rapidly than large particles and the rate of scattered light intensity varies accordingly. These changes in the intensity of scattered light are detected as the particles move under Brownian motion. PCS determines particle size by characterising the time scale of the intensity fluctuations caused by the diffusing particles. By correlating sections of the signal with themselves at different periods of time (autocorrelation), this time dependency can be evaluated, resulting in an autocorrelation function from which particle size and size distribution can be determined. For a monosized distribution of spheres the function is an exponential function of time. For a polydisperse system, multiple values of the correlation coefficient are determined and a first-, second and third order fit of the data yields a size distribution and standard deviation. The translational diffusion coefficient can be measured, which in turn can be used to determine the mean hydrodynamic radius of the particle using the Stokes-Einstein equation (for monosized particles):

$$D = \frac{kT}{6\pi\eta r}$$

(D=diffusion coefficient, k=Boltzmann's constant, T=absolute temperature (Kelvin),  $\eta$ =solvent viscosity, r=mean equivalent spherical hydrodynamic radius)

In the Sematech correlator, the time increments separating the two copies of the signal to be processed are termed channels. The overall time separation between channels can be varied by altering the channel sampling time. The choice of sample time is critical in achieving meaningful results. Although the Sematech instrument can automatically determine the sample time by comparing calculated and measured background values, this parameter was set manually before analysis. Commonly, a sample time of 5 or 10 $\mu$ s was chosen depending on the relative size of the vesicles to be sized. Extruded vesicles were measured using the shorter time of 5 $\mu$ s and unextruded preparations were sized using the longer sampling time to account for the presence of larger, more slowly moving vesicles. A total running time of 100sec was used for all experiments. Similar parameters for PCS sizing of liposomal preparations have been described by Elorza *et al.*, (1993).

PCS is the most widely and commonly used method to determine size distribution of liposomes in the submicron range (Barenholz & Amselem, 1993). The limitations of PCS concern the size range over which the validity of the technique is maintained. The range of PCS measurement is usually given as 3nm-3 $\mu$ m, although for most instruments the practical upper limit is 1 $\mu$ m. As with laser light diffraction, the presence of a few large particles may obscure smaller particles and result in skewing of the size distribution towards the higher size range. The Sematech multiangle goniometer used throughout this study is equipped with a high power laser source (Helium-Neon 5mW,  $\lambda$ =632.8nm) and advanced photomultiplier detection system combined with data analysis by a singular system algorithm. It is claimed that this specification enables particle size distributions to be determined over the 5nm-5 $\mu$ m range, even for polydisperse samples.

Results from PCS sizing are quoted as the mean hydrodynamic diameter of the intensity cumulants distribution plus or minus the dispersion. The dispersion is a measure (in nm) of the width of the distribution relative to the mean. The Sematech algorithm also generates a value of polydispersity which is similar to the value used in Malvern PCS software. The polydispersity value varies from 0 to 1, with low values representing monosized systems and higher values indicating multimodal distributions or polydispersity.

Samples were prepared by diluting a quantity (50 $\mu$ l) of liposome dispersion with 5ml of filtered buffer (0.22 $\mu$ m polycarbonate filter, Millipore, UK) and sized using the Sematech multiangle goniometer. Samples were contained within a low volume glass tube mounted in a sample holder in an index matching bath. Measurements were made at 25 $\pm$ 0.1 $^{\circ}$ C at an angle of 90 $^{\circ}$ . The values quoted are the intensity mean for the liposomal hydrodynamic diameter.

### 3.3.7. Zeta potential analysis

The zeta potential of liposomes can be determined by measuring the particle mobility in an electric field. Using the equations of Smoluchowski, Henry or Debye-Huckel (Müller *et al.*, 1986) the zeta potential ( $\zeta$ ) may be calculated from the liposome mobility. The electrophoretic mobility ( $\mu_E$ ) is defined as the velocity of the particle under unit electric field and is usually expressed in relation to the particle velocity ( $v$ ) and the applied field strength ( $E$ ), as in the equation:

$$\mu_E = \frac{v}{E}$$

where  $v$  is measured in m/s, and  $E$  in V/m, so that  $\mu_E$  has the dimensions m<sup>2</sup>/s/V (Kayes, 1988). The equation used for converting the electrophoretic mobility into zeta potential depends upon the values of the Debye-Hückel parameter ( $k$ ), which depends on electrolyte

concentration, and the particle radius ( $a$ ). At large values of  $ka$  the Smoluchowski equation can be applied. This was the equation used throughout the course of this study due to the conditions of measurement employed (aqueous medium, moderate electrolyte concentration and an average particle radius of 0.5-5 $\mu$ m). Zeta potential is defined as:

$$\zeta = \mu_E \frac{4\pi\eta}{\epsilon}$$

where  $\eta$  is the viscosity of the medium (in poises) and  $\epsilon$  is the respective dielectric constant. The value of  $\zeta$  is measured in mV. It follows from this equation that the electrophoretic mobility of a non-conducting particle for which  $ka$  is large at all points on the surface, should be independent of its size and shape provided the zeta potential is constant (Shaw, 1980). Determinations were undertaken using the following parameters listed in table 3.2.

Parameter	Value
Cell type	Zetamaster standard cell
Cell voltage	100mV (constant)
Current	buffer dependent
Conductivity	buffer dependent
Temperature	25.5 $\pm$ 0.1 $^{\circ}$ C
Dielectric constant	79.0
$f(ka)$	1.50

Table 3.2. Parameters used in zeta potential measurements (from Malvern technical information)

A laser doppler anemometry instrument consists of two coherent laser beams derived from the output of a low power laser that intersect within the sample cell, forming a beam crossover pattern of interference fringes. Particles moving across the fringes in response to the applied electric field scatter light with an intensity which fluctuates at a frequency related to their velocity. The frequency of the scattered laser light differs from the frequency of the initial laser beam. This shift is caused by the Doppler effect and is a function of the particle velocity. The signal from individual photons of scattered light are detected by a

photomultiplier and analysed by a digital correlator to give a frequency spectrum from which the particle mobility and the zeta potential are calculated (McFayden, 1986; Müller, 1991).

Zeta potentials of empty and loaded vesicles were measured to investigate the effect of drug loading on liposome surface charge. Two different buffer systems were used to evaluate liposomal zeta potentials. PBS pH 7.4 was used as measurements in this medium would reflect the surface characteristics under physiological conditions whilst a lower ionic strength diphosphate buffer allowed greater sensitivity in assessing zeta potential changes. Liposome dispersion (20 $\mu$ l,  $\sim$ 0.3 $\mu$ mol lipid) was added to 10ml of 0.02M diphosphate buffer ( $\text{Na}_2\text{HPO}_4 \cdot 2\text{H}_2\text{O}$ , 3.598g/L;  $\text{KH}_2\text{PO}_4$ , 2.72g/L; pH 7.4) or PBS pH 7.4, filtered through a 0.2 $\mu$ m filter before use, and zeta potentials then measured at  $25^\circ\text{C} \pm 0.1^\circ\text{C}$  using a Zetamaster instrument (Malvern Instruments, Ltd., Malvern, UK). Machine operation was periodically checked using a standard latex with a defined electrophoretic mobility. A carboxy-modified polystyrene latex (AZ55, Malvern Instruments, Malvern, UK) was diluted in a supplied buffer and measured using the parameters listed above. This latex has a charge of -55mv at  $25^\circ\text{C}$  and the acceptable deviation from this value is  $\pm 5\text{mV}$ .

### **3.3.8. Light Microscopy**

Vesicle morphology could be investigated using light microscopy for preparations whose size distribution was greater than 0.5 $\mu$ m. Preparations were diluted in PBS pH 7.4 and viewed using phase contrast microscopy under 40X and 100X magnification (Zeiss Axioscope, Zeiss Optical Instruments, Germany).



### 3.3.9. Transmission electron microscopy (TEM)

A variation of the drop method of TEM was used to investigate gross liposomal morphology, membrane integrity and size. This method utilises a negative stain provided by a heavy metal salt which strongly scatters electrons. As electron scattering is directly related to atomic number, the phospholipid bilayers of vesicles, composed principally of carbon and hydrogen, will scatter fewer electrons than the stain and therefore appear in negative contrast (New, 1990). A single drop of freshly prepared liposomes was placed onto a carbon coated copper grid, left to stand for 1 min, and then dried using a wick of filter paper (Whatman, No. 2). The stain, 2% w/v ammonium molybdate, was then dropped onto the grid and left for a further minute. Fresh filter paper was used to remove excess stain from the grid. When dry, the sample was imaged with a transmission electron microscope (Phillips EM 301G) operating at an accelerating voltage of 100kv with zero tilt.

### 3.3.10. Thin layer chromatography

TLC was used periodically to confirm the purity of phospholipid stock solutions. The stationary phase used was silica gel (Sigma Chemical Company, UK) which is surface coated with a layer of tightly bound water. The mobile phase used was chloroform: methanol: water (65:25:4 v/v). Using these conditions, phospholipids were separated principally according to headgroup differences. Lipids were visualised by iodine uptake. Lipids which have undergone extensive degradation would be observed as a long smear with a tail trailing to the origin. Pure material should run as a clearly defined spot. Lipids extracted from natural sources such as egg yolk will be stained as a broader spot compared with their synthetic counterparts, reflecting their heterogeneity in composition (New, 1990).

### 3.3.11. Gel exclusion chromatography (GEC)

GEC was used to separate vesicles with small diameters (50-400nm) from non-entrapped PXB due to difficulty in obtaining a vesicle pellet after centrifugation. GEC separates materials on the basis of molecular weight and as such is particularly suitable for liposomes as they are, in most cases, much larger than non-entrapped drugs. A gel should be chosen which excludes liposomes from the gel matrix and so elutes liposomes in the void volume, but which includes non-entrapped drug in the gel matrix and so elutes the drug in a later fraction depending on its molecular weight. The gel matrix is commonly a cross-linked dextran (Sephadex) which is insoluble in water but swells in aqueous media, forming gel particles suitable for gel filtration.

Initially the rapid minicolumn separation method (Barenholz & Amselem, 1993) was seen to be unsuitable for the separation of PXB from liposomes due to overlap in the eluted samples. Successful separation was achieved using a larger column (1x30cm, Pharmacia, Sweden) packed with Sephadex G-50 (molecular exclusion limit ~50000Da, medium grade 1-50µm particle size). Liposomes were eluted with PBS at a flow rate of 0.33ml min<sup>-1</sup> delivered by a peristaltic pump (12000 Varioperpex pump, LKB/Bromma, Sweden). Sample collection (2ml) was *via* an automated fraction collector (2112 Redirac fraction collector, LKB/Bromma, Sweden).

### 3.3.12. Ultrafiltration separation of non-entrapped PXB from LPXB preparations

Vesicles were separated from non-entrapped drug by ultrafiltration using Microcon 100 microconcentrators (Amicon Ltd., Gloucestershire, England). The microconcentrator fits in an ependorff tube and utilises an ultramembrane with a molecular weight cut off of 100000 to separate liposomes from non-entrapped drug. A 300µl sample of liposomes was added to the sample reservoir and centrifuged at 1000g for 3min (MSE Microfuge, UK). The filtrate

containing only non-entrapped drug was sampled and analysed for PXB content by scintillation counting.

### **3.3.13. Reduction of liposome size by extrusion**

Liposome extrusion is the process whereby multilamellar liposomes are forced through filters with defined pore sizes to obtain a liposomal preparation with a size distribution similar to the diameter of the filter pore. A custom-made extrusion device was used. The 'extruder' (Lipex Biomembranes Inc., Vancouver, B.C.) is a stainless steel filter holder capable of operating at pressures up to 800lb/in<sup>2</sup>. Sample ports facilitate multiple extrusion and the water-jacketed filter barrel enables the extrusion of lipids which have gel-liquid phase transitions that are above room temperature. The extruder was operated as defined in the Lipex technical information document. Samples were extruded by passing multilamellar (DRV) liposomes through two stacked nucleopore polycarbonate filters with the required pore size (Costar, UK) ten times. This has previously been shown to produce vesicles with a homogenous size distribution. Following extrusion liposomes were separated from free drug by GEC (section 3.3.11) and size distribution was verified by PCS (section 3.3.6)

### **3.3.14. Differential scanning calorimetry (DSC)**

Thermal analysis of the liposome preparations was performed with a Perkin-Elmer DSC-4 instrument using the Thermal Analysis Data Station (TADS) for data collection, handling and presentation (thermatograms were normalised). The liposome pellet (20µL) was hermetically sealed in an aluminium pan. An empty pan was used as the blank. Sample and blank were continually purged with nitrogen gas (20kg/cm<sup>2</sup>) and heated from 20 to 70°C, at a scan rate of 5°C/min. Temperature calibration was performed with an indium standard (melting point

156.4°C). For each liposome preparation, the transition temperature ( $T_m$ , °C) and the enthalpy of the transition (J/g) were determined from triplicate samples.

### 3.4. Results and Discussion

#### 3.4.1. Preparation of PXB DRV formulations: identification of compatible phospholipids

The previously reported interaction of PXB with phospholipids prompted a range of DRV formulations to be prepared and evaluated. Table 3.3 shows the phospholipid composition of the formulations initially tested. Results from the screening process enabled important guidelines to be established for the encapsulation of PXB.

Formulation	Lipid ratios ( $\mu\text{M}$ )	PXB added (mg)	Comments
EPC	33	2	milky-white suspension, vesicles seen using light microscopy
EPC:CH (2:1)	66:33	2	milky-white suspension, vesicles seen using light microscopy
EPC:CH (1:1)	33:33	10	milky-white suspension, vesicles seen using light microscopy
EPC:PG (9:1)	29.7:3.3	0.4	milky-white suspension, vesicles seen using light microscopy
EPC:PS (9:1)	29.7:3.3	0.4	milky-white suspension, vesicles seen using light microscopy
EPC:DCP (9:1)	29.7:3.3	2	milky-white suspension, vesicles seen using light microscopy
EPC:PI (9:1)	29.7:3.3	2	aggregate/white precipitate
EPC:PA (9:1)	29.7:3.3	2	aggregate/white precipitate
EPC:PG (9:1)	29.7:3.3	4	aggregate/white precipitate
EPC:PG (9:1)	29.7:3.3	6	aggregate/white precipitate
EPC:CH:PG (7:2:1)	23.1:6.6:3.3	2	aggregate/white precipitate
EPC:CH:DCP (9:5:1)	26.4:33:6.6	2	aggregate/white precipitate
EPC:SA (9:1)	29.7:3.3	2	vesicles formed gel-like pellet after washing

Table 3.3. Compatibility of phospholipids for the preparation of PXB DRVs

Vesicular preparations were obtained with all formulations composed solely of neutral lipids. Liposomes composed of egg PC with and without increasing ratios of cholesterol (10, 33, and 50% molar ratios) appeared well suspended and vesicular as determined by light microscopy. Previous studies using model liposome systems and lipid monolayers have shown that PXB interacts only weakly with zwitterionic phospholipids. The interaction of PXB with PC liposomes resulted in low levels of release of entrapped marker (glucose) which could be further diminished by the incorporation of cholesterol (Imai *et al.*, 1975). The adsorption of PXB to PC monolayers was found to be very low compared with phospholipids (Teuber & Miller, 1977). However care is needed in the extrapolation of monolayer interactions to liposome systems due to the influence exerted by surface curvature in binding events. PXB has been shown to interact with DMPC, but at much higher concentrations than those required for biological activity, indicating a different mechanism of destabilisation at this concentration (Mushayakarara & Levin, 1984). Similar activity with DPPC was observed in an earlier study (Pache *et al.*, 1972) which showed that PXB in high concentrations reduced the lipid endothermic transition. This result was not repeated by Hartmann *et al.* (1978) who did not observe any changes in the phase transition of DPPC when incubated with molar ratios of PXB up to 50 mol%. At the concentrations required for biological activity it is generally accepted that PXB does not appreciably bind to zwitterionic lipids such as the phosphatidylcholines (Babin *et al.*, 1987). This may partly explain the selectivity of PXB towards bacterial membranes which are devoid of PC and cholesterol (Hsuchen & Feingold, 1973). During the initial screening process a number of drug lipid ratios were used. Encapsulations (determined indirectly by the BCA or bioassay) varied from 0.018-0.034  $\mu\text{M}$  PXB/ $\mu\text{M}$  lipid for EPC, 0.003-0.014  $\mu\text{M}$  PXB/ $\mu\text{M}$  lipid for EPC:CH (2:1) and 0.03-0.054  $\mu\text{M}$  PXB/ $\mu\text{M}$  lipid for EPC:CH (1:1). However, the importance of these values lies in the qualitative confirmation of PXB encapsulation in vesicles which appeared to possess the correct gross morphology using light microscopy. A more systematic study of encapsulation efficiencies is described in section 3.4.2.

Successful encapsulation was also achieved with liposomes composed of egg PC and 10 mol% of the positively charged amphiphile, stearylamine. Due to the cationic nature of PXB at physiological pH, it would not be expected to adsorb to positively charged bilayers. Teuber *et al.* (1977) did not show any absorption to stearylamine monolayers and SA was effective in reducing binding of PXB to *E. coli* lipids. Initial encapsulation values were obtained as for neutral liposomes and varied from 0.015-0.017  $\mu\text{M}$  PXB/ $\mu\text{M}$  lipid. Vesicular structures were seen using light microscopy, although a looser/gel-like pellet was obtained after centrifugation and washing, possibly due to highly repulsive electrostatic forces between vesicles.

Although PXB was successfully encapsulated within neutral and positively charged DRV, the incorporation of negatively charged phospholipids resulted in a number of unsuccessful preparations. The difficulties encountered with anionic phospholipids are predictable given the wealth of data accumulated through studies intended to elucidate the mechanism of antimicrobial action and selectivity of PXB, or, which utilised PXB as a simple model for membrane-protein interactions.

The first negative amphiphile used was phosphatidic acid (PA) which carries a single negative charge at physiological pH. On addition of PXB to a solution of SUV composed of EPC:PA (9:1 molar ratio), prior to freezing and lyophilisation, an increase in turbidity was noted, indicating vesicle fusion and aggregation (Aramaki & Tsuchiya, 1989). Rehydration resulted in instant formation of a gritty white precipitate, which when viewed using light microscopy, appeared devoid of vesicular structures. A strong interaction has previously been noted with PA bilayers whose lateral chain packing was considerably disturbed by the peptide region of PXB. It was also proposed that the branched fatty acid tail served to anchor the peptide within the matrix (Beurer *et al.*, 1988). Freeze-fracture microscopy of liposomes composed of DPPA appeared aggregated, large and multilamellar after incubation with PXB. These morphological alterations were greater with increased PXB concentration and were interpreted as the result of fusion and leakage events (Kubesch *et al.*, 1987). The presence of

depressions in fractured membranes indicated the formation of lipid-polymyxin domains. The importance of hydrophobic/electrostatic interactions in the formation of domains has been studied using polymyxin B nonapeptide (PXBN). PXBN differs from PXB in possessing only the peptide portion of the molecule, the branched fatty acid tail is removed by enzymatic cleavage using ficin (Vaara & Viljanen, 1985). It was found that both PXB and PXBN caused interdigitation of DPPA, inferred from effects on chain motion using spin probes, which indicated that penetration of hydrophobic peptide side-chains bound electrostatically on the surface was sufficient to induce this phenomenon. However interdigitation may be maintained more easily using PXB due to greater penetration of its acyl chain. The phase transition of DPPA was decreased by 20°C after incubation with PXB, indicating disordering of the hydrocarbon chains. PA monolayers have also been shown to have a strong affinity for PXB (Teuber & Miller, 1977). A model for the high affinity binding of PXB with acidic phospholipids has been proposed by Hartmann *et al.* (1978). According to this model, one molecule of PXB carries five positive charges at physiological pH and binds up to 5 molecules of PA. This results in elastic distortion of the lipid membrane with the formation of domains of PXB-bound lipids. Each domain exhibits a heterogeneous structure with an inner core in which strong electrostatic and hydrophobic interactions are present, surrounded by a hydrophobic annular ring. Binding curves for this process are sigmoidal suggesting that the interaction is a cooperative process. The spatial arrangement of PXB with acidic monolayers is such that the fatty acid chain penetrates the lipid bilayer with the short-charged chain anchoring the peptide within the phospholipid head-group region. The polar head-group of PXB has the shape of an elliptical disc and is orientated flat on the membrane surface. The whole molecule is completely asymmetric and will thus cause a strong asymmetric distortion of the lipid matrix. The precipitation observed with EPC:PA DRV preparations can therefore be explained through interaction of PXB with PA through a combination of hydrophobic and electrostatic forces resulting in the formation of a non-colloidal hydrophobic aggregate.

Phosphatidylglycerol (PG) was also used as a negatively charged amphiphile. In this case the interaction with PXB was more complex than that observed with PA. Initially it was



observed that liposome preparations formed below a PG:PXB ratio of 8:1. Increasing PXB concentration resulted in the formation of a white precipitate similar to that observed with PA. When the supernatants of the successful preparations were analysed for PXB, using either the BCA or bioassay, no PXB was detected. This indicated that PXB was completely bound to PG within the lipid bilayer or that any PXB in the supernatant was bound to PG and therefore unable to react with the BCA reagent or retain any antimicrobial activity. The difficulties encountered with determining encapsulation directly using BCA/bioassay meant that this hypothesis could not be confirmed at this stage of development.

Babin *et al.* (1988) studied the binding of PXB with DPPG bilayers by spectroscopic methods. A macroscopic phase separation was noted when excess PXB was present. This was dependent on the charge saturation with a precipitate observed when the PXB:DPPG ratio  $>5$ , but at a ratio  $<5$ , DPPG remained associated with the vesicles. Although the data indicated formation of stable vesicles at a ratio of  $<8$ , the presence of EPC may exert a protective effect hence allowing the drug lipid ratio to be slightly increased (Imai *et al.*, 1975). Both electrostatic and hydrophobic forces participate in stabilising PXB at the bilayer/solution interface (El Mashak & Tocanne, 1980). It was suggested that the hydrophobic tail of PXB penetrates the bilayer and interacts with the phospholipid acyl chains. This interaction has been described for PG in both the fluid and gel states. The binding of PXB to PG differs from that of PA in that it is not cooperative (Babin *et al.*, 1987). Therefore it appears that stable preparations were obtained when PXB was added in a low concentration (approximately below that required for charge saturation).

The binding of radiolabelled PXB to a number of anionic phospholipids was studied by Teuber *et al.* (1977). Binding of PXB was found to be of a similar magnitude for phosphatidic acid, phosphatidylserine, phosphatidylinositol, dicetylphosphate and phosphatidylglycerol. Therefore it can be assumed that the quantity of bound PXB is independent of the chemical nature of the phospholipid headgroup. In the current study similar preparations were obtained with EPC:PS (9:1), EPC:DCP (9:1) and EPC:PG (9:1)

formulations. However the inclusion of cholesterol (50% molar ratio) resulted in precipitation. Cholesterol may hinder PXB penetration of the bilayer or induce a macroscopic phase separation of PXB-lipid conjugates. PI appeared to bind in the same way as PA to PXB as all preparations immediately precipitated upon rehydration.

In summary, the initial screening of phospholipids for use in DRV formulations was successful in identifying compatible lipids. Neutral and positive formulations produced vesicular preparations. Anionic phospholipids differed in suitability for liposome formulations, with PA and PI precipitating with all PXB concentrations. PG, PS and DCP formed liposomes when PXB was added in quantities less than that required for charge saturation. Aggregation occurred when PXB was present in excess of this level and cholesterol caused aggregation in all cases. Direct measurements of encapsulation are needed to confirm complete sequestration of PXB within the vesicular compartment as was suggested by preliminary analysis of supernatant washes by the BCA and bioassays.

#### **3.4.2. Encapsulation efficiencies of PXB DRVs: effect of initial drug loading**

Four neutral formulations, EPC, EPC:CH (9:1), EPC:CH (2:1) and EPC:CH (1:1) were formulated with increasing PXB concentrations in order to establish an optimal PXB loading for a constant quantity of lipid (66 $\mu$ M). All formulations were prepared by the DRV method and assayed for PXB content by scintillation counting of [<sup>3</sup>H] PXB (section 2.3.4). Encapsulations were estimated both directly from the resuspended liposome pellet and indirectly from the supernatant washes. Good agreement was seen between direct and indirect encapsulation values. The results discussed are those determined by the direct method.

The amount of PXB added to SUV, prior to freezing and lyophilisation, was increased over the range 3, 6, 9 and 12mg/66 $\mu$ M lipid. With EPC liposomes, drug encapsulation, expressed

as a percentage of the total PXB initially added, decreased from  $47.46 \pm 0.43\%$  (3mg loading) to  $27.42 \pm 0.31\%$  (12mg loading) (figure 3.3). However, when expressed as an encapsulation efficiency ( $\mu\text{M PXB}/\mu\text{M lipid}$ ), encapsulations rise with loadings up to 9mg after which efficiencies appear to plateau (figure 3.4). The entrapment yields observed with EPC liposomes are of a similar magnitude to values described for amikacin, tobramycin, ticarcillin and chloramphenicol (Lagacé *et al.*, 1991; Onur *et al.*, 1992; Ravaoarino *et al.*, 1993). The reduced efficiencies observed at the highest loading may indicate some interference with vesiculation or a saturation of membrane binding of PXB. However, given the weak interaction with neutral phospholipids, binding to EPC bilayers is not likely to be the major site of encapsulation as the majority of PXB should be encapsulated within the aqueous volume of the DRVs. The critical micelle concentration of PXB has been previously reported as 6% (w/v) (Lawrence *et al.*, 1993). As the first rehydration step routinely used an aqueous volume of  $200\mu\text{l}$ , a 12mg drug loading would result in the formation of PXB micelles which may not be encapsulated as efficiently as free PXB or they may interfere with bilayer assembly during the initial rehydration step. The 9mg loading was adopted as the maximum drug to lipid ratio when  $66\mu\text{M}$  lipid was used. Loadings may be increased with higher lipid quantities (Wichert *et al.*, 1992) but the  $66\mu\text{M}$  was used to maximally encapsulate PXB using minimal phospholipid quantities.

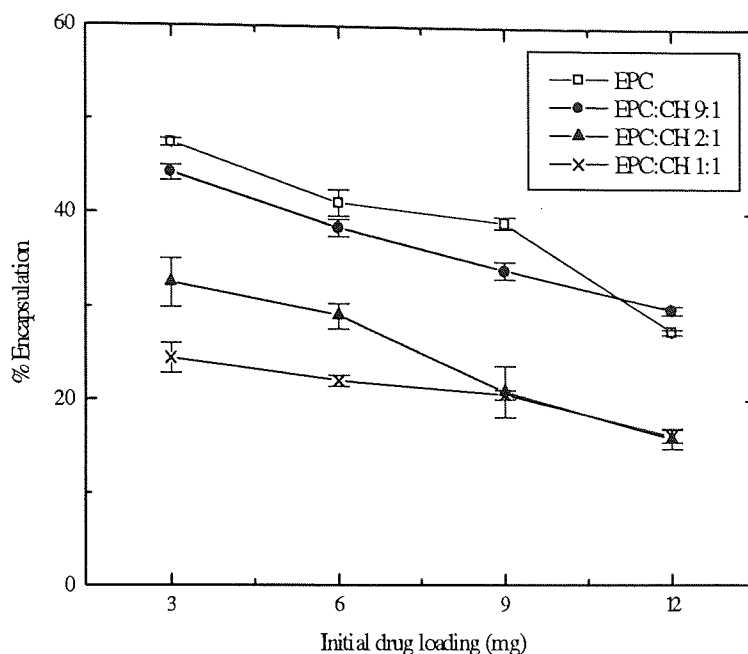


Figure 3.3. Encapsulation of PXB within EPC based DRVs as a function of cholesterol concentration and initial PXB loading. Each point represents the percentage mean  $\pm$  standard deviation of three independent preparations

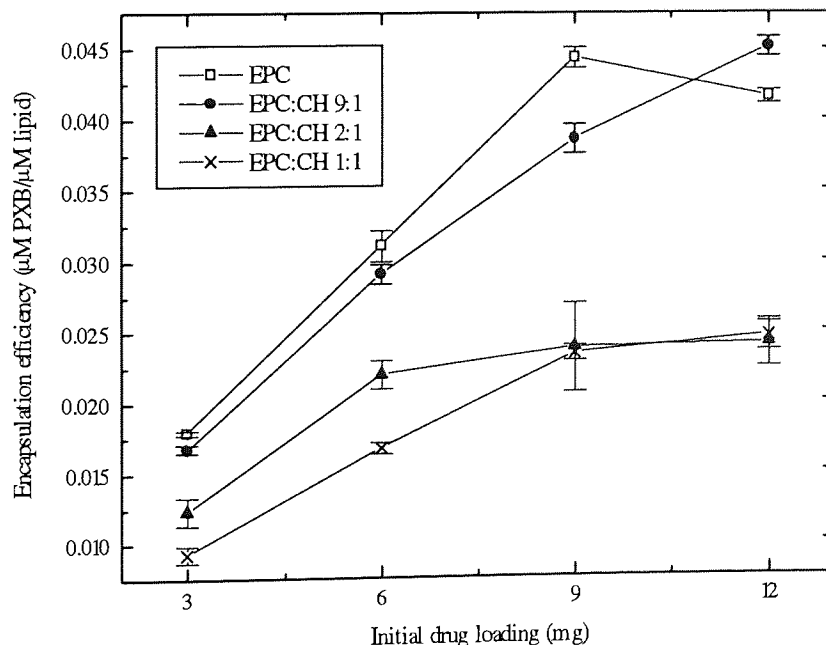


Figure 3.4. Encapsulation efficiencies of DRVs as a function of cholesterol concentration and initial PXB loading. Each point represents the mean  $\pm$  standard deviation of three independent preparations

Encapsulation studies were performed using increasing PXB concentrations with increasing molar ratios of cholesterol (0, 10, 30 and 50% with egg phosphatidylcholine (EPC), total lipid 66 $\mu$ M). It was found at all PXB loadings (3,6,9,12mg) that encapsulations decreased with increased cholesterol (CH) molar ratio (figure 3.3). This effect on drug loadings can be attributed to the changes in membrane packing caused by cholesterol. Above the transition temperature, high CH concentrations ( $\geq 30\%$ ) cause closer membrane packing which decreases bilayer fluidity (New, 1990). This condensing effect may reduce the interaction of the fatty acyl chain of PXB with the hydrophobic hydrocarbon chains of the bilayer. This effect was clearly observed with DRV preparations which contained high molar ratios of cholesterol. In the presence of CH, a PXB loading of 9mg appeared to be the optimal loading concentration, as observed with EPC vesicles.

Using the optimal loading of 9mg (with 66 $\mu$ M total lipid), the effect of CH on encapsulation was investigated using DSPC vesicles. DSPC has a phase transition of 54 $^{\circ}$ C (Szoka & Papahadjopoulos, 1980), therefore at room temperature DSPC vesicles are in the 'solid' gel state. The encapsulation efficiency of DSPC liposomes was 33.09 $\pm$ 5.32%, which was significantly different from the value observed with EPC vesicles (59.61 $\pm$ 2.89%). Although EPC and DSPC vesicles exist in the fluid and gel states respectively at room temperature, encapsulation and annealing are carried out above the  $T_m$ . Therefore membrane interaction with PXB always occurs in the disordered fluid liquid crystalline phase. The reduced encapsulation seen with DSPC liposomes may suggest preferential association of PXB with bilayers composed of unsaturated phospholipids.

As with EPC based liposomes, the incorporation of CH resulted in reduced encapsulation efficiencies. Below the  $T_m$ , cholesterol pushes the phospholipids apart, the packing of the headgroups is weakened and the fluidity of the gel phase is increased (New, 1990). However as vesiculation is performed at a temperature above the  $T_m$ , where cholesterol decreases membrane fluidity and induces closer packing with a reduction in the freedom of acyl chains. Therefore the lower encapsulations with DSPC CH (2:1) (22.65 $\pm$ 1.49) and DSPC:CH (1:1)

( $24.43 \pm 1.37$ ) may also be attributable to membrane condensation during the rehydration stage. In addition to reducing bilayer penetration of the hydrophobic tail of PXB, CH may also disrupt hydrogen bonding of the cationic headgroup of PXB with phosphate groups of the phospholipid headgroups. This may be mediated by the positioning of CH within the membrane. The hydroxyl group of CH is positioned level with the acyl chain carboxyl groups and the planar steroid nucleus parallel with the first nine carbon atoms of the acyl chain. However as the effect of CH is not significantly different ( $p < 0.05$ ) with 30% and 50% molar ratios, reduced encapsulations are more likely to be due to the membrane modifying properties of CH.

Decreased encapsulation efficiencies with increased CH have previously been described for suramin, the hexasodium salt of bis(naphthalenetrisulfonic acid) (Chang & Flanagan, 1994). Suramin is a large polyanion (mw 1429) with six negative charges under physiological conditions. It was proposed that in addition to bilayer condensation reducing accessibility of suramin to the lipid interior, CH also interrupted suramin intercalation *via* ionic effects with choline headgroups. Gross and Ehrenberg (1989) have also described decreased binding constants for a haematoporphyrin derivative and photofrin II in the presence of CH. The encapsulation of a cationic tridecapeptide, indolicidin, was also reduced by CH (Ahmad, 1995)

In summary, the encapsulation results with EPC and DSPC based vesicles have illustrated the importance of membrane composition. Encapsulations are reduced by the use of a saturated lipid such as DSPC and are further reduced by the inclusion of CH. Although the PXB binding interaction with neutral phospholipids has been classed as negligible, encapsulation values indicate a fraction of PXB which is membrane associated. Further evidence for surface/membrane localisation from zeta potential studies is discussed in section 3.4.7.

### 3.4.3. Effect of charged phospholipids on encapsulation efficiencies

The inclusion of negatively charged lipids or amphiphiles such as PS, PA, PI, PG and DCP, or positively charged amphiphiles such as SA will tend to increase interlamellar repeat distances and swell the vesicle structure leading to a greater entrapped aqueous volume (Kulkarni *et al.*, 1995). The magnitude of this effect is increased in low-ionic strength buffers or non-electrolytes because the electrostatic forces that mediate the effect are even greater under these conditions. The presence of charged lipids also increases the physical stability of the preparation by decreasing aggregation (Martin, 1990; Riaz *et al.*, 1989). The encapsulation efficiency of doxorubicin, a positively charged amphiphile, is increased by the presence of negatively charged lipids (Amselem *et al.*, 1990). The influence of anionic and cationic lipids on the encapsulation of gentamicin in DRV has been studied by Cajal *et al.* (1992). Encapsulation was decreased by PS and increased with SA, a surprising result given the cationic character of gentamicin. The authors did not speculate on the mechanism of this effect.

The effect of the positively charged amphiphile, SA, on PXB encapsulation was studied by incorporating a 10% molar ratio in EPC DRV. Again, a drug loading of 9mg/66 $\mu$ M total lipid was used. It was found that the encapsulation (table 3.4) was significantly reduced ( $p < 0.05$ ). As PXB is highly cationic at physiological pH, it appears reasonable to suggest that repulsive electrostatic interactions deter the association of PXB with or within the aqueous space of positively charged bilayers. The interaction of PXB with bilayers containing SA has previously been reported as minimal (Teuber & Miller, 1977).

As previously discussed only a few anionic phospholipids were suitable for the encapsulation of PXB (section 3.4.1). From this group of anionic phospholipids, DCP was further studied for DRV formulation. A 10% molar ratio was included in EPC liposomes and PXB loaded in a 9mg/66 $\mu$ M lipid ratio. An encapsulation percentage (table 3.4) of  $48.10 \pm 4.96$  ( $n=3$ ) was observed which was not significantly different from that seen with EPC liposomes ( $50.52 \pm$

7.42, n=9). BCA analysis of the supernatants of these liposomes indicated ~90% encapsulation contradicting the value calculated using [<sup>3</sup>H] counts. PXB binds with DCP through charge interaction of cationic amino residues and negatively charged phosphate groups (Hsueh & Feingold, 1973). The masking of the positively charged sites of PXB by DCP prevents coupling with BCA and therefore gives a low result for PXB concentration in the supernatant. Bioassay analysis of these supernatants failed to detect PXB. This is consistent with the charge interaction between PXB and DCP forming an inactive PXB/DCP complex. A previous study noted that PXB induced the phase separation of DPPG from DMPC/DPPG bilayers (Babin & Pezolet, 1988). The PXB/DPPG complex precipitated under the charge saturation condition.

It would therefore appear that the encapsulation of PXB within anionic vesicles results in removal of DCP from the bilayer or the neutralisation of bilayer-bound DCP negative charge. The reduction of negative groups at the vesicle surface would reduce the surface potential (*i.e.*, make it less negative), an effect which has been confirmed by zeta potential studies (section 3.4.7). In addition the similarity of encapsulation values of neutral and anionic vesicles supports the hypothesis that PXB/DCP complexes are not held within the liposome compartment. The failure of negative lipids to augment encapsulation efficiencies and to maintain a surface charge diminishes their utility for the formulation of LPXB.

#### 3.4.4. Inclusion of stealth lipids

The development of hydrophilic lipids which could delay vesicle uptake by the MPS has revitalised the use of liposomes in the treatment of a wide range of diseases involving non-MPS tissues (Gregoriadis, 1993). MPS-avoiding or Stealth<sup>®</sup> liposomes appear to have considerable potential for the treatment of extracellular bacterial infections. Stealth liposomes show increased accumulation in the inflamed lungs of *Klebsiella pneumoniae* infected rats (Bakker-Woudenberg *et al.*, 1993). Using the same animal model, stealth vesicles loaded with ceftazidime or gentamicin increased the survival outcomes of infected animals (Bakker-



Woudenberg, 1995). This highlights the potential of a stealth PXB formulation to systemically treat CF lung infections. DSPE-PEG<sub>1900</sub> was included in a 10% molar ratio with EPC and DSPC formulations which also contained 33% molar ratio of CH. Such formulations have demonstrated extended blood residence times (Allen, 1994). DSPE-PEG carries a single negative charge at physiological pH which is shielded by hydrophilic PEG chains. Although PXB interacts strongly with negatively charged lipids, the steric hindrance appears to prevent charge-coupling occurring. Successful formulation of PXB in long-circulating liposomes has been achieved although the low entrapment efficiencies of DSPC-based vesicles may limit their therapeutic usefulness.

The encapsulation efficiency of EPC:CH:PEG (2:1:0.2) was significantly lower than the equivalent formulation without DSPE-PEG. This may be related to the steric effects of the PEG polymer chains reducing interaction of PXB with the bilayer. This effect is not limited to DSPE-PEG as similar encapsulation values were obtained when GM<sub>1</sub> was used (table 3.4). This points to the lower encapsulation being a general effect of stealth-type lipids and not specifically related to the hydrophilic polymer or hydrophobic anchor lipid.

The lowest encapsulation of all DRV tested was seen with DSPC:CH:DSPE-PEG (2:1:0.2). This is likely to be the sum of the effects of unfavorable formulation components. As previously noted, entrapment is reduced by DSPC and CH. The addition of DSPE-PEG further reduces entrapment compared to that seen in the absence of PEG-lipid.

Formulation	Phospholipid molar ratio	Encapsulation %	Encapsulation efficiency ( $\mu\text{M}$ PXB/ $\mu\text{M}$ lipid)	Drug:lipid ratio
EPC	-	50.52 $\pm$ 7.42	0.057	1:17.5
EPC:CH	2:1	38.96 $\pm$ 1.58	0.044	1:22.7
EPC:CH	1:1	32.88 $\pm$ 4.84	0.037	1:27.0
EPC:SA	9:1	33.8 $\pm$ 4.35	0.038	1:26.3
EPC:DCP	9:1	48.10 $\pm$ 4.96	0.055	1:18.2
EPC:CH:PEG	2:1:0.2	27.2 $\pm$ 2.13	0.031	1:32.3
EPC:CH:GM <sub>1</sub>	2:1:0.2	27.72 $\pm$ 1.38	0.032	1:31.2
DSPC	-	33.09 $\pm$ 5.32	0.038	1:26.3
DSPC:CH	2:1	22.65 $\pm$ 1.49	0.026	1:38.5
DSPC:CH	1:1	24.43 $\pm$ 1.37	0.028	1:35.7
DSPC:CH:PEG	2:1:0.2	11.85 $\pm$ 0.59	0.014	1:71.4

Table 3.4. Encapsulation of PXB within liposomes of varying composition prepared by the DRV method. Drug loading 9mg/66 $\mu\text{M}$  lipid. Each encapsulation represents the mean $\pm$ standard deviation of at least three preparations

### 3.4.5. Differential scanning calorimetry (DSC) of the interaction between PXB and DSPC bilayers

Although the interaction of PXB with neutral phospholipids has been regarded as negligible, the marked influence of membrane composition on DRV entrapment of PXB suggests that bilayer association may represent a significant site for encapsulation. In a previous study (Lawrence *et al.*, 1993), DSC studies of PXB and aqueous phospholipid dispersions showed an apparent interaction. High concentration of entrapped and exogenous PXB (up to 12%w/v) reduced the transition of hydrogenated egg phosphatidylcholine (HEPC). However, this was most likely the result of surfactant activity of PXB at this concentration disrupting

bilayer structure. In order to elucidate the effect of increased loadings on the formation of DRV, PXB was loaded in increasing ratios (9, 18, 27 and 36mg) with DSPC (66 $\mu$ M) vesicles. The resulting preparations were separated from free drug by centrifugation and encapsulation determined by scintillation counting. The centrifuged preparations were subsequently used for DSC analysis as described in section 3.3.14.

The entrapment values are shown in table 3.5. Light microscopy was used to confirm gross morphology and preparations appeared vesicular with all loadings.

Initial loading	% Encapsulation	Encapsulation efficiency ( $\mu$ M PXB/ $\mu$ M lipid)
9mg	33.09 $\pm$ 1.07	0.038
18mg	21.73 $\pm$ 2.41	0.049
27mg	20.05 $\pm$ 1.63	0.068
36mg	17.72 $\pm$ 1.49	0.081

Table 3.5. Encapsulation efficiencies of DSPC DRV loaded with high PXB levels. Values determined directly from liposomal pellet by scintillation counting of [ $^3$ H]-PXB (each point represents the mean $\pm$ sd of three determinations).

Encapsulations with the 9mg/66 $\mu$ M ratio were similar to those previously observed. With higher PXB loadings entrapment percentage diminished but the drug to lipid ratio after entrapment increased showing greater total amount of PXB was entrapped. Therefore it was possible to study the effects of the increased vesicular load of PXB on DSPC thermal events.

Initial loading (mg)	Transition temperature (°C)	Enthalpy of transition (J/g)	Comments
0	54.31±0.28	5.62±2.32	Sharp peak
9	54.63±0.53	4.07±1.38	Sharp peak
18	54.34±0.70	3.22±1.23	Shoulder on peak
27	54.45±0.23	0.94±0.30	Flattened/broad peak
36	54.24±0.57	1.44±0.73	Flattened/broad peak

Table 3.6. Changes induced in DSPC peak gel-liquid crystalline phase transition temperature by entrapped PXB (each point represents the mean±sd of six determinations).

The thermatogram of empty DSPC vesicles shows a major transition endotherm centered at 54°C (figure 3.5). This peak is sharp and symmetrical with an enthalpy of 5.62±2.32 J/g. With the incorporation of PXB the temperature of the main transition does not change, even at the highest loading. The peak shape is maintained with an initial loading of 9mg and the phase transition enthalpy is not significantly reduced (4.07±1.38 J/g). However, at and above an entrapped drug to lipid ratio of 0.049µM PXB/µM lipid, the transition begins to broaden and a shoulder on the peak is evident. With further increases in entrapped PXB the transition is gradually flattened. This information may be used to investigate the mechanism of PXB binding to the bilayer. As the  $T_m$  of empty DSPC vesicles does not significantly differ from that of loaded vesicles (see table 3.6), it may be proposed that PXB has little effect on the mobility of individual DSPC acyl side-chains. Cortisol-21 also has a similar effect on bilayers and although this compound is lipophilic, its interaction model with phospholipids has similarities to that of PXB. The primary interaction is with the phospholipid headgroup followed by subsequent penetration of the steroid nucleus into the lipid bilayer (Fildes & Oliver, 1978). Penetration of PXB into the bilayer is limited to the short length of the fatty acyl chain. A cholesterol-like action has been proposed for PXB (Pache *et al.*, 1972) but although a the DSPC endotherm displayed progressive broadening, the position of the  $T_m$  remained unaffected by drug loading. The insertion of the fatty acid side chain in the absence of significant headgroup binding is insufficient to completely disrupt DSPC vesicles. Vesicular preparations were observed with all loadings and no evidence of solubilisation was

seen. The broadening of the transition at 18, 27 and 36mg loadings may indicate that PXB is non-uniformly dispersed in the bilayer. Domains of bound PXB may therefore exist within the lamellae. The broadening of the endotherm can be interpreted as a decrease in the cooperativity of the transition reflecting some degree of disorder of the bilayer. Although dipole-dipole interaction of PXB with DSPC at the headgroup region may play a role, it is more likely that the interaction events demonstrated by DSC of loaded are the result of acyl chain penetration.

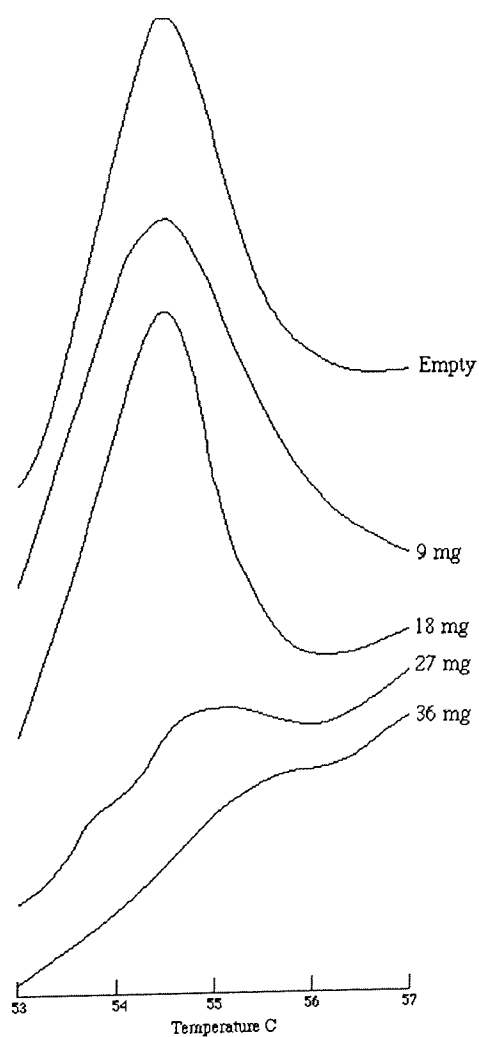


Figure 3.5. Changes in the main transition of DSPC by entrapped PXB.

#### 3.4.6. Membrane interaction of PXB: adsorption of PXB to preformed EPC vesicles

DSC studies of DSPC DRV containing entrapped PXB have confirmed that PXB does interact with neutral bilayers. It is also of interest to investigate adsorption or binding of PXB to preformed vesicles. EPC vesicles were chosen for this study in order to use bilayers which were in the fluid liquid-crystalline state at the conditions used. Binding under these conditions would be facilitated by the loose-packing of the bilayers. Under these conditions it would not be expected to incorporate a significant quantity within the aqueous core of the vesicles. EPC DRV were formed in the standard way and extruded 10 times through 0.8 $\mu$ m polycarbonate filters using the Extruder<sup>®</sup> (see section 3.3.13). A tracer quantity of [<sup>14</sup>C]-cholesterol was used as a lipid marker. The rationale for extrusion to produce vesicles with size diameter was to maximise the surface area for binding but minimise the possibility of PXB being entrapped within the aqueous core, a possibility if unilamellar vesicles are used. Vesicles with this size distribution (confirmed by laser diffraction, volume mean 0.87 $\pm$ 0.44 $\mu$ m, figure 3.7) are oligolamellar (Mayer *et al.*, 1986). Vesicles (33 $\mu$ M) were resuspended in phosphate buffer (5ml) containing a 0.5mg/ml solution of PXB and incubated at 37°C for 3hr. Scintillation counting was used to detect free and adsorbed PXB. Separation between vesicles and free drug was achieved by size exclusion gel chromatography as described in section 3.3.11. Liposomes were detected in the void volume by the appearance of [<sup>14</sup>C]-CHOL peak. Any [<sup>3</sup>H]-PXB associated with this peak was taken to represent adsorbed PXB. Free drug appeared separated in the included volume of the column.

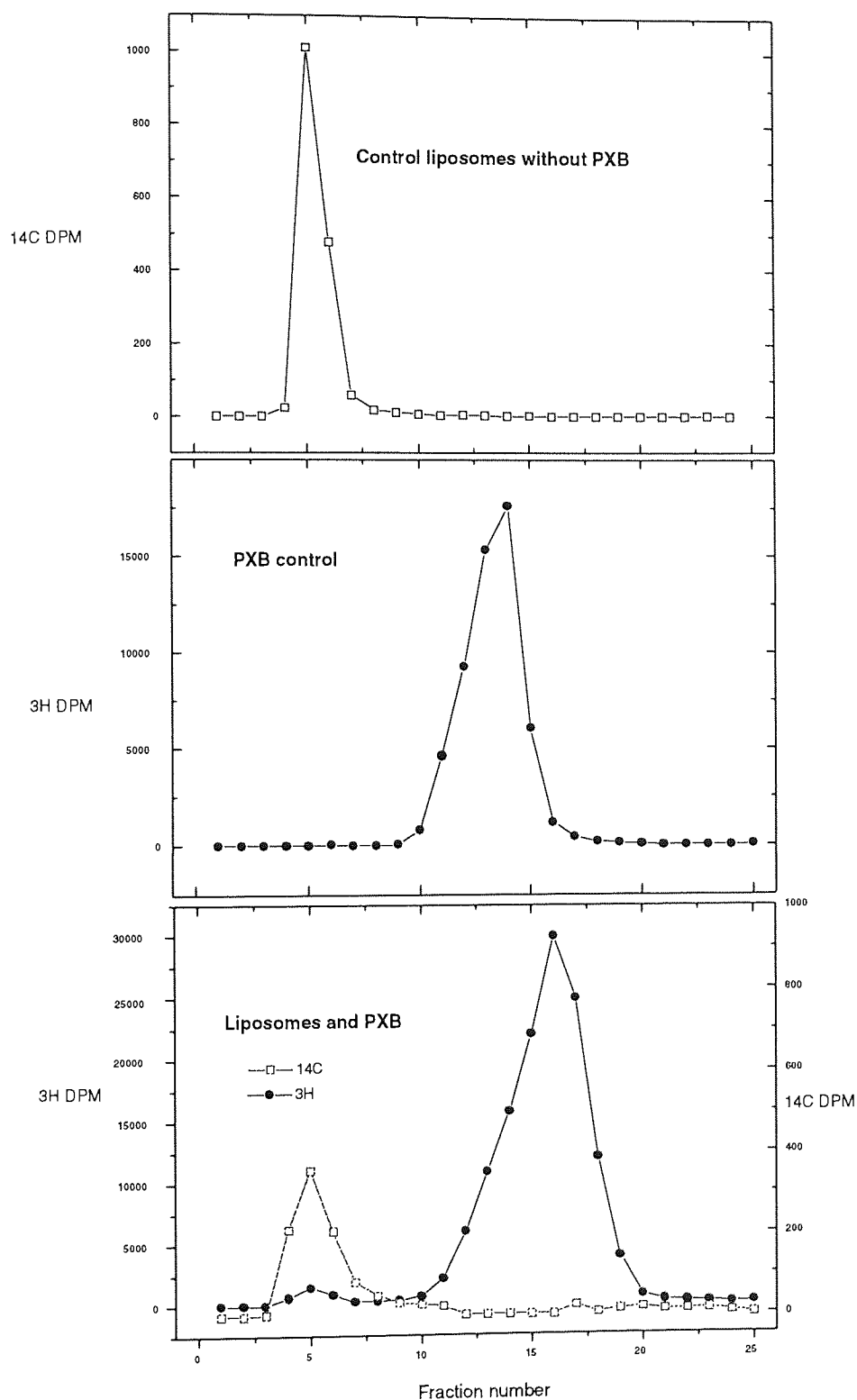


Figure 3.6. Adsorption of PXB to preformed EPC  $0.8\mu\text{m}$  vesicles: separation of vesicles and drug by gel exclusion chromatography

As can be seen from the chromatograms efficient separation is achieved between free drug and vesicles. Empty vesicles display a single peak due to  $[^{14}\text{C}]\text{-CHOL}$  which is evident in the void volume. Similarly when free PXB is applied to the column it is eluted as a single peak in

the later fractions (*i.e.*, the included volume). When the drug/vesicle suspension is applied to the column the two peaks due to the respective components are still resolved. However in addition to the [ $^{14}\text{C}$ ]-CHOL peak in the void volume a small [ $^3\text{H}$ ]-PXB peak was detected.

Therefore PXB would appear to associate with neutral bilayers in the fluid, loosely packed, liquid crystalline state. The quantity adsorbed is small, but as binding during the adsorption experiment is only to the outer surface of multilamellar vesicles, the bulk of lipid is unavailable for binding of PXB. Surface effects of membrane-associated/encapsulated PXB were further investigated by zeta potential studies (see section 3.4.7).

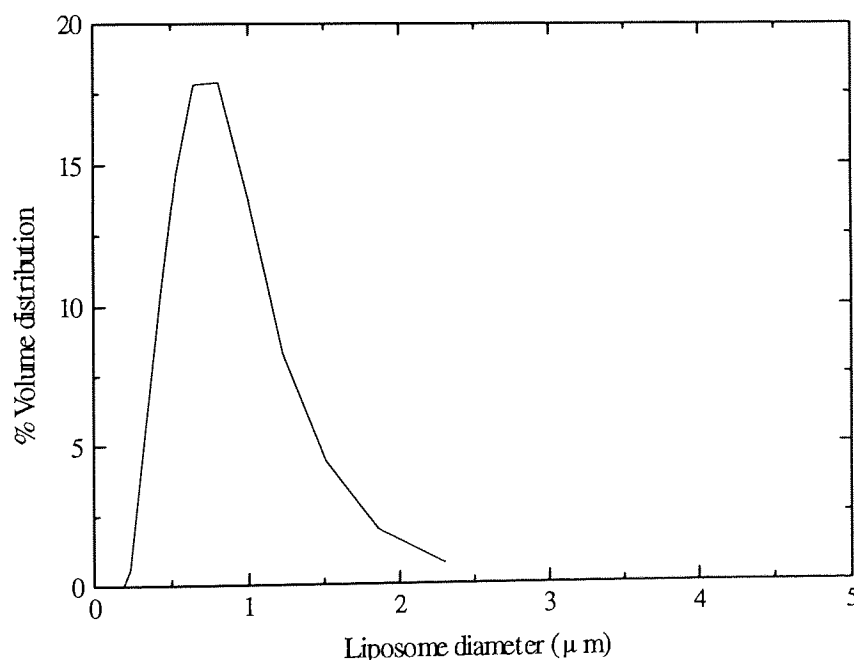


Figure 3.7. Laser diffraction size distribution (Malvern Mastersizer E) of DSPC vesicles after 10 extrusions through a 0.8µm filter.



### **3.4.7. Membrane interaction of PXB: zeta potential of LPXB formulations**

The formulation, DSC and adsorption studies have shown that PXB associates with the bilayers of EPC and DSPC based DRV formulations. The topology of binding may have several implications for the release profiles and stability of LPXB. PXB with its five positive charges at physiological pH would be expected to influence the surface charge of vesicles. Several methods may be used for the determination of surface charge and zeta potential of liposomal formulations.

The electrostatic surface potential of liposomes may be measured directly or indirectly by a variety of techniques which have been reviewed comprehensively by Cevc (1993a). Direct methods utilise molecular probes which may be fluorescent, paramagnetic or nuclear magnetic resonance probes. Partitioning of charged probes to bilayers is a function of the electrostatic forces involved. However, the concentration of the probe used may effect the electrostatic potential measured and the probe concentration needs to be constant or systematic measurements involving a range of probe concentrations need to be performed. A compromise between probe concentration and sensitivity needs to be made in order to minimise probe-induced membrane defects. High concentrations of probes tend to form separate domains and may also induce liposome fusion (Cevc, 1993a). These concerns along with the need for calibration make the use of direct methods a time-consuming method of characterising liposomal surface charge. For these reasons the method of choice for this work is laser doppler velocimetry, a indirect microelectrophoretic technique which can reproducibly and reliably detect surface potential changes at the millivolt level. Commercial instruments such as the Malvern Zetamaster® used in this study, offer several advantages over classical microelectrophoresis. With the classical technique a voltage is applied between two electrodes and the velocity of microscopically visible vesicles travelling between the electrodes is measured. This method is time-consuming and tedious and measurements are made using a relatively small number of particles. Non-biased operator selection of particles is inevitable. With commercial instruments statistically significant results may be obtained

with a small number of measurements as a large number of particles are measured each time. The principles and equations used to convert electrophoretic mobility to zeta potential are discussed in section 3.3.7.

The electrophoretic surface potential of liposomes is an important determinant of both *in vivo* and *in vitro* stability. The presence of charged lipids can reduce the likelihood of aggregation following liposome formation (Martin, 1990). The surface charge may also effect *in vivo* properties with negatively charged phospholipids such as PS and PG enhancing opsonic clearance from the circulation (Allen & Paphadjopoulos, 1993). Therefore binding of PXB may change physical stability and *in vivo* characteristics through modification of liposomal zeta potential. The extent of zeta potential alteration was investigated by routine measurement of this parameter whenever a DRV formulation was prepared. The methodology and sample preparation are detailed in section 3.3.7.

Formulation	Zeta potential in PBS pH 7.4 (mV)	Zeta potential in 0.02M diphosphate buffer pH 7.4 (mV)
EPC empty	-2.6±1.0	-3.9±3.6
EPC loaded	+1.2±0.3	+3.2±2.3
EPC:CH (2:1) empty	-3.0±1.0	-4.7±1.7
EPC:CH (2:1) loaded	-1.0±0.4	+1.1±1.4
EPC:CH (1:1) empty	-1.8±1.2	-2.6±0.7
EPC:CH 1:1 loaded	-2.9±0.8	-2.2±1.2
EPC:CH:PEG 2:1:0.2 empty	-2.2±1.0	-3.2±0.3
EPC:CH:PEG 2:1:0.2 loaded	-1.5±0.8	-1.4±0.9
DSPC empty	-0.7±1.0	-1.7±1.5
DSPC loaded	-2.0±1.2	-0.5±0.4
DSPC:CH 2:1 empty	-3.8±1.7	-8.6±2.0
DSPC:CH 2:1 loaded	-6.0±0.3	-7.2±1.4
DSPC:CH 1:1 empty	-5.8±1.9	-9.4±0.4
DSPC:CH 1:1 loaded	-5.4±0.8	-6.8±1.0
DSPC:CH:PEG 2:1:0.2 empty	-2.3±1.0	-4.1±0.5
DSPC:CH:PEG 2:1:0.2 loaded	-2.5±0.8	-3.9±0.2
EPC:SA empty	+13.6±0.8	+22.8±0.7
EPC:SA loaded	+12.8±0.2	+24.2±0.4
EPC:DCP empty	-19.6±0.9	-44.5±0.8
EPC:DCP loaded	-5.5±0.3	-10.9±0.7

Table 3.7. Zeta potential values of unloaded and loaded LPXB DRV formulations. All loaded values relate to washed vesicles after a standard initial loading of 9mg PXB/66µM lipid. Zeta potentials are the mean of those determined from five measurements for at least three preparations.

The neutral unloaded liposomes (both EPC and DSPC) had a small negative potential in both isotonic PBS pH 7.4 and 0.02M diphosphate buffer. The lower values of zeta potential observed for this and other formulations in PBS relative to 0.02M diphosphate are related to the tonicity of the media. Increased ionic strength results in increased shielding of the surface potential which gives rise to a decreased zeta potential (Shaw, 1980). The values obtained are in agreement with those previously reported for vesicles with this lipid composition (Lawrence *et al.*, 1993). Neutral EPC liposomes were shown by Schlieper *et al.* (1983) to have zero zeta potential at pH 7. However Law *et al.* (1988) found similar preparations to have a slightly negative potential. Although the liposomes are composed of a zwitterionic phospholipids, negative values may be caused by differences in buffer pH, ionic strength or adsorption of negative ions such as hydroxyl ions (Makino *et al.*, 1991; Shaw, 1980).

Loaded vesicles composed of EPC had a small positive potential in both buffers. Bilayer associated PXB is likely to be the source of the surface potential change. The small magnitude of the positive potential is due to the low drug to phospholipid ratio (see table 3.7). The molar ratio of encapsulated drug also accounts for any non-bilayer interacting PXB, encapsulated within the aqueous volume of DRV. Interaction of bilayer bound PXB through hydrogen bonding and dipole interactions with phospholipid headgroups will further diminish the positive potential at the vesicle surface. It is of note that a positive potential was not observed with loaded DSPC vesicles. This may be due to a number factors. Firstly, the drug to phospholipid ratio of DSPC vesicles is ~35% less than that of EPC formulations. It is also possible that the spatial arrangement of PXB within solid DSPC bilayers does not facilitate interaction of PXB and choline headgroups resulting in a smaller proportion of encapsulated drug interacting with the bilayer. Therefore it would appear from these observations that the charge imparted to a bilayer by PXB is, unsurprisingly, a concentration related phenomenon.

The incorporation of CH in 33 and 50% molar ratios did not change the zeta potential of EPC and DSPC based formulations which remained essentially neutral. CH is neutral and

therefore lacks an effect on the zeta potential of neutral phospholipid bilayers (Woodle *et al.*, 1992). DSPC based preparations have slightly more negative potentials than their EPC counterparts, which may be due to small differences in headgroup interactions brought about through packing changes. The aetiology of the small negative charge of both formulation types may again be due to the reasons outlined above. Only EPC:CH (2:1) preparations showed a change in zeta potential after loading with PXB. In addition this effect was only observed in the lower ionic strength buffer which perhaps indicates a smaller quantity of surface associated PXB. The zeta potential in 0.02M diphosphate ( $+1.1 \pm 1.4$  mV) was lower than that of EPC vesicles although this difference was not significantly different. All other formulations did not show a positive potential on loading which may reflect the reduced drug to lipid ratios observed with CH containing vesicles (see table 3.4).

The inclusion of DSPE-PEG<sub>1900</sub> in a 10% molar ratio in a typical Stealth formulation (EPC:CH:PEG/DSPC:CH:PEG 2:1:0.2) resulted in essentially neutral vesicles as expected. Woodle *et al.* (1992) have reported a neutral zeta potential for similar formulations. In this study a discrepancy between surface potential and electrophoretic mobility (or zeta potential) was seen. Surface potential was measured directly using a fluorescent probe and was found to be strongly negative in PEG containing formulations. It was proposed that the reduced zeta potential relative to surface potential was caused by hydrodynamic drag effects related to the polymer chains. The PEG chains also serve to shield the single negative charge of the lipid-polymer conjugate, an effect which is of paramount importance to the Stealth properties of this lipid (Allen & Paphadjopoulos, 1993). Loaded PXB did not alter the zeta potential of these formulations suggesting that PXB was prevented from interacting electrostatically with the negative charge of DSPE-PEG<sub>1900</sub> through steric hindrance by the PEG polymer chains. Surface located PXB would also be similarly masked by the polymer chains thereby minimising any PXB-induced zeta potential changes. It should be noted that the drug to lipid ratios of this phospholipid composition, particularly DSPC based vesicles, are lower than that seen with EPC/DSPC vesicles.

Positively charged vesicles were prepared by incorporating SA in a 10% molar ratio with EPC. Unloaded vesicles had a potential of  $+13.6 \pm 0.8$  mV in PBS pH 7.4 and  $+22.8 \pm 0.7$  mV in 0.02M diphosphate. No significant increase was observed with loaded vesicles. As the incorporation of PXB is reduced in cationic vesicles and perhaps more importantly, bilayer interaction is minimal due to repulsive electrostatic forces, PXB would not be expected to contribute to the zeta potential in this case. The detection of surface-located PXB using zeta potential data is made more difficult as any small positive charge imparted to the bilayer would be overshadowed by the presence of the positive amphiphile.

A 10% molar ratio of DCP in EPC based vesicles resulted in a strongly negative zeta potential in both PBS ( $-19.6 \pm 0.9$ ) and 0.02M diphosphate ( $-44.5 \pm 0.8$ ). However the zeta potential was strongly affected by the loading of PXB. As previously discussed, PXB interacts strongly with DCP resulting in removal of the negative amphiphile from bilayers. Remaining DCP may also interact with PXB changing the charge of the vesicles from a nominally negative value to neutral. The zeta potential of loaded vesicles in PBS ( $-5.5 \pm 0.3$ ) and 0.02M diphosphate ( $-10.9 \pm 0.7$ ) is significantly different from empty vesicles and approaches the zeta potentials of nominally neutral formulations. These data support the hypothesis of neutral liposome formation from anionic liposomes by PXB loading, as suggested from encapsulation data (section 3.4.3).

To summarise, zeta potential characterisation of LPXB has confirmed that PXB is bilayer-associated and may alter the zeta potential of these vesicles. This phenomenon is phospholipid dependent and appears related to drug to phospholipid ratio. There are implications of surface potential changes for *in vitro* and possibly *in vivo* stability of LPXB. Aggregation of vesicles increases as the zeta potential tends towards zero (Riaz *et al.*, 1989). As PXB creates a very small positive potential in neutral EPC vesicles and EPC:CH (2:1) the tendency towards aggregation and fusion may be increased. These events may increase liposome size and decrease the retention of PXB on storage. Release of PXB is discussed in section 3.4.12. *In vivo* interaction with tissue fluids is largely dependent on liposomal surface

characteristics. Of these, zeta potential plays a major role (Juliano & Stamp, 1975). Positively charged vesicles may exhibit accelerated *in vivo* clearance due to a number of mechanisms. Liposome size may be increased by adsorption of negatively charged plasma factors. Also, increased cellular interactions may be mediated by positive charge or adsorbed negatively charged proteins (Senior *et al.*, 1991). However as the positive charge imparted by PXB is, even at its greatest, a fraction of that seen with SA, it is necessary to confirm these hypotheses through release studies in biologically relevant media before commencing *in vivo* studies.

### 3.4.8. Size characterisation of LPXB formulations

#### 3.4.8.1. Laser diffraction sizing

Laser diffraction sizing of LPXB formulations was performed using a Malvern Mastersizer E. The principles of this technique and method of sample preparation are described in section 3.3.5.

As shown in table 3.8, the mean diameter of vesicles is described in two ways; (a) the mean diameter of the volume distribution and (b) the mean diameter of the number distribution. The result is determined directly from the volume distribution and this data is then used to calculate a number distribution. As a result, the number distribution needs to be treated with caution as it is an estimate based on computation and transformation of the volume size distribution.

Although numerous investigations have utilised the DRV technique for the encapsulation of antimicrobials (Cajal *et al.*, 1992; Lagace *et al.*, 1991; Onur *et al.*, 1992; Ravaoarino *et al.*, 1993) and other agents (Alino *et al.*, 1990; Seltzer *et al.*, 1988) there is a paucity of information on the size range of vesicles produced by this technique. Most investigations

have characterised the size distributions of DRVs after a further processing step *i.e.*, extrusion through polycarbonate filters or microfluidisation. However, it is generally accepted that the DRV method produces vesicles with a heterogenous size distribution which can approach the micrometer range in diameter (Gregoriadis & Florence, 1993). DRVs (equimolar egg PC and cholesterol) were originally reported to have a maximum size of  $2\mu\text{m}$  with 95% of vesicles less than  $1\mu\text{m}$  (Kirby & Gregoriadis, 1984). Another study reported the size distribution of DRV, determined by negative stain electron microscopy, to be  $0.1\text{-}0.5\mu\text{m}$  (Perkins *et al.*, 1993). The importance of the method used to characterise the size distribution and the nature of the distribution (*i.e.* volume, mass or number) is highlighted by the results reported by Gregoriadis *et al.* (1993) for egg PC based DRV. In this study vesicles were sized using PCS and the number and mass diameters reported. The number distribution ranged from  $300\text{-}400\text{nm}$  whilst the mass distribution had a much larger range from  $1\text{-}3\mu\text{m}$ . This reflects the importance that each result presentation gives to the proportion of vesicles at each end of the size range. With the number mean the average diameter is weighted towards a lower value as the presence of a few large particles is far outweighed by the much greater presence of smaller vesicles. However, with the volume mean, a few large vesicles may have the equivalent mass of a much larger number of smaller particles and as a result the reported size distribution is skewed toward the higher range.

The presentation code used in the calculation of size distribution can greatly affect actual size reported. This parameter is related to refractive index of the measured material. The approach taken to applying a presentation code to liposomes samples was to use a code (2OHD) previously used for Intralipid emulsions which would be expected to have similar characteristics to liposome suspensions. The use of 2OHD appears to be valid when the size distributions of extruded vesicles are considered. Using both EPC and DSPC DRVs, vesicles were extruded ten times through a  $0.8\mu\text{m}$  filter. This procedure is reported to give vesicles with a mean diameter approximating that of the filter used. Both preparations had mean volume diameters of  $\sim 0.8\mu\text{m}$  confirming that the reported volume mean and size distribution was a reasonably accurate estimation.



The size distributions, as determined by laser diffraction measurements, of LPXB formulations are shown in table 3.8. Figure 3.8 also shows the size distributions of a representative sample for each formulation tested. The volume mean of EPC DRV ( $4.19 \pm 2.28 \mu\text{m}$ ) was comparable to that of EPC MLV ( $4.27 \pm 2.64 \mu\text{m}$ ). Phospholipid composition appeared to affect mean size. With empty liposomes, cholesterol appeared to increase the volume mean ( $6.04 \pm 3.04 \mu\text{m}$ ,  $6.60 \pm 2.69 \mu\text{m}$  respectively) compared to vesicles composed solely of EPC ( $4.19 \pm 2.28 \mu\text{m}$ ). This may be due to increased fusion of CH containing vesicles. The inclusion of a 10% molar quantity of a charged amphiphile also increased the mean diameter. The increased sizes of SA and DCP containing vesicles were similar and this phenomenon is most likely the result of increased interlamellar spacing due to repulsive electrostatic forces between charged bilayers. EPC:CH:PEG vesicles had a similar diameter ( $4.51 \pm 2.18 \mu\text{m}$ ) to EPC vesicles. The large standard deviations associated with the volume means suggest a wide size distribution, possibly due in part to the presence of aggregates. Formulations containing PEG and charged amphiphiles did not flocculate after rehydration whereas neutral formulations were susceptible to flocculation. Vesicles were routinely formulated and stored in PBS, conditions which may induce flocculation of uncharged vesicles (Gregoriadis & Florence, 1993a). The mean size diameter and size distributions are therefore likely to include the diameters of vesicular aggregates which may explain the relatively high mean diameters of LPXB formulations. Such aggregates are unlikely to contribute to electron microscopy size determinations as vesicles forming aggregates would be individually sized. Large aggregates would also be outside the working range of common PCS techniques. Therefore the mean diameters of DRVs sized using these methods may approximate the number distribution determined by laser diffraction. The number size mean is considerably less than the equivalent volume mean although in some cases, mathematical transformation of the volume distribution gives rise to anomalous results (*e.g.* EPC:CH 2:1 empty vesicles). These considerations apply equally to unloaded and loaded vesicles.

The mean diameter of some formulations was also influenced by the presence of PXB. EPC loaded vesicles had a greater mean diameter than their unloaded counterparts. This may be due to the diminution of the small potential of nominally neutral vesicles by bilayer associated PXB. This was also observed with EPC:CH (2:1). Loaded EPC:SA vesicles had a slightly greater mean diameter than empty vesicles possibly due to increased repulsion between bilayers because of interlamellar PXB. Loading of PXB in EPC:DCP formulations reduced the mean diameter to  $4.88 \pm 4.68 \mu\text{m}$ , a value close to that observed with empty neutral vesicles. This may support the hypothesis of neutral vesicle formation with loaded EPC:DCP vesicles (see section 3.4.3.). If PXB masked bilayer associated DCP then an increase in size diameter through aggregation may be expected (Aramaki & Tsuchiya, 1989). However if PXB complexes and removes DCP from bilayers less drug would be bilayer bound and the mean diameter of nominally negative vesicles would be similar to that of empty neutral vesicles. No effect of drug was seen with PEG containing formulations suggesting that the action of PXB was an intervesicular effect which was negated through steric stabilisation of vesicles by PEG-lipid.

As observed with EPC vesicles, the volume mean of DSPC DRV ( $5.98 \pm 3.74 \mu\text{m}$ ) was similar to that of DSPC MLV ( $5.78 \pm 2.92 \mu\text{m}$ ). DSPC based vesicles were also generally larger than EPC based vesicles. With empty vesicles, cholesterol again increased the mean diameter to  $8.25 \pm 3.7 \mu\text{m}$  (2:1) and  $8.65 \pm 4.00 \mu\text{m}$  (1:1). Steric stabilisation with DSPE-PEG<sub>1900</sub> reduced the mean diameter to  $6.97 \pm 3.21 \mu\text{m}$ . The relatively large standard deviations associated with these means suggests the presence of aggregates. This was confirmed by light microscopy (see section 3.3.8). Drug loading appeared to increase the mean diameter of all DSPC based formulations by 1-2  $\mu\text{m}$ . This was greatest with DSPC vesicles, where a  $\sim 2 \mu\text{m}$  shift was observed although the effect was less ( $\sim 1.0 \mu\text{m}$ ) with all other formulations. The reason for the different behaviour of loaded DSPC and EPC vesicles is unclear but may be related to possible packing changes induced by PXB which may alter intervesicular surface interactions.

Formulation	Volume mean ( $\mu\text{m}$ )	Number mean ( $\mu\text{m}$ )
	$\pm\text{sd}$	$\pm\text{sd}$
EPC MLV empty	4.27 $\pm$ 2.64	2.57 $\pm$ 2.10
EPC MLV extruded (0.8 $\mu\text{m}$ filter)	0.95 $\pm$ 0.54	0.33 $\pm$ 0.21
EPC empty	4.19 $\pm$ 2.28	1.63 $\pm$ 0.96
EPC loaded	6.56 $\pm$ 2.70	3.86 $\pm$ 1.72
EPC:CH (2:1) empty	6.04 $\pm$ 3.07	0.98 $\pm$ 1.20
EPC:CH (2:1) loaded	7.04 $\pm$ 2.94	3.18 $\pm$ 1.95
EPC:CH (1:1) empty	6.6 $\pm$ 2.69	3.42 $\pm$ 1.82
EPC:CH (1:1) loaded	6.55 $\pm$ 3.58	2.77 $\pm$ 2.34
EPC:CH:PEG (2:1:0.2) empty	4.51 $\pm$ 2.18	2.18 $\pm$ 1.16
EPC:CH:PEG (2:1:0.2) loaded	3.91 $\pm$ 2.08	0.80 $\pm$ 0.75
EPC:SA (9:1) empty	5.06 $\pm$ 3.69	2.86 $\pm$ 1.35
EPC:SA (9:1) loaded	5.96 $\pm$ 4.02	0.44 $\pm$ 0.64
EPC:DCP (9:1) empty	5.76 $\pm$ 4.48	4.10 $\pm$ 2.61
EPC:DCP (9:1) loaded	4.88 $\pm$ 4.68	4.13 $\pm$ 2.59
DSPC MLV empty	5.78 $\pm$ 2.92	0.63 $\pm$ 1.00
DSPC MLV extruded (0.8 $\mu\text{m}$ filter)	0.87 $\pm$ 0.44	0.50 $\pm$ 0.21
DSPC empty	5.98 $\pm$ 3.74	0.27 $\pm$ 0.41
DSPC loaded	3.90 $\pm$ 2.33	1.24 $\pm$ 0.79
DSPC:CH (2:1) empty	8.25 $\pm$ 3.70	0.49 $\pm$ 0.85
DSPC:CH (2:1) loaded	7.03 $\pm$ 3.17	3.02 $\pm$ 0.22
DSPC:CH (1:1) empty	8.65 $\pm$ 4.00	0.52 $\pm$ 0.88
DSPC:CH (1:1) loaded	6.86 $\pm$ 2.82	3.49 $\pm$ 1.90
DSPC:CH:PEG (2:1:0.2) empty	6.97 $\pm$ 3.21	0.79 $\pm$ 1.35
DSPC:CH:PEG (2:1:0.2) loaded	5.78 $\pm$ 2.70	2.72 $\pm$ 1.52

Table 3.8 Mean size determined by laser diffraction sizing of LPXB formulations. All vesicles prepared by the DRV technique unless otherwise indicated. Loading refers to a standard initial loading of 9mg PXB/66 $\mu$ M total lipid. All volume and number means and sd are the average of three independent preparations.

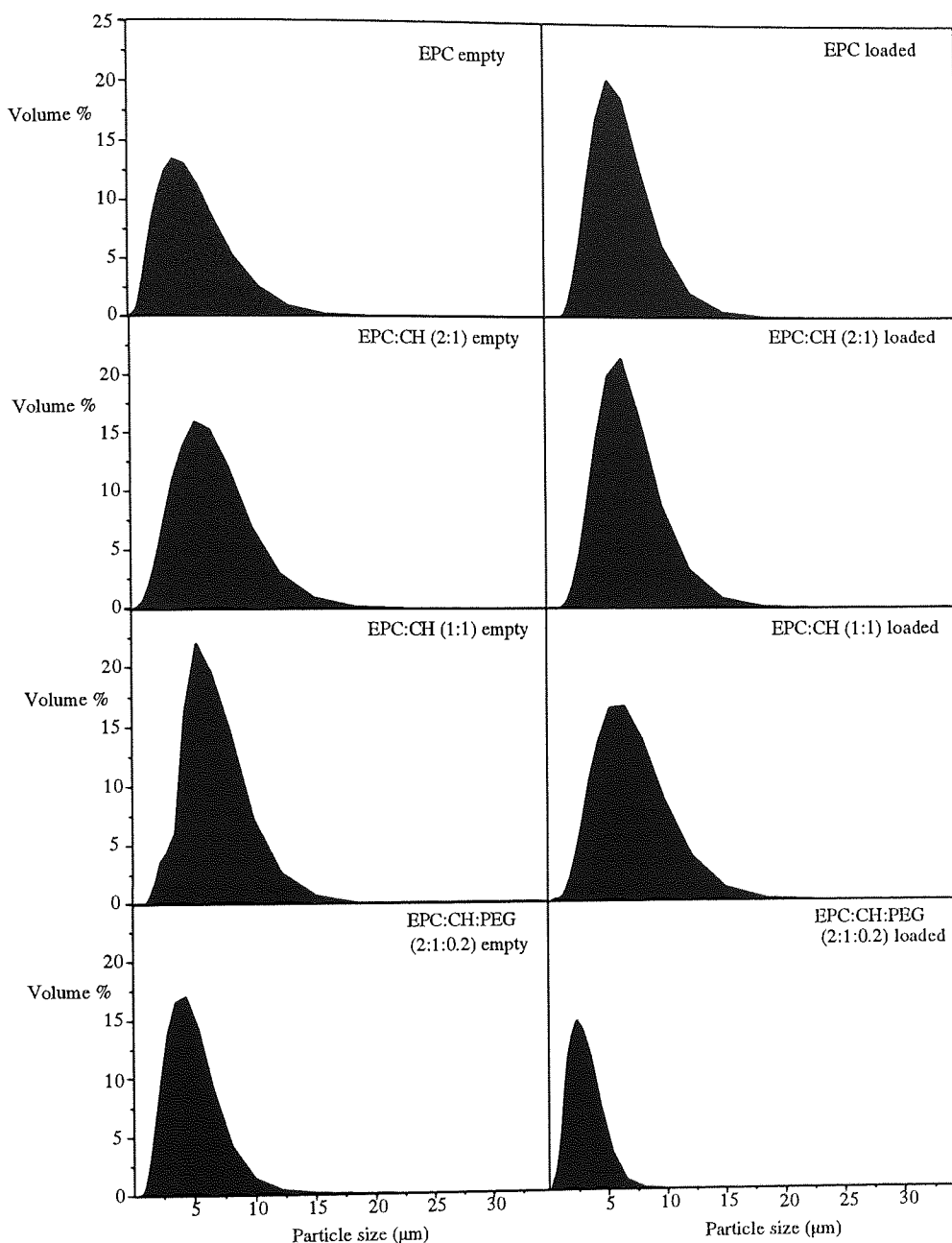


Figure 3.8. Representative size distributions of LPXB DRV formulations as determined by laser diffraction sizing. Loading refers to a standard initial loading of 9mg PXB/66 $\mu$ M total lipid

### 3.4.8.2. Photon correlation spectroscopy (PCS)

PCS sizing of LXPB formulations was performed using a Sematech multiangle goniometer (Nice, France). The principles of this technique and the method of sample preparation are discussed in section 3.3.6. The formal range of PCS is accepted to be 3 to 3000nm.

However, in practice  $1\mu\text{m}$  is often the upper limit if heterogenous dispersion of vesicles are to be sized (Barenholz & Amselem, 1993). The advantage of the Sematech instrument for sizing of liposomal preparations in the micron range is that the working range of the technique has been effectively extended to  $5\mu\text{m}$  and, in some cases to  $10\mu\text{m}$ . This extended effective has been achieved through a number of hardware modifications (high power laser and ultra-low-noise photomultiplier detector) and advanced software algorithms for data manipulation (see section 3.3.6). Resolution between bi- or multimodal distributions has also been improved. The improvements have been made through hardware modifications and the use of a new method of software analysis (Sematech technical information).

Table 3.9 shows the mean hydrodynamic diameter of liposomes determined from an intensity cumulants distribution. Figures 3.9-3.12 illustrate representative size distributions of liposomes determined by this technique. The accuracy of the machine was checked using a latex standard with a nominal diameter of  $1.1\mu\text{m}$  (Polysciences, UK). The geometric mean diameter determined by PCS was  $1.092\pm 0.022\mu\text{m}$ . This confirmed the accuracy of the reported mean for micron sized particles with a narrow size distribution. Verification of accuracy with liposomal preparations was performed as with laser diffraction. EPC MLV were sized by PCS and found to have a hydrodynamic mean diameter of  $1.369\pm 1.173\mu\text{m}$ . This value is substantially lower than that observed with laser diffraction sizing ( $4.27\pm 2.64\mu\text{m}$ ). After ten extrusions through a  $0.4\mu\text{m}$  polycarbonate filter (Costar, England) the mean was reduced to  $0.422\pm 0.238\mu\text{m}$ . EPC DRV without PXB were found to have a mean diameter of  $1.776\pm 0.444\mu\text{m}$ . Drug loading decreased the mean diameter to  $0.846\pm 0.341\mu\text{m}$ . DSPC empty DRV had a mean diameter of  $0.718\pm 0.428\mu\text{m}$ . Drug loading was found to decrease the mean size of EPC:CH 1:1 vesicles from  $1.964\pm 0.950\mu\text{m}$  to  $1.350\pm 1.066\mu\text{m}$ . The lower values obtained for the mean size of DRVs by PCS is close to previously published values (Gregoriadis & Florence, 1993a; Kirby & Gregoriadis, 1984). The disparity in size distributions determined by PCS and laser diffraction is due to the size ranges covered by both techniques. Although the Sematech allows an effective increase in the working range of PCS, large aggregates which contribute substantially to the volume distribution

determined by laser diffraction, are not detected and therefore do not skew the distribution towards the upper end. Indeed large vesicles/aggregates may obscure smaller particles (Barenholz & Amselem, 1993). This may account for the still relatively large diameters of LPXB formulations compared to previously published results. It may be concluded that the size means determined by PCS for LPXB formulations have been shown to be in the range of that accepted for vesicles produced by the DRV technique.

Formulation	Hydrodynamic mean diameter (nm)	Dispersion (nm)
Latex standard	1092	±22
EPC MLV empty	1369	±1173
EPC MLV empty (after 0.4µm extrusion)	422	±238
EPC DRV empty	1776	±444
EPC DRV loaded	862	±341
EPC:CH 1:1 empty	1964	±950
EPC:CH 1:1 loaded	1350	±1066
DSPC DRV empty	718	±428

Table 3.9. Geometric mean diameters and dispersions of LPXB formulations determined by PCS using a 90° scattering angle. Loading refers to a standard loading of 9mg PXB/66µM total lipid.

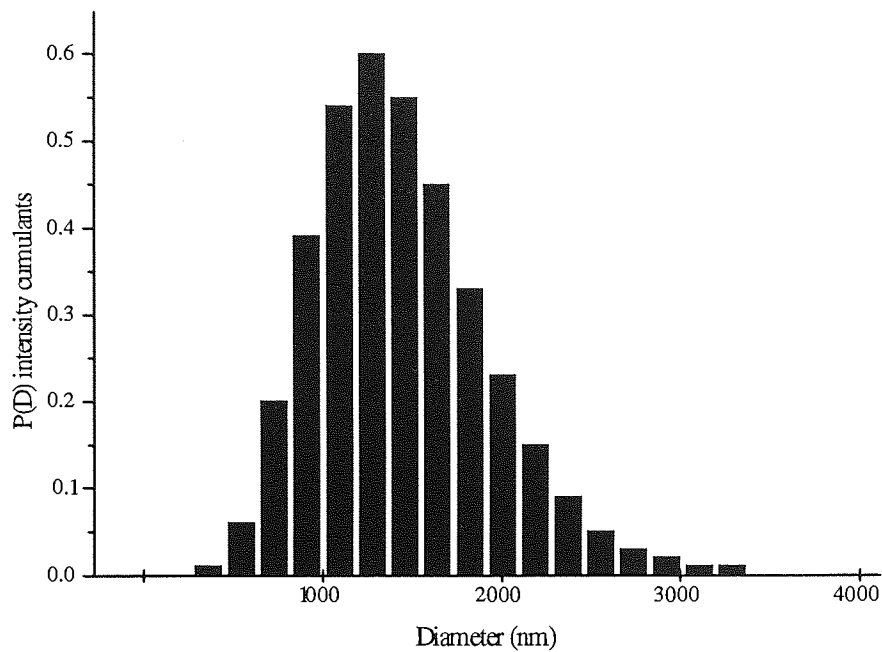


Figure 3.9. Intensity weighted size distribution of empty EPC DRV determined using PCS. Hydrodynamic mean diameter  $1776 \pm 444$  nm.

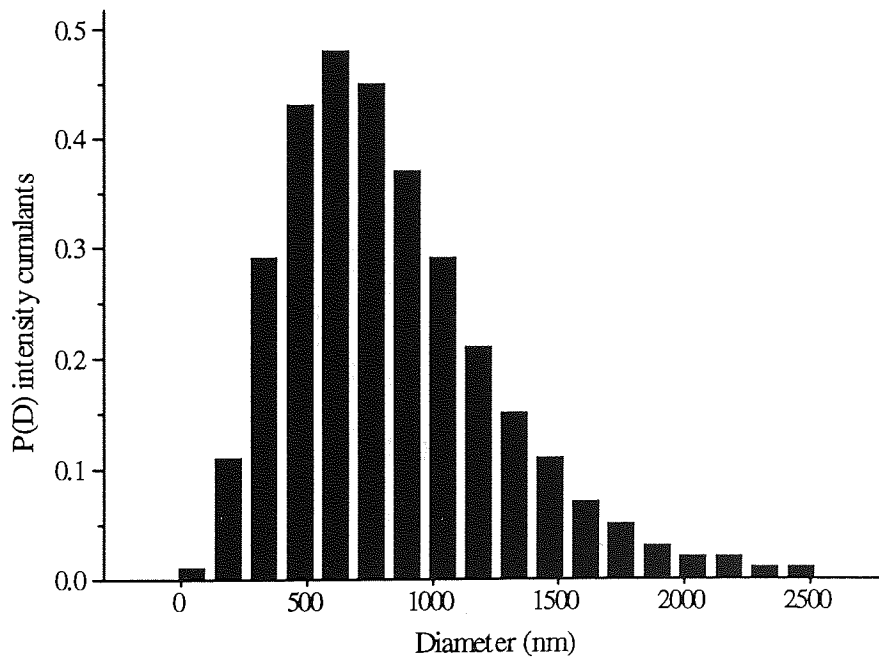


Figure 3.10. Intensity weighted size distribution of loaded EPC DRV determined using PCS. Hydrodynamic mean diameter  $862 \pm 341$  nm.

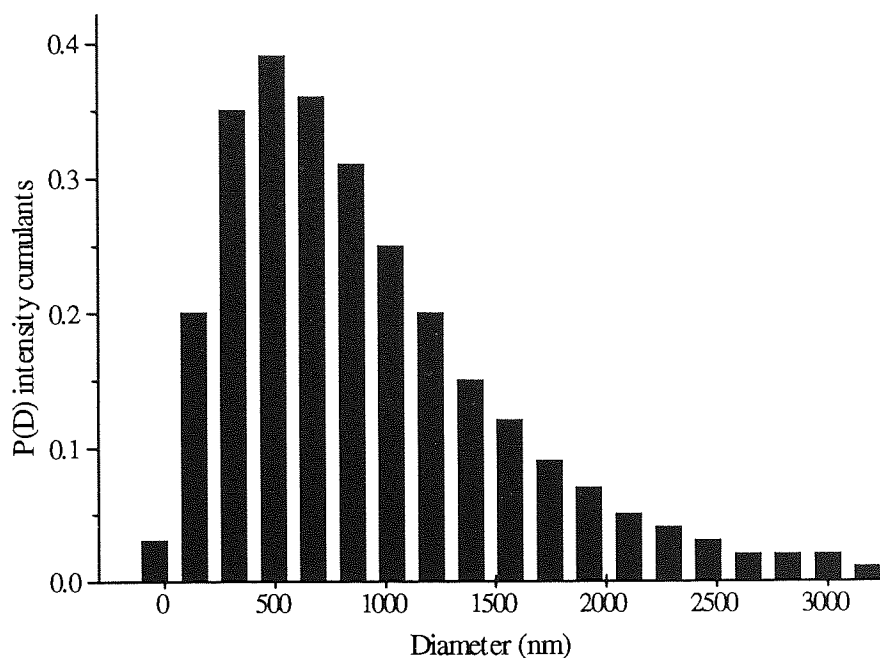


Figure 3.11. Intensity weighted size distribution of empty EPC:CH 1:1 DRV determined using PCS. Hydrodynamic mean diameter  $743 \pm 430$  nm.

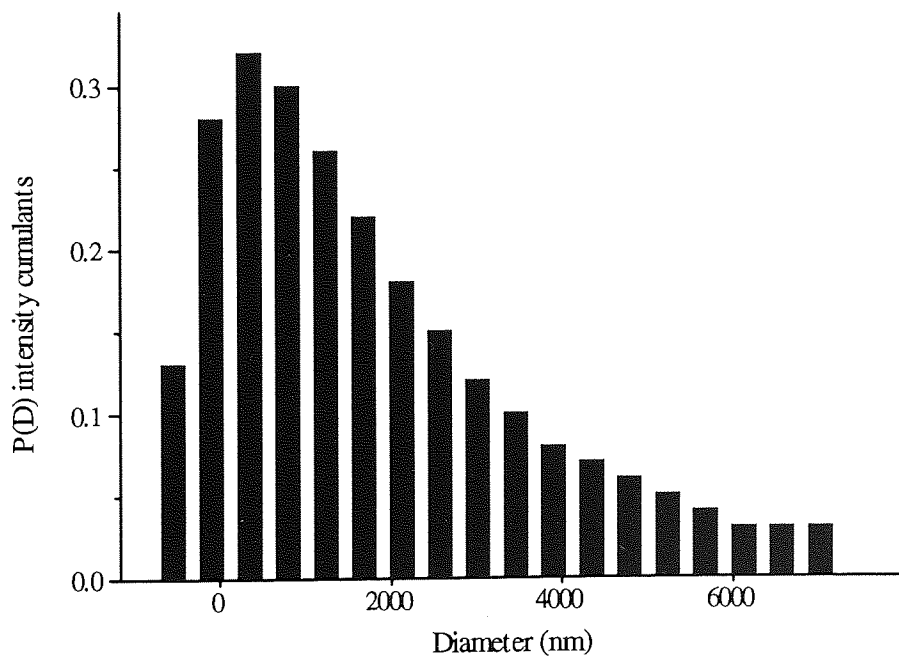


Figure 3.12 Intensity weighted size distribution of loaded EPC:CH 1:1 DRV determined using PCS. Hydrodynamic mean diameter  $1350 \pm 1066$  nm.



### 3.4.9. Transmission electron microscopy of LPXB formulations

The morphology and membrane structure of LPXB formulations were investigated using negative stain electron microscopy (TEM). Particle size distributions were not determined by this method due to the difficulty in obtaining a sufficient number of vesicles. However the diameters of imaged vesicles may give an indication of liposome size. Samples were prepared and imaged as described in section 3.3.9. All vesicles illustrated are loaded DRV preparations. Encapsulation efficiencies, laser diffraction and PCS sizing and zeta potential characterisation are described in the preceding sections.

Figures 3.13-3.18 show the appearance of LPXB formulations after negative stain TEM. Fig 3.13 shows an aggregate of EPC:CH (2:1) at 57k magnification. The vesicles are heterogenous in size (~100nm-400nm) and are oligolamellar with typically 4-6 lamellae. Figure 3.14 shows an aggregate of EPC:CH (2:1) from another preparation. Again, the vesicles are small (50-100nm) and are oligolamellar. Using laser diffraction and PCS such an aggregate would appear to have a diameter of 500-750nm as it would be detected as a single particle. EPC:CH:PEG DRVs provided excellent images using this technique. Figure 3.15 shows a micrograph at 25k magnification. Vesicles have a wide range of diameters (50-500nm) and appear to possess bilayers encapsulating a darker core region. Larger structures are present but it is unclear whether or not they are vesicular or artefacts of the process. On higher magnification (120k) (figure 3.16) the bilayer structure is clearly visible with vesicles appearing to have seven to eight lamellae around a central core region. Vesicles in this micrograph have a diameter of ~200nm. Figure 3.17 shows a single oligolamellar DSPC:CH (1:1) vesicle at a magnification of 150k. This vesicle is ~150nm in diameter. A lower magnification (60k) micrograph (figure 3.18) of DSPC vesicles showed vesicular structures with a diameter of 50-200nm. However, bilayer structure was not well resolved in this micrograph. Again larger structures were also observed but the nature of these is unclear. The possibility that they are artefacts of the staining procedure cannot be excluded.

TEM confirmed the presence of bilayers in a range of liposome formulations. The representative micrographs shown here illustrate the size and morphology of LPXB formulations. The relatively small size of the imaged vesicles is consistent with previously reported DRV diameters determined by this method. This indicates that the LPXB formulations had the typical characteristics of a DRV preparation in terms of size and morphology.

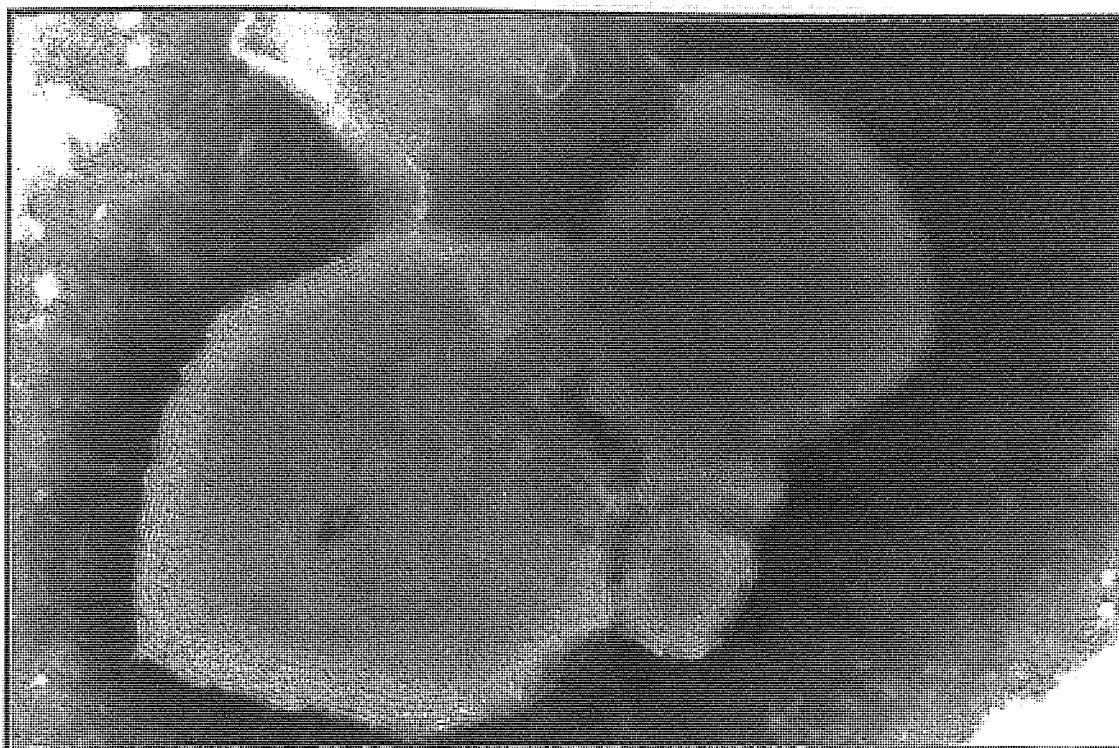


Figure 3.13. Negative stain TEM of EPC:CH (2:1) loaded DRVs. Magnification 57K.

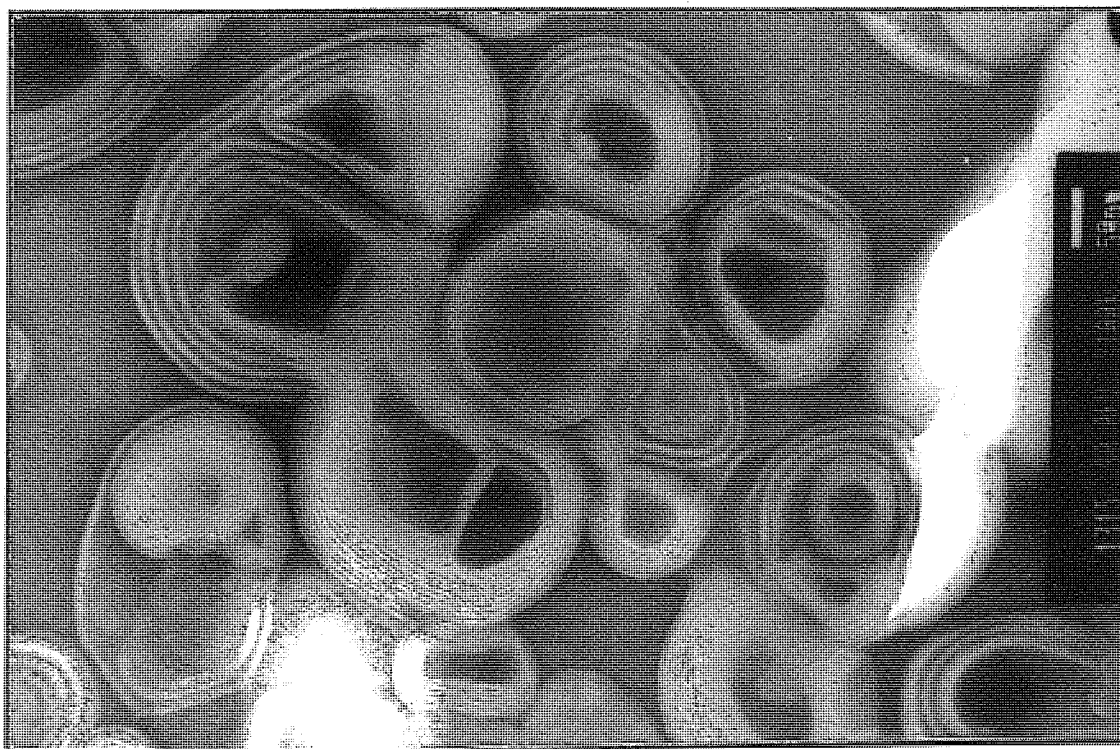


Figure 3.14. Negative stain TEM of EPC:CH (2:1) loaded DRVs. Magnification 100K.

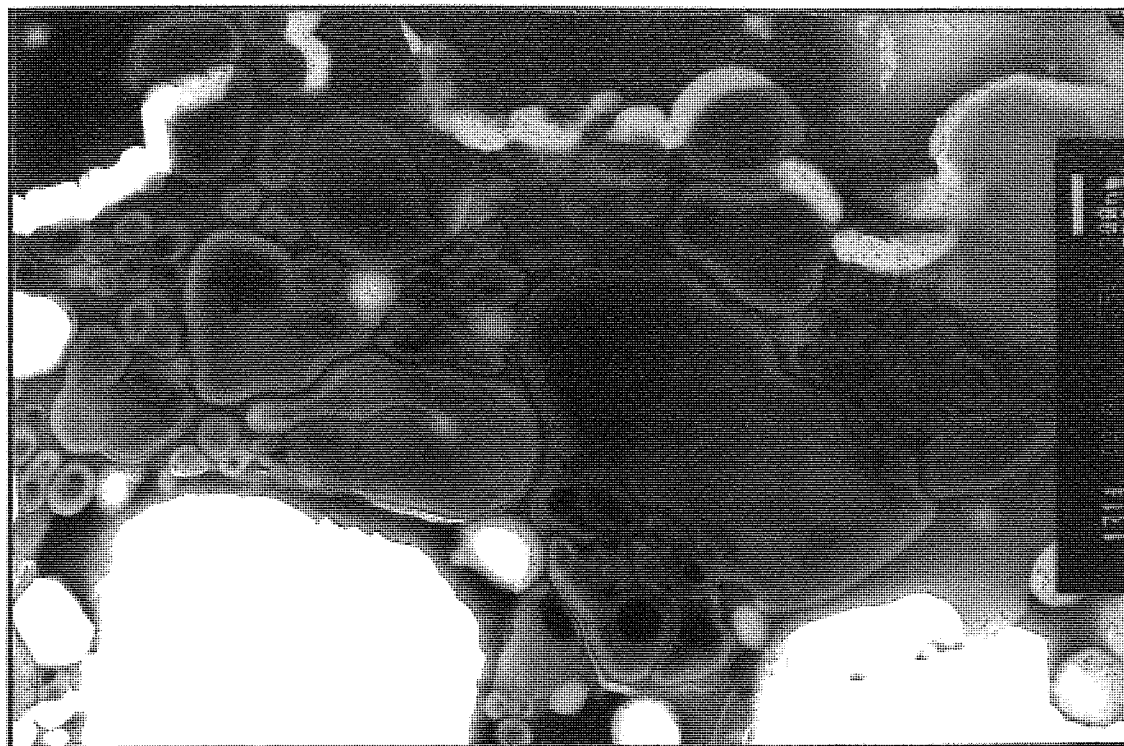


Figure 3.15. Negative stain TEM of EPC:CH:PEG (2:1:0.2) loaded DRVs. Magnification 25K.

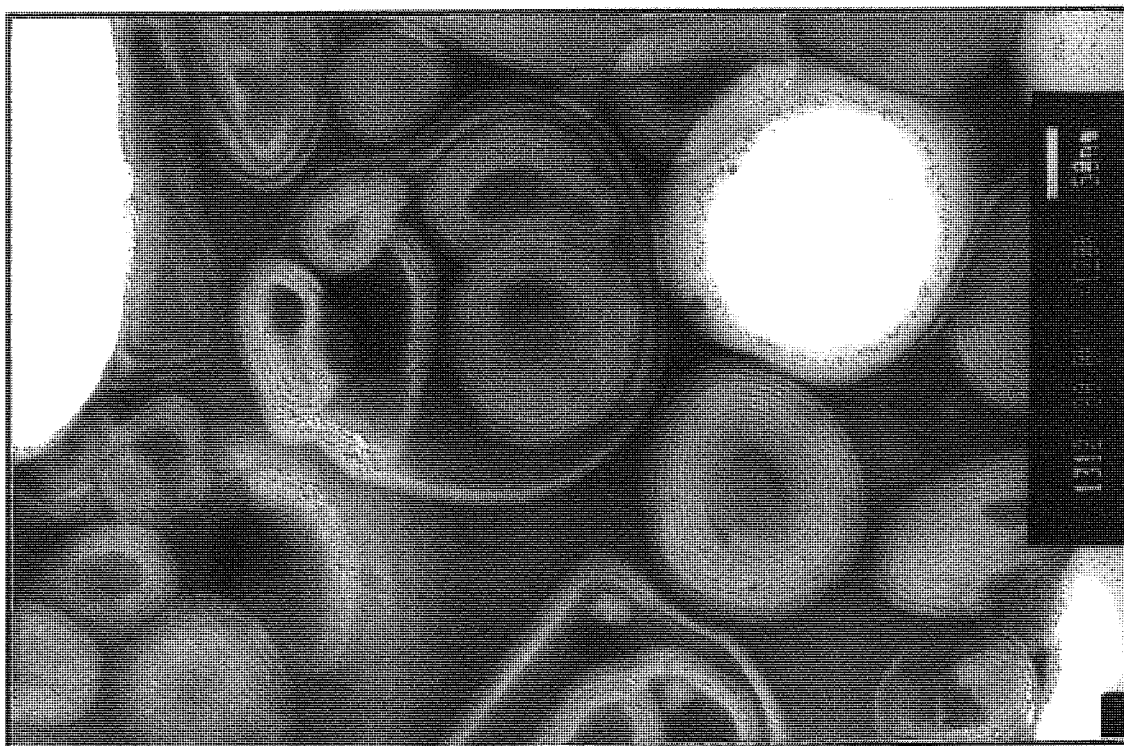


Figure 3.16. Negative stain TEM of EPC:CH:PEG (2:1:0.2) loaded DRVs. Magnification 120K.



Figure 3.17. Negative stain TEM of DSPC:CH (1:1) loaded DRV. Magnification 150K.

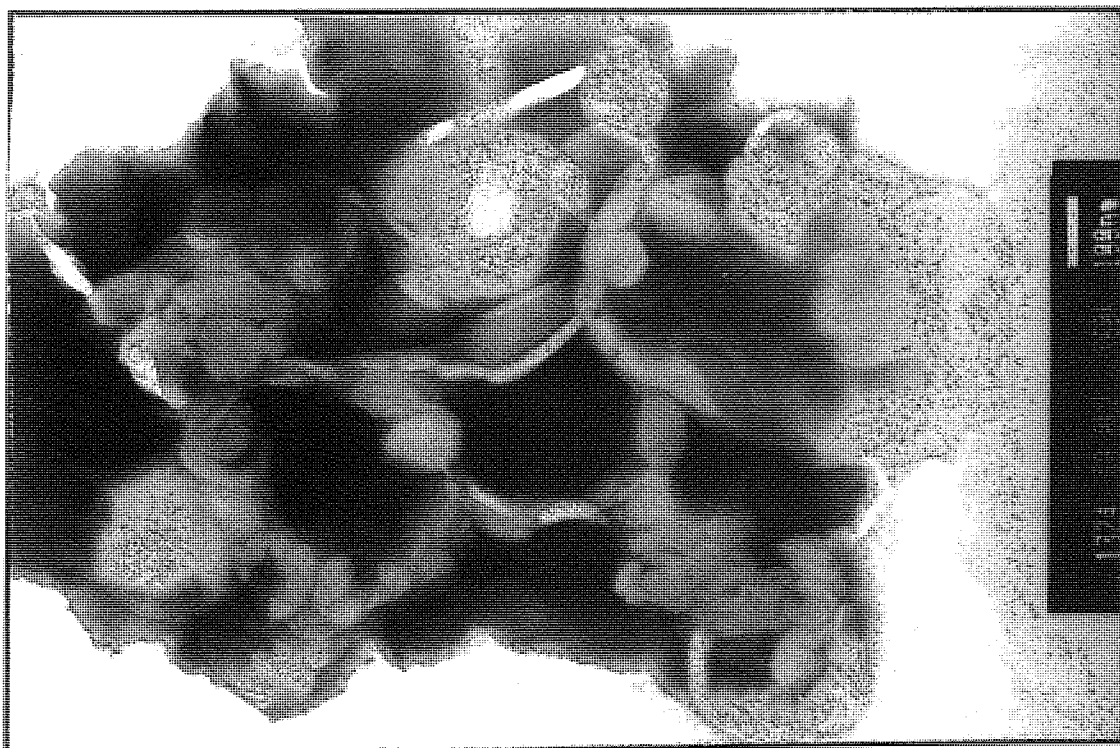


Figure 3.18. Negative stain TEM of DSPC loaded DRVs. Magnification 60K.

#### **3.4.10. Light microscopy assessment of LPXB formulations**

Light microscopy was used to determine the gross morphology and the degree of aggregation in LPXB preparations. Samples were prepared and viewed using phase contrast microscopy as described in section 3.3.8. Table 3.10 illustrates the characteristic features of LPXB preparations observed using light microscopy. Representative light micrographs also illustrate the morphology of several formulations.

The gross morphology of LPXB formulations was observed to be phospholipid dependent. Empty EPC liposomes appeared to have the smallest vesicles of the preparations observed, although a heterogenous size population was present. Small aggregates composed of 5-15 liposomes were observed. Drug loading resulted in the presence of much larger aggregates (30-50 vesicles). This was also observed with all EPC:CH formulations. Both empty and loaded EPC:CH appeared as large aggregates of vesicular material (figures 3.19 and 3.20), indicating that cholesterol played a major role in this type of intervesicular interaction. Aggregates were not observed with either empty or loaded EPC:CH:PEG liposomes. The lack of influence of drug loading on the morphology of this formulation suggests that PXB does not interfere with the steric stabilisation conferred by PEG polymer chains.

The observation of morphology of EPC based liposomes are of use in the interpretation of sizing data, particularly that generated by laser diffraction sizing. The large aggregates and heterogenous size range observed by optical microscopy reinforce the relatively large volume means and ranges determined from sizing data.

Optical microscopy observations showed a difference in morphology between DSPC and EPC based vesicles. Unloaded DSPC vesicles appeared mainly as free vesicles with some small clumps of 2-5 vesicles visible. Loading did not appear to increase the size of the aggregates observed in contrast with the equivalent EPC formulations. This suggests a lower degree of membrane interaction of PXB with DSPC possibly coupled with different fusion

behaviour as a result of the ordered gel state of DSPC. Cholesterol did not appear to increase the formation of aggregates as was observed with EPC vesicles. Both DSPC:CH (2:1) and (1:1), loaded and unloaded formulations, appeared with small aggregates and dispersed vesicles visible.

However, laser diffraction data indicates a larger volume mean for DSPC:CH vesicles relative to their EPC:CH counterparts. The inconsistency with optical microscopy observation may be explained by a vortex mixing step during laser diffraction sample preparations. Vortex mixing may only be partly successful in dispersing aggregates, possibly downsizing aggregates to just a few liposomes. The higher means observed may therefore reflect an increase in the mean diameter of free vesicles compared with those observed in EPC preparations. DSPC:CH:PEG vesicles appeared well dispersed with single vesicles observed with unloaded and loaded preparations. A heterogenous size distribution of vesicles was observed with all DSPC based preparations.

The effect of charge stabilisation of liposomes was seen with EPC:SA liposomes (empty and unloaded) and EPC:DCP vesicles (empty formulation only). Vesicles from these preparations were of a wide size range and were well dispersed. Significantly, EPC:DCP loaded vesicles had a similar morphology to EPC loaded preparations, again suggesting changes in the negative surface potential as a result of PXB loading.

Formulation	Gross morphology
EPC empty	Aggregates (5-15 vesicles)
EPC loaded	Aggregates (30-50 vesicles)
EPC:CH (2:1) empty	Aggregates (30-50 vesicles)
EPC:CH (2:1) loaded	Aggregates (30-50 vesicles)
EPC:CH (1:1) empty	Aggregates (30-50 vesicles)
EPC:CH (1:1) loaded	Aggregates (30-50 vesicles)
EPC:CH:PEG (2:1:0.2) empty	Free vesicles
EPC:CH:PEG (2:1:0.2) loaded	Free vesicles
DSPC empty	Free vesicles and aggregates (2-5 vesicles)
DSPC loaded	Free vesicles and aggregates (2-5 vesicles)
DSPC:CH (2:1) empty	Free vesicles and aggregates (2-5 vesicles)
DSPC:CH (2:1) loaded	Free vesicles and aggregates (2-5 vesicles)
DSPC:CH (1:1) empty	Free vesicles and aggregates (2-5 vesicles)
DSPC:CH (1:1) loaded	Free vesicles and aggregates (2-5 vesicles)
DSPC:CH:PEG (2:1:0.2) empty	Free liposomes
DSPC:CH:PEG (2:1:0.2) loaded	Free liposomes
EPC:DCP (9:1) empty	Free liposomes
EPC:DCP (9:1) loaded	Aggregates (5-10 vesicles)
EPC:SA (9:1) empty	Free liposomes
EPC:SA (9:1) loaded	Free liposomes

Table 3.10. Gross morphology of LPXB formulations observed using phase contrast light microscopy with x40 magnification.



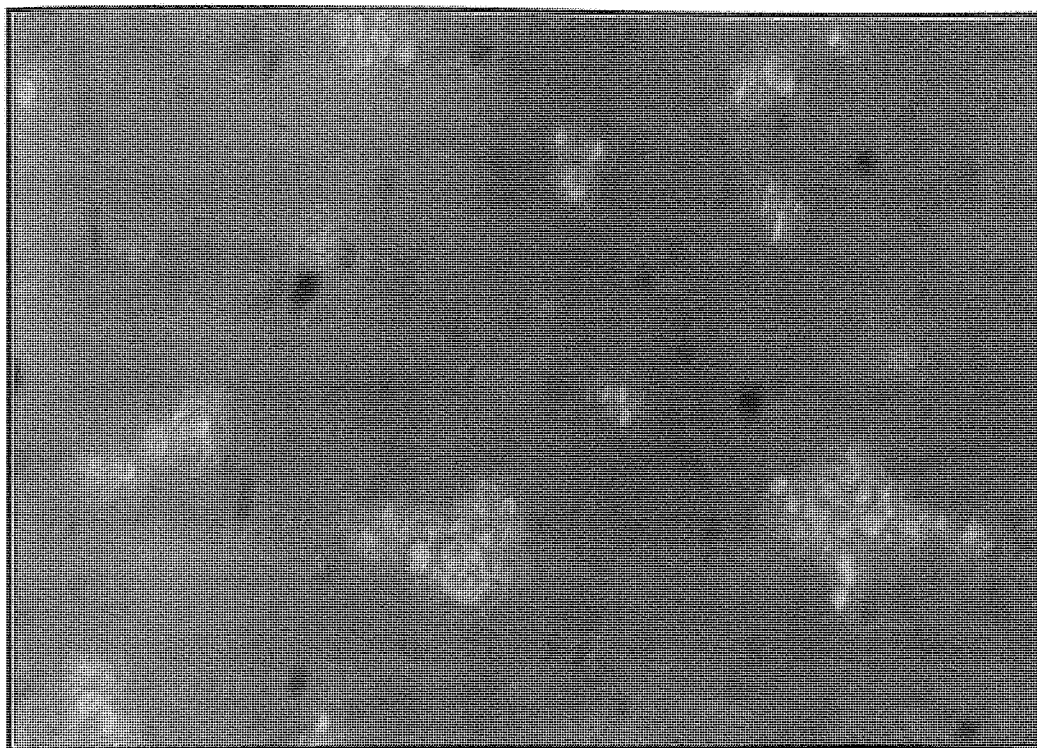


Figure 3.19. Phase contrast micrograph of EPC:CH (2:1) empty DRV using x40 objective.

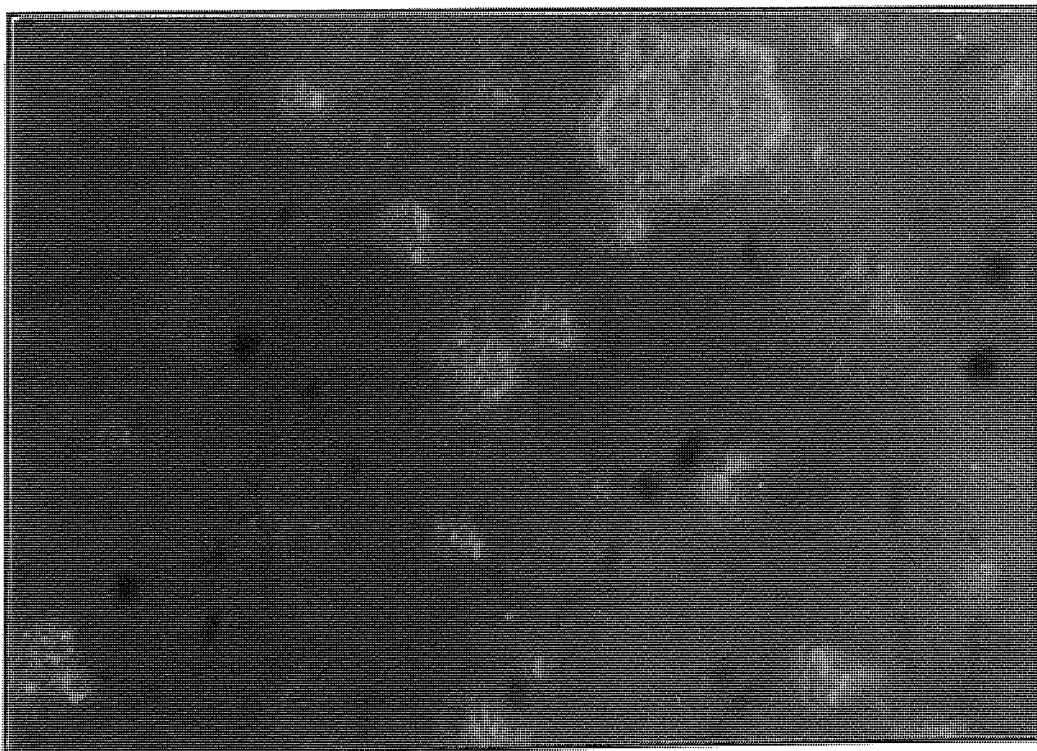


Figure 3.20. Phase contrast micrograph of EPC:CH (2:1) loaded DRV using x40 objective.

### 3.4.11. Phospholipid measurement of LPXB DRV

The determination of phospholipid content of DRV was performed using two methods. Firstly, the Stewart procedure (Stewart, 1980) is a direct determination of intact phospholipids based on the quantification of the complex formed between the phosphate group of phospholipids and ammonium ferrothiocyanate. The complex is extracted using chloroform and determined spectrophotometrically (Barenholz & Amselem, 1993). This is a simpler approach than the Bartlett assay which indirectly quantifies phospholipids through digestion and measurement of inorganic phosphate. The protocol for the Stewart assay is described in section 3.3.4.

An alternative approach was to measure [ $^{14}\text{C}$ ] cholesterol by scintillation counting of the liposomal pellet after preparation. Comparison of [ $^{14}\text{C}$ ] content before and after preparation was used to quantitate total phospholipid. This is based upon the assumption that the ratio of [ $^{14}\text{C}$ ]-CHOL and bulk phospholipid remains constant and that any loss affects both components equally.

The Stewart assay was used with initial preparations to confirm that efficient transfer of phospholipids was occurring during the DRV procedure. Phospholipids may be lost through transfer losses by pipetting or through incomplete conversion to SUV with pelleting of large vesicles and titanium probe particles after sonication. However, sonication produced clear solutions indicating complete conversion of MLV to SUV. Therefore any loss of phospholipid would be expected to occur through simple transference losses. To minimise such losses, washing steps were used and the efficiency of the DRV process was confirmed with the high recoveries of EPC witnessed for EPC vesicles (98.58%) and EPC:CH (2:1) ( $101.77 \pm 4.92\%$ ,  $n=3$ ). Although useful for the direct determination of phospholipids, the Stewart assay suffers from several drawbacks which curtailed its use for routine phospholipid determination. The time-consuming nature of this method restricts the number of samples which may be assayed. Also, the assay is specific for the type of phospholipid headgroup and

is unresponsive to phosphatidylglycerol (New, 1990). Calibration curves are required to assay each phospholipid and for lipid mixtures, identical mixtures have to be used to construct calibration plots (Barenholz & Amselem, 1993). It is necessary to achieve clean separation between the phases as the phospholipids are determined spectrophotometrically from the lower chloroform phase. As a result of these drawbacks, phospholipids were quantified by measuring [ $^{14}\text{C}$ ]-CHOL retention. With the assumption of identical losses of cholesterol and phospholipid components, cholesterol counts of vesicles before and after preparation allowed losses to be determined. This value varied for a number of formulations between  $87.21 \pm 4.77\%$  to  $95.73 \pm 4.61\%$ . As a general approximation, 90% of the phospholipid (determined with respect to cholesterol) remains after washing. The slightly lower values obtained with scintillation counting compared with the Stewart assay may suggest that the losses of cholesterol and phospholipid are not totally equivalent. Loss of CH in excess of phospholipids may occur through the formation of cholesterol microcrystals, a possibility given the chloroform/methanol solvent commonly used to form thin lipid films. Overall it may be concluded that no significant loss of bulk phospholipid was detected. Table 3.11 shows the retention values determined using both methods for a number of formulations.

Formulation	Assay method	Phospholipid retained after DRV preparation (% $\pm$ sd)
EPC	Stewart assay	98.58 $\pm$ 3.17
EPC:CH (2:1)	Stewart assay	101.77 $\pm$ 4.92
EPC:CH (1:1)	Scintillation counting	95.73 $\pm$ 4.61
EPC:CH:PEG (2:1:0.2)	Scintillation counting	88.72 $\pm$ 1.82
EPC:CH:GM <sub>1</sub> (2:1:0.2)	Scintillation counting	87.21 $\pm$ 4.77
DSPC:CH (1:1)	Scintillation counting	89.77 $\pm$ 5.22
DSPC:CH:PEG (2:1:0.2)	Scintillation counting	90.88 $\pm$ 3.80

Table 3.11. Phospholipid determination for a number of LPXB DRVs. Phospholipid retained is expressed as a percentage of the starting quantity and represents the mean of three samples  $\pm$  standard deviation

### 3.4.12. Drug release from LPXB formulations

After successful encapsulation within liposomes it is necessary to minimise the leakage of entrapped drugs (Betageri, 1993). The release rate at low temperatures (e.g. 4°C) is relevant to pharmaceutical stability (Law *et al.*, 1994) and knowledge of the *in vitro* release profile at 37°C is a prerequisite before *in vivo* investigations may commence (Betageri & Parsons, 1992; Elorza *et al.*, 1993; Taylor *et al.*, 1990). The rate of drug release from liposomes is largely determined by the physicochemical properties of the drug and the liposomal system. Liposomes are freely permeable to water, but cations are released at a slower rate than anions (Bangham *et al.*, 1965). Aqueous hydrogen bonding may determine the release rate of non-electrolytes (Cohen, 1975).

Liposome permeability is a function of the degree of disorder of the lipid bilayer. Phospholipids in the liquid crystalline state show greater permeability to entrapped material than comparative bilayers in the gel state (Betageri & Parsons, 1992; Taylor *et al.*, 1990). Loss of entrapped material is therefore temperature dependent, with greatest efflux around the phospholipid phase transition temperature ( $T_m$ ). Increased permeability at this temperature is a result of regions of high bilayer disorder where gel and liquid crystalline phases temporarily coexist (Betageri, 1993). Cholesterol can decrease the efflux rate through interaction with phospholipid hydrocarbon chains. Electrostatic interactions with charged phospholipids may also affect drug release (Law *et al.*, 1994).

The aim of this study was to evaluate the role of phospholipid composition in PXB release at 4°C/37°C in PBS and at 37°C in 20% fetal calf serum (FCS). Liposomes were separated from released PXB by centrifugation (18000g x 30min, Beckmann JII) and extraliposomal PXB quantified by scintillation counting (section 2.3.4).

### 3.4.12.1 Release of PXB from LPXB formulations stored at 4°C in PBS pH 7.4

Figures 3.21 and 3.22 show the retention of PXB in LPXB preparations throughout a 4 week storage period at 4°C.

EPC and EPC:CH:PEG vesicles released approximately 40% of entrapped PXB after one week of storage at 4°C. Leakage of PXB continued over 4 weeks until almost 55-60% was released from both formulations. The incorporation of cholesterol in 33 and 50 mol% was successful in reducing the leakage of PXB. Initially release was reduced to approximately 10% at 1 week and was followed by a second slow phase of release which totalled 12-17% at the end of the 4 week period. The phase transition of EPC is -15°C to -7°C (Szoka & Papahadjopoulos, 1980). Therefore at 4°C EPC is in the relatively permeable liquid crystalline state. At this temperature, *i.e.*, above the  $T_m$ , the inclusion of cholesterol modulates membrane fluidity by decreasing the rotational freedom of phospholipid hydrocarbon chains thereby reducing bilayer permeability (Betageri & Parsons, 1992; Taylor *et al.*, 1990). At 50 mol% CHOL, the phase transition is lost and the efflux rate is reduced. Due to the relatively large molecular weight and highly charged nature of PXB, the mechanism of release is presumably diffusion through water-filled defects in the liposome membrane.

The release profiles of EPC, EPC:CH:PEG (2:1:0.2) are similar. This result is surprising as the EPC:CH (2:1) formulation exhibited greater retention than EPC. The presence of a 6.25 mol% ratio of DSPE-PEG<sub>1900</sub> appears to negate the effect of cholesterol. It has previously been reported that a 5-7.5 mol% (Allen *et al.*, 1991) is the optimum level of PEG-lipid incorporation. At 15 mol% DSPE-PEG<sub>1900</sub> begins to disperse vesicles with the formation of non-vesicular structures such as tubules (Lasic *et al.*, 1991). Although the 6.25 mol% used in the present formulations would be insufficient to cause such gross effects on liposome morphology, an interaction with membrane associated PXB may be sufficient to promote membrane defects with a subsequent rise in permeability. In phase behaviour studies of

DSPE-PEG<sub>1900</sub> in EPC liposomes, it has been reported that at 5 mol% DSPE-PEG<sub>1900</sub> liposomes had similar leakage characteristics as pure EPC vesicles. In the same study it was suggested that the interaction of PEG-PE with bilayers involves changes in the relative area of the inner and outer monolayers (Lasic *et al.*, 1991). Such changes may increase the permeability to PXB or may decrease bilayer interaction with the drug.

The release profile of EPC based vesicles were similar in shape for the range of phospholipid compositions tested. After initial release at 1 week, a small increase in released PXB was observed over a 4 week period. The profile may therefore consist of an initial phase of rapid release followed by a second phase of slow efflux. A phase of rapid release has previously been described for hydroxycobalamin from charged vesicles (Alpar *et al.*, 1981), for hydrophobic drugs from charged liposomes (Juliano & Stamp, 1979) and for hydrophobic materials from uncharged liposomes (Arrowsmith *et al.*, 1983). The released fraction of PXB may reflect loss of bilayer associated drug, with a following phase of slow flux of entrapped drug across the lipid bilayers. The much higher initial release of PXB from EPC vesicles may be attributed to desorption of surface located PXB (the extent of which is greater with this formulation, see section 3.4.7), although the high release observed with EPC:CH:PEG suggests that membrane disorder may be the dominant factor. As cholesterol was effective in increasing the retention of PXB in EPC vesicles it would appear that membrane permeability controls the release of PXB.

The release of PXB at 4°C from EPC:SA (9:1) vesicles was investigated over a two week period. Again, an initial burst of PXB was observed with 39% of PXB originally entrapped released after 5 days storage. Slow leakage of PXB followed, with approximately 45% released after two weeks storage. This profile does not differ considerably from that of EPC/EPC:CH:PEG vesicles indicating that electrostatic repulsion between SA and PXB did not increase release rates.

The high initial release observed with EPC and EPC:CH:PEG vesicles was not observed with DSPC based preparations (initial release 6-12%). Retention of PXB over the storage period by all DSPC based vesicles was equivalent to that of the more stable EPC:CH (2:1 and 1:1) vesicles. The difference in release characteristics is related to the phase behaviour of the lipids used. At 4°C, DSPC ( $T_m$  54°C, Szoka, 1980) is in the relatively stable gel state, whereas EPC is liquid crystalline at this temperature. Small differences in efflux of PXB were observed with cholesterol containing DSPC liposomes. A 2:1 molar ratio of cholesterol did not augment the release of PXB, whereas a 1:1 ratio approximately doubled the initial quantity released. These results may be explained by the effect of CHOL on bilayers below their  $T_m$ . Previous studies have shown that CHOL increases the disorder of gel-state bilayers by forcing apart the rigid hydrocarbon chains with an increase in vesicle permeability (New, 1990). Therefore the decreased retention observed with DSPC:CH (1:1) liposomes contrasts with the increased stability of the corresponding EPC:CH (1:1) formulation.

DSPC:CH:PEG (2:1:0.2) vesicles had greater retention of PXB than their EPC based counterparts. This would appear to be related to the increased rigidity of the DSPC bilayer. However, there was a small increase in release over the DSPC:CH (2:1) formulation, again indicating a negative effect of DSPE-PEG<sub>1900</sub> on PXB release. The reasons for such an increase are unclear but may be related to a weak permeabilising interaction of PXB with the anchor lipid or possibly the polymer fraction of this lipid. Interestingly, a previous study has noted that the surface association of cyanuric chloride coupled PEG<sub>5000</sub>-DSPE increased the permeability to entrapped glucose by a factor between 7 and 12 in the PEG content range 0-5 mol% (Nicholas *et al.*, 1994). It is however important to remember that the stealth properties of DSPE-PEG<sub>1900</sub> serve to protect vesicles from opsonin induced clearance and that vesicle permeability to entrapped solutes remains sensitive to the phospholipid/cholesterol composition of the bilayer (Needham *et al.*, 1992; Woodle & Lasic, 1992).

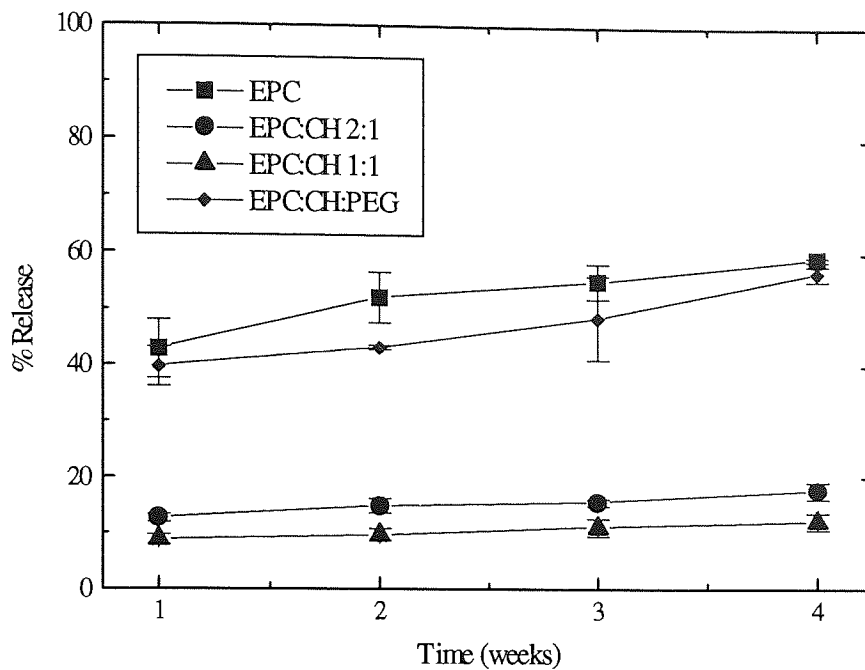


Figure 3.21. Release of PXB from EPC based DRV at 4°C in PBS pH 7.4. Each point represents the mean  $\pm$  standard deviation for three preparations.

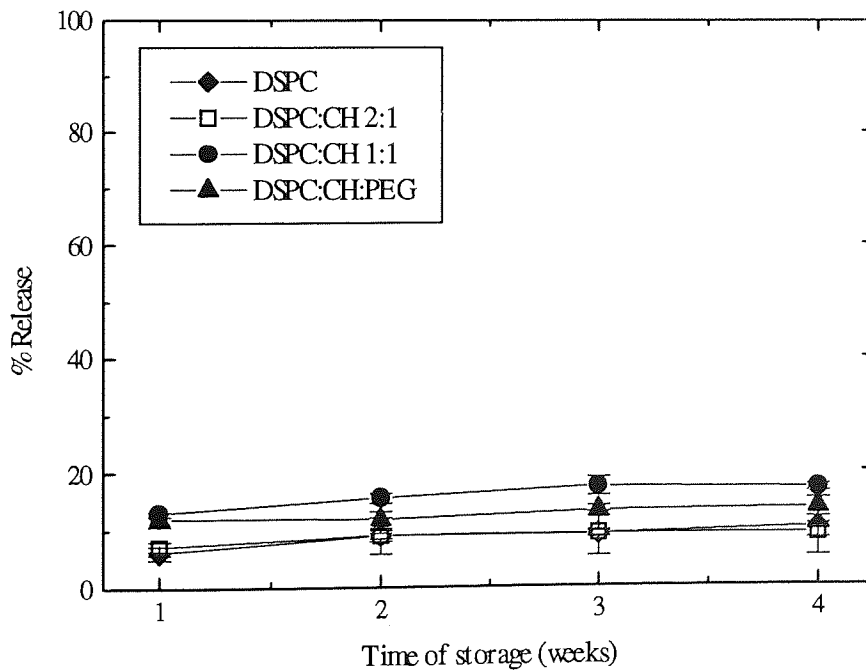


Figure 3.22. Release of PXB from DSPC based DRV at 4°C in PBS pH 7.4. Each point represents the mean  $\pm$  standard deviation for three preparations.



### 3.4.12.2 Release of PXB from LPXB formulations stored at 37°C in PBS pH 7.4

The effect of physiological temperature on the release of PXB was studied by incubation of LPXB formulations in PBS pH 7.4, at 37°C, over a seven day period. Drug release was quantified as detailed in section 2.3.4.

Table 3.12 shows the percentage PXB released from EPC based vesicles over the seven day study period. Phospholipid composition does not appear to influence the release characteristics of the formulations tested. The release profiles of most preparations were biphasic in nature. A period of rapid release over 72 hours was followed by a second stage of slow release up to 168 hours. The release profiles observed at 4°C suggested a biphasic release although the lack of early time measurements precluded any further analysis of the release profile at this temperature. However, release at early time points release was monitored with preparations incubated at 37°C and the profiles show efflux of PXB to be greatest in the initial 72 hour period of incubation.

The release at 4°C was dependent on lipid composition, with cholesterol modulating bilayer permeability as previously reported in a number of studies (Betageri & Parsons, 1992; Taylor *et al.*, 1990). At 37°C, a comparison of the release profiles of EPC, EPC:CH (2:1) and (1:1) does not show the permeability reducing effects of cholesterol. Also, the higher release with EPC:CH:PEG at 4°C was not observed at 37°C. The reasons for this anomalous behaviour are unclear but may be attributable to a temperature dependent interaction between PXB and cholesterol/phosphatidylcholine. Release of phosphorothioate oligonucleotides has also been shown to be independent of phospholipid composition. The rate of permeation was a result of the large molecular weight (~5000) and the highly polar (polyanionic) nature of the oligonucleotides used (Akhtar & Juliano, 1992).

Several formulations showed small deviations from the bulk of release profiles. PXB release from EPC, EPC:CH (1:1), EPC:CH:PEG and EPC:CH:SA was similar in profile and

magnitude at all time points tested. However, release from positively charged EPC:SA vesicles was less at early time points (up to 72hr). This may be explained by electrostatic repulsion effects between PXB and SA reducing the efflux of drug, possibly by repelling PXB diffusion through membrane defects. EPC:CH:GM<sub>1</sub> also showed a reduction in early time release. The initial rapid phase observed with other preparations was decreased in the case of GM<sub>1</sub> containing vesicles. The profile of release assumed a first-order pattern (figure 3.25). The reasons for this are unclear but may be related to decreased intervesicular interaction and it is also likely that the PXB/GM<sub>1</sub> interaction differs from that seen with PXB/DSPE-PEG<sub>1900</sub>.

Time (hrs)	Formulation						
	% Released (Mean±sd)						
	EPC	EPC:CH (2:1)	EPC:CH (1:1)	EPC:SA (9:1)	EPC:CH:SA (6:3:1)	EPC:CH:PEG (2:1:0.2)	EPC:CH:GM <sub>1</sub> (2:1:0.2)
0	18.73 ±4.37	17.49 ±7.67	8.85 ±1.34	16.74 ±0.73	12.86 ±1.19	14.32 ±0.09	19.28 ±4.82
4	32.66 ±1.70	ND	22.06 ±4.78	27.14 ±1.70	32.32 ±10.77	34.48 ±4.82	24.99 ±5.24
24	46.95 ±4.16	54.14 ±3.31	41.82 ±7.97	34.81 ±3.00	54.67 ±7.89	49.17 ±4.61	34.54 ±2.89
48	55.04 ±10.09	67.72 ±7.10	50.32 ±9.14	39.8 ±2.3	58.05 ±1.67	54.80 ±4.83	40.98 ±1.86
72	66.75 ±9.03	77.56 ±4.08	65.75 ±7.52	44.49 ±5.37	60.01 ±4.16	62.96 ±10.46	48.12 ±5.07
96	65.10 ±7.55	ND	66.31 ±7.73	62.40 ±8.40	62.31 ±6.34	67.06 ±5.14	52.10 ±5.10
168	66.79 ±4.36	83.83 ±0.20	66.01 ±6.35	74.26 ±11.4	63.99 ±4.70	74.12 ±6.70	60.13 ±0.86

Table 3.12. Release of PXB from EPC based DRV incubated in PBS pH 7.4 at 37°C. Each value represents the mean±standard deviation of three independent preparations.

Whilst vesicles containing EPC as the main lipid did not illustrate the classical effects of CH on bilayer permeability, the incorporation of CH within DSPC based vesicles resulted in predictable release profiles. DSPC vesicles, in the ordered gel state at 37°C showed the lowest release with  $34.51 \pm 4.70\%$  released after 144 hours. However 33 and 50 mol% ratios of CH increased the release to  $49.0 \pm 4.16\%$  and  $66.74 \pm 1.84\%$  respectively after 144 hours incubation. CH is recognised as increasing the permeability of vesicles composed of lipids below their  $T_m$  through effects on chain spacing and rotation (Inoue, 1974; Taylor *et al.*, 1990). The release from DSPC:CH:PEG was not significantly different from DSPC vesicles again suggesting a reduction in the membrane effects of CH by PEG-lipid in the presence of PXB.

Time (hrs)	Formulation			
	% Released (Mean $\pm$ sd)			
	DSPC	DSPC:CH (2:1)	DSPC:CH (1:1)	DSPC:CH:PEG (2:1:0.2)
0	4.79 $\pm 0.53$	10.18 $\pm 2.42$	10.22 $\pm 1.20$	11.87 $\pm 0.59$
4	8.68 $\pm 0.40$	24.24 $\pm 6.10$	21.48 $\pm 5.21$	16.92 $\pm 1.34$
24	15.10 $\pm 1.28$	36.16 $\pm 10.75$	45.04 $\pm 6.49$	28.17 $\pm 2.28$
48	18.68 $\pm 2.80$	39.28 $\pm 11.62$	48.97 $\pm 0.73$	28.40 $\pm 3.90$
72	24.83 $\pm 3.39$	40.66 $\pm 9.20$	51.68 $\pm 3.68$	31.45 $\pm 5.94$
96	30.68 $\pm 5.52$	50.58 $\pm 11.89$	59.98 $\pm 4.54$	36.0 $\pm 4.02$
144	34.51 $\pm 4.70$	49.0 $\pm 9.16$	66.94 $\pm 1.89$	36.24 $\pm 8.18$

Table 3.13. Release of PXB from DSPC based DRV preparation incubated in PBS pH 7.4 at 37°C. Each value represents the mean $\pm$ standard deviation of three independent preparations.

The release profiles observed with LPXB formulations are similar to those described for other antimicrobials encapsulated with the DRV technique. Tobramycin retention in DSPC:DMPG (10:1 molar ratio) DRV was very stable for 24 hours after rehydration with greater than 83% retained for samples stored at 4°C and 37°C in PBS. In the same study, retention of ticarcillin in DRV of identical composition was approximately 70% after 24 hours at 4°C and 37°C (Lagacé *et al.*, 1991). Cajal *et al.* (1992) have determined gentamicin leakage from DRV composed of EPC:CH (1:1) stored at 4°C in PBS. A biphasic profile was noted with approximately 20% released after 1 week, followed by a slow increase up to 25% after 4 weeks. The second slow phase of release was attributed to intra and extraliposomal gentamicin concentrations reaching an equilibrium value which possibly indicated non-sink conditions for release. In general the high stability of DRV to release of entrapped solutes is a function of the multilamellar nature of the vesicles produced.

The mechanism of PXB release will depend on drug diffusion through lipid bilayers. As intact liposomes are essentially impermeable to multivalent ions and macromolecules (Szoka & Papahadjopoulos, 1980), release of a hydrophilic drug such as PXB will be through water-filled defects in the bilayer structure (Juliano & Stamp, 1979). The mechanism of mitoxantone release from liposomes was shown to be a diffusion-controlled process. This was demonstrated through linear fitting of percentage drug released against square root of time (Higuchi, 1961). Linear behaviour was observed with correlation coefficients between 0.962-0.968. This approach was also taken with PXB. Figures 3.23-3.26 show the release profiles plotted as the percentage of PXB released vs the square root of time for EPC and DSPC based vesicles. The correlation coefficient of EPC based vesicles demonstrated a reasonably linear fit with all compositions. Values ranged from 0.898 (EPC:CH:SA) to 0.997 (EPC:CH:GM<sub>1</sub>). Linear behaviour was also seen with DSPC based vesicles. In this case correlation coefficients ranged from 0.964 (DSPC:CH 2:1) to 0.995 (DSPC). Therefore it would appear that PXB release from EPC/DSPC based vesicles is a diffusion controlled process. It is of note that the release of PXB from both vesicle types was greater at 37°C than 4°C at comparable time-points (figures 3.21 and 3.22), indicating that diffusion was

increased at the higher temperature. The mechanism of temperature enhanced release is likely to be due to increased rotational movement of acyl chains creating membrane defects therefore decreasing diffusional resistance to PXB.

The rate of release is indicated by the slope of the Higuchi plots. The values shown in table 3.14 reinforce the earlier comments regarding the effect of cholesterol on the release rate of PXB at 37°C. All EPC based liposomes, with the possible exception of EPC:CH:GM<sub>1</sub>, possess similar release rate constants. The release rate is lower with DSPC and DSPC:CH:PEG vesicles and is augmented by the addition of cholesterol.

Formulation	Slope ( $\pm$ sd)
EPC	3.94 $\pm$ 0.59
EPC:CH (2:1)	5.27 $\pm$ 0.97
EPC:CH (1:1)	4.87 $\pm$ 0.71
EPC:CH:PEG (2:1:0.2)	4.46 $\pm$ 0.49
EPC:CH:GM <sub>1</sub> (2:1:0.2)	3.26 $\pm$ 0.10
EPC:SA (9:1)	4.29 $\pm$ 0.46
EPC:CH:SA (6:3:1)	3.83 $\pm$ 0.84
DSPC	2.46 $\pm$ 0.11
DSPC:CH (2:1)	3.08 $\pm$ 0.38
DSPC:CH (1:1)	4.47 $\pm$ 0.45
DSPC:CH:PEG (2:1:0.2)	2.03 $\pm$ 0.22

Table 3.14. Slopes of linear regression plots for PXB release from LPXB preparations in PBS pH 7.4 at 37°C.

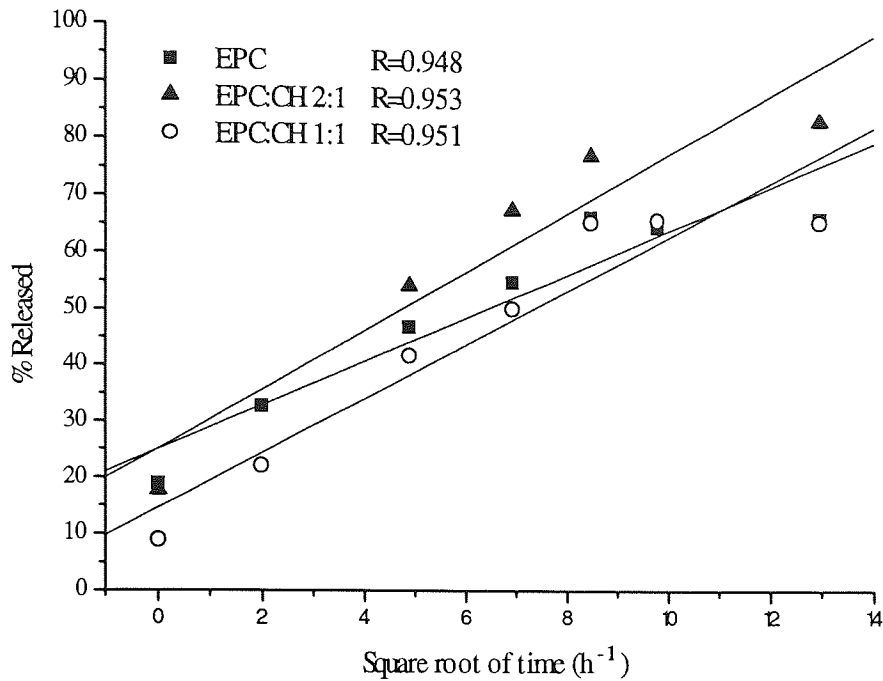


Figure 3.23. Percentage released against square root of time for EPC, EPC:CH (2:1) and (1:1) LPXB formulations. Each point represents the mean of three preparations.

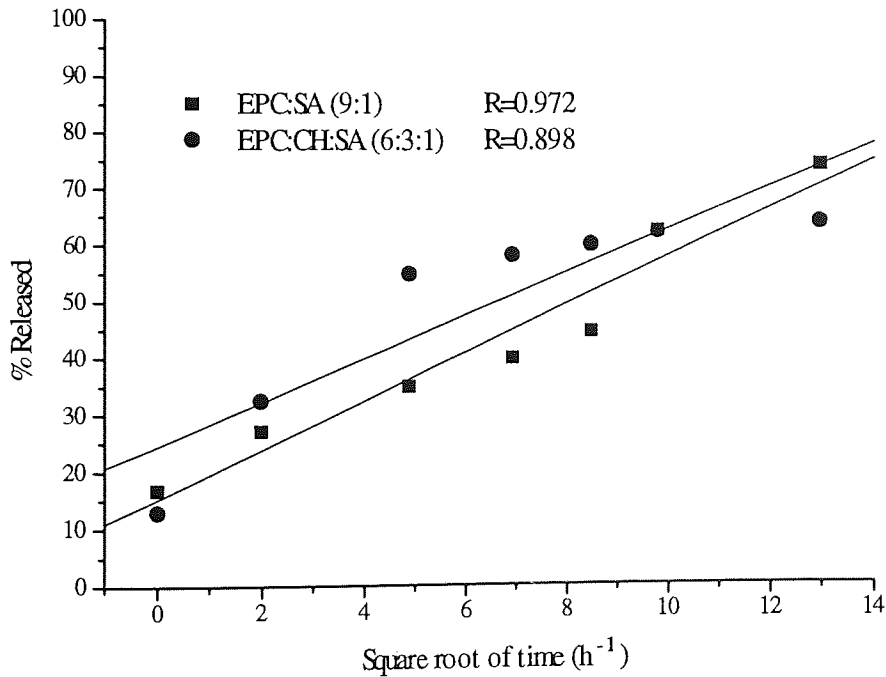


Figure 3.24. Percentage released against square root of time for EPC:SA (9:1) and EPC:CH:SA (6:3:1) LPXB formulations. Each point represents the mean of three preparations.

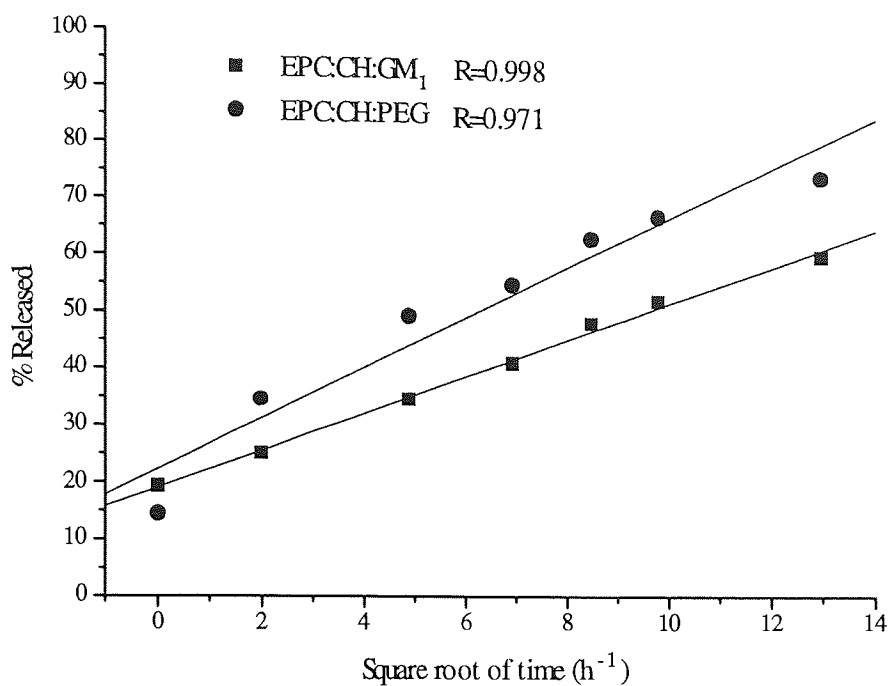


Figure 3.25. Percentage released against square root of time for EPC:CH:GM<sub>1</sub> (2:1:0.2) and EPC:CH:PEG (2:1:0.2) LPXB formulations. Each point represents the mean of three preparations.

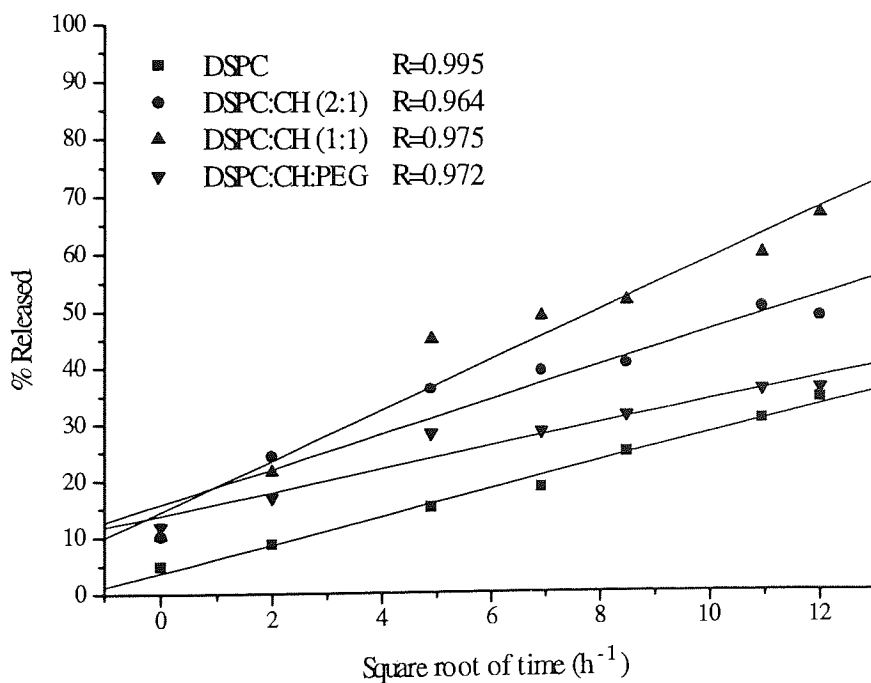


Figure 3.26. Percentage released against square root of time for DSPC based LPXB formulations. Each point represents the mean of three preparations.

### 3.4.12.3 Release of PXB from LPXB formulations in 20% FCS in PBS pH 7.4

The release studies performed in buffer systems have yielded information on the permeability characteristics of LPXB formulations. However, release *in vivo* is mediated by a variety of biomolecules including high density lipoproteins, lipid transfer proteins, phospholipases, clotting and complement enzymes (Jones & Nicholas, 1991; Senior, 1987). Plasma-induced leakage of solutes has been found to be highly dependent on lipid composition (Kirby *et al.*, 1980) and knowledge of stable formulations is a necessity before commencing *in vivo* studies. Serum-induced leakage was studied by Allen and Cleland (1980) and it was shown that the release of entrapped solutes was influenced by the concentration of serum in the release medium. Higher levels of serum resulted in enhanced leakage, although the biggest differential was observed with 0 and 10% serum concentrations. High serum concentrations can be difficult to manipulate for drug separation purposes, particularly low-speed centrifugation and for these reasons it was decided to use a 20% level in release experiments. The use of a 25% serum level has been described as a suitable model for biological fluids as 90% of the effects of full serum may be obtained (Bonte & Juliano, 1986). FCS (non-heat inactivated) was used as it could be obtained in sterile large volumes. Although the serum components differ from those of human serum, this assay provides data on the stability of LPXB formulations in the presence of potentially destabilising proteins.

The release of PXB from EPC based vesicles incubated in PBS at 37°C failed to show the stabilising effect of cholesterol. However, when identical preparations were incubated in the presence of 20% FCS, cholesterol was shown to reduce efflux of PXB over the 24 hour test period (figure 3.28). As the release was followed by centrifugation and analysis of supernatant PXB concentrations, transient destabilisation of EPC vesicles prevented the inclusion of early time release data (0 and 30mins) using this method of separation. After 1 hr incubation, a pellet was obtained and the supernatant was successfully separated from liposomes. The failure to pelletise EPC vesicles reflects the degree of destabilisation induced by serum. Separation of vesicles was problematic throughout the incubation period and



contamination of the supernatant phase with liposomal PXB invalidated the release values obtained in this manner.

An alternative approach was utilised to obtain early time release data for EPC. An ultrafiltration method using Microcon 100 microconcentrators (Amicon Ltd., Gloucestershire, England) was used to separate liposomes from free PXB. This method was used as described in section 3.3.12 and has been previously used to separate vesicles from untrapped steroids (Taniguchi *et al.*, 1987). The ultrafiltrate obtained was analysed for free PXB and the release profile compared with that obtained from centrifugation. As figure 3.28 shows, the profile obtained using ultrafiltration separation showed an immediate release of ~20% PXB on contact with serum followed by a rapid release which continued up to 6 hours when ~45% of the entrapped contents had been released. After 24hr the ultrafiltration value (54.43%) compared well with that determined by centrifugation ( $54.9 \pm 1.92\%$ ).

Transient destabilisation of EPC:SA vesicles was also observed and as a result, early time release has been disregarded. The release after 24hr is of the same extent as EPC vesicles. Electrostatic repulsion between SA and PXB does not appear to influence release characteristics in the buffer system (section 3.4.12.2) and SA did not increase the serum-induced leakage of PXB. EPC and EPC:SA vesicles have therefore shown similar release profiles in all test systems. The time-dependent destabilisation of both EPC and EPC:SA vesicles may be the result of the rapid adsorption of proteins to the liposomal surface. This absorption produces a rise in permeability by altering membrane packing and is followed by a sequence of membrane/protein rearrangement to form a new surface. Membrane permeability may therefore sharply increase on contact with serum and then decline as membrane lipids and adsorbed proteins form their most stable configuration (Hunt, 1982).

Cholesterol is often included in liposome preparations to protect against serum-induced destabilisation (Kirby *et al.*, 1980). In this regard its inclusion in EPC vesicles was successful in reducing the release of entrapped PXB. A 33 mol% ratio reduced the efflux at all time

points and further stabilisation was observed with a 50 mol% ratio. The failure of cholesterol to decrease permeability at 37°C in PBS may be directly related to an unfavourable interaction with PXB which was suggested by the results of encapsulation studies (section 3.4.2). However, the serum protective effect may be considered separately from any compound-dependent effects on membrane permeability as it is a result of the decreased penetration of serum proteins due to the presence of a high molar ratio of cholesterol. The profiles of cholesterol containing vesicles were biphasic although the initial rapid phase of release and subsequent slow efflux were much reduced. Cholesterol is able to stabilise bilayers through effects on bilayer fluidity and thereby prevent or inhibit the association of high density lipoproteins, particularly apolipoprotein A-I (Allen & Cleland, 1980). Biphasic release may be due to a two-phase transfer of high-density lipoprotein (HDL) (Bonte & Juliano, 1986). The first phase occurs rapidly and is followed by a saturable phase during which 50-60% of membrane lipid may be transferred to HDL.

Saturated lipids are regarded as forming vesicles with greater serum stability than those composed of unsaturated lipids (Senior, 1987). DSPC vesicles demonstrated greater retention of PXB than their EPC counterparts over 24hr of incubation (figure 3.28). Transient destabilisation (*i.e.* a failure to pellet liposomes) was not seen with DSPC vesicles. The incorporation of cholesterol in DSPC vesicles was not as successful in further reducing PXB leakage as was seen with EPC based vesicles. A small reduction, although not statistically significant was seen with DSPC:CH (2:1) liposomes. A 50 mol% ratio resulted in increased efflux at all time points. This is presumably due to the fluidising effect on the gel DSPC bilayer outweighing the protective effect against serum afforded by cholesterol. Interestingly the profiles (figure 3.27) obtained with DSPC based liposomes were flat with drug release occurring immediately, with no further increase apparent over the 24 hour incubation period. This contrasts with the clearly biphasic profiles seen with EPC vesicles.

The inclusion of DSPE-PEG<sub>1900</sub> failed to stabilise EPC/DSPC based vesicles in the presence of FCS. This is consistent with the similarity between buffer release values obtained with and

without PEG-lipid. Although the data suggest that PEG-lipid was not successfully incorporated in LPXB preparations, good colloidal stability was seen with these samples on prolonged storage, illustrating that a degree of steric stabilisation was achieved. Comparing EPC:CH (2:1) with EPC:CH:PEG (2:1:0.2) (or the DSPC equivalents) shows that PEG-lipid has a negative effect on stability at 4°C in PBS and 37°C in 20% FCS. A complex three way interaction between PEG-lipid, PXB and cholesterol may limit the therapeutic utility of this form of LPXB.

The release of PXB in 20% FCS/PBS was found to be influenced by the presence of cholesterol and the degree of saturation of the bulk lipid. The *in vivo* use of LPXB would appear to require the use of cholesterol-rich liposomes composed of saturated lipids. Liposome composition would also need to be tailored to provide a stealth capability if vesicles are to be efficiently targeted *via* the systemic circulation to the inflamed CF lung. In this respect GM<sub>1</sub> appears to be a more promising candidate than DSPE-PEG<sub>1900</sub> due to the increased stability observed with this type of vesicle (figure 3.25). The use of GM<sub>1</sub> and possibly other stealth lipids (*e.g.* polyglycerols) warrants further investigation.

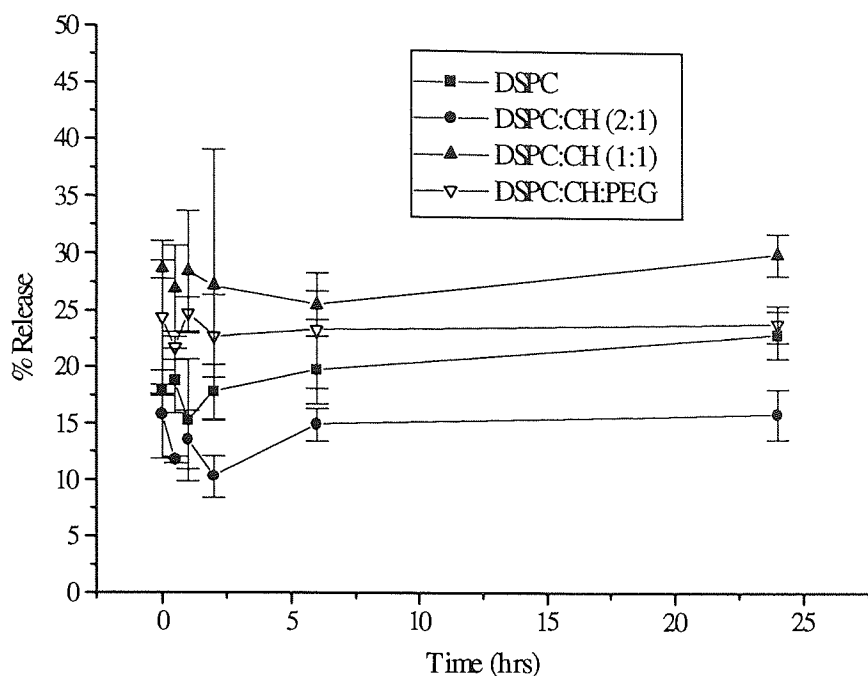


Figure 3.27. FCS induced-release of PXB from DSPC-based DRV expressed as a percentage of that originally entrapped. Each point represents the mean  $\pm$  standard deviation of three preparations.

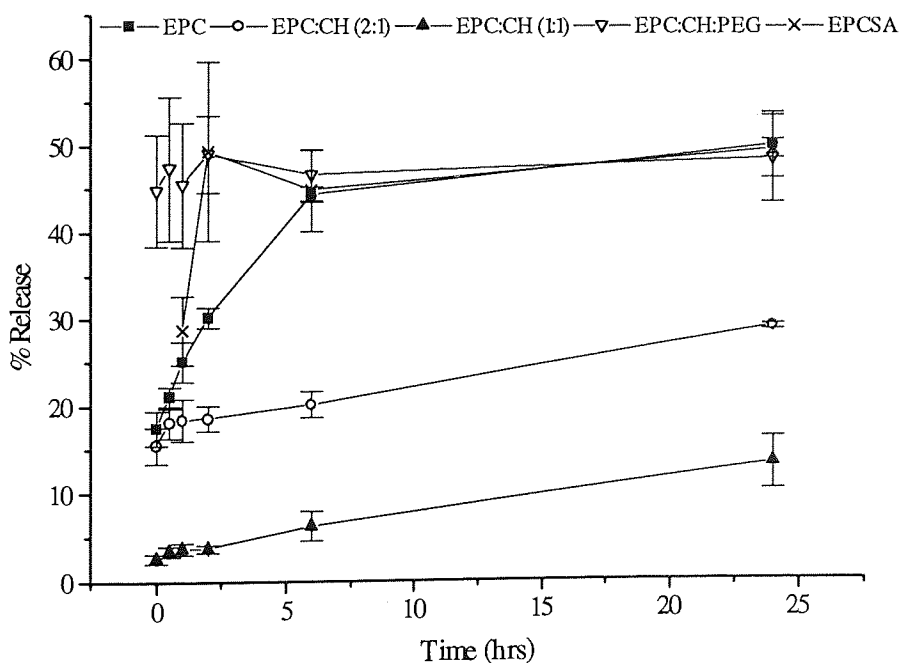


Figure 3.28. FCS induced-release of PXB from EPC-based DRV expressed as a percentage of that originally entrapped. Each point represents the mean  $\pm$  standard deviation of three preparations.

## Chapter 4

### *In vivo* testing of liposomal polymyxin B formulations

---

#### ABSTRACT

Formulation studies have shown that PXB may be encapsulated within liposomes with a range of phospholipid compositions. The *in vivo* behaviour of these formulations was investigated by intratracheal instillation in rats. Liposome formulations of PXB successfully prolonged the lung residence time compared to the free drug which was rapidly cleared. *In vitro* macrophage uptake assays were performed to quantitate the role of macrophage uptake in phagocytic liposome clearance in the lung. The intravenous route was also investigated with a stealth type formulation of PXB prolonging the blood circulation time relative to non-entrapped drug. The effect of formulation variables and vesicle characteristics on the *in vivo* performance of LPXB are discussed.

---

## 4.0. *In vivo* testing of LPXB formulations

### 4.1. Introduction

The rationale for LPXB development was to improve the current therapy of CF lung infections. The perceived advantages of LPXB have been discussed in section 1.2.7. In order to assess the *in vivo* performance of LPXB it was necessary to deliver the drug to its site of action, the lung. This may be achieved through a number of animal models. Firstly, a drug solution may be nebulised and small rodents exposed to the aerosol in a sealed chamber. However, this approach requires the use of specialised equipment, the dose administered to each animal is not easy to quantitate and the dose delivered is relatively small (Jurima-Romet *et al.*, 1990). The intratracheal administration of a drug solution is an alternative approach which offers a simpler means of delivery of a large dose of liquid suspension directly to the lung. Intratracheal instillation has been previously used to quantify the absorption of antibiotics from the rat lung (Burton & Schanker, 1974; Omri *et al.*, 1994; Schreier *et al.*, 1994). The pharmacokinetics of liposomally entrapped antimicrobials have also been assessed using this technique (Demaeyer *et al.*, 1993; Omri *et al.*, 1994). There are differences between the pulmonary distribution of intratracheally instilled and aerosolised drug solutions. With intratracheal instillation, a drug solution is distributed unevenly between the various lobes of the lung, whereas aerosolisation produces a more uniform distribution with greater penetration into the alveolar regions (Brown Jr. & Schanker, 1983; Jurima-Romet *et al.*, 1990). However, given the practical difficulties of aerosolisation, intratracheal instillation was the most pragmatic technique for the *in vivo* evaluation of pulmonary administered LPXB.

The treatment of lung infections may also be achieved through the use of systemically administered antimicrobials. Recently, interest has focused on the potential of intravenously (i.v.) administered long-circulating liposomes for the treatment of infections caused by extracellular bacteria (Bakker-Woudenberg, 1995). For this reason the pharmacokinetics of LPXB were also evaluated after i.v. administration.

Numerous mechanisms contribute to the clearance of liposomal compounds delivered to the lung. Non-specific processes such as mucociliary clearance remove vesicles from the bronchoalveolar epithelia (Schreier *et al.*, 1993) and the fluids lining these surface can promote vesicle destabilisation with subsequent release and absorption of entrapped agents (Jurima-Romet *et al.*, 1992). Macrophage clearance also plays a role and may be dependent on formulation variables (Kyung-Dall *et al.*, 1993). *In vitro* uptake studies of several formulations were performed using a well-characterised murine macrophage cell-line to give information on the potential avidity of formulations for this mechanism of clearance.

## **4.2. Materials**

### **4.2.1 Polymyxin B**

As section 2.2.1

### **4.2.2 Phospholipids**

As section 2.2.2.

### **4.2.3. Chemicals**

All chemicals and reagents not specified in the text were supplied by BDH Chemicals Ltd. (Poole, UK), Sigma Chemical Company (Poole, UK) and Fisons (Loughborough, UK) and were of Analar grade or equivalent.

### 4.3. Methods

#### 4.3.1. Preparation of LPXB for intratracheal instillation

DRV preparations of LPXB were prepared as described in section 3.3.1 and encapsulations determined by scintillation counting of [<sup>3</sup>H]-PXB. A standard drug loading of 9mg PXB/66 $\mu$ M total lipid was used for all preparations. In order to use liposomes with a defined size distribution, preparations were filtered ten times through a 0.8 $\mu$ m polycarbonate filter using a filter barrel or Extruder<sup>®</sup> device (Lipex Biomembranes, Vancouver, Canada). This technique has been previously shown to generate vesicles with a diameter approximating that of the pore size used (section 3.3.13). The diameter of extruded vesicles necessitated the use of high-speed centrifugation to efficiently separate vesicles from non-entrapped drug. Vesicles were spun at 40000g for 1hr and the resulting pellet was resuspended and washed with 25ml PBS pH 7.4. After separation vesicles were resuspended to give a LPXB dose equivalent to 1mg/ml of PXB. Vesicles were characterised by laser Doppler velocimetry (zeta potential) in PBS pH 7.4 and 0.02M diphosphate as previously described (section 3.3.7).

#### 4.3.2 Intratracheal instillation of LPXB

Adult male rats weighing 200-250g were used for this study. The method of Enna and Schanker (1972) for measurement of instilled compounds from the lungs of anaesthetised rats was modified to allow measurements of LPXB levels in animals for periods up to 24hr after instillation.

Animals were anaesthetised prior to dosing by i.m. injection of Hypnorm (0.3mg/kg) followed by i.p. injection of diazepam (2.5mg/kg). Anaesthetised animals were placed in a supine position and a small midline incision was made over the trachea. The trachea was exposed by blunt dissection of the sternohyoideus muscle. An incision was made between the fifth and sixth tracheal rings using a 20-gauge needle and a short length (2.5cm) of Portex



polyethylene catheter advanced to within 1cm of the lung bifurcation. Endotracheal delivery was then achieved using a 1ml syringe containing 0.1ml of liposomal or free PXB (1mg/ml PXB). The solution was instilled with sufficient air to clear the catheter of any residual dose. Following instillation the animals heads were immediately elevated 30° above the horizontal and the tracheal hole plugged with a small piece of hydrocolloid dressing to promote wound healing. The incision was then closed with two or three sutures and the animal allowed to recover under a heating lamp. After recovery, animals were placed in metabowls with free access to food and water.

At the appropriate time-points, blood samples were obtained by tail-vein bleeding into heparinised eppendorf tubes. When required animals were sacrificed and tissues (lungs, spleen, liver and kidneys) excised, weighed and homogenised in PBS pH 7.4 using an Ultraturrax homogeniser (20000rpm for 2min). The sample was diluted to an appropriate volume and 200µl transferred to a scintillation vial containing 15ml of Optiphase Hisafe II scintillation cocktail. Samples were dark-adapted for 24hr before counting in a Packard 1600TR Tri-Carb scintillation counter. Samples were corrected for quench by comparison to a standard quench curve and the dpm value determined ( $[^3\text{H}]$ -PXB and/or  $[^{14}\text{C}]$ -CHOL).

### **4.3.3 Intravenous administration of free and LPXB**

#### **4.3.4. Preparation of EPC:CH:PEG extruded DRV for intravenous (i.v.) administration**

DRVs, composed of EPC:CH:PEG (2:1:0.2), were prepared as before (section 3.3.1), using a drug loading of 9mg PXB and 66µM total lipid. After rehydration and separation from free drug by centrifugation, vesicles were extruded ten times through a 100nm polycarbonate filter using an Extruder<sup>®</sup> device (Lipex Biomembranes, Vancouver, Canada). Scintillation counting of  $[^3\text{H}]$ -PXB was used to determine encapsulation. Cholesteryl  $[1-^{14}\text{C}]$  oleate

(0.185MBq) was incorporated as a liposomal bilayer marker (specific activity 3.11MBq/mg, Amersham International, England).

#### 4.3.5. Ion-exchange separation of 100nm extruded EPC:CH:PEG vesicles from non-entrapped PXB - preparation and activity of Dowex-50WX4 cation exchange resin

Due to the small size of the extruded vesicles, separation from non-entrapped drug required the use of an alternative method to centrifugation. Gel exclusion chromatography may be used for this purpose, although sample dilution limits its usefulness in this case. Cation exchange has previously been used to remove unencapsulated amikacin (Wichert *et al.*, 1992) and doxorubicin (Amselem *et al.*, 1990; Barenholz & Amselem, 1993) from liposomal suspensions. PXB is strongly positively charged and would be expected to be chelated strongly by the resin.

Dowex 50WX-4 (hydrogen form, 100-200 mesh, Sigma, Poole, Dorset) is supplied as a strongly acidic resin and it was necessary to convert it to the sodium form by successive washings with 100ml 2M NaOH *per* 25g of resin using a Buchner funnel. The NaOH was removed by a 500ml wash with 1M NaCl after which the pH returned to neutral. The resin was finally washed with 0.9% w/w NaCl and dried overnight at 80°C.

The removal of free PXB by activated Dowex was confirmed by incubating 1ml aliquots of a 5mg/ml solution of PXB with 10, 20, 30, 40, 50, 75 and 100mg of resin for 15min at room temperature in a shaking water bath. The samples were centrifuged at 2000g for 2min and the supernatant assayed for PXB by BCA assay of PXB (section 2.3.2). The percentage of PXB adsorption by Dowex was calculated by dividing the PXB concentration of the supernatant by the PXB concentration of an untreated sample. Figure 4.1 shows this percentage plotted against the weight of Dowex used. Dowex resin was found to remove all PXB when the resin to drug ratio was greater than 6:1.

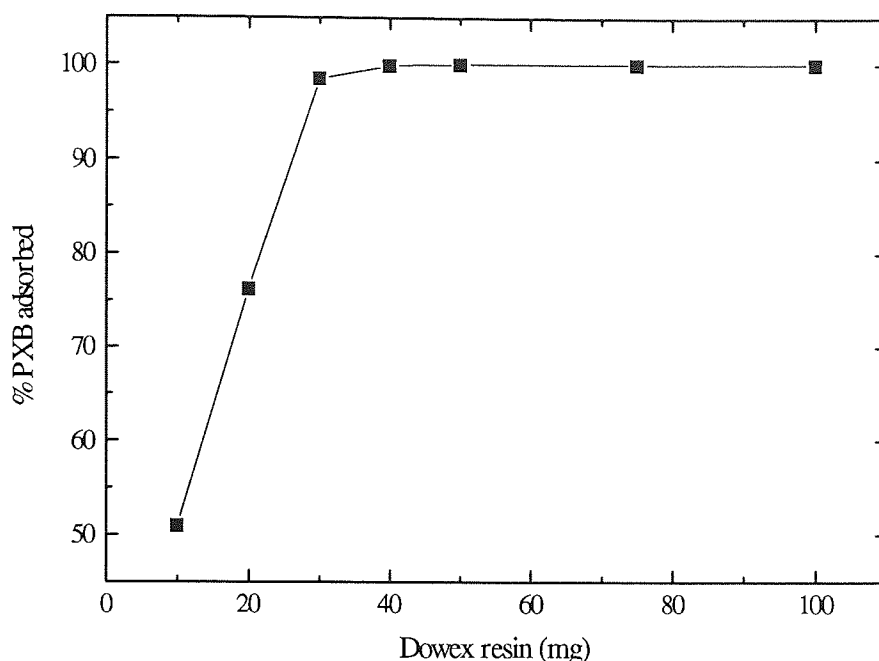


Figure 4.1. Adsorption of PXB (5mg) by Dowex 50WX-4. Each point represents the mean of duplicate samples

As the removal of PXB was successfully achieved using Dowex, this method was used to separate EPC:CH:PEG vesicles from non-entrapped PXB. Extruded vesicles (1ml,  $\sim 40\mu\text{M}$  lipid) were mixed with dry activated Dowex (200mg) in a round bottomed flask under the above conditions. After incubation, the mixture was transferred to a 1ml syringe, plugged with glass wool, and centrifuged at 200g for 2min. The eluate contained vesicles separated from resin. In order to verify separation a small aliquot (50 $\mu\text{l}$ ) of resin treated vesicles was applied to a G-50 column and GEC performed as previously described. A sample of non-resin treated vesicles was also fractionated by GEC and the profiles compared. Vesicle size distribution was compared before and after resin treatment. Zeta potential of the separated vesicles was determined by laser doppler velocimetry (section 3.3.7). TEM (section 3.3.9) was used to confirm downsizing and vesicle morphology after extrusion.

#### 4.3.6. Intravenous administration of non-encapsulated PXB and LPXB

Animals were anaesthetised prior to dosing by i.m. injection of Hypnorm (0.3mg/kg) followed by i.p. injection of diazepam (2.5mg/kg). Anaesthetised animals were placed in a supine position and 200µl of PXB or LPXB administered *per* the tail vein. PXB was administered in two doses; 0.8mg/kg and 2.7mg/kg. A single dose of LPXB was used (0.1mg/kg PXB, ~6µmol lipid). At the appropriate time-points, blood samples were obtained by tail-vein bleeding into heparinised eppendorf tubes. Urine was collected over 24hr using metabowls. When required animals were sacrificed and tissues (lungs, spleen, liver and kidneys) excised and analysed for [<sup>14</sup>C]-cholesteryl oleate and [<sup>3</sup>H]-PXB content as after intratracheal instillation (section 4.3.2).

Serum samples were also treated with Dowex resin to differentiate between liposomal and free PXB in the circulation. Serum (100µl) was incubated with 10mg activated resin for 15min at room temperature with shaking. It was then separated from resin by applying to a 200µl pipette tip plugged with glass wool and centrifuging at 2000g for 2min (Microfuge, MSE, UK). Eluted serum was then analysed for [<sup>14</sup>C]-CHOL and [<sup>3</sup>H]-PXB as previously detailed.

#### 4.3.7. Preparation of LPXB for macrophage uptake assay

In order to increase the uptake of vesicles by the chosen murine macrophage cell-line, J774.1, DRVs were extruded ten times through a 0.2µm polycarbonate filter using an Extruder (Lipex Biomembranes, Vancouver). These vesicles were separated from free drug by gel exclusion chromatography using a Sephadex G-50 column and fraction collector as described previously (section 3.3.11). Confirmation of vesicle size distribution was performed by PCS (section 3.3.6).

#### 4.3.8. Macrophage uptake assay for LPXB

Murine J774.1 macrophages were cultured in 75cm<sup>2</sup> flasks using RPMI 1640 buffered with HEPES at 37°C supplemented with 5mM L-glutamine and 10% foetal calf serum (FCS). Uptake studies were performed in twelve well culture dishes (Costar, UK), each well containing 1x10<sup>6</sup> viable cells. Uptake was quantified with and without 10% FCS. Extruded liposomes (0.1µm lipid/well) were incubated with cells for 3hr at 4°C or 37°C. The culture medium was removed and the cells gently washed before resuspension and lysis with 0.5% (w/v) SDS in PBS. The extent of uptake was quantified by scintillation counting of [<sup>3</sup>H] PXB in lysate samples.

### 4.4. Results and Discussion

#### 4.4.1. Characterisation of LPXB formulations used for intratracheal (i.t.) instillation

The encapsulation of PXB within DRV has previously been shown to be formulation dependent. The effects of phospholipid composition have been discussed in section 3.4.3. The encapsulations (table 4.1) determined for the single preparations used for i.t. instillation largely follow the trends previously observed. Exceptions were the EPC:CH (2:1) and (1:1) formulations which had higher entrapments (49.62±1.01% and 54.32±0.93% respectively). Zeta potential characterisation (table 4.1) in both buffer systems confirmed that all preparations possessed similar surface charge characteristics as earlier preparations (section 3.4.7). Laser diffraction sizing was not performed due to the relatively large amount of sample required. However the extrusion process had demonstrated reproducible downsizing of vesicles to sizes which approached the pore-size of filter used.

Downsizing of vesicles using extrusion through polycarbonate filters results in deformation of liposomes as they pass through filter pores (Hope *et al.*, 1993). Vesicles can deform to a

certain extent but the pressure differential on the opposite side of the pore causes the bilayer to rupture. Immediate annealing occurs and results in the formation of smaller vesicles (Olson *et al.*, 1979). This process has been envisaged as successive layers of MLV 'peeling' off until only unilamellar vesicles remain (Martin, 1990). Evidence for bilayer rupture comes from the observation that sequential extrusion results in loss of aqueous marker (Olson *et al.*, 1979). Microfluidisation of DRV also downsizes vesicles with loss of entrapped contents (Gregoriadis & Florence, 1993a). The extrusion process reduced PXB entrapment within DRV (table 4.1). The loss of contents presumably reflects rupture of vesicle structure and release of entrapped PXB. A consistent reduction was seen across the range of formulations extruded and amounted to 45-50% of the originally entrapped drug. When [<sup>14</sup>C]-CHOL was included as a bilayer marker little or no loss was detected after extrusion. This suggests that PXB lost during extrusion originated from the fraction of drug encapsulated within the aqueous compartment of vesicles. Microfluidisation of washed DRV caused a similar reduction in the entrapment of maltose and tetanus toxoid (Gregoriadis & Florence, 1993a). This study also demonstrated that it is possible to minimise loss of entrapped solute by processing in the presence of untrapped drug. Olson *et al.* (1979) noted an increase in the entrapment of solutes when extrusion was carried out in the presence of untrapped solute. Therefore it may be possible to minimise the loss of PXB by extruding unwashed DRV.

Formulation	Entrapment before extrusion (%)	Entrapment after extrusion (%)	Retention of [ <sup>14</sup> C]-CHOL marker (%)	Zeta potential (mV) in PBS pH 7.4	Zeta potential in 0.02M diphosphate pH 7.4
EPC	45.41±0.51	24.83±0.46	ND	-3.7±0.7	1.8±0.4
EPC:CH (2:1)	49.62±1.01	27.71±2.05	99.84±1.12	-5.9±0.2	0.4±0.4
EPC:CH (1:1)	54.32±0.93	32.82±1.40	98.69±2.00	-8.3±0.9	0.3±0.2
EPC:SA (9:1)	38.25±0.72	18.96±1.52	ND	13.6±1.5	23.8±0.3
EPC:CH:SA (2:1:0.2)	41.36±1.31	23.98±1.01	ND	4.6±0.5	9.4±0.4
EPC:CH:GM <sub>1</sub> (2:1:0.2)	27.72±1.38	15.88±1.37	88.28±4.7	-6.0±1.4	-15.8±0.6
EPC:CH:PEG (2:1:0.2)	33.73±0.11	17.72±1.41	88.64±3.81	-0.1±0.6	-1.4±0.7

Table 4.1. Characterisation of DRV used for i.t. administration. Each encapsulation is the mean±standard deviation of three determinations for a single preparation. Zeta potentials are the mean of five individual measurements in each buffer system

#### 4.4.2. Pulmonary retention of non-encapsulated PXB after intratracheal administration

After i.t. instillation of non-entrapped PXB, low lung levels at 4hr (3.29±2.64%) and 24hr (3.05±2.24%) were observed (table 4.3). These levels of PXB are consistent with those of a previous study which investigated the absorption of antibiotics with a range of hydrophobicities from the rat lung after i.t. instillation (Burton & Schanker, 1974). It was shown that absorption was related to lipophilicity with chloramphenicol absorbed most rapidly followed by doxycycline, erythromycin and tetracycline, with benzylpenicillin showing

the slowest absorption rate. Pulmonary absorption of polymyxins has been noted after clinical use with blood levels detected after aerosol inhalation (Halliday, 1967).

Absorption of compounds from the lung is governed by a number of factors. For PXB, a decapeptide with a molecular weight of ~1350Da, factors such as size, charge and interactions with lung phospholipids contribute to the absorption rate (Wall, 1995). In general the rate and extent of absorption of non-lipid soluble compounds varies in inverse order with the molecular weight of the compound (Folkesson *et al.*, 1990). It was shown that the absorption of dDAVP (1-deamino-cysteine-8-D-arginine vasopressin), a peptide with a molecular weight of 1067Da, was greater than those of bovine IgG with a molecular weight of 150000Da. The existence of several populations of water-filled pores of different radii in the alveolar epithelium was suggested to account for the observed differences in transport rates of compounds of various molecular weight. An effective molecular weight cut-off for the occurrence of sieving was proposed to be between 4 and 7kD (Brown Jr. & Schanker, 1983; Enna & Schanker, 1972). Cytochemical staining and absorption studies have indicated that macromolecular transport may be mediated by pericellular or transcytotic processes (Bensch & Dominguez, 1971; Gil, 1983), with subsequent transport from the underlying interstitium occurring *per* lymph drainage (Meyer *et al.*, 1969; Smith *et al.*, 1989), or through the leaky pericellular junctions of the capillary endothelium to the bloodstream (Schneeberger, 1978).

Transport across epithelia, including tracheal and bronchial epithelia, shows charge related permselectivity (Rojanasakul *et al.*, 1992). As many components of the alveolar-capillary barrier have been characterised as negatively charged (Simionescu & Simionescu, 1983), electrostatic interaction with charged molecules may affect absorption with neutral and anionic compounds exhibiting higher transport rates than cationic agents. As PXB is positively charged at physiological pH, interaction with epithelial cell surface components may account for the residual level observed after 24hr. However, diffusion through water-



filled pores is obviously favoured with the bulk of the administered dose absorbed from the lung.

Interaction with lung phospholipids is an important factor which may affect lung absorption. In addition to the phospholipids of cell membranes, pulmonary administered compounds interact with phospholipids of the pulmonary surfactant. The pulmonary surfactant monolayer is the first phospholipid surface that a lung-delivered drug contacts upon reaching the alveoli. This layer is ~4nm thick and decreases the surface tension of alveolar membranes which aids liquid haemostasis and may play a role in pulmonary defence (van Golde *et al.*, 1988). The surfactant is composed of 80-90% lipid of which phosphatidylcholines and phosphatidylglycerols constitute 70-80% and 5-10% of the total lipid by weight respectively (King & Clements, 1972). Approximately 60% of the PC in surfactant is in the form of DPPC. Other surfactant lipids include cholesterol, fatty acids and triglycerides. Endogenous surfactant proteins and plasma proteins from exudate (e.g. albumin) are also present.

PXB has previously been shown to interact weakly with neutral phospholipids and strongly with anionic phospholipids (see section 3.4.1). The extent of interaction with pulmonary phospholipids does not appear to be sufficient to prolong lung levels. This is in contrast to the lung profiles observed for peptides with a similar molecular weight. Detirelix is an amphipathic decapeptide (mol. wt 1540) which has two cationic sites at physiological pH. The i.t. administration of the free drug resulted in prolonged absorption with a reported mean residence time of  $14.7 \pm 2.5$  hr (Bennett *et al.*, 1994b). A liposomal formulation provided sustained release (mean residence time  $57.4 \pm 4.2$  hr) in excess of that seen with free drug (Bennett *et al.*, 1994a). Efficient liposome loading was achieved as a result of specific and non-specific interactions between detirelix and phospholipid bilayers. Electrostatic interactions between the cationic amino-acid residues initiated association which was followed by insertion of the hydrophobic tail with the lipid bilayer. Optimal insertion occurs with peptides with 10-12 amino acids (Williams & Weiner, 1989) which may explain the strong association seen with detirelix. Cyclosporin A (CsA) is a neutral lipophilic cyclic undecapeptide (mol. wt 1203) which also shows prolonged lung retention (Dowling *et al.*,

1990; Zenati *et al.*, 1991). The lung has been noted as having an avidity for CsA when administered parenterally (Keenan *et al.*, 1992; Stepkowski *et al.*, 1989). Therefore CsA readily crosses the alveolar-capillary barrier. Binding to lung tissue components, such as phospholipids, may account for prolonged pulmonary residence of CsA. A strong interaction with liposomal phospholipids has previously been described in a number of studies (Stuhne-Sekalec & Stanacev, 1991; Waldrep *et al.*, 1993). As with detirelix, the structural properties of CsA facilitate this interaction. Lipopeptide analogues of echinocandin B and cilofungins are cyclic hexapeptides with amide-linked hydrocarbon chains (mol. wt ~1200) (Rouse *et al.*, 1992). A strong hydrophobic interaction between the hydrocarbon chains and liposomal bilayers was revealed in a spectroscopic study (Ko *et al.*, 1994). The cyclic peptide head-group is of a similar size to that of PXB, although the hydrocarbon chain is seven methylene units longer. The dimethylmyristoyl chains may also facilitate association with the phospholipid bilayers of tissues explaining the prolonged lung retention of this group of compounds. Prolonged lung levels of pentamidine have been attributed to binding of the multiple positively-charged amino groups of pentamidine to acidic phospholipids (Debs *et al.*, 1987).

PXB, detirelix, CsA and cilofungins share a similar molecular weight and peptide structure. However, the structural features which promote interaction with phospholipids may determine pulmonary retention of these compounds. The weak interaction of PXB with phosphatidylcholine is unlikely to reduce rapid absorption from the lung as observed in the current study.

#### 4.4.3. Pulmonary retention of LPXB after intratracheal administration

The lung retention of [<sup>3</sup>H]-PXB was significantly increased following i.t. instillation of all LPXB formulations compared to non-liposome-entrapped PXB. There was no significant difference in the percentage of original radiolabel retained within the lung at 4hrs among the

neutral liposomal formulations tested: EPC ( $48.9 \pm 2.4\%$ ), EPC:CH (2:1) ( $56.4 \pm 10.1\%$ ) and EPC:CH (1:1) ( $62.6 \pm 12.7\%$ ). EPC:CH:PEG (2:1:0.2) vesicles had a similar retention value ( $51.26 \pm 5.96\%$ ). The retention of EPC:SA vesicles ( $65.38 \pm 16.07\%$ ) was significantly greater than EPC vesicles 4hr after instillation. Lung levels of PXB obtained with the positively charged EPC:CH:SA (6:3:1) formulation ( $73.4 \pm 4.4\%$ ) and EPC:CH:GM<sub>1</sub> ( $85.66 \pm 4.32\%$ ) at 4hr were significantly increased ( $p < 0.05$ ) compared with the use of neutral vesicles. After 24hr, the lung retention of PXB decreased and indicated the ongoing clearance of liposomal formulations from the lung. PXB lung levels were not significantly different among the neutral formulations at 24hr: EPC ( $40.3 \pm 3.7\%$ ), EPC:CH (2:1) ( $27.7 \pm 9.0\%$ ) and EPC:CH (1:1) ( $40.0 \pm 15.2\%$ ). EPC:CH:PEG retention ( $36.14 \pm 11.92\%$ ) was again comparable to this group. The retention of EPC:SA ( $59.11 \pm 11.27\%$ ) was not significantly different from that of EPC vesicles after 24hr. Lung retention of PXB at 24hr remained significantly ( $p < 0.05$ ) increased with the EPC:CH:SA formulation ( $52.3 \pm 4.1\%$ ) and EPC:CH:GM<sub>1</sub> ( $50.29 \pm 8.81\%$ ) compared with the EPC and EPC:CH (2:1) formulations, although the difference was not significant when compared with the EPC:CH (1:1) formulation.

The incorporation of the bilayer marker [<sup>14</sup>C]-CHOL allowed the clearance of liposomes from the lung to be evaluated and compared to the clearance of [<sup>3</sup>H]-PXB. Table 4.2 shows the recoveries (as a fraction of the dose originally administered) of [<sup>14</sup>C]-CHOL at 4hr and 24hr. The clearance of liposomes from rat lungs lagged behind the clearance of PXB. After 4hr all formulations show >75% retention in the lung and inter-formulation differences are small. On-going clearance is also seen with [<sup>14</sup>C]-CHOL counts falling after 24hr. At this time-point [<sup>14</sup>C]-CHOL recoveries were similar for EPC:CH (2:1) ( $46.69 \pm 15.42\%$ ), EPC:CH (1:1) ( $58.43 \pm 24.84\%$ ) and EPC:CH:PEG ( $50.22 \pm 13.82\%$ ). Higher recoveries were observed with EPC:CH:SA ( $73.82 \pm 6.00\%$ ) and EPC:CH:GM<sub>1</sub> ( $64.63 \pm 10.57\%$ ). The latter formulations showed elevated [<sup>3</sup>H]-PXB levels at both time-points suggesting that [<sup>3</sup>H]-PXB remained associated with liposomes and that liposomal clearance was the rate-limiting parameter for [<sup>3</sup>H]-PXB clearance. As the clearance of non-entrapped PXB is rapid, release of drug from liposomes would result in rapid absorption of PXB from the lung, with a

decreasing [ $^3\text{H}$ ]-PXB/[ $^{14}\text{C}$ ]-CHOL ratio. Measurement of [ $^{14}\text{C}$ ]-CHOL does not necessarily indicate recovery of intact liposomes as molecular exchange and transfer of lipid can occur. However, the determination of [ $^{14}\text{C}$ ]-CHOL/[ $^3\text{H}$ ]-PXB ratios provides a good indication of liposomal integrity, as was observed in this case (Jurima-Romet & Shek, 1991).

Formulation	% [ $^{14}\text{C}$ ]-CHOL remaining after 4hr	% [ $^{14}\text{C}$ ]-CHOL remaining after 24hr
EPC	Not done	Not done
EPC:CH (2:1)	84.96±8.87	46.69±15.42
EPC:CH (1:1)	87.14±7.90	58.43±24.84
EPC:SA (9:1)	Not done	Not done
EPC:CH:SA (6:3:1)	75.82±3.31	73.82±6.00
EPC:CH:PEG (2:1:0.2)	82.27±10.76	50.22±13.82
EPC:CH:GM <sub>1</sub> (2:1:0.2)	87.90±6.96	64.63±10.57

Table 4.2. Lung levels of [ $^{14}\text{C}$ ]-CHOL in DRV, 4 and 24hr, after i.t. administration. Each point represents the percent of the original quantity of [ $^{14}\text{C}$ ]-CHOL administered (average±s.d., n=3).

The release of encapsulated PXB may be facilitated through the destabilisation of liposomes by protein components of the epithelial lining fluid (Jurima-Romet *et al.*, 1992). The presence of cholesterol may decrease solute permeability through liposomal bilayers and may protect liposomes from destabilisation (Fielding & Abra, 1992). However this effect was not observed with LPXB formulations. Specifically the retention of PXB in the lung with EPC vesicles was not significantly different from PXB retention with EPC:CH (2:1 and 1:1) and EPC:CH:PEG formulations. The elevated levels of EPC:SA (compared to EPC at 4hr), EPC:CH:SA and EPC:CH:GM<sub>1</sub> (at 4 and 24hr) suggested that vesicle destabilisation was not the sole contributing factor to PXB clearance from the lung.

Several mechanisms contribute to the clearance of liposomes from the lung. The mucociliary escalator, consisting of ciliated epithelial cells lining the upper tracheobronchial region to the peripheral terminal bronchioles, are an extremely efficient clearance mechanism. The major clearance mechanism in the alveolar regions is uptake by pulmonary alveolar macrophages. Liposomes are cleared by incorporation into the surfactant phospholipid pool where recycling of phospholipids by alveolar type II cells takes place (Schreier *et al.*, 1993). Higher uptake of i.t. instilled formulations may be mediated through charge interaction as it is known that positively charged vesicles show higher macrophage uptake than uncharged counterparts (Alpar *et al.*, 1990). Such an effect would contribute to the higher levels seen with positively charged vesicles. An *in vitro* assay for uptake was established and the relevance of this to the observed lung levels is discussed in section 4.4.9.

A number of studies have shown that liposomal encapsulation is a successful means of increasing the lung retention times of i.t. delivered drugs. Liposomal encapsulation of atropine increased drug concentration within pulmonary tissue for a more prolonged period as compared to free drug (Meisner *et al.*, 1989). The retention of i.t. administered  $\alpha$ -tocopherol was significantly increased when liposomally encapsulated (Suntres *et al.*, 1993). Glutathione, a water-soluble tripeptide, is rapidly cleared from the lung when delivered as the free drug. However, liposomal entrapment significantly enhances the lung residence time through the slow release of entaped glutathione (Jurima-Romet *et al.*, 1990; Jurima-Romet & Shek, 1991; Suntres & Shek, 1994). The i.t. administration of free and liposomal benzylpenicillin showed that the onset of peak plasma concentration could be delayed by encapsulation. Oxytocin, a water-soluble nine amino-acid peptide (mol. wt. 1007), also showed decreased systemic absorption when administered as a liposomal formulation. For both drugs it was concluded that the lung acts as the rate-limiting barrier for absorption although the amount of drug entering the circulation was dependent on the fraction released from liposomes (Mihalko *et al.*, 1988). Liposomal encapsulation of sodium cromoglycate produced sustained plasma levels of drug and decreased the peak plasma level observed after inhalation of free drug solution by human volunteers, indicating prolonged retention (Taylor

*et al.*, 1989). After i.t. administration of free gentamicin a peak plasma level was achieved in 30 minutes. No peak was observed with liposomal gentamicin and the plasma concentrations remained significantly lower than after unencapsulated drug administration (Demaeayer *et al.*, 1993). The influence of pulmonary infection on the lung-retention of free and liposome-encapsulated tobramycin was investigated by Omri *et al.* (1994). The i.t. instillation of liposome-encapsulated tobramycin resulted in a prolonged retention time (15 min for free drug and a minimal duration of 960 minutes for the liposomal formulation). The presence of infection (created by *P. aeruginosa* impregnated agar beads) decreased pulmonary levels of both free and encapsulated tobramycin. This was attributed to enhanced passage of antibiotic across lung epithelia due to vasodilation and increased vascular permeability. It would appear reasonable that the clearance of PXB would be similarly enhanced in the infected and inflamed CF lung. Also, as mucociliary clearance is impaired in CF, clearance of LPXB would be reduced relative to clearance from healthy lungs.

The effect of phospholipid composition on the clearance of terbutaline-loaded vesicles was studied by Fielding and Abra (1992). The lung kinetics of liposomal terbutaline were found to be sensitive to liposomal composition. The presence of cholesterol and phospholipids with saturated hydrocarbon chains increased pulmonary liposome retention. Increasing cholesterol content allowed the pulmonary half-life of terbutaline to be increased almost 10-fold. This was attributed to the protection of liposomes from destabilisation and a decrease in membrane permeability. The lung retention of entrapped glutathione was also affected by liposome composition. The release of glutathione from vesicles composed of DMPC, which is in the liquid crystalline state at body temperature, was modulated by the presence of cholesterol. However, the differences between DPPC and DSPC vesicles, with and without cholesterol, were minimal (Jurima-Romet & Shek, 1991). A subsequent *in vitro* study showed that glutathione release could be induced by bronchoalveolar lavage fluid (Jurima-Romet *et al.*, 1992). Again the leakage of glutathione was formulation dependent. Release from DMPC vesicles in lavage fluid was not significantly different from that in buffer and could be reduced by the incorporation of cholesterol. Cholesterol increased release from

DPPC and DSPC vesicles, both lipids which are in the gel state under the test conditions. Accordingly, EPC vesicles should be stabilised in the presence of bronchoalveolar fluids by the presence of cholesterol. However, release studies (section 3.4.12) conducted in PBS pH 7.4 at 37°C failed to show a decreased permeability for cholesterol-containing preparations compared with their cholesterol-free counterparts. Release induced by 20% FCS in PBS was reduced by cholesterol and it was concluded that cholesterol was effective in reducing protein-induced destabilisation of LPXB but not effective for reducing the membrane permeability related efflux of PXB. Therefore the similarity of *in vivo* lung profiles of EPC, EPC:CH (2:1 and 1:1) and EPC:CH:PEG may be attributable in part to their shared efflux kinetics in PBS. Although bronchoalveolar fluid contains a number of proteins (albumin, IgG, surfactant-associated proteins) it lacks lipoproteins, the main mediators of liposome destabilisation in serum. The release profiles obtained in buffer-only conditions may therefore be a more relevant indication of release in the lung. PXB release in PBS from EPC:SA and EPC:CH:GM<sub>1</sub> was significantly different at 24hr from comparator formulations. This may partly explain the higher recovery of [<sup>3</sup>H]-PXB from EPC:CH:GM<sub>1</sub> although this was not seen with EPC:SA. It is likely that release as a result of vesicle destabilisation or PXB diffusion is only one of several mechanisms for LPXB clearance, with mucociliary clearance and macrophage uptake also important.

In conclusion, the prolonged retention times observed with LPXB formulations are consistent with previous studies that demonstrated the potential of liposome-encapsulation for prolonging the pulmonary residence of i.t. drugs.

#### **4.4.4. Biodistribution of PXB and LPXB after intratracheal administration**

The prolonged lung retention of LPXB demonstrates the existence of a pulmonary reservoir of drug. As a result of sustained lung levels, systemic absorption and exposure were reduced.

Accordingly the biodistribution of [ $^3\text{H}$ ]-PXB after i.t. instillation of free drug differed from that seen with entrapped drug.

The serum profile of [ $^3\text{H}$ ]-PXB after i.t. instillation of free drug is shown in figure 4.2. Levels were detected 15 minutes after instillation ( $2.00 \pm 1.16\%$  of the originally administered dose) and subsequently decreased over the 24hr period. The early peak is indicative of rapid absorption of PXB from the rat lung. At the 4hr time-point when the lung level had decreased to  $3.29 \pm 2.64\%$ , [ $^3\text{H}$ ]-PXB could still be detected in serum, albeit at a low level ( $0.51 \pm 0.33\%$ ). Levels were detected at the 24hr time-point although they had decreased still further ( $0.37 \pm 0.16\%$ ). These levels are expected given the variable and low levels seen after intravenous injection (Brownlee *et al.*, 1952).

PXB also distributed to the liver with levels detectable after 4hr and 24hr ( $6.24 \pm 0.89\%$  and  $5.14 \pm 1.32\%$  respectively). Lower levels were detected in the spleen at both time-points ( $0.51 \pm 0.33\%$  at 4hr and  $0.37 \pm 0.16\%$  at 24hr). The main site of PXB distribution was in the kidney. At 4hr,  $14.66 \pm 0.90\%$  of the administered dose was recovered from the kidney and this value decreased to  $10.54 \pm 3.17\%$  after 24hr. The fraction recovered in the urine after 24hr ( $12.72 \pm 1.72\%$ ) was consistent with previous studies which demonstrated a delayed excretion of PXB with a maximum of 20% of the administered dose excreted after 48hr (Brownlee *et al.*, 1952; Kucers & Bennett, 1987). Approximately 30% of the dose was recovered from these tissues. The unrecovered fraction reflects that PXB may bind to and persist in other tissues such as the brain, heart and muscle (Kunin & Bugg, 1971). The fate of PXB in these tissues remains uncertain although it is likely that it is slowly enzymatically inactivated (Brownlee *et al.*, 1952).



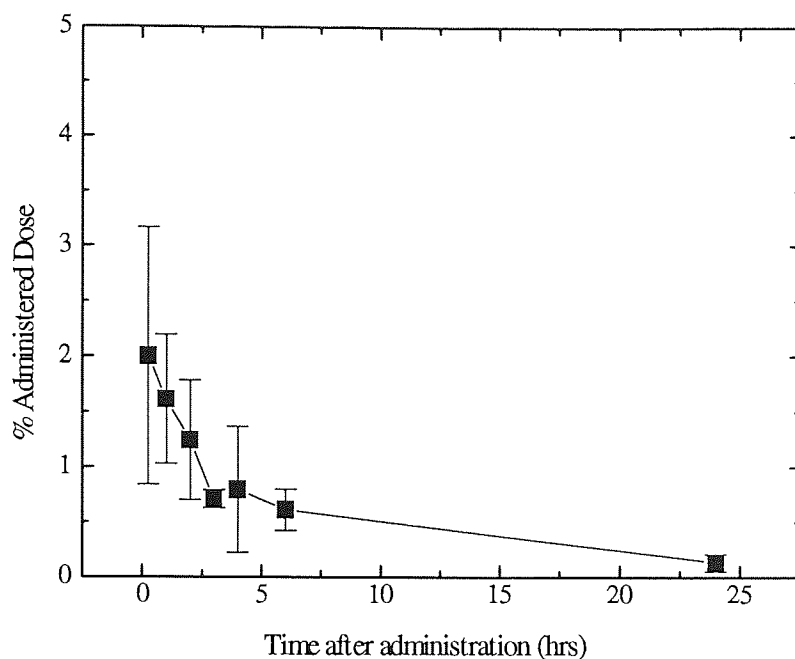


Figure 4.2. Serum levels of [ $^3\text{H}$ ]-PXB after i.t. instillation of free drug in male rats. Each point represents the percentage of the administered dose expressed as the mean  $\pm$  standard deviation of three animals

Reduced systemic absorption of [ $^3\text{H}$ ]-PXB from LPXB formulations resulted in decreased tissue levels relative to free drug. Serum levels of [ $^3\text{H}$ ]-PXB were seen only with EPC:CH:PEG vesicles, although these were highly variable. At 4hr a serum level of  $8.37 \pm 5.94\%$  was detected which decreased to  $2.87 \pm 2.12\%$  after 24hr. Both levels are in excess of the values seen with free drug and although the reasons for the anomalous behaviour of EPC:CH:PEG are unclear, the presence of PEG may have facilitated vesicular extravasation. Confirmation of the presence of intact liposomes in serum was not achieved as [ $^{14}\text{C}$ ]-CHOL was not detected. However, this may be due to a low concentration of label or exchange of cholesterol during extravasation. Increased blood levels ( $13.8 \pm 9.0\%$ ) after i.t. instillation of liposomes containing PEG5000-conjugated stearylamine were higher than control vesicles and indicated a trend for these vesicles to partition in blood relative to lung (Greco *et al.*, 1994).

The high kidney levels observed at 24hr with free drug were decreased with LPXB formulations (EPC;  $6.8 \pm 1.95\%$ , EPC:CH (2:1);  $2.55 \pm 1.75\%$ , EPC:CH (1:1);  $3.01 \pm 1.57\%$ ,

EPC:CH:SA;  $2.10 \pm 1.31\%$ , EPC:CH:PEG;  $2.17 \pm 1.41\%$  and EPC:CH:GM1;  $1.89 \pm 0.53\%$ ). Extrapulmonary [ $^3\text{H}$ ]-PXB was detected only in urine with EPC:SA due to a low 3H-PXB/cold PXB ratio (the loading solution of this preparation was erroneously prepared). Interestingly kidney levels for all other LPXB formulations increased over 24hr again indicating the sustained release of PXB from the lung. This was not seen after free drug instillation which reflects the altered lung kinetics of free and entrapped drug. Further evidence of reduced systemic absorption and exposure with liposome-entrapped drug was observed with lower [ $^3\text{H}$ ]-PXB urine levels after 24hr than those seen with free drug. Also, [ $^3\text{H}$ ]-PXB was not detected in the spleen with liposomal formulations.

To summarise, liposomal encapsulation was successful in decreasing systemic absorption and organ accumulation of PXB. This property has previously been observed with a number of i.t instilled drugs such as glutathione (Jurima-Romet *et al.*, 1990), atropine (Meisner *et al.*, 1989) and sodium cromoglycate (Taylor *et al.*, 1989). Reduced extrapulmonary absorption may be of clinical benefit as aerosolised PXB is administered as aggressive long-term prophylactic treatment and reduced organ levels (especially renal) may be important in preventing long-term side-effects.

Formulation	Lung		Liver		Spleen		Kidney		Serum		Urine	
	4hr	24hr	4hr	24hr	4hr	24hr	4hr	24hr	4hr	24hr	4hr	24hr
Free Drug	3.29± 2.64	3.05± 2.24	6.24± 0.89	5.14± 1.32	0.51± 0.33	0.37± 0.16	14.66± 0.9	10.54± 3.17	0.79± 0.57	0.13± 0.08	12.72± 1.72	
EPC	48.93± 2.44	40.33± 3.66	1.06± 0.52	1.56± 1.08	ND	ND	5.64± 1.37	6.8± 1.95	ND	ND	8.88± 1.44	
EPC:CH (2:1)	56.41± 10.12	27.68± 8.97	0.68± 0.6	0.54± 0.73	ND	ND	2.52± 1.09	2.55± 1.75	ND	ND	Not done	
EPC:CH (1:1)	62.55± 12.74	39.96± 15.21	0.51± 0.62	1.10± 0.73	ND	ND	1.66± 0.32	3.01± 1.57	ND	ND	Not done	
EPC:SA (9:1)	65.38± 16.07	39.11± 11.27	ND	ND	ND	ND	ND	ND	ND	ND	7.60± 1.27	
EPC:CH:SA (6:3:1)	73.35± 4.38	52.29± 4.11	1.07± 0.49	1.13± 0.72	ND	ND	2.47± 1.53	2.10± 1.31	ND	ND	8.52± 0.71	
EPC:CH:PEG (2:1:0.2)	51.26± 5.96	36.14± 11.92	0.78± 0.52	0.95± 0.38	ND	ND	1.14± 0.84	2.17± 1.41	8.37± 5.94	2.87± 2.12	7.8± 2.88	
EPC:CH:GM <sub>1</sub> (2:1:0.2)	85.66± 4.32	50.29± 8.81	1.21± 0.48	1.15± 0.78	ND	ND	1.58± 0.61	1.89± 0.53	ND	ND	10.23± 2.36	

Table 4.3. Biodistribution of i.t. instilled PXB and LPXB in male rats at a dose of 0.4mg kg<sup>-1</sup> PXB. Each point represents the percent of the original dose of [<sup>3</sup>H]-PXB administered (averages.d., n=3). ND denotes that [<sup>3</sup>H] levels were not detectable above background.

#### 4.4.5. Characterisation of EPC:CH:PEG 100nm extruded vesicles used for i.v. injection

The zeta potential of this preparation was  $-2.3 \pm 2.4$  mV, indicating a neutral surface as previously observed. A low PXB to lipid ratio ( $0.012 \mu\text{mol}/\mu\text{mol}$  lipid) was achieved, probably due to increased rupture of vesicles as they passed through the small diameter pores (100nm) of the polycarbonate filter. The size distribution was determined by PCS both before and after Dowex treatment and is shown in figure 4.3. The hydrodynamic intensity means of the distributions were not affected by resin treatment (mean before Dowex;  $122 \pm 57$  nm, mean after Dowex;  $120 \pm 54$  nm). Negative stain TEM confirmed the downsizing of vesicles (figures 4.5 and 4.6).

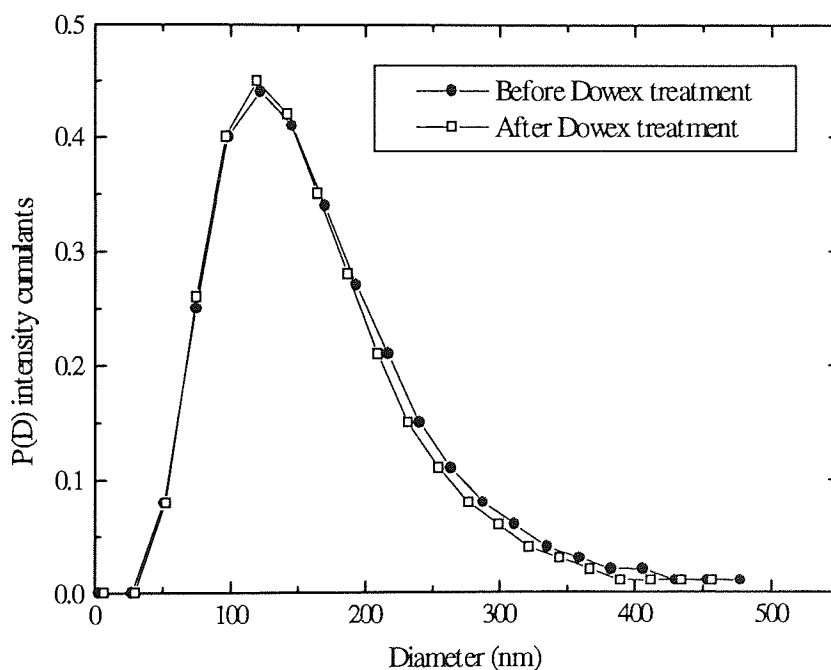


Figure 4.3. Size distributions of EPC:CH:PEG vesicles extruded 10 times through a  $0.1 \mu\text{m}$  filter, before and after Dowex treatment.

GEC was used in order to confirm that Dowex treatment was successful in removing free PXB. The gel elution profiles for the sample before and after Dowex treatment are shown in figure 4.4. This profile shows that although Dowex successfully removed the bulk of PXB without loss of liposomally-entrapped drug, a small residue of free drug remained (10.47% of initial free drug quantity). This was not observed during the initial method validation (figure

4.1). However the sensitivity of the BCA assay is much less than [ $^3\text{H}$ ]-PXB scintillation counting, the method used to obtain the gel profiles. Further separation was not attempted and the vesicle/free drug mixture was used for i.v. administration.

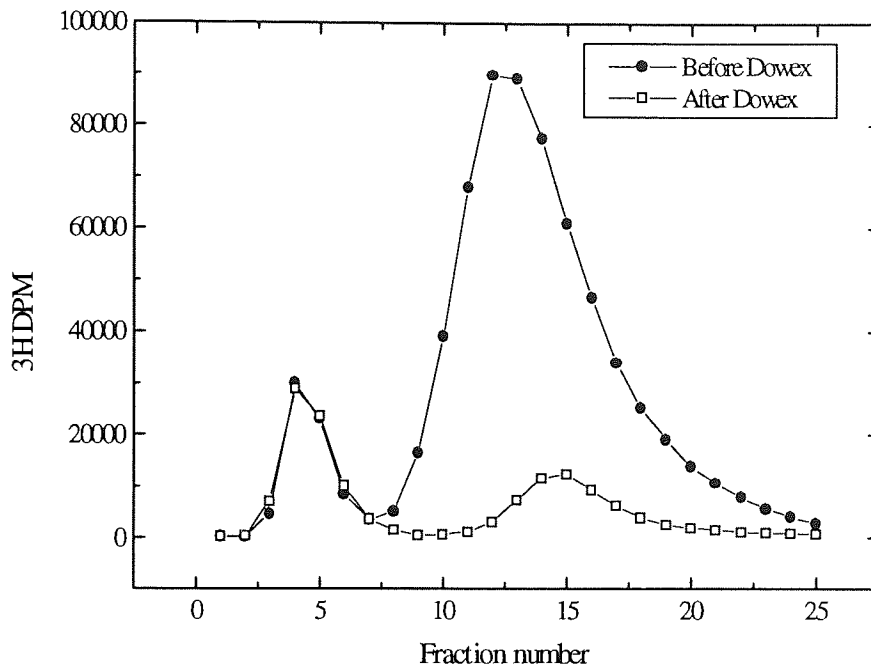


Figure 4.4. Gel exclusion chromatograms of extruded EPC:CH:PEG vesicles before and after Dowex resin treatment.

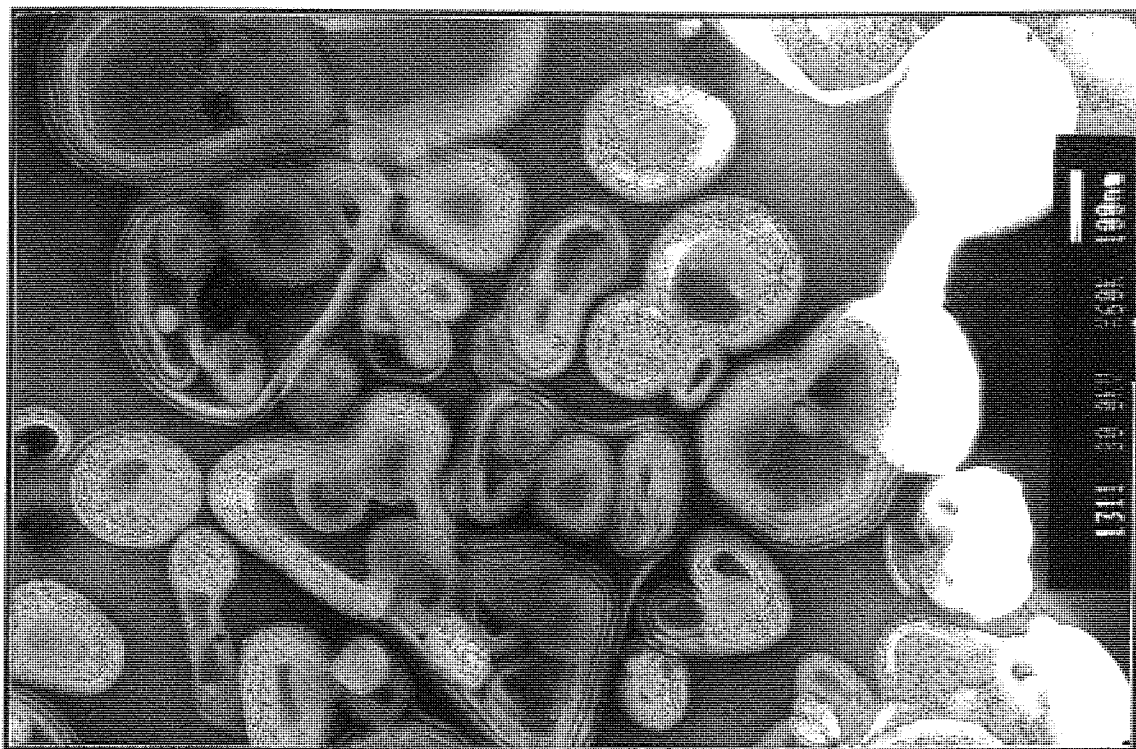


Figure 4.5. TEM of EPC:CH:PEG vesicles before 10 extrusions through a 100nm filter. Magnification 60k

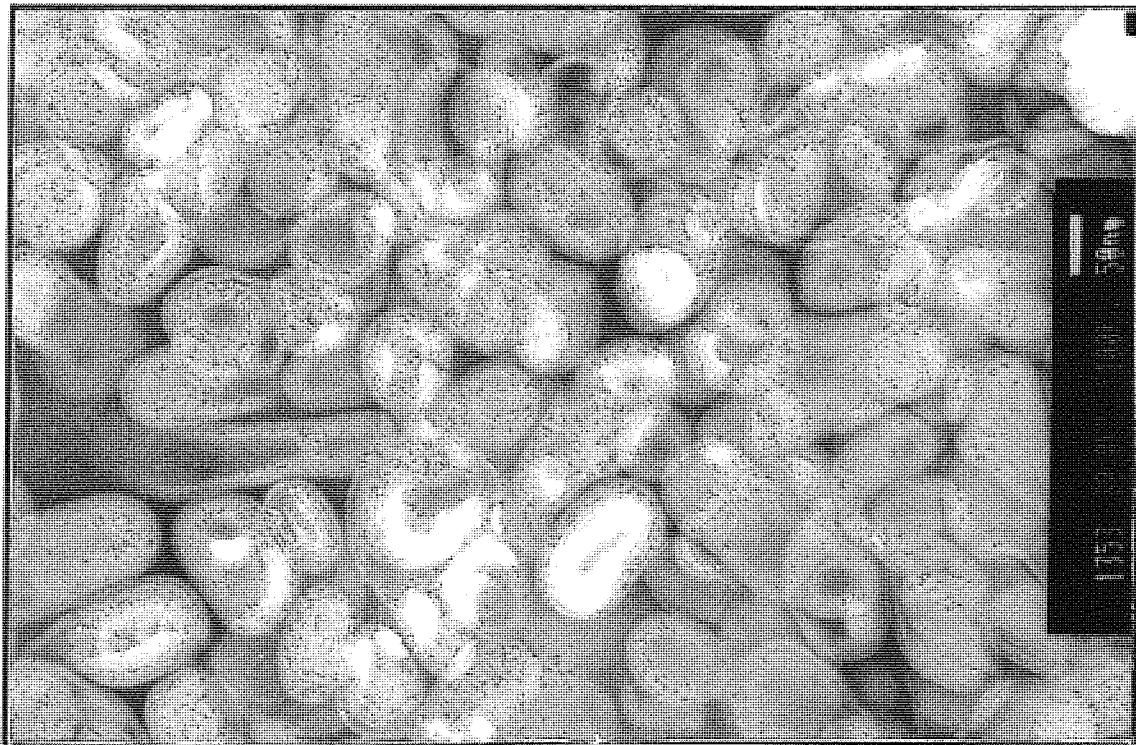


Figure 4.6. TEM of EPC:CH:PEG vesicles after 10 extrusions through a 100nm filter. Magnification 100k

#### 4.4.6. Biodistribution of non-entrapped PXB after i.v. administration

When administered at a dose of 0.8mg/kg, free PXB exhibited widely varying early serum levels as shown in figure 4.7. 1hr after administration, blood levels varied from  $2.33 \pm 0.12\%$  to  $47.98 \pm 3.05\%$  (expressed as a percentage of the originally administered dose). Levels after 2hr still varied but on-going clearance and redistribution was evident with a decline in serum levels. After 4hr serum levels of PXB converged to  $\sim 3-5\%$  for all animals. Thereafter levels in all animals slowly decreased until after 24hr less than 3% remained in the bloodstream. A high dose (2.5mg/kg) was also evaluated. The serum levels displayed the same trends as the lower dose with equivalent levels observed at all time-points (figure 4.8).

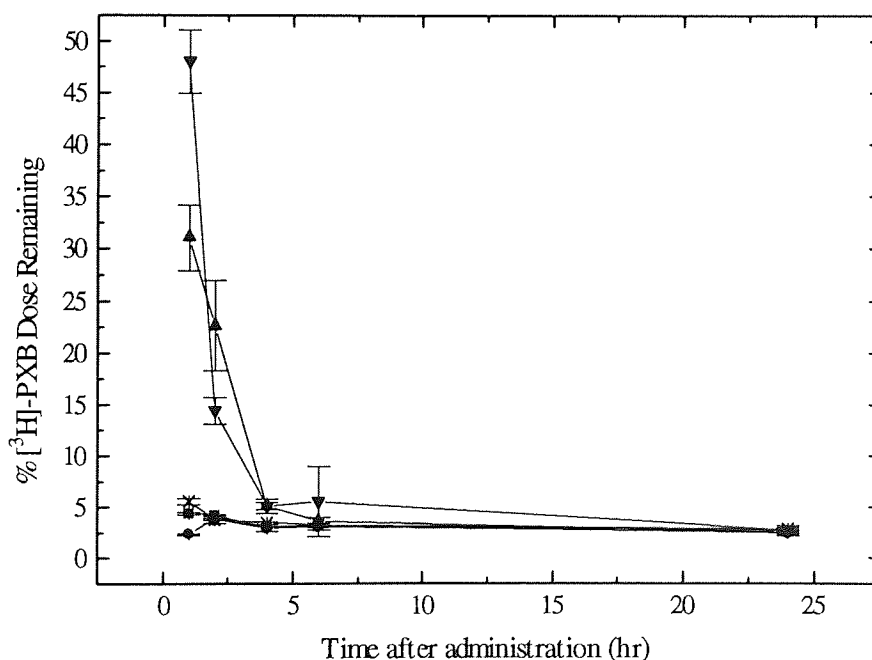


Figure 4.7. Serum levels of PXB after i.v. administration of a 0.8mg/kg dose to five adult male rats. Each time-point represents the mean  $\pm$  standard deviation of three samples for each individual animal.

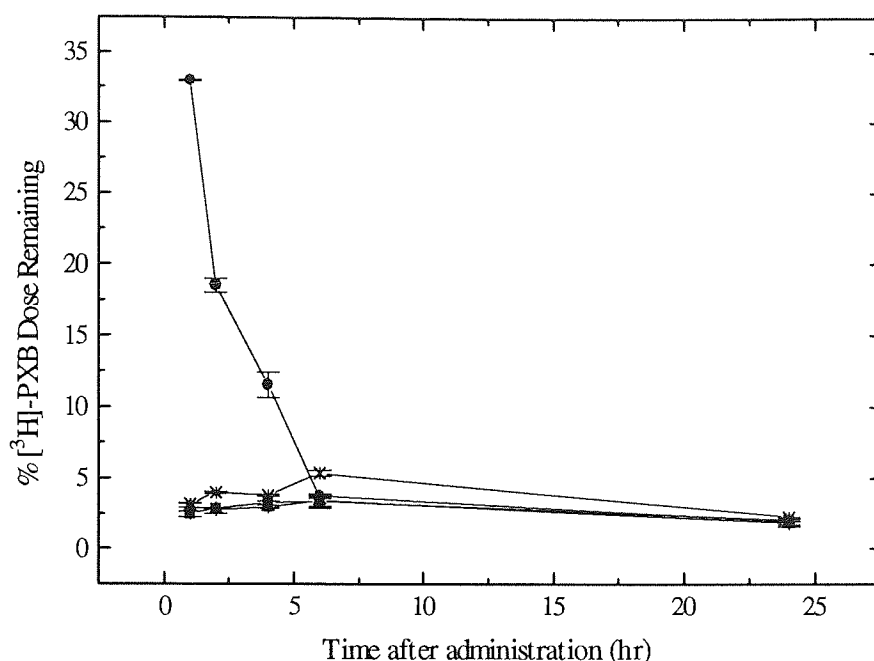


Figure 4.8. Serum levels of PXB after i.v. administration of a 2.5mg/kg dose to five adult male rats. Each time-point represents the mean  $\pm$  standard deviation of three samples for each individual animal.

Brownlee *et al.* (1952) noted that PXB blood levels showed a great deal of individual variation in rabbits. When given intravenously, no antibiotic could be detected after 4hr. Although levels continued to be detected after 24hr in the present study, radiolabel detection is much more sensitive than the bioassay used in these early experiments (Brownlee *et al.*, 1952).

Tissue and urine levels of PXB were also investigated 24hr after i.v. administration (figure 4.9). With the low dose (0.8mg/kg), urine recovery of PXB reached  $12.33 \pm 3.70\%$ . Urine levels ( $13.37 \pm 1.87\%$ ) were not significantly different with the higher dose (2.5mg/kg). The high recovery of PXB in the urine is not surprising, given that polymyxins are mainly excreted by the kidney (Kucers & Bennett, 1987). Low values for urine recovery in man have been previously published, with 0.1% detected after 12hr (Kucers & Bennett, 1987) and only  $0.3 \pm 0.08\%$  excreted after 24hr in dogs (Brownlee *et al.*, 1952).



Accordingly, the kidney represented a major site of distribution for PXB. Again, recoveries after 24hr were similar for both doses (low dose;  $7.32 \pm 0.74\%$ , high dose;  $7.49 \pm 1.17\%$ ). PXB may accumulate in the kidney through binding to anionic phospholipids in the renal cortex. The strong affinity of PXB for acidic phospholipids is well established (Storm *et al.*, 1977). Binding is mediated through amino groups and such an interaction has been proposed as a possible mechanism of aminoglycoside renal toxicity (Aramaki & Tsuchiya, 1989; Sastrasinh *et al.*, 1982). Liver levels of PXB were also significant with  $7.08 \pm 1.20\%$  recovered with a  $0.8\text{mg/kg}$  dose and  $11.14 \pm 3.37\%$  with the higher dose. It was proposed that liver levels were a result of the presence of PXB in the large volume of blood present in this organ (Brownlee *et al.*, 1952). However, given the relatively low blood levels at 24hr, some accumulation in the liver would appear necessary to account for the observed recoveries. Both low and high doses resulted in negligible levels in the lung ( $0.29 \pm 0.04\%$  and  $0.35 \pm 0.07\%$  respectively) and in the spleen ( $0.23 \pm 0.05\%$  and  $0.34 \pm 0.12\%$  respectively), indicating a low affinity of PXB for these tissues. The low lung levels achieved after i.v. injection highlight the potential for a stealth type formulation to treat pulmonary infections.

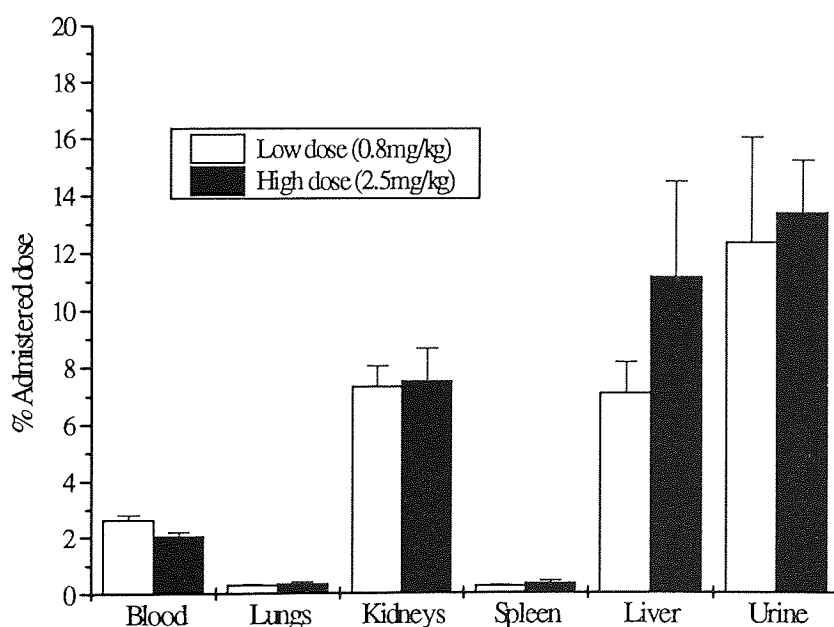


Figure 4.9. Tissue distribution of PXB after i.v. injection of  $0.8\text{mg/kg}$  ( $n=5$ ) and  $2.5\text{mg/kg}$  ( $n=4$ ) doses. Each point represents the % administered dose expressed as the mean  $\pm$  standard deviation.

The total dose recovered was ~30% with both dose levels used. The low recovery has been noted in previous studies and the fate of PXB in the body is not well understood (Brownlee *et al.*, 1952; Kunin, 1967). PXB may also bind to heart, brain and muscle and it is likely that the bulk of drug is inactivated slowly in the body, possibly by proteolytic enzymes (Kucers & Bennett, 1987; Kunin & Bugg, 1971).

The blood and tissue levels observed after i.v. injection are consistent with the fate of systemically absorbed PXB after i.t. instillation. Particularly, the low blood levels seen after 4hr and 24hr with i.t. administered PXB, are similar to those seen after i.v. injection. As the majority of the i.t. dose had been cleared from the lung at these time-points, the low blood levels appeared anomalous with rapid clearance. However the biodistribution of i.v. administered PXB correlates with this observation.

#### 4.4.7. Biodistribution of PXB after i.v. administration of EPC:CH:PEG 100nm vesicles

Figure 4.10 shows the serum profile of [ $^3\text{H}$ ]-PXB before and after Dowex treatment. Untreated serum samples show rapid clearance of PXB with  $21.50 \pm 1.40\%$  of the originally administered dose remaining after 1hr. Sustained levels are seen up to 6hr after administration with  $16.58 \pm 5.08\%$  still in the circulation at this time-point. On-going clearance was evident with a decreased recovery of  $6.90 \pm 1.64\%$  after 24hr. Although a large proportion of the administered dose was cleared or redistributed, the serum profile achieved with LPXB resulted in sustained higher levels than seen with non-entrapped drug. It is important to note that the preparation used contained a considerable fraction of free PXB (53.77% entrapped, 46.23% as free PXB) which would be subject to rapid and variable clearance kinetics as previously noted.

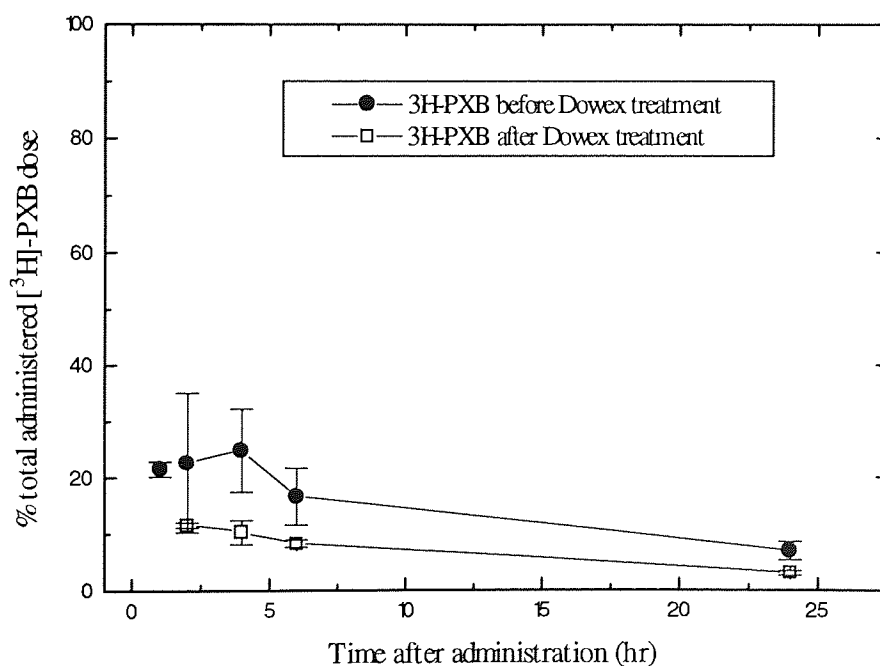


Figure 4.10. Serum levels of PXB determined by scintillation counting of [ $^3\text{H}$ ]-PXB in untreated (free and liposomal drug) and Dowex treated (liposomal drug only) samples, expressed as a percentage of the total [ $^3\text{H}$ ]-PXB dose administered. Each point represents the mean  $\pm$  standard deviation for five animals.

Serum treatment with Dowex cation exchange resin has been used to separate free from liposomal drug (Amselem *et al.*, 1990; Barenholz & Amselem, 1993). When this technique was used with PXB serum samples (figure 4.10), approximately 10% of [<sup>3</sup>H]-PXB was present as the free drug at 2, 4 and 6hr time-points. This represents a higher free serum level than that achieved by non-entrapped drug administration and is likely to be the result of sustained release of drug from EPC:CH:PEG vesicles. A lower quantity of free drug was detected after 24hr with  $3.91 \pm 1.24\%$  removed by resin treatment. These values represent recoveries of <sup>3</sup>H-PXB expressed as a percentage of the total i.v. [<sup>3</sup>H]-PXB dose administered. As the resin treated serum represents encapsulated or liposome-associated PXB, calculation of the treated [<sup>3</sup>H]-PXB serum values as a percentage of the total liposomal [<sup>3</sup>H]-PXB dose will allow differentiation between the clearance of free and liposomally entrapped drug.

Entrapped PXB values are therefore expressed as a percentage of the liposomal [<sup>3</sup>H]-PXB dose administered. [<sup>14</sup>C]-cholesteryl oleate was used as a liposomal marker (New, 1990; Woodle, 1993). Dowex treatment of plasma was shown not to affect [<sup>14</sup>C] levels (figure 4.12) as previously reported by Amselem (1990). Figure 4.11 shows the clearance of both markers over a 24hr period. Parallel clearance of both markers was observed suggesting that initial rapid clearance or uptake of vesicles from the circulation was followed by a phase of slow release and/or decreased rate of vesicle uptake. Prior to administration, vesicles had a [<sup>3</sup>H]/[<sup>14</sup>C] ratio of 3.16 which was observed to decrease sharply after 2hr (1.26) followed by a slow decline over the remaining period (4hr; 1.18, 6hr; 1.11, 24hr; 1.08). This is consistent with release studies conducted with this formulation in FCS which showed high initial loss of drug followed by a slow efflux phase (section 3.4.12.3). The lower values for recovery of [<sup>3</sup>H]-PXB relative to [<sup>14</sup>C]-cholesteryl oleate (expressed as a percentage of the administered liposomal dose) confirm release of PXB with subsequent removal from the circulation.

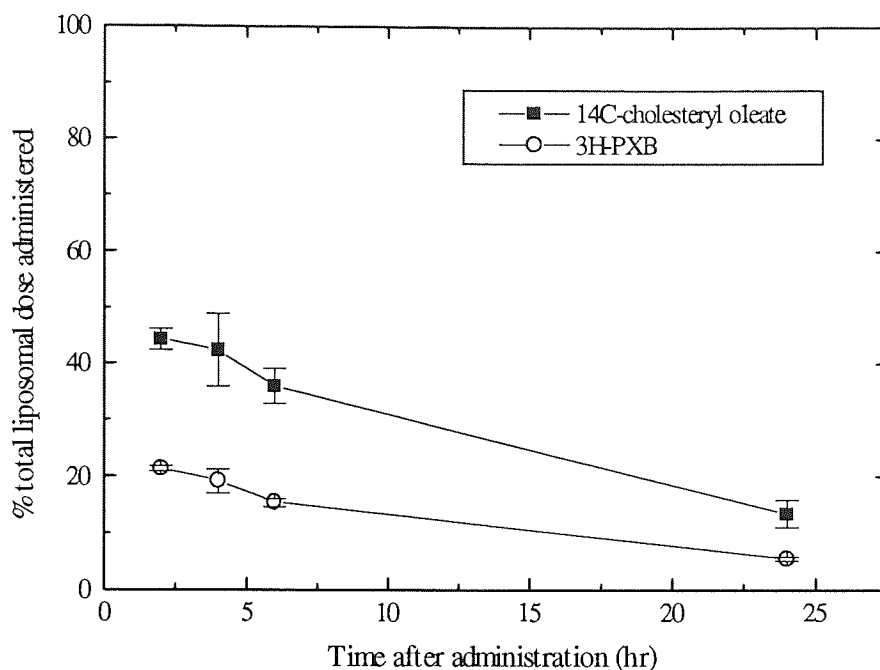


Figure 4.11. Serum levels of liposomal [ $^3\text{H}$ ]-PXB and [ $^{14}\text{C}$ ]-cholesteryl oleate determined by scintillation counting of Dowex treated (liposomal drug only) samples, expressed as a percentage of the total [ $^3\text{H}$ ]/[ $^{14}\text{C}$ ] dose administered. Each point represents the mean  $\pm$  standard deviation for five animals.

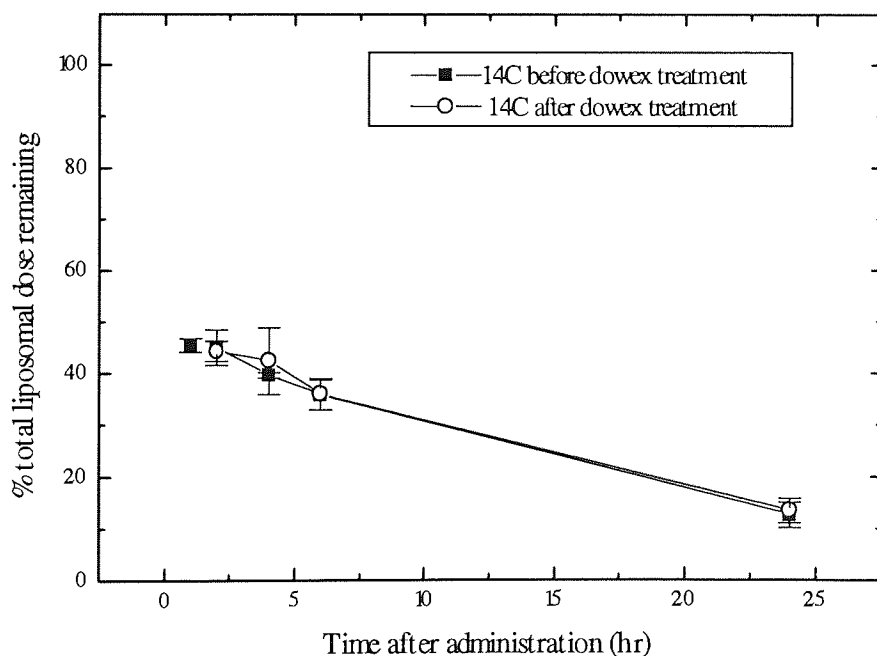


Figure 4.12. Serum levels of [ $^{14}\text{C}$ ]-cholesteryl oleate determined by scintillation counting of untreated and Dowex treated samples, expressed as a percentage of the total [ $^{14}\text{C}$ ]-cholesteryl oleate dose administered. Each point represents the mean  $\pm$  standard deviation for five animals.

The biodistribution of EPC:CH:PEG delivered PXB (figure 4.13) was compared to that observed with free drug. Liver levels were similar with  $11.41 \pm 1.35\%$  ( $^3\text{H}$ )-PXB recovered after 24hr. This organ was also the main extracirculatory site for liposomal recovery with  $6.30 \pm 0.90\%$  detected after 24hr, suggesting significant vesicle uptake (although relatively much less than would be seen with conventional liposomal formulations). Spleen levels were elevated compared to free drug, with  $2.71 \pm 0.42\%$  of  $^3\text{H}$ -PXB recovered compared with  $0.34 \pm 0.12\%$  for free drug. A lower recovery of  $^{\text{14}}\text{C}$ -cholesteryl oleate ( $0.84 \pm 0.12\%$ ) in this organ may suggest release of PXB from vesicles before uptake, or cellular processing of the marker lipid with subsequent redistribution (Woodle, 1993). The combined liver and spleen levels are slightly higher than those described for a comparable formulation and dose after i.v. administration to rats (Woodle *et al.*, 1992). Lung and kidney levels of liposomal marker were low with  $0.71 \pm 0.08\%$  and  $0.60 \pm 0.3\%$  of  $^{\text{14}}\text{C}$ -cholesteryl oleate recovered in each organ respectively. These tissues are not main sites for liposome accumulation and higher lung levels would only be expected in the presence of inflammation (Bakker-Woudenberg *et al.*, 1993). Accordingly  $^3\text{H}$ -PXB recoveries in both organs were also low. In the lung a comparable recovery to free drug was seen ( $0.32 \pm 0.03\%$  compared with  $0.35 \pm 0.07\%$  for free drug). Kidney levels were much reduced with the liposomal formulation ( $1.22 \pm 0.06\%$  compared with  $7.32 \pm 0.74\%$  for free PXB) and indicate that a potential reduction in renal toxicity may be achieved with LPXB. The lower kidney levels were surprising as urine recovery of  $^3\text{H}$ -PXB with the liposomal formulation was not significantly different to that seen with both doses of free drug. This anomaly may be due to sustained low level release of PXB from liposomes. The dynamics of renal binding and excretion may be altered with the low dose of entrapped  $^3\text{H}$ -PXB administered ( $0.2\text{mg/kg}$ ). As expected, recovery of  $^{\text{14}}\text{C}$ -cholesteryl-oleate was low ( $0.60 \pm 0.13\%$ ), although the detectable levels may indicate excretion of marker metabolites.

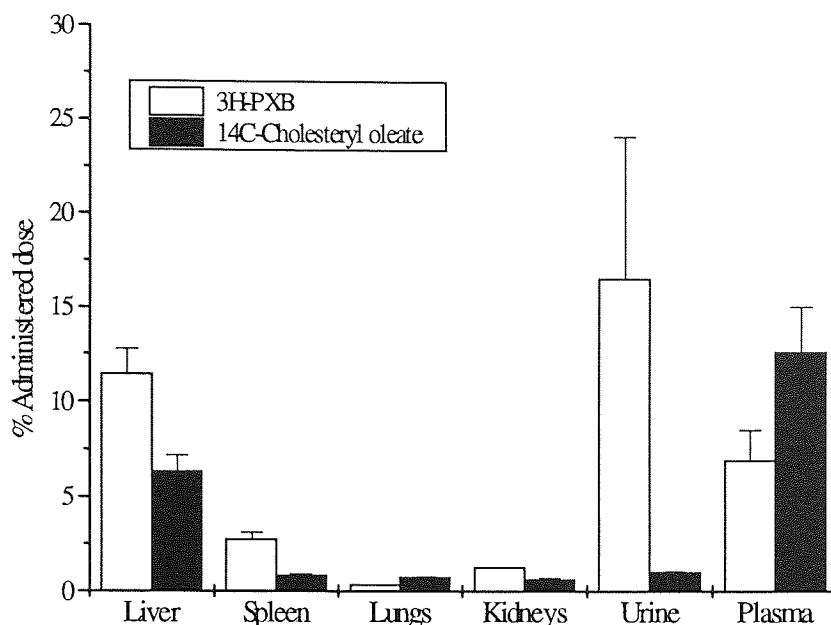


Figure 4.13. Tissue distribution of [<sup>3</sup>H]-PX B and [<sup>14</sup>C]-cholesteryl oleate 24hr after administration of EPC:CH:PEG vesicles. The recovery of each label is expressed as a percentage of the originally administered dose. Each point represents the mean  $\pm$  standard deviation of five animals.

The rationale for the systemic use of this formulation came from recent studies which showed accumulation of stealth formulations in inflamed lungs (Bakker-Woudenberg *et al.*, 1993; Bakker-Woudenberg *et al.*, 1992). Extravasation into inflamed areas is most probably a result of locally increased capillary permeability or injured endothelial linings secondary to infection (Bergers *et al.*, 1995). The long-circulating properties of stealth vesicles permit accumulation (up to 9% of the injected dose) in such sites. Uptake remains low when inflammation is not present. (Bakker-Woudenberg *et al.*, 1993). The therapeutic advantages of stealth vesicles are evident from studies with stealth formulations of gentamicin and ceftazidime used in the treatment of *Klebsiella pneumoniae* pneumonia model in rats. Both antibiotics showed increased therapeutic activity when given as the encapsulated form (Bakker-Woudenberg, 1995; de Marie *et al.*, 1994). The incorporation of DSPE-PEG<sub>1900</sub> in a 5-7.5% molar ratio has previously been reported to extend circulation half-lives of i.v. administered vesicles (Zalipsky *et al.*, 1994). In addition to lipid composition, particle size also is an important determinant of liposomal circulation times (Senior, 1987). The vesicles

used in the present study had a diameter of  $120 \pm 54$  nm which is similar to vesicles reported to possess long-circulating properties (Allen, 1994a; Bakker-Woudenberg *et al.*, 1993). The relatively low dose of lipid ( $12 \mu\text{mol/kg}$  containing  $0.20 \text{ mg/kg}$  PXB) used in this study should not affect the circulation time of EPC:CH:PEG vesicles as stealth formulations have been shown to possess dose-independent kinetics in rats (Woodle *et al.*, 1992) and in mice (Allen & Hansen, 1991). Therefore the vesicles used in the current study possessed the characteristics of a typical stealth formulation. However, liposome blood levels (as determined from [ $^{14}\text{C}$ ]-cholesteryl oleate recovery) at early time-points was lower than that seen with comparable formulations in a previous rat study (Woodle *et al.*, 1992). The percentage of injected dose recovered after 24 hr ( $13.4 \pm 2.39\%$ ) was also less than reported values ( $23.4 \pm 2.0$  for partially hydrogenated EPC:CH:PEG<sub>1900</sub>, 2:1:0.1). The lipid bilayer marker employed is important and in this respect [ $^{14}\text{C}$ ]-cholesteryl oleate may not be ideal for long-circulating vesicles, as metabolism and release from cells may occur over the period of study (Woodle, 1993). However, the lower levels achieved may be related to the incorporation of PXB, as this formulation displayed a degree of instability in release studies (sections 3.4.12). Further work is necessary to clarify the mechanism of this interaction. The results do indicate that it is possible to augment the blood levels of PXB through encapsulation. They also show that a long-circulating formulation of PXB to treat CF lung infections is achievable, although the optimal stealth lipid and vesicle composition remain to be determined. GEC separation of LPXB from non-entrapped drug would be preferable to Dowex treatment and may be coupled to a concentration step (such as ultramembrane centrifugation) to circumvent vesicle dilution.



#### 4.4.8. Characterisation of LPXB preparations used for macrophage uptake studies

Vesicles were prepared by the DRV process, using a 9mg PXB loading with 66 $\mu$ M total lipid. Three formulations were prepared, EPC, EPC:SA (9:1) and EPC:CH:PEG (2:1:0.2). After rehydration and separation from non-entrapped drug by centrifugation, encapsulations were determined as before (section 3.3.1). In order to maximise the surface lipid available for cell interaction and to produce vesicles with a defined size distribution, liposomes were extruded through a 0.2 $\mu$ m polycarbonate filter as previously described (section 3.3.13). Due to their small size extruded vesicles were separated from non-entrapped material using GEC (section 3.3.11). The gel chromatogram for EPC:SA is shown in figure 4.16 and illustrates the separation achieved. Fractions which were eluted in the void volume and showed counts for [<sup>3</sup>H]-PXB and [<sup>14</sup>C]-CHOL (added in a tracer quantity which was unlikely to affect membrane properties) were pooled and the encapsulation after extrusion determined. As previously observed (section 4.4.1) PXB was lost during the extrusion process and encapsulation efficiencies were therefore reduced (figure 4.14). The hydrodynamic means of the intensity size distributions were determined by PCS and were 161 $\pm$ 79nm (EPC), 169 $\pm$ 69nm (EPC:SA; 9:1) and 119 $\pm$ 49nm (EPC:CH:PEG; 2:1:0.2). The formulations exhibited similar distributions and a representative distribution (EPC:SA; 9:1) is shown in figure 4.15. Surface characteristics were defined in terms of zeta potential and hydrophobicity (sections 3.3.7 and 5.2.6). Although the vesicles characterised by these methods were larger than those used for macrophage uptake studies, size would not be expected to influence relative differences between formulations.

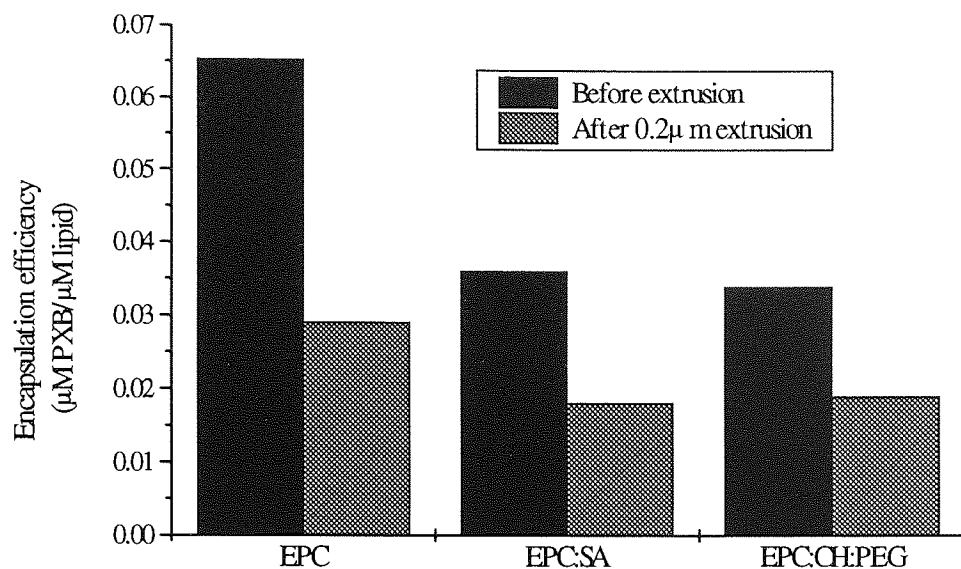


Figure 4.14. Encapsulation efficiencies ( $\mu\text{M PXB}/\mu\text{M lipid}$ ) of LPXB formulations before and after 10 extrusions through a  $0.2\mu\text{m}$  filter.

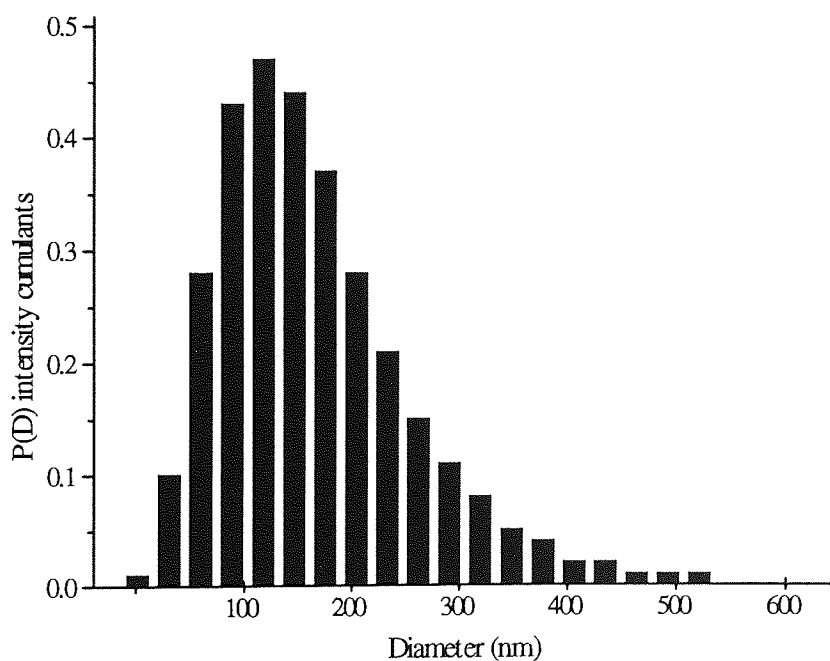


Figure 4.15. PCS Size distribution of EPC:SA vesicles after 10 extrusion through a  $0.2\mu\text{m}$  filter (mean diameter  $169\pm 69\text{nm}$ )

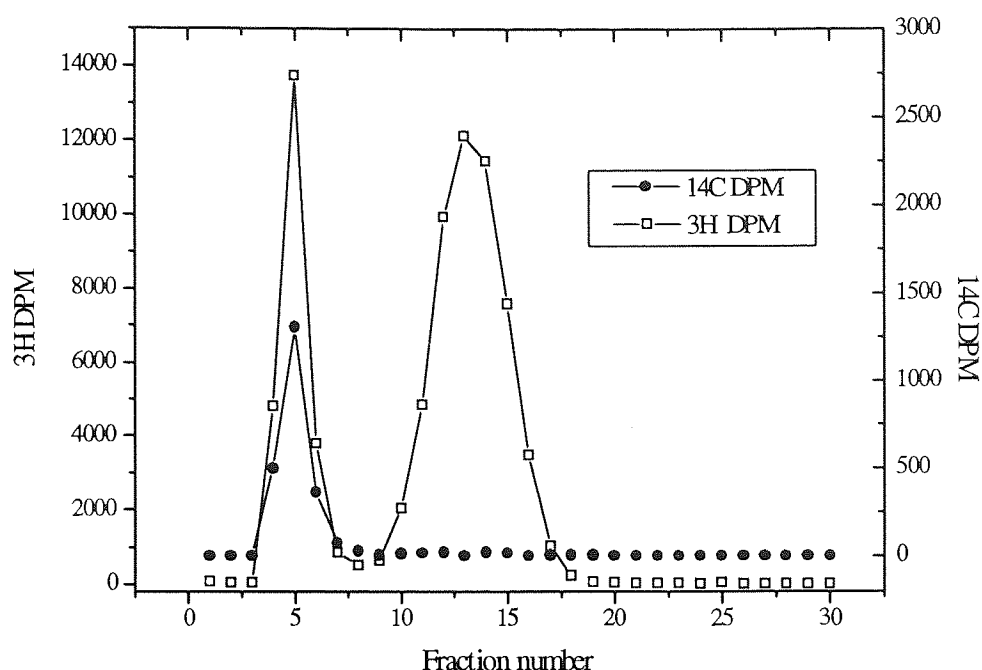


Figure 4.16. Gel exclusion chromatogram of EPC:SA 200nm extruded vesicles.

#### 4.4.9. Macrophage uptake of extruded LPXB formulations.

The rationale for performing macrophage uptake studies was to investigate the role of surface characteristics on cellular interaction. The phospholipid compositions were chosen to provide vesicles with different surface characteristics which may influence this interaction. In the lung, vesicles are cleared through a combination of processes which include uptake by pulmonary macrophages. Previous studies have investigated the *in vitro* interaction of liposomes with macrophage function (Gonzalez-Rothi *et al.*, 1991) and the efficacy of liposomal amikacin against MAI-infected macrophages (Wichert *et al.*, 1992). Both studies utilised murine alveolar macrophages harvested by lung lavage. Several other studies have investigated the interaction of liposomes with a murine macrophage cell-line, J774 (Daleke *et al.*, 1990; Kyung-Dall *et al.*, 1993; Stevenson *et al.*, 1983; Stevenson *et al.*, 1984). Although not alveolar in origin, this tumour cell-line exhibits non-specific phagocytosis and allows the conditions for uptake to be easily standardised.

Macrophage experiments were performed at 4°C and 37°C. Incubation of macrophages and liposomes at 4°C inhibits phagocytosis (Stevenson *et al.*, 1983) and allows cell surface interactions, such as adsorption, to be quantified. Incubation at 37°C allowed both surface association and uptake to be measured. From these results, the percentage of vesicles phagocytosed could be calculated. The effect of FCS was also investigated with incubation at 4°C/37°C carried out both with and without FCS.

Phagocytosis by J774.1 was confirmed under the test conditions by incubation at 37°C with fluorescent latex particles (1.0µm ±0.1µm Polysciences, UK). Figure 4.17 shows the appearance of a macrophage with internalised particles after 3hr incubation at 37°C in the absence of FCS.

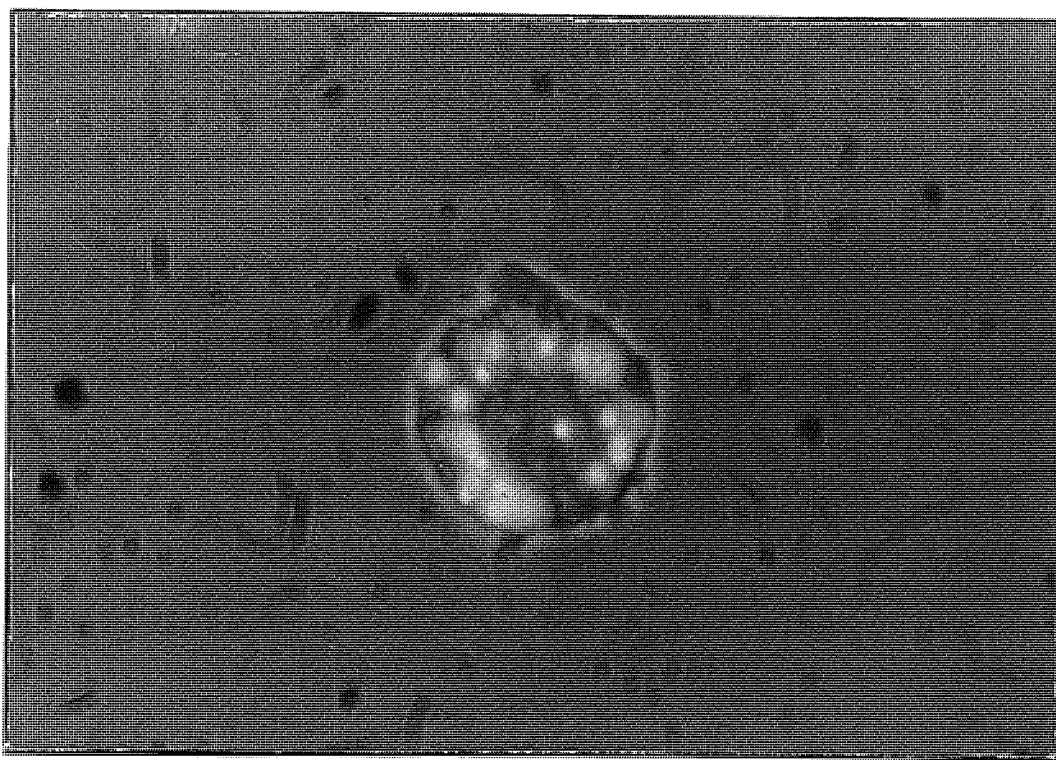


Figure 4.17. J774.1 macrophage with ingested fluorescent latex particles after 3hr incubation at 37°C without FCS

Figure 4.18 shows the binding of vesicles (expressed as the percentage of the quantity of [<sup>3</sup>H]-PXB initially added *per well*) to macrophages at 4°C. [<sup>3</sup>H]-PXB was used to quantitate vesicular uptake and binding. Release from vesicles at 4°C and 37°C was not detected and it

was therefore possible to use [ $^3\text{H}$ ]-PXB counts obtained after lysis of the cell monolayer to determine the percentage uptake. [ $^{14}\text{C}$ ]-CHOL was added as a very dilute tracer to enable detection during gel chromatography and as vesicles were used in a low concentration (200nM *per well*), there were insufficient counts to enable uptake of liposomal lipid to be used to measure cell interaction. In the presence of 10% FCS, highest binding was observed with EPC:SA ( $3.86\pm 0.06\%$ ), intermediate binding with EPC ( $2.60\pm 0.35\%$ ) and lowest binding with EPC:CH:PEG ( $1.05\pm 0.36\%$ ). In the presence of 10% FCS this order was maintained, although less binding was observed with EPC:SA ( $2.26\pm 0.08\%$ ) and EPC ( $1.51\pm 0.27\%$ ). There was no significant change in the binding of EPC:CH:PEG ( $1.05\pm 0.36\%$ ).

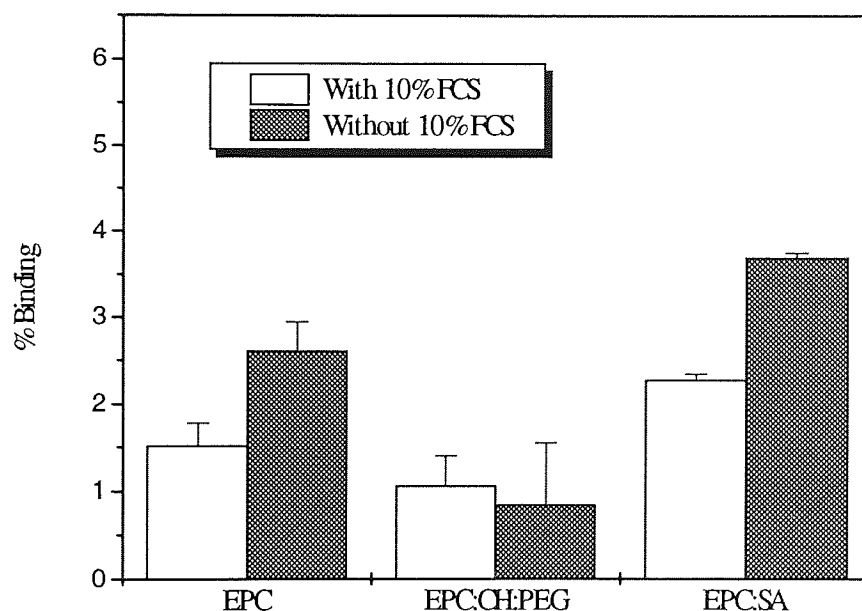


Figure 4.18. Binding of LPXB to J774.1 cells after 3hr incubation at 4°C. Each point represents the mean  $\pm$  standard deviation of three experiments

The high adsorption of EPC:SA may be explained through a strong electrostatic interaction with the cell membranes of J774.1. In PBS, EPC:SA vesicles had a positive potential of  $13.6 \pm 0.8\text{mV}$  whilst J774.1 cells were strongly negatively charged ( $-12.8 \pm 1.0\text{mV}$ ). Whilst the positive charge of SA increases the hydrophilicity of this formulation (see figure 4.20) the electrostatic interaction would take precedence in mediating cell association. The effective delivery of FITC labelled albumin by SA-containing vesicles to non-phagocytic HL-60 cells

was proposed to be due to a strong electrostatic interaction between liposomes and cells which was possibly followed by fusion (Alpar *et al.*, 1990). As binding is the initial event in liposome uptake by macrophages (Torchilin *et al.*, 1980) it would be likely that higher association would result in higher uptake. The majority of liposomes that become cell-associated are internalised (Schroit *et al.*, 1986). This was observed with EPC:SA at 37°C with  $6.12 \pm 0.20\%$  (with 10% FCS) and  $3.75 \pm 0.49\%$  (without 10% FCS) uptake after 3hr (figure 4.19). Phagocytosis was greatest with this formulation with an observed value of  $1.49 \pm 0.50\%$  (with FCS) and  $2.44 \pm 0.21\%$  (without FCS).

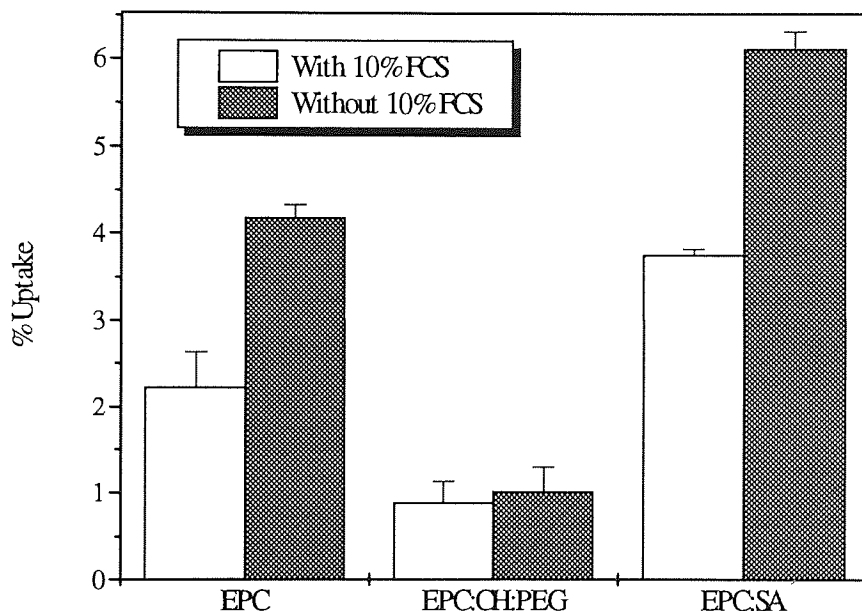


Figure 4.19. Uptake of LPXB to J774.1 cells after 3hr incubation at 37°C. Each point represents the mean  $\pm$  standard deviation of three experiments

EPC vesicles showed intermediate binding at 4°C. This lipid composition gives rise to an essentially neutral surface (zeta potential  $-3.7 \pm 0.7\text{mV}$  in PBS) which was also the most hydrophobic (figure 4.20) of the formulations used in the macrophage uptake assays. A hydrophobic surface would facilitate macrophage interaction with adsorption and subsequent uptake (Senior, 1987). The uptake of EPC vesicles was also intermediate with  $4.18 \pm 0.15\%$  (without FCS) and  $2.22 \pm 0.42\%$  uptake after 3hr incubation at 37°C. Phagocytosis of this formulation was  $0.71 \pm 0.50\%$  (with FCS) and  $1.58 \pm 0.38\%$  (without FCS).

EPC:CH:PEG vesicles showed the lowest binding values at 4°C and the lowest uptake values at 37°C. Phagocytosis appeared to be negligible as binding and uptake was not significantly different ( $p < 0.05$ ). The surface presence of PEG-polymer chains reduces the interaction of the liposomal surface with proteins and cell surfaces (Senior *et al.*, 1991; Zalipsky *et al.*, 1994). The ability of stealth liposomes to avoid capture by cells of the MPS is directly related to this property. Although EPC:CH:PEG had a similar zeta potential ( $-2.9 \pm 1.9$  mV) to EPC, the presence of PEG-polymer endows the surface with a much higher degree of hydrophilicity (figure 4.20). The hydrophilic barrier contributes to the steric-stabilisation observed with this type of vesicle (Allen, 1994b) and is likely to mediate reduced binding and uptake as seen in this experiment.

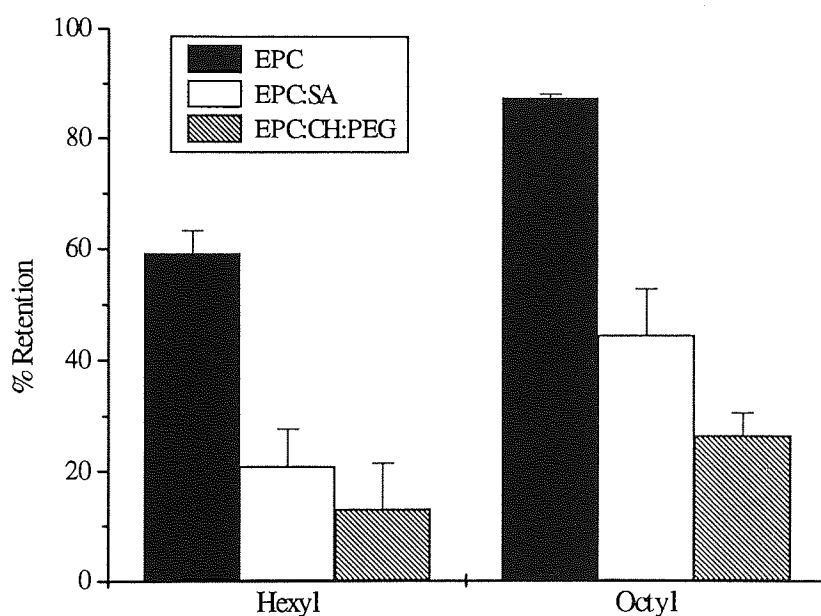


Figure 4.20. HIC of EPC, EPC:SA and EPC:CH:PEG vesicles using hexyl and octyl stationary phases. Retention values are the mean  $\pm$  standard deviation for three triplicates

The reduction in binding noted in the presence of FCS may be explained by the interaction of proteins with liposomal surfaces. Adsorption of proteins to positively charged vesicles renders the surface less positive (Senior *et al.*, 1991). A reduction in the positive potential of EPC:SA would diminish the attractive electrostatic forces involved in binding with the negatively charged cell membrane. Similarly, adsorption of proteins to EPC surfaces may hinder interaction with the macrophage surface. Torchillin *et al.* (1980) have described

reduced capture of liposomes by macrophages in the presence of proteins due to blocking of potential liposomal binding sites. The stealth properties of PEG-lipids are in part due to the reduced adsorption of proteins onto the vesicle surface (Allen & Paphadjopoulos, 1993; Tilcock *et al.*, 1993). The similarity in binding values of EPC:CH:PEG, in the presence and absence of FCS, suggests that incorporation of DSPE-PEG<sub>1900</sub> successfully prevented protein-coating of the liposome surface.

Negatively charged formulations were not investigated due to the difficulty in producing PXB-loaded vesicles with a negative surface (section 3.4.3). However, previous studies have shown that MLV containing negatively charged phospholipids such as PG, PS, PI or cardiolipin are phagocytosed more avidly than vesicles composed exclusively of PC. The negative headgroup is an important determinant of binding as PA does not seem to facilitate adsorption or internalisation (Alpar *et al.*, 1990; Schroit *et al.*, 1986). Negatively charged PS-containing liposomes were phagocytosed to a greater extent by J774.1 than neutral PC liposomes (Daleke *et al.*, 1990). Stevenson *et al.* (1984) have also reported uptake of anionic vesicles containing phosphatidylserine by J774.2. The existence of a J774 cell surface protein receptor for PS-containing vesicles was proposed as an explanation of the high binding and uptake observed with this formulation (Kyung-Dall *et al.*, 1993).

In conclusion, the macrophage uptake assay discriminates between formulations on the basis of surface characteristics. Zeta potential was an important determinant of binding with attractive electrostatic interaction favouring subsequent uptake. Hydrophobicity was also important with higher uptake seen with hydrophobic EPC vesicles relative to hydrophilic EPC:CH:PEG vesicles. The primary aim of this study was to establish an assay which could be used to provide information on the phagocytosis of vesicles. Although not immediately relevant to lung clearance by alveolar macrophages, this assay may be useful to identify differences between formulations which may affect cell uptake. For example, the high lung recovery at 4hr of EPC:SA compared with EPC after i.t. instillation may reflect greater uptake of this formulation by lung macrophages. PXB would therefore be sequestered within



cells and released only after liposome degradation and drug efflux. Fewer vesicles would be subject to mucociliary clearance or destabilisation with rapid absorption of free drug. However, before extrapolation to *in vivo* profiles can be made, further work is necessary to clarify relevant differences between J774.1 and alveolar macrophages.

## Chapter 5

### Surface characterisation of liposomes by hydrophobic interaction chromatography

---

#### ABSTRACT

The surface properties of liposomes play a major role in determining their physical characteristics and *in vivo* performance. Recently, attention has focused on the importance of surface hydrophilicity in achieving liposomes with prolonged circulation times. Hydrophobic interaction chromatography (HIC) allows surface hydrophilicity/hydrophobicity to be assessed and relative differences between formulations may be quantified. Although HIC has been applied to the surface characterisation of microspheres, it has not been previously used to evaluate liposomal surface characteristics. The work presented in this chapter compares HIC characterisation of liposomes with a range of phospholipid compositions with a number of previously reported phase-partitioning studies.

---

## 5.0. Surface characterisation of liposomes by hydrophobic interaction chromatography (HIC)

The biological fate of systemically administered liposomes is governed by a number of parameters which include particle size, bilayer fluidity, surface charge and surface hydrophilicity (Allen & Paphadjopoulos, 1993). Liposome charge and size may be investigated by a wide range of established techniques (Barenholz & Amselem, 1993) and membrane fluidity can be investigated using DSC or fluorescent membrane probes. Recent work has highlighted the importance of surface hydrophilicity for achieving liposomes with long-circulating properties (Allen, 1994a). Liposomal hydrophilicity has been investigated in several studies which used partition of vesicles between aqueous two-phase systems as an index of relative hydrophobicity (Eriksson & Albertsson, 1978; Eriksson, 1981; Zaslavsky *et al.*, 1984). Water-soluble polymers such as dextran and polyethylene-glycol form two immiscible phases whose properties may be adjusted to provide suitable pH and tonicity conditions. Vesicles partition between the interface and one of the bulk phases to different degrees depending on their surface characteristics (Sharpe, 1985). Although simple in principle, this technique requires the optimisation of both phases to resolve differences between formulations and a careful sampling technique is required to avoid contamination from adjacent regions (Tilcock *et al.*, 1993). The aim of this study was to evaluate an alternative technique, HIC, which has not previously been applied to liposomal surface characterisation.

HIC has been previously used to measure the hydrophobicity of bacteria by comparing retention in an uncharged bed of sepharose modified with hydrophobic groups (Mozes & Rouxhet, 1987; Smyth *et al.*, 1978). HIC is a column chromatography technique which separates particles on the basis of hydrophobic interactions with a gel matrix. Neutral gel matrices such as hydrophobically-modified agaroses are used in order to avoid interference from electrostatic effects. A variation of this technique has proved successful in the

characterisation of microspheres (Müller, 1991). The method used in this study was based on that described by Alpar and Almeida (1994).

## **5.1. Materials**

### **5.1.1. Phospholipids**

As section 2.2.1.

### **5.1.2. Chemicals**

Agarose, propyl-agarose, pentyl-agarose, hexyl-agarose and octyl-agarose used as stationary phases in HIC were purchased from Sigma Chemical Company (Poole, UK). All chemicals and reagents not specified in the text were supplied by BDH Chemicals Ltd. (Poole, UK), Sigma Chemical Company (Poole, UK) and Fisons (Loughborough, UK) and were of Analar grade or equivalent.

## **5.2. Methods**

### **5.2.1. Preparation of MLV by thin-film hydration**

As section 3.3.2.

### **5.2.2 Preparation of DRV**

As section 3.3.1.

### **5.2.3. Extrusion of MLV and DRV**

Both types of vesicle were extruded ten times through 0.8 $\mu$ m filters as described in section 3.3.11.

#### 5.2.4. Laser Diffraction Sizing

As section 3.3.5.

#### 5.2.5. Zeta potential analysis

As section 3.3.6.

#### 5.2.6. HIC

Glass pasteur pipettes were plugged with glass wool and used as chromatography columns (figure 5.1). The stationary phases (agarose, propyl-agarose, pentyl-agarose, hexyl-agarose and octyl-agarose) were washed several times in distilled water to remove any traces of preservatives and then resuspended in a NaCl solution of the required osmolarity (typically 0.2M) to produce a thick slurry of approximately 70% agarose. Stationary phases were loaded by applying on top of the glass wool sinter in the Pasteur pipette to a height of 30mm (~1ml of packed gel volume). The column was prepared for use by washing with 10ml of the required NaCl solution. The agarose-bed was maintained in a hydrated state until samples were applied.

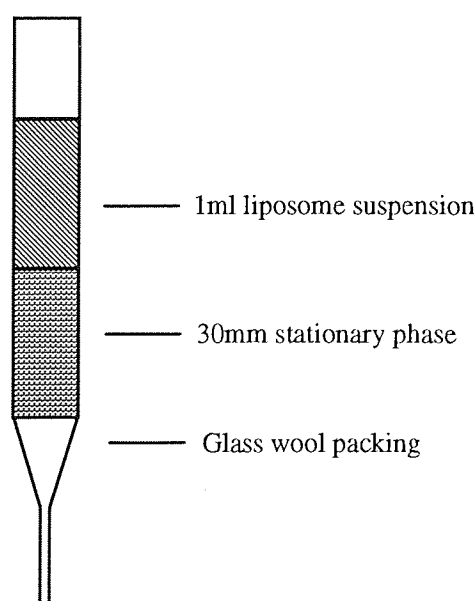


Figure 5.1. Schematic of Pasteur pipette columns used for HIC

Three identical columns were run for each type of agarose used. Suspensions of liposomes were adjusted to an  $OD_{470nm}$  of 0.5 (Phillips UV/Vis spectrophotometer PU 8370) and 1ml volumes were loaded onto columns, followed by 2 x 1ml of 0.2M NaCl pH 7.4 and 2 x 1ml of double-distilled water. The  $OD_{470nm}$  of the eluates (five fractions of 1ml each) were compared to the  $OD_{470nm}$  of 1ml of the original suspension and graphs of cumulative elution and final retention values plotted. The hydrophobicity of formulations determined by this method was calculated as a percentage of liposomes eluted from the column and the total percentage retained on the column.

### 5.2.7. Statistical analysis

Comparison between liposomes retained or eluted from HIC columns were analysed for significance using a two-tailed unpaired t-test. Differences with  $p < 0.05$  were considered significant.

## 5.3. Results and Discussion

As this technique had not previously been applied to liposomes, it was necessary to investigate the influence of ionic strength and particle size before differences between formulations could be compared.

### 5.3.1. Effect of Molarity on elution of liposomes from HIC columns

Ionic strength of the eluting medium plays a major role in determining the extent of particulate interaction with the stationary phase. A characteristic effect of all hydrophobic interactions is that they diminish upon decreasing ionic strength of the medium (Hjertén, 1973). Therefore, addition of salts can promote or reduce hydrophobic interaction between

particles and the gel matrix. Anions such as  $\text{Cl}^{-1}$  and  $\text{PO}_4^{-3}$  increase hydrophobic interactions ('salting-out' effect), whereas the addition of cations such as  $\text{Ca}^{2+}$  and  $\text{Ba}^{2+}$  disrupts the structure of water ('chaotropic' effect) and leads to a decrease in retention. Sodium chloride solutions of varying molarity have been used to perform HIC with microspheres (Müller, 1991). This technique used non-ionic surfactants such as Triton-X100 to elute retained particles. As liposome structure is readily disrupted by such agents (Hernandez-Borrell *et al.*, 1990), ionic strength of the eluting medium was reduced by following saline washes with two distilled water washes. Figure 5.2 shows the variation in total retention of EPC liposomes with saline molarity in both the least hydrophobic (agarose) and most hydrophobic (octyl-agarose) stationary phases. A concentration of 0.2M NaCl was found to give large retention differences between phases. As this was the lowest concentration to give adequate resolution between phases, it was chosen for further investigation of the technique.

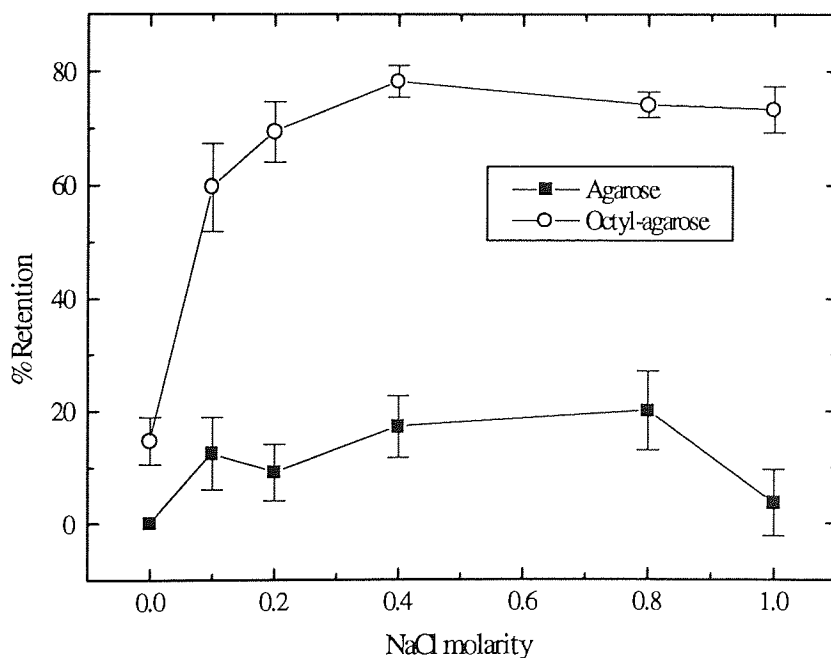


Figure 5.2. Influence of saline ionic strength on the retention of 0.8 $\mu\text{m}$  extruded EPC liposomes (each point represents the mean $\pm$ sd of three experiments)

### 5.3.2. Effect of liposome extrusion on vesicle elution from HIC columns

The relative elution of 0.8 $\mu$ m extruded EPC liposomes and non-extruded vesicles is shown in figure 5.3. Unsized MLV had higher retention values in both stationary phases although a larger difference was seen in the agarose phase. This may be attributed to trapping of large lipid aggregates in the gel matrices. The agarose derivatives used in this study have a dried bead diameter of 60 to 140 $\mu$ m which may increase on rehydration. Large lipid aggregates have been shown not to permeate gel columns (New, 1990). The size profile of unextruded vesicles (figure 5.4) shows the presence of large particles and the removal of these would account for the increased retention observed. The shape of the elution profiles for extruded and non-extruded liposomes were similar, suggesting that the behaviour of the bulk of vesicles (*i.e.*, those which were not subject to sieving) was comparable for both formulations. However, the increased retention of non-extruded vesicles in the agarose phase indicates a significant sieving effect with larger vesicles/aggregates.

The elution of extruded vesicles illustrated the importance of comparing liposomes with defined size distributions that are not subject to physical sieving effects. The interaction *per* unit surface area of each vesicle may also be expected to influence extent of retention. For this reason, vesicle preparations were standardised by extrusion through 0.8 $\mu$ m filters for all subsequent investigations.



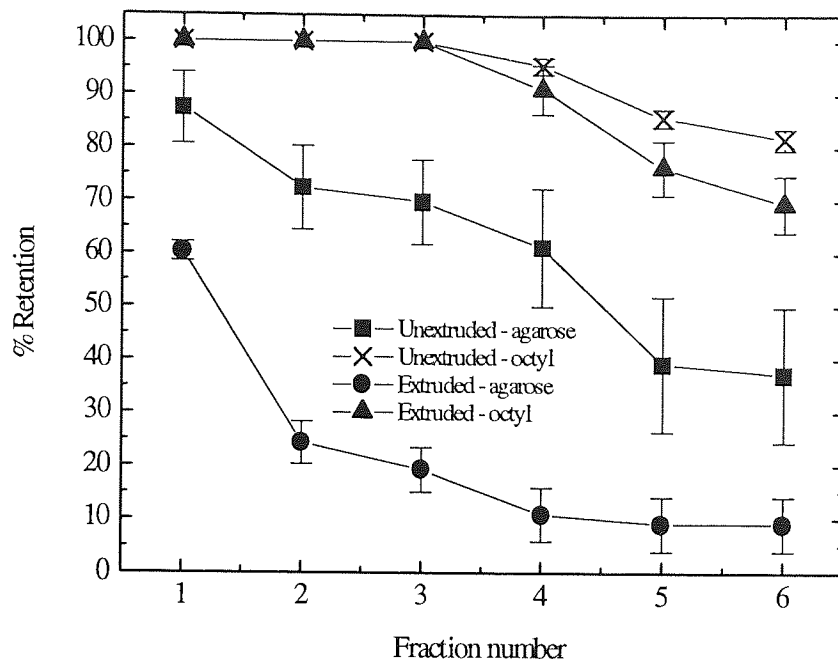


Figure 5.3. Influence of extrusion on the retention of EPC liposomes in agarose and octyl-agarose phases. Eluting medium 0.2M NaCl, (each point represents the mean $\pm$ sd of three experiments).

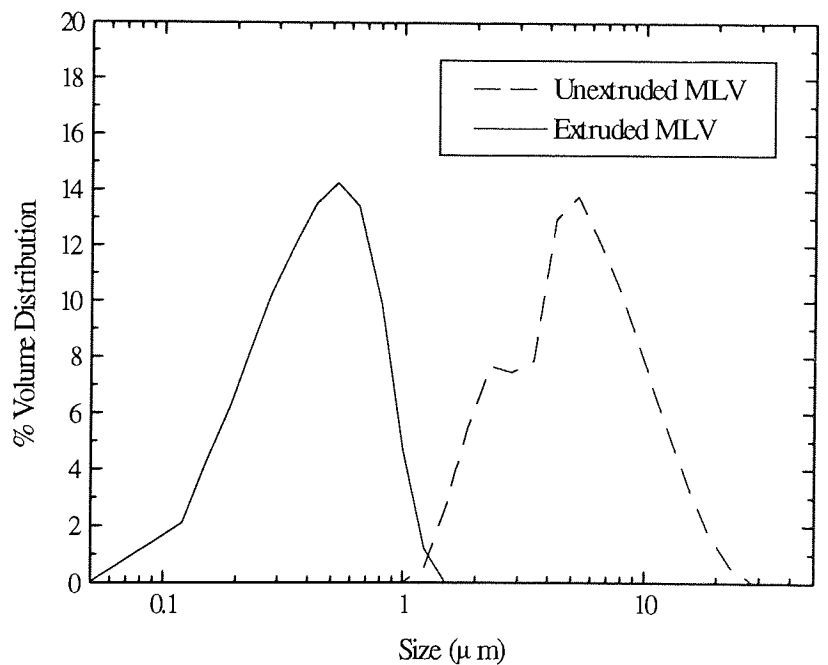


Figure 5.4. Particle size distribution determined by laser diffraction of non-extruded and 0.8 $\mu$ m extruded EPC liposomes in 0.2M NaCl.

### 5.3.3. Influence of phospholipid composition on elution profiles from HIC columns

#### 5.3.3.1. Effect of surface charge

The inclusion of a charged phospholipid or amphiphile in a 10% molar ratio resulted in strongly anionic vesicles (PI, PA, DCP, PG and PS) or positively charged vesicles (SA). The zeta potentials of these formulations are shown in table 5.1. With negatively charged components, zeta potentials determined in the eluting medium (0.2M NaCl, pH 7.4) were similar for DCP ( $-20.1 \pm 0.6 \text{mV}$ ), PI ( $-18.5 \pm 1.2 \text{mV}$ ), PA ( $-19.7 \pm 0.7 \text{mV}$ ) and PS ( $-16.7 \pm 0.4 \text{mV}$ ), although PG gave rise to a smaller negative potential ( $-11.3 \pm 0.8 \text{mV}$ ). The zeta potential of SA vesicles was  $+11.3 \pm 1.7 \text{mV}$ . As HIC had not previously been applied to liposomes, elution was performed using a range of agaroses modified with hydrophobic groups. As figure 5.5 demonstrates, resolution between formulations which reflected differences in phospholipid composition, was increased as the hydrophobicity of the stationary phases increased. Highest resolution was achieved in hexyl and octyl phases. In both phases, EPC liposomes were the most hydrophobic with retention values of  $59.09 \pm 4.2\%$  and  $87.34 \pm 0.75\%$  respectively. All formulations containing a charged component had significantly reduced retention in both phases. Surface expression of a charged component can increase hydrophilicity (Allen & Paphadjopoulos, 1993). Affinity of a phosphatidylethanolamine polar head group for an aqueous environment exceeded that of a phosphatidylcholine headgroup (Zaslavsky *et al.*, 1984). This was proposed to be consistent with the hypothesis that an ionisable moiety is more hydrophilic than a non-ionogenic moiety of a similar structure. This may explain the reduced retention (or increased hydrophilicity) observed with charged formulations. In charge-sensitive two-phase systems, increased wetting of membrane surfaces, in the presence of PA and PS, was proposed to affect partitioning (Tilcock *et al.*, 1993). The decreased retentions observed with both positively and negatively charged formulations suggests that the elution of such vesicles is independent of charge, as would be expected with the neutral agaroses used.

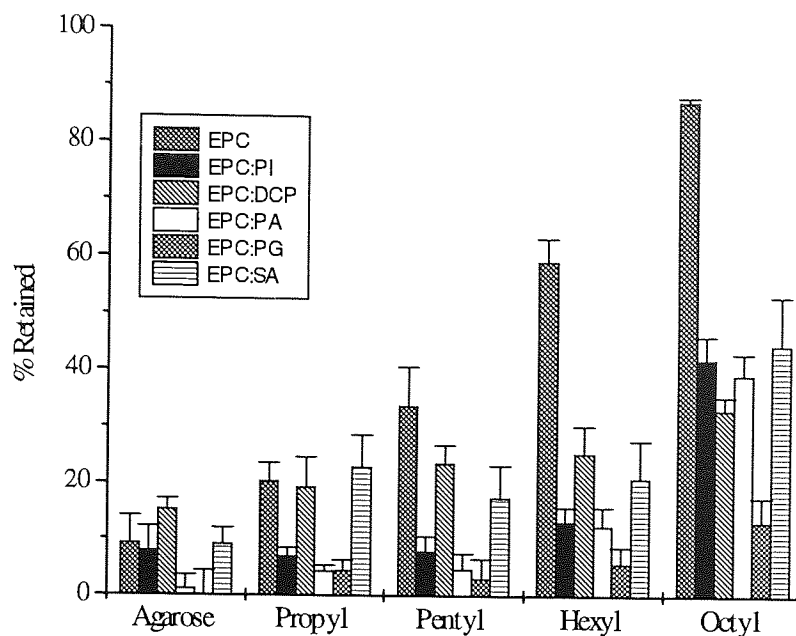


Figure 5.5. Influence of charged phospholipids on hydrophobicity of surfaces of EPC based liposomes (each point represents the mean  $\pm$ sd of three experiments)

Differences between charged formulations are evident in the more hydrophobic octyl phase. There was no significant difference in retention between EPC:PI, EPC:DCP, EPC:PA, EPC:SA and EPC:PS. However the retention of EPC:PG liposomes was significantly reduced. EPC:PG had a less negative potential than the other negatively charged formulations, although this is unlikely to be the reason for the increased hydrophilicity observed. The importance of the polar head-group for the phase-partitioning of liposomes has been well documented (Eriksson & Albertsson, 1978, Zaslavsky, 1984; Tilcock *et al.*, 1993). The structure of the polar head-group may be expected influence hydrophilicity, with small groups such as PA, DCP, SA showing relatively less hydrophilic surfaces than bulkier groups such as PS, PI and PG. The stationary phases used do not appear to resolve any such differences. This hypothesis would appear more reasonable if PI (used as the hydrogenated form in stealth formulations, Bakker-Woudenberg, 1993) showed similar or greater hydrophilicity than PG. As this was not observed, the rationale for decreased retention of EPC:PG liposomes remains unclear.

Formulation	Zeta Potentials (mV)		
	0.2M NaCl	PBS pH 7.4	0.02M diphosphate
EPC	-2.4±1.2	-2.9±1.6	-1.7±1.0
EPC:CH (2:1)	-2.5±1.5	-1.9±1.1	-5.2±0.4
EPC:CH (1:1)	-2.2±0.6	-1.6±1.1	-2.6±0.7
EPC:DCP (9:1)	-20.1±0.6	-26.0±1.8	-54.9±2.7
EPC:PS (9:1)	-16.7±0.4	-22.7±1.0	-59.7±0.9
EPC:PI (9:1)	-18.5±1.2	-19.0±0.9	-53.9±0.9
EPC:PA (9:1)	-19.7±0.7	-25.6±0.8	-63.8±1.7
EPC:PG (9:1)	-11.3±0.8	-15.2±1.3	-47.8±0.3
EPC:SA (9:1)	+11.3±1.7	+13.6±0.8	+37.6±1.1
EPC:PEG (9:1)	-1.8±1.2	-3.2±2.3	-9.6±1.4
EPC:CH:PEG	-2.9±1.9	-6.2±0.7	-1.8±0.4

Table 5.1. Zeta potentials, determined by laser doppler velocimetry, of liposome formulations used for HIC experiments. Each value represents the mean of five determinations for a single preparation

### 5.3.3.2. Effect of cholesterol

The retention of cholesterol containing formulations was compared to vesicles composed solely of EPC (figure 5.6). In the hexyl phase, a 30% molar ratio of cholesterol did not significantly reduce retention although the trend appeared to be towards a lower value. A significant reduction was achieved with a 50% molar ratio. The lower value observed in the hexyl phase with EPC:CH (1:1) ( $28.7 \pm 4.56\%$ ) was significantly different from EPC:CH (2:1) ( $42.76 \pm 3.57\%$ ). Higher retention of all formulations was seen in the octyl phase although the pattern of retention remaining the same. The retention of EPC liposomes was not significantly greater than EPC:CH (2:1) ( $79.62 \pm 5.09\%$ ). However, the retention of EPC:CH (1:1) ( $76.66 \pm 2.36\%$ ) was significantly reduced relative to EPC. Again the retention values of cholesterol containing formulations were not significantly different. An increase in liposome surface hydrophilicity was observed with cholesterol-containing formulations in ficoll-dextran biphasic systems (Zaslavsky *et al.*, 1984). The addition of cholesterol was proposed to increase the separation of phospholipid head-groups which induces an increase in the

hydration of the liposome surface. In contrast, cholesterol was reported to exert only a minor effect in dextran-polyethylene glycol systems (Eriksson & Albertsson, 1978). The results observed in the current study suggest that cholesterol produces a small increase in surface hydrophilicity which was less than that observed with charged components.

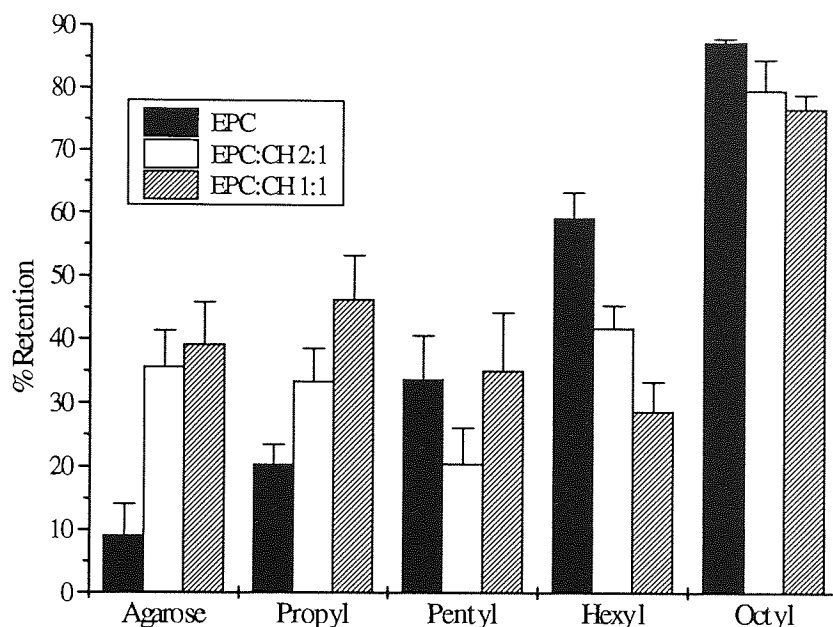


Figure 5.6. Influence of cholesterol on retention of EPC based liposomes (each point represents the mean  $\pm$  sd of three experiments)

### 5.3.3.3. Effect of acyl chain

Figure 5.7 shows the elution profiles of EPC and DSPC vesicles. There was no significant difference in the elution of these vesicles in all phases. Therefore it would appear that only surface characteristics determine the interaction of phospholipid vesicles with hydrophobically-modified agaroses. Both lipids share the phosphatidylcholine headgroup and possess similar zeta potentials in 0.2M NaCl (table 5.1). The equivalent behaviour of both lipids is consistent with phase-partition studies which demonstrated that the degree of

unsaturation was relatively unimportant for surface characteristics (Eriksson, 1981; Eriksson & Albertsson, 1978).

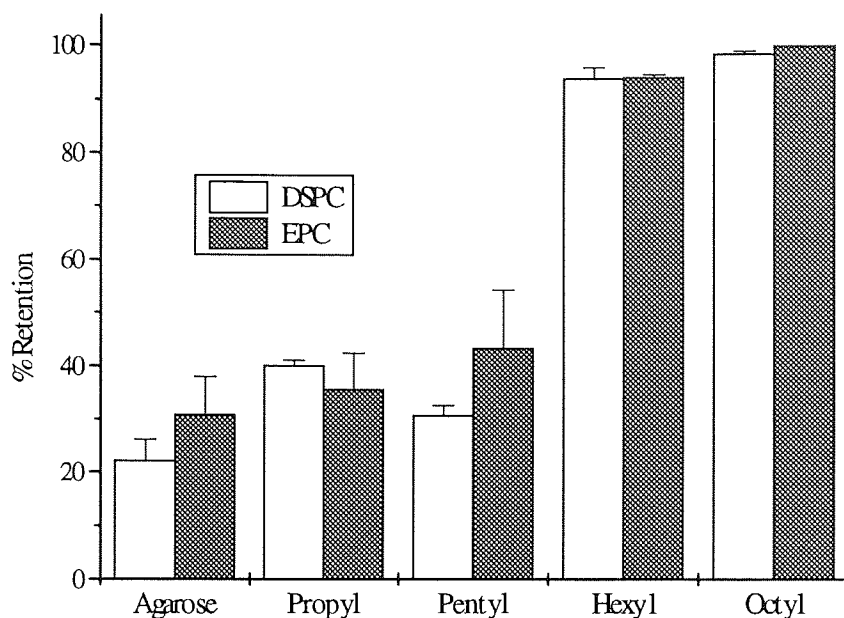


Figure 5.7. Influence of acyl chain saturation on retention of liposomes (each point represents the mean  $\pm$  sd of three experiments)

#### 5.3.3.4. Effect of pegylated lipids

The presence of hydrophilic group at liposome surfaces is postulated to contribute to the long-circulating properties of vesicles containing GM<sub>1</sub>, hydrogenated phosphatidylinositol and DSPE-PEG (Blume & Cevc, 1993; Gabizon & Papahadjopoulos, 1992). Liposomes derivatised with tresyl-coupled monomethoxy PEG 5000 were shown to exhibit increased hydrophilicity in phase-partitioning experiments (Senior *et al.*, 1991; Tilcock *et al.*, 1993). Figure 5.8 shows the elution of liposomes containing DSPE-PEG<sub>1900</sub> compared to EPC vesicles. EPC liposomes containing a 10% molar ratio of PEG-lipid were as hydrophilic as the most hydrophilic example of negatively charged formulations (EPC:PG). The presence of

cholesterol did not change the elution profile, with no significant differences between EPC:PEG and EPC:CH:PEG. The surfaces of these vesicles were confirmed to have an essentially neutral zeta potentials (table 5.1), reflecting shielding of the negative charge of DSPE-PEG<sub>1900</sub> by PEG polymer chains (Allen, 1994; Zalipsky *et al.*, 1994). PEG is regarded as one of the most hydrophilic polymers due to its water-compatible (CH<sub>2</sub>-CH<sub>2</sub>-O)<sub>n</sub> chain. The ether oxygen atoms form strong hydrogen bonds with water which result in highly orientated water around the polymer (Woodle & Lasic, 1992). The increased hydrophilicity of the liposome surface created by this polymer may decrease interaction with hydrophobic agaroses. HIC may be a useful technique for the characterisation of hydrophilic surfaces. Although hexyl-agarose provided the best resolution between charged and uncharged formulations, resolution of differences between very hydrophilic surfaces may require the use of more hydrophobic agaroses than octyl-agarose (*e.g.* decyl-agarose). The greater hydrophobic interaction of vesicles with such agaroses may facilitate further differentiation between polymer hydrophilicity and that derived from an exposed negative charge. It appears reasonable that the resolution that may be achieved with a particular agarose derivative will be related to the range of vesicle surface hydrophobicities.

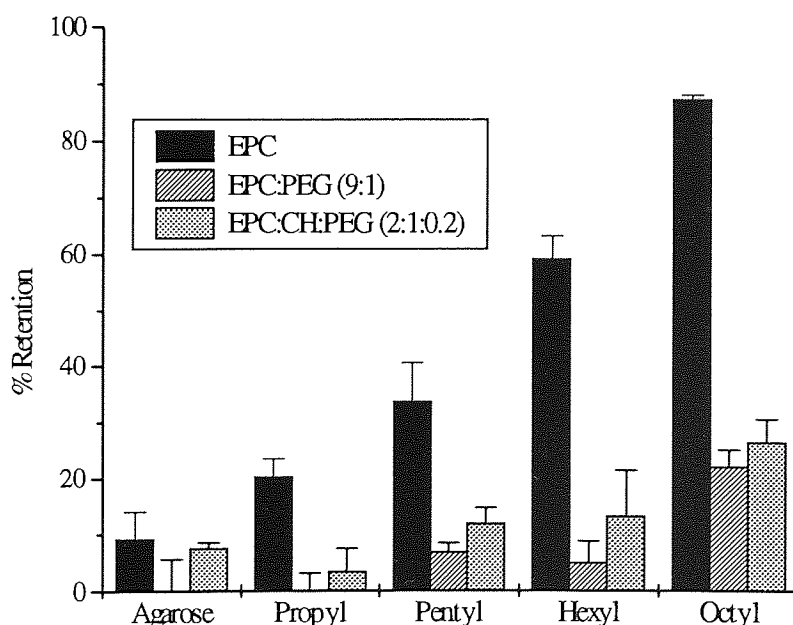


Figure 5.8. Influence of DSPE-PEG<sub>1900</sub> on retention of liposomes (each point represents the mean  $\pm$  sd of three experiments)

### 5.3.3.5. HIC characterisation of drug-loaded vesicles

HIC characterisation of charged vesicles showed that an exposed negative charge increased surface hydrophilicity. Drug loading of EPC:DCP formulations resulted in a decrease in surface charge, consistent with complexation of DCP and PXB (section 3.5.7). In addition to surface charge measurements, changes in hydrophilicity were investigated by comparing the retention of drug loaded EPC:DCP vesicles with the empty preparation. PXB was loaded in DRV using an initial drug to lipid ratio of 9mg PXB to 66 $\mu$ M total lipid. PXB loading efficiency for this preparation was found to be 0.056 $\mu$ mol PXB/ $\mu$ mol lipid. Zeta potential (table 5.1) was affected by drug loading with a value of  $-9.0\pm 1.3$ mV observed in 0.2M NaCl. The retention of these vesicles relative to EPC and EPC:DCP unloaded liposomes is shown in figure 5.9.

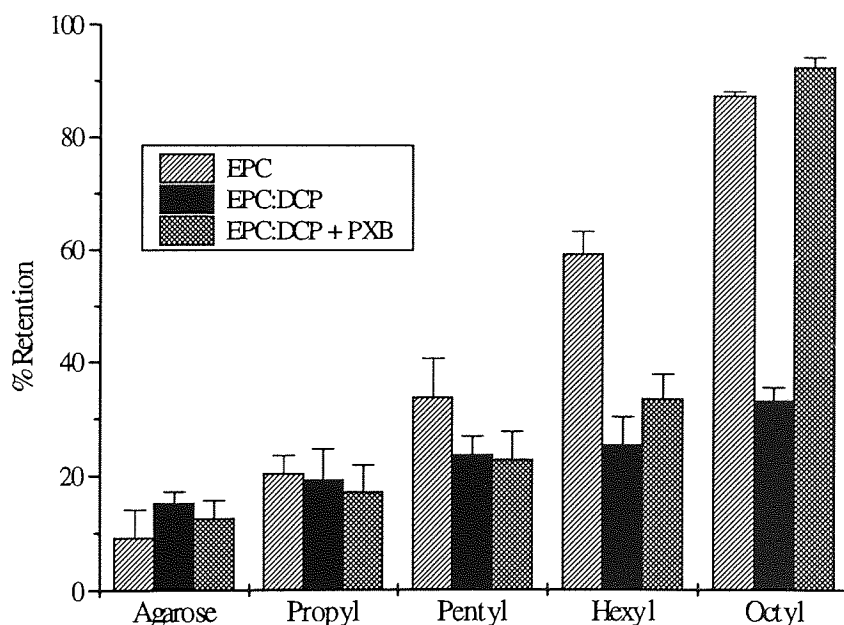


Figure 5.9. Influence of drug-loading on retention of EPC:DCP liposomes (each point represents the mean $\pm$ sd of three experiments)

Retention in the hexyl phase of loaded liposomes ( $33.40\pm 4.36\%$ ) was not significantly different to that of empty EPC:DCP liposomes ( $25.32\pm 4.89\%$ ). Therefore both formulations



were significantly more hydrophilic than EPC liposomes in this phase. Contrasting results were obtained in the octyl phase. Retention of EPC:DCP loaded liposomes was significantly greater than the unloaded preparation and there was no significant difference when compared to the retention of EPC vesicles. This suggests that the surface resembled that of empty EPC vesicles. The interaction of PXB with DCP would be expected to involve proton exchange (Hsuchen & Feingold, 1973) with subsequent diminution of DCP negative charge. As an unionised group is less hydrophilic than an ionised group of the same structure, an increase in retention would be expected (Zaslavsky *et al.*, 1984). However this explanation does not correlate with the similarity in retention of loaded and unloaded vesicles in the hexyl phase. It is possible that PXB mediates an increased interaction of vesicles with octyl-agarose relative to hexyl-agarose, perhaps through direct interaction of its amino-acid headgroup with the stationary phase. Further work is required to investigate the exact arrangement of bilayer-associated PXB/DCP, using bilayer probe or NMR analytical techniques. Such data may help to explain the anomalous behaviour of loaded vesicles in hexyl and octyl-agaroses.

#### 5.4. Conclusions

HIC successfully resolved differences between liposomes of various phospholipid compositions. Hydrophobicity of liposomes has been previously performed by partition in two-phase systems. The results reported by HIC are in general agreement with those determined by partitioning. The phospholipid polar head-group was found to have the dominant role in determining surface hydrophilicity. Surface charge, negative and positive in polarity, increased hydrophilicity. Cholesterol had a smaller influence on hydrophilicity and the degree of acyl chain saturation was relatively unimportant. HIC reflected the changes in surface properties induced by the presence of PEG. Practically, HIC has several advantages over phase-partitioning methods. Firstly, the columns are simple to prepare and the commercially available agaroses may be used after washing with distilled water. The detection of vesicle interaction may be achieved with optical density measurements as

opposed to detecting labelled phospholipids/tracers in phase-partitioning experiments. Additionally, this technique may be modified to allow automation with a greater sample handling potential. Automated HIC has been previously used to characterise microsphere surfaces (Müller, 1991). HIC may also be useful for detecting changes in surface properties mediated by plasma protein adsorption and this may be applied to the identification of the lipids with stealth properties. Although the current data indicated a change in surface properties with drug-loaded vesicles, further work, is necessary to evaluate the relevance of HIC data to bilayer surface changes.

## Chapter 6

### Antimicrobial and antiendotoxin properties of polymyxin B

---

#### ABSTRACT

Liposomal PXB has been demonstrated to have a favourable lung clearance profile relative to free drug. However, it is essential that the antimicrobial activity of PXB is maintained after encapsulation. In order to verify that LPXB formulations were active against the target organism, *P. aeruginosa*, the bactericidal activity of both free and encapsulated PXB was investigated. The minimal inhibitory concentrations of LPXB formulations were also compared to free drug. It was found that vesicle surface characteristics played a major role in the interactions with bacterial cells and influenced the activity of liposomal formulations.

The activity of PXB in CF may be also the result of an anti-endotoxin effect related to the high affinity of PXB for the lipid A region of LPS. This interaction was investigated using electrophoretic and immunoblotting techniques. It was found that PXB caused structural distortion of the lipid A region but did not prevent binding to anti-LPS antibodies. The relevance of this finding to the pathophysiology and treatment of CF lung infections with aerosolised polymyxins is discussed.

---

## 6.0. Antimicrobial and anti-endotoxin properties of PXB

Liposomal encapsulation of PXB has proved successful in extending the pulmonary residence time of this antibiotic in adult rats. In addition to changing pulmonary pharmacokinetics of PXB, liposomal encapsulation may also influence antibacterial efficacy (Nacucchio *et al.*, 1988). Encapsulation has been shown to enhance the activity of piperacillin against Staphylococci (Nacucchio *et al.*, 1985) and tobramycin/ticarcillin against resistant strains of *P. aeruginosa* (Lagace *et al.*, 1991). Phospholipid composition may play an important role in determining interaction between liposomes and bacteria, with positively charged lipids mediating electrostatic attraction between liposomes and negatively charged bacterial membranes (Jones *et al.*, 1994).

The aim of this study was to investigate the efficacy of a range of LPXB formulations against a clinical isolate of *P. aeruginosa* grown in chemically defined media. Minimal inhibitory concentrations (MICs) were measured and antimicrobial bactericidal studies performed comparing the activity of LPXB with equivalent concentrations of non-entrapped PXB.

In addition to antimicrobial activity, PXB also possesses potent anti-endotoxin/LPS effects (see section 1.2.6). Previous studies have used densitometric (Moore *et al.*, 1986) and probe displacement (David *et al.*, 1992) methods to demonstrate that PXB has a high affinity for LPS. PXB binds, through a combination of hydrophobic and electrostatic forces, to the lipid A moiety of LPS causing structural distortion and this interaction leads to an endotoxin neutralising effect (Danner *et al.*, 1989; Morrison & Jacobs, 1976). The aim of this work was to use sodium dodecyl sulphate-polyacrylamide gel electrophoresis (SDS-PAGE) and immunoblotting techniques to determine if the interaction of PXB with LPS results in a reduction in antigenicity of the lipid A region. Such an interaction may interfere with the inflammatory cascade and reduce immune-complex formation in the CF lung (fig 1.1).

## 6.1. Materials

### 6.1.1 Polymyxin B

As section 2.2.1.

### 6.1.2 Phospholipids

As section 2.2.2.

### 6.1.3. Chemicals

All chemicals and reagents not specified in the text were supplied by BDH Chemicals Ltd. (Poole, UK), Sigma Chemical Company (Poole, UK) and Fisons (Loughborough, UK) and were of Analar grade or equivalent.

### 6.1.4. Organism and culture maintenance

The organism used in the studies was *Pseudomonas aeruginosa* NCTC 6750 (PA 6750). It was maintained at 4°C on nutrient agar (Lab M Ltd., Bury) plates. Long term storage was -70°C in chemically defined media (CDM12).

### 6.1.5. Chemically defined medium (CDM12)

PA 6750 was grown in CDM liquid medium and shaken on a rotating incubator (New Brunswick G10) at 37°C. CDM12 is isotonic with serum and its composition is listed in table 6.1. The value 12 is the theoretical optical density at 470nm which can be obtained by batch culture growth of cells in this medium. The pH was adjusted to 7.8 using 1M NaOH and the medium was autoclaved at 121°C for 20 minutes. Glucose and  $K_2HPO_4 \cdot 3H_2O$  were autoclaved separately in order to prevent caramelisation and precipitation respectively.

Component	Quantity (mM)
Glucose	48.00
KCl	0.74
NaCl	0.60
(NH) <sub>4</sub> SO <sub>4</sub>	48.00
MgSO <sub>4</sub> ·7H <sub>2</sub> O	0.48
MOPS (3-(N-Morpholino)	60.00
Propane-sulphonic acid)	
K <sub>2</sub> HPO <sub>4</sub> ·3H <sub>2</sub> O	3.84
ddH <sub>2</sub> O to	1 litre

Table 6.1. Components of CDM12.

## 6.2. Methods

### 6.2.1. Preparation of LPXB for antimicrobial bactericidal assay and MIC studies

DRV preparations of LPXB were prepared as described in section 3.3.1 and encapsulations determined by scintillation counting of [<sup>3</sup>H]-PXB. A standard drug loading of 9mg PXB/66μM total lipid was used for all preparations. All buffers were autoclaved at 121°C for 30min and liposomes were prepared aseptically in a laminar air-flow cabinet.

### 6.2.2. Zeta potential analysis of LPXB formulations

As section 3.4.7.

### 6.2.3. Laser diffraction sizing of LPXB formulations

As section 3.4.8.1.

#### 6.2.4. Antimicrobial bactericidal assay

The growth of an iron-restricted batch culture of PA6750 was followed by the measurement of optical density at 470nm at regular intervals. Cells in the early logarithmic phase of growth were used for bactericidal studies. Tubes containing appropriate concentrations of non-entrapped PXB and LPXB to give final concentrations of 0.1µg/ml and 0.3µg/ml in CDM salt solution were prepared aseptically in triplicate and pre-warmed at 37°C. Control tubes were prepared by omitting antimicrobial solutions and using an appropriate volume of CDM12 salts solution. Additional control tubes containing empty liposomes at the same lipid concentration as loaded vesicles were also prepared. Cultures of PA6750 were used at optical densities between 0.04 and 0.08 and then standardised by dilution with CDM12 salts solution to an OD<sub>470nm</sub> of 0.04. Aliquots of this suspension (100µl) were added to the antimicrobial solutions (4.9ml) to give the desired cell density ( $1 \times 10^6$  cfu/ml) and incubated at 37°C for 1hr.

To determine cell numbers after exposure to free and LPXB, viable counts were determined using the spread plate method (Crone, 1984). The treated cells and controls were diluted 1:10 and 1:100 in Lethen broth (Difco Laboratories, Detroit, USA) and 100µl samples plated onto predried nutrient agar in triplicate. Plates were incubated at 37°C overnight to produce between 30-300 colonies *per* plate and colonies enumerated using a colony counter. The viable count for the original suspension was established from the mean number of colony forming units (cfu) from a triplicate set of plates and multiplied by the dilution factor (cfu/ml). The relative reductions in cfu were compared and expressed as percentage surviving fraction for each test solution.

#### 6.2.5. Determination of the minimal inhibitory concentrations of PXB and LPXB

Aliquots of double strength CDM (2.4ml) were dispensed into test-tubes with 0.5ml glucose (0.4M). PXB/LPXB solutions and distilled water were added in a 2ml volume to give the

desired concentration in a final volume of 5ml and finally a 100 $\mu$ l inoculum (diluted in CDM to give 1x10<sup>6</sup> cfu/ml) from an overnight culture was added. The final concentration (in 5ml) of both free and LPXB was 0.1-0.8 $\mu$ g/ml. The tubes were vortexed and incubated at 37°C on a shaker for 18hr. The tubes were examined for growth and the MIC defined as the lowest concentration of antibiotic that inhibited the development of visible growth.

Drug released from liposomes during the period of MIC testing was determined by incubating a control tube containing CDM salts solution with LPXB in the absence of inoculum. After 18hr incubation at 37°C, samples were taken and free drug separated using Microcon 100 microconcentrators (Amicon, Herts.). Release was expressed as the % of drug initially encapsulated and this value was used to determine the concentration of free PXB in solution.

#### 6.2.6. Extraction and purification of *P. aeruginosa* LPS

LPS was extracted by an adaptation of the hot phenol technique of Westphal and Jann (1965). A 2L over-night culture of PA01, grown in iron-restricted chemically defined medium (CDM), was harvested by centrifugation at 5000 x g for 10min. The cells were washed once in 0.85% (w/v) saline, resuspended in 20ml 30mM Tris-HCl, pH 8.0 and broken by 10 x 30s pulses of sonication in an ice bath, with 30s intervals for cooling. Deoxyribonuclease (Bovine pancreas type III), ribonuclease (Bovine pancreas type 1-AS) and lysozyme (to digest the DNA, RNA and peptidoglycan respectively) was added to a final concentration of 0.1mg/ml, and the preparation was incubated for 2hrs at 37°C. Five ml tetrasodium EDTA (0.5M) (to remove cations binding the LPS together), and protease (*Strep. griseus* type XIV; final concentration 1mg/ml) were added. The preparation was incubated overnight at 37°C with constant shaking. The protease was destroyed by heating the mixture to 80°C for 20min. The digested cell suspension mixed with an equal volume of 90% w/v phenol, pre-heated to 80°C. The preparation was stirred vigorously for 5min and then centrifuged at 5000 x g for 25min to permit phase separation. The upper aqueous layer



(containing LPS) was removed, care being taken not to disturb any of the proteinaceous material at the interface. Two further phenol-water extractions were performed by reheating the phenol layer to 80°C and adding a further 50ml water at the same temperature. The pooled aqueous fractions were dialysed for 48hrs against tap water to remove phenol.

Following dialysis, magnesium chloride was added to a final concentration of 50mM. The LPS was pelleted by centrifugation at 100,000 x g for 4hrs, washed in double distilled water, re-centrifuged and lyophilised.

### **6.2.7. Gel electrophoresis of LPS**

Polyacrylamide gel electrophoresis (Laemmli, 1970) is a powerful technique for the determination of molecular weight of macromolecules such as proteins. SDS-PAGE has been also used extensively to characterise LPS (Maskell, 1991). The lipid A portion of LPS contains negatively charged pyrophosphate groups which give this macromolecule an overall negative charge. As LPS possesses ionisable groups it can exist as electrically charged species in solution at physiological pH. Differences in charge to mass ratios resulting from differences in molecular weight cause a differential migration of ions in solution when subjected to an electric field. Cations move to the cathode and anions to the anode at rates depending on the impelling force of the electric field on the charged ion and the frictional and electrostatic retarding effects between the sample and the surrounding medium. The sample must be dissolved or suspended in buffer for electrophoresis to take place and any supporting medium must also be saturated with buffer to conduct the current and to maintain a constant state of ionisation since any changes in pH would alter the charges on the molecules being separated. LPS must first be treated so as to produce uniform charge/mass ratios for the subsequent separation in gels to be achieved solely on molecular size. This is accomplished by treating LPS with SDS and 2-mercaptoethanol which breaks disulphide bonds, assists solubilisation and attaches an ionic group at regular intervals along the LPS structure.

LPS was separated by SDS-PAGE using 14% acrylamide gels according to the methods described by Lugtenberg *et al.* (1975), as modified by Anwar *et al.* (1983). Running and stacking gels contained 4M urea. The Mini-Protean system (Bio-rad, Herts, UK) was used throughout this work.

The running and stacking gels were prepared as described in table 6.2 and polymerisation was initiated by the addition of N,N,N',N'-tetramethylethylene diamine. The running gel was poured between the glass plates separated by 0.5mm plastic spacers and allowed to set for 10min. A spray of electrode buffer on top of the gel ensured complete polymerisation. This buffer solution was removed and the stacking gel was cast in a similar manner. A teflon comb was inserted between the plates to create wells for sample application. Samples were denatured at 100°C for 10min with an equal volume of a denaturing mix containing mercaptoethanol (sample buffer, see table 6.2) before loading onto the gel. Samples were loaded (5µl of a 2.5mg/ml solution of LPS) and electrophoresis carried out at a constant voltage of 100V (power pack Bio-rad model 500/200). Electrophoresis continued until the tracking dye had migrated to within 0.5cm of the bottom of the gel. Electrode buffer contained 0.0025M Tris, 0.19M glycine and 0.1% w/v SDS. Gels were either used directly for immunoblotting (see section 6.2.9.) or stained with silver (see section 6.2.8.).

Constituent	Running gel (14% w/v)	Stacking gel (14% w/v)	Sample Buffer
Stock 1 <sup>1</sup>	6.25ml	-	-
Stock 2 <sup>2</sup>	-	1.7ml	-
1.5M Tris <sup>3</sup> pH 8.8	6.25ml	-	-
0.5M Tris <sup>3</sup> pH 6.8	-	2.5ml	5ml
10% w/v SDS	0.5ml	0.1ml	10ml
Distilled water	6.16ml	5.3ml	10ml
10% w/v AMPS <sup>4</sup>	70µl	30µl	-
TEMED <sup>5</sup>	45µl	25µl	-
Glycerol	-	-	5ml
2-Mercaptoethanol	-	-	0.5ml
5% w/v bromophenol blue	-	-	0.4ml
Urea	4.64g	2.32g	-

1) Stock 1= 44% w/v acrylamide and 0.8% w/v N,N'-methylene-bis-acrylamide (BIS)

2) Stock 2 = 30% w/v acrylamide and 0.8% w/v BIS

3) Tris (hydroxymethyl) aminoethane

4) Ammonium persulphate (freshly prepared)

5) N,N,N',N' - tetramethylethylene diamine

Table 6.2. Composition of running gel, stacking gel and sample buffer for SDS-PAGE of LPS

### 6.2.8. Silver stain of LPS

LPS separated by SDS-PAGE was visualised by silver staining following the method of Tsai and Frasch (1982). After electrophoresis the gel was immersed overnight in 40% (v/v) ethanol/5% (v/v) acetic acid solution. This fixing solution was then replaced with fresh solution containing 1% (v/v) periodic acid and the LPS oxidised for 30min. After 4x30 min washes with double distilled water to remove any unreacted periodic acid, staining reagent was poured over the gel. The silver stain was freshly prepared by slowly adding 2.5ml of

20% w/v silver nitrate solution to a mixture of 1ml concentrated ammonium hydroxide and 14ml 0.1M sodium hydroxide. The solution was made up to 75ml with double distilled water and the gel shaken for 30min. After further washing was performed for 10min with two changes of water, a developing solution consisting of 25mg citric acid, 0.5ml formaldehyde (37% v/v) in 500ml double distilled water was added to the gel.

When the LPS was stained to the desired intensity (2 to 5 min), the colour development was terminated by replacing the developer with fixing solution. Gels were photographed immediately.

### 6.2.9. Immunoblotting of LPS

Transfer of LPS separated by SDS-PAGE to a nitrocellulose membrane and investigation of antigenic sites was performed following the method of Towbin *et al.*, (1979), as modified by Anwar *et al.*, (1984). Following electrophoresis, the gel and nitrocellulose (Trans Blot Membrane, pore size 0.45 $\mu$ m, Bio-Rad Laboratories Ltd., Maidstone, Kent) were sandwiched between chromatography paper, Scotch-brite pads (Bio-Rad Laboratories Ltd., Maidstone, Kent) and perforated plastic support grids. Electroblothing was performed in a Trans-blot cell, at 50V for 60min in ice-cold blot buffer (192mM glycine, 25mM Tris, 20% (v/v) methanol, pH 8.3). After transfer, the nitrocellulose was removed from the cell, and soaked in Tris-buffered saline (TBS, 10mM Tris HCl, 0.9% w/v NaCl, pH 7.4), containing 0.3% (v/v) Tween 20 and 1% (w/v) bovine serum albumin (BSA), for 60min to saturate non-specific binding sites on the paper (Batteiger *et al.*, 1982). Complete quantitative transfer of LPS was confirmed by staining the gel after blotting with silver (section 6.2.8.).

Specific immunological detection of antigenic sites was achieved by incubating the immunoblot with pooled human antisera from CF patients infected with *P. aeruginosa*, adjusted to an appropriate dilution (1:50 in TBS-Tween), for 3hrs at 37°C, with shaking. Following this the blot was washed in TBS-Tween and incubated for a further 2hrs with

protein-A-HRP (horse radish peroxidase).

HRP conjugates were visualised using a solution containing 25µg/ml 4-chloro-1-naphthol and 0.01% (v/v) hydrogen peroxide in 10mM Tris, pH 7.4. The colour was allowed to reach an optimum intensity and then the reaction was terminated by placing the immunoblot in water.

#### **6.2.10. Investigation of the PXB/LPS interaction using SDS-PAGE and immunoblotting techniques**

The effect of PXB on the structure of LPS was investigated using SDS-PAGE. Aliquots (20 µl) of LPS extracted from PA01 were incubated with 80µl of various concentrations of PXB (0, 5000, 10000, 25000, 50000, 75000, and 100000 units/ml, PXB activity 7730 units/mg) prior to loading on the gel for 1hr at 37°C. The gel profile after separation was visualised by silver staining (section 6.2.8).

PXB was further investigated for its ability to mask the antigenicity of LPS by transfer of electrophoretically separated LPS, after incubation with PXB as above, onto nitrocellulose membranes as described in section 6.2.9. and probing with pooled human serum (1:50 dilution in TBS-Tween) from CF patients infected with *P. aeruginosa*.

Competitive immunoblotting was performed using LPS without PXB. After transfer of LPS to nitrocellulose, the blot strips were incubated with a number of concentrations of PXB (0, 10000, 25000, 100000, 500000 units/ml) for 1hr at 37°C. The blot strips were rinsed with TBS-Tween and probed with CF patient sera (1:50). Developed blots were then visually inspected for any changes in binding of human antibodies in the presence of increasing PXB concentrations.

## 6.4. Results and Discussion

### 6.4.1. Characterisation of DRV used in antimicrobial bactericidal assays and MIC studies

DRV were prepared using phospholipid compositions which would give nominally neutral (EPC), negatively (EPC:DCP 9:1) and positively charged vesicles (EPC:SA 9:1). The entrapment of PXB within these formulations is shown in figure 6.1. Encapsulations were similar to those previously reported for such phospholipid compositions (section 3.4.2). The loadings achieved with EPC ( $45.41 \pm 0.51\%$ ,  $n=3$ ) and EPC:DCP vesicles ( $50.81 \pm 0.79\%$ ) were similar. Positively charged vesicles had a significantly lower entrapment ( $31.92 \pm 2.08\%$ ). Electrophoretic mobility measurements in 0.02M diphosphate pH 7.4 illustrate the different surface characteristics of the liposome preparations used (figure 6.2). Empty liposomes composed solely of EPC had a zeta potential of  $-0.3 \pm 0.3$  mV. The inclusion of a 10% molar ratio of SA resulted in a positive potential of  $12.8 \pm 1.1$  mV. Liposomes containing the negative amphiphile, DCP, had a strongly negative zeta potential of  $-54.9 \pm 2.7$  mV. When the zeta potential of liposomes with entrapped PXB was measured, all preparations became more positive. These findings indicate a degree of bilayer/surface association of PXB and are consistent with those reported in section 3.4.7. Liposome diameter was determined by laser diffraction and the volume means of all loaded preparations were found to be similar (EPC;  $5.05 \pm 2.31 \mu\text{m}$ , EPC:DCP;  $5.98 \pm 4.02 \mu\text{m}$ , EPC:SA;  $5.70 \pm 4.36 \mu\text{m}$ ).

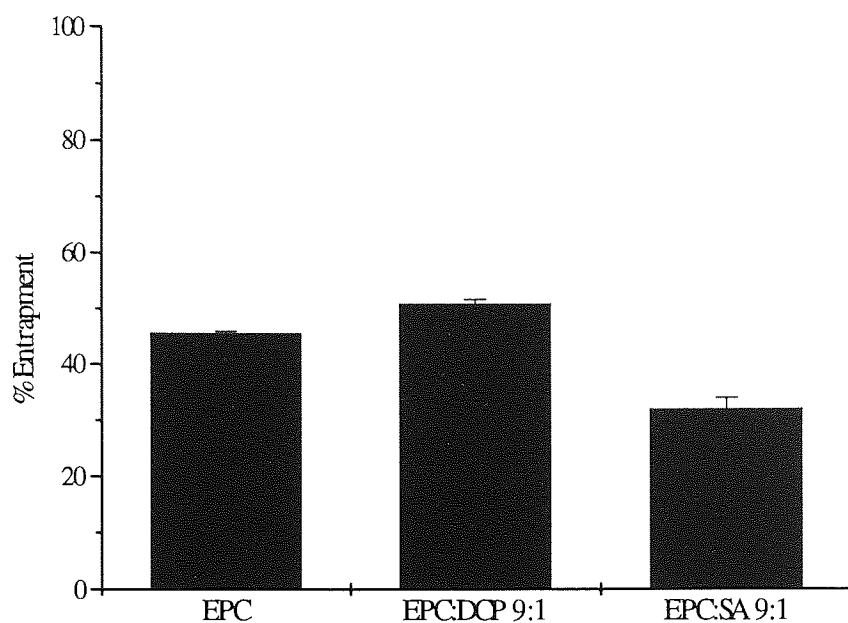


Figure 6.1. Entrapment of PXB within DRV. Entrapment values expressed as a percentage of the initial drug loading (9mg PXB/66 $\mu$ M total lipid). Each point represents the mean $\pm$ sd for three replicates.

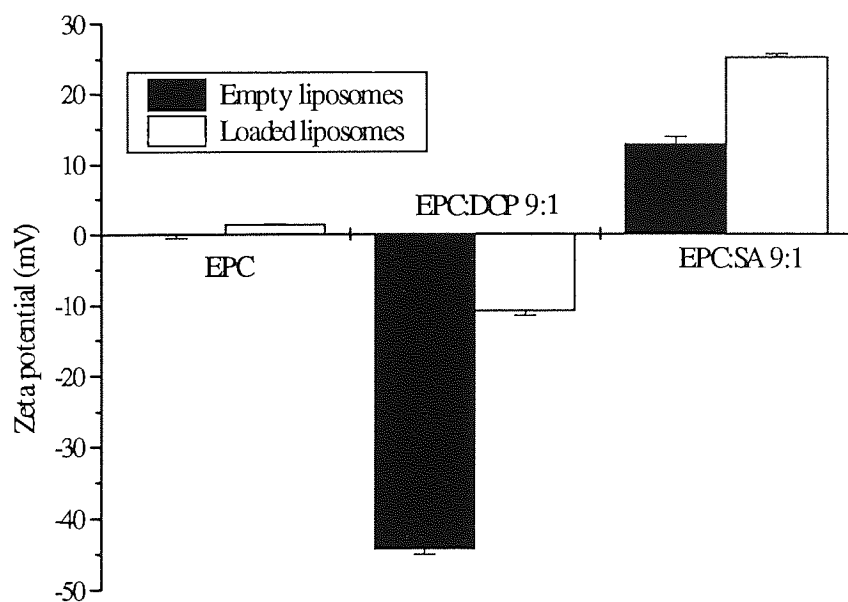


Figure 6.2. Zeta potential of loaded and unloaded DRV in 0.02M diphosphate buffer pH 7.4. Each point represents the mean $\pm$ sd for five measurements.

#### 6.4.2. Antimicrobial bactericidal testing of PXB and LPXB

The antimicrobial activity of PXB was assessed using two concentrations; 0.1 µg/ml and 0.3 µg/ml. Figure 6.3 shows the relative differences in bactericidal activity expressed as the % surviving fraction for non-entrapped PXB and liposomal PXB at a concentration of 0.3 µg/ml. Incubation of empty vesicles at equivalent lipid concentrations as loaded vesicles gave similar results to those of CDM salt control tubes, indicating that the phospholipids used had no effect on organism growth. At 0.3 µg/ml, positively charged and negatively charged liposomes produced a greater reduction in cell numbers than neutral liposomes. As *P. aeruginosa* cells are negatively charged ( $-11.4 \pm 2.9$  mV) in PBS (Nicholov *et al.*, 1993), the enhanced activity of positively charged vesicles may be attributable to increased cell association through attractive electrostatic interactions. The enhanced activity of negatively charged liposomes is unlikely to be the result of electrostatic interactions. It is possible that the surface polarity of DCP-containing vesicles results in increased surface hydrophilicity which may facilitate association with hydrophilic PA6750 cells. However, HIC characterisation of loaded EPC:DCP vesicles gave ambiguous results for this parameter (section 5.3.3.5). Alternatively, increased surface association of polycationic PXB with the anionic headgroup of DCP may increase the availability of PXB at the liposome surface which may in turn interact with the target LPS molecules on the bacterial surface.

As both non-entrapped and LPXB formulations produced a 100% cell kill at 0.3 µg/ml, it was not possible to determine any additional enhancement of activity achieved with encapsulated drug. However, it is clear that PXB maintains antimicrobial activity after the DRV process. Enhancement of activity was not observed at the lower concentration (0.1 µg/ml) with no significant difference between the bactericidal activity of free and entrapped PXB (figure 6.4). Although positively charged vesicles decreased cell numbers to a greater extent than neutral or negatively charged liposomes, there was no significant difference between cell-kill observed with free and entrapped drug.



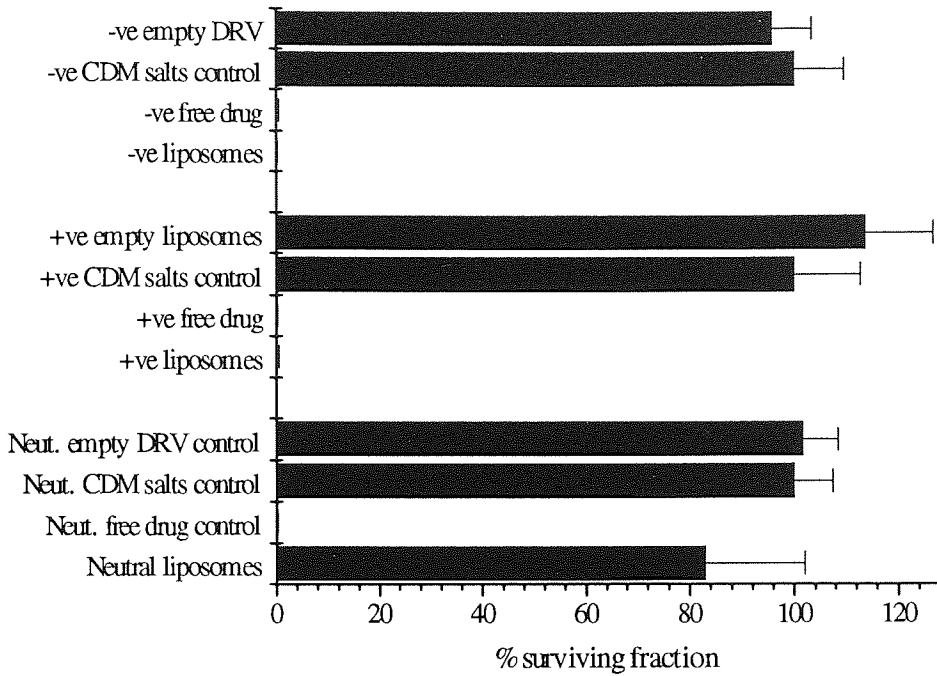


Figure 6.3. Bactericidal activity of PXB and LPXB (0.3µg/ml dose) against *P. aeruginosa* after 1hr incubation at 37°C. Controls with CDM salts only, empty liposomes and free drug only were run with each liposome formulation. Liposomes are denoted: Neut.=EPC, +ve=EPC:SA and -ve=EC:DCP. Each point represents the mean±sd for three triplicates.

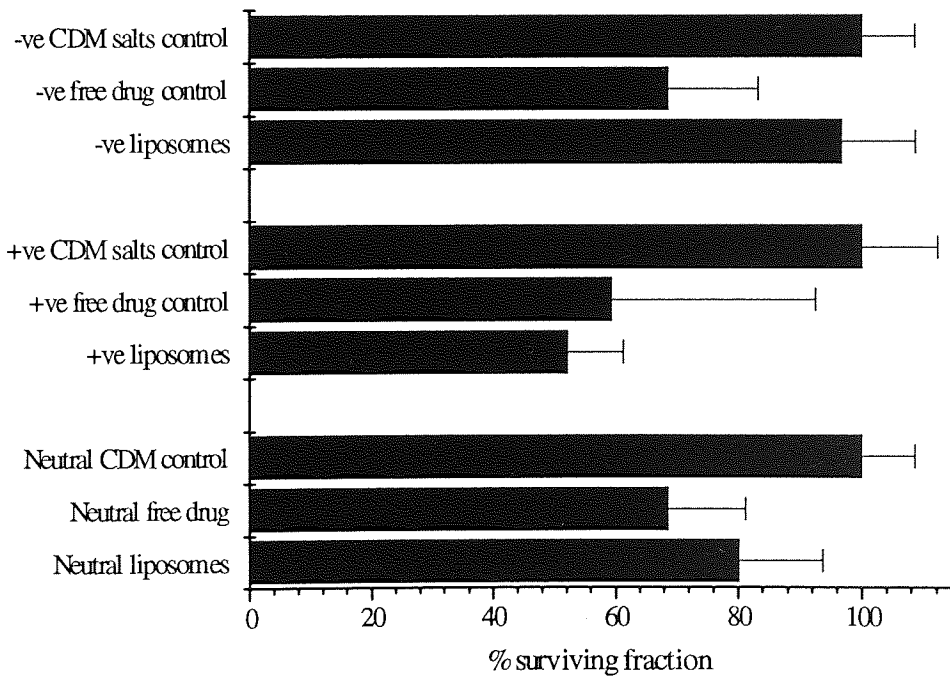


Figure 6.4. Bactericidal activity of PXB and LPXB (0.1µg/ml dose) against *P. aeruginosa* after 1hr incubation at 37°C. Controls with CDM salts only and free drug only were run with each liposome formulation. Liposomes are denoted: Neut.=EPC, +ve=EPC:SA and -ve=EC:DCP. Each point represents the mean±sd for three triplicates.

A number of previous studies have investigated the effect of liposome encapsulation on *in vitro* bactericidal activity. Negatively charged tobramycin-loaded liposomes were more active than free drug at sub-MIC levels against PAO1, a pseudomonas clinical isolate. It was suggested that there was sufficient cell-liposome attraction to overcome any electrostatic repulsion although a mechanism was not proposed (Poyner *et al.*, 1993). These findings are similar to those seen with negatively-charged PXB formulations at a 0.3µg/ml dose. Charge effects were also reported by Young-Ho and Jones (1994) who described a strong association of cationic liposomes (DPPC:CH:SA) with films of adsorbed Streptococci and Staphylococci. It was found that the number of liposomes (100-140nm in diameter) *per* bacterium ranged from 1000 to 3000 depending on the bacterial strain. Positive charge was also shown to increase the activity of ciprofloxacin-loaded liposomes against a clinical isolate of *P. aeruginosa* (Nicholov *et al.*, 1993). Variation of lipid acyl chain and cholesterol content were shown to have little effect on cell-association. However liposomes possessing a small positive charge (mediated by phosphatidylethanolamine) had significantly increased association with bacterial cells. It was demonstrated that liposomal attachment to bacterial cells screened part of the bacterial negative surface charge. Electrostatic attraction was proposed as the mechanism for increased association of these vesicles. Positively charged SUV also showed increased suppression of bacterial growth. Enhanced antistaphylococcal activity of piperacillin was noted when encapsulated within liposomes composed of equimolar PC and cholesterol (Nacucchio *et al.*, 1985). Liposomal entrapment was proposed to protect piperacillin from hydrolysis by  $\beta$ -lactamase, thereby increasing the concentration of active drug. In a follow-up study (Nacucchio *et al.*, 1988) it was shown that entrapped gentamicin and piperacillin were effective against strains of *E. coli* and *P. aeruginosa* resistant to the free antibiotics. The mechanism of enhancement was proposed to include protection of drug from enzymatic degradation and facilitated diffusion of liposome-associated drug across the bacterial envelope. Translocation of phospholipids between the outer and inner membranes of *Salmonella typhimurium* occurs after direct fusion of phospholipid vesicles (Jones & Osborn, 1977). Sekeri-Pataryas *et al.* (1985) showed that liposomes containing entrapped penicillin could overcome the cell wall barrier of resistant *P.*

*aeruginosa* and effectively deliver the antibiotic to the cell. Liposome-bacterial fusion was demonstrated with the delivery of a liposome-entrapped enzyme, horse-radish peroxidase, to bacterial cells (Tomlinson *et al.*, 1989). Facilitated diffusion by phospholipid vesicles was proposed to deliver this molecule which is normally too large to diffuse across the outer membrane of bacterial cells. Fusion was dependent on calcium ion concentration, time, temperature, buffer composition, pH, LPS chemotype and cell/liposome concentration. DRV entrapment of ticarcillin and tobramycin enhanced activity against resistant strains of *P. aeruginosa* (Lagacé *et al.*, 1991). It was suggested that encapsulation of antibiotics promotes their diffusion across the bacterial envelope of resistant strains, although the mechanism was unknown. Protection from enzyme degradation was also proposed.

Other studies have demonstrated the importance of the availability of entrapped drug in determining antibiotic *in vitro* activity. The inactivity of encapsulated chloramphenicol and streptomycin against *E. coli* in broth culture was noted by Stevenson *et al.* (1983). The vesicles were loaded with sufficient antibiotic, which if present as free drug in solution, would have inhibited bacterial growth. Similarly, ampicillin loaded liposomes failed to inhibit growth of *Listeria monocytogenes* in culture (Bakker-Woudenberg *et al.*, 1985). Gentamicin and ceftazidime loaded stealth vesicles possessed low bactericidal activity against *Klebsiella pneumoniae* in culture yet were effective against infection *in vivo* (Bakker-Woudenberg, 1995). In such cases the release of entrapped antibiotic would determine *in vitro* activity. It is likely that for each particular bacteria-liposomal antibiotic interaction, a number of the above mechanisms are appropriate and generalisations regarding *in vitro* activity cannot be made.

In the case of LPXB, entrapment within phospholipid vesicles does not result in a reduction in activity at the two concentrations tested. As LPXB did not show enhanced activity relative to free drug at 0.1 µg/ml, it would appear that facilitated diffusion is an unimportant delivery mechanism in this case. The results achieved with LPXB must be qualified in terms of the fraction released and therefore PXB available for bactericidal activity. Although release experiments were not conducted in CDM salts solution, release in PBS pH 7.4 indicated only

a fraction of the entrapped contents was released after early time-points (generally <30% after 4hr, section 3.8.2). The activity of LPXB may therefore be attributable to release of PXB at or near the cell surface which would expose bacterial cells to a transiently high PXB concentration. Protection of PXB from enzymatic degradation is unlikely to significantly enhance activity as the drug is not extensively hydrolysed by bacterial enzymes. Although LPXB did not possess significantly enhanced antimicrobial bactericidal activity, the altered pulmonary pharmacokinetics of this formulation may produce a more effective treatment of infection *in vivo* than that achievable with free drug (Drusano, 1988).

#### 6.4.3. MIC studies with PXB and LPXB

The entrapment of PXB within DRV used for MIC studies is shown in table 6.3. The values demonstrate the formulation dependency discussed in section 3.5.3. The MIC for free PXB against stationary phase cells of PA6750 grown in iron-depleted CDM12 was found to be 0.1-0.2 $\mu$ g/ml. The MICs of neutral EPC-based liposomes varied when expressed as the total concentration of PXB. However when the effective free PXB concentration was calculated using the percentage of drug released, the MIC for all neutral EPC-based formulations was similar (~0.1-0.2 $\mu$ g/ml). The value is similar to that seen with free drug and suggests that liposomal encapsulation did not promote diffusion/delivery to bacterial cells. The MIC clearly depended on the availability of free drug in solution. Only EPC:SA liposomes had a lower MIC value (0.044-0.066 $\mu$ g/ml). This may reflect association of EPC:SA vesicles with bacterial cells which would increase PXB released in the cell microenvironment. The increased activity of PXB in the MIC assay are consistent with the greater bactericidal activity of this formulation relative to neutral vesicles. The MICs observed with DSPC-based vesicles were lower than those of free drug. This is surprising given that release from this type of vesicle was less than that seen with EPC-based formulations and resulted in lower concentrations (sub-MIC) of free drug in the incubation medium. Also, previous studies have noted that the acyl chain composition of vesicles has little effect on association with *P.*

*aeruginosa* cells (Nicholov *et al.*, 1993). As the entrapment of DSPC-based vesicles was generally lower than that of comparable EPC-based vesicles, a larger lipid dose needed to be used to achieve the equivalent PXB dose. Therefore a greater number of DSPC-based vesicles were added to each tube. Accordingly the relative ratio of vesicles/cell is increased and this may facilitate greater liposome-cell adsorption with correspondingly higher amounts of PXB released within the immediate vicinity of bacterial membranes. Alternatively the altered membrane fluidity of DSPC-based vesicles may promote adsorption of cells to liposomal surfaces.

In summary MIC studies with LPXB have indicated that facilitated diffusion of PXB does not occur. The amount of available drug is controlled by liposomal release characterisation and it is this fraction of free drug which determines the MIC. Increased association of positively charged vesicles decreases the MIC, presumably through localised release of PXB at the outer membranes of *P. aeruginosa*. The lower MICs observed with DSPC-based vesicles are likely to be the result of increased liposome/cell ratios.

Formulation	% Entrapment (n=3) $\pm$ sd	Nominal MIC ( $\mu$ g/ml)	% Release during test period (n=3) $\pm$ sd	Effective free drug concentration ( $\mu$ g/ml)
Free drug	N/A	0.1-0.2	N/A	0.1-0.2
EPC	60.96 $\pm$ 3.10	0.2-0.3	43.66 $\pm$ 1.02	0.087-0.131
EPC:CH (2:1)	39.24 $\pm$ 1.37	0.2-0.3	62.51 $\pm$ 3.17	0.125-0.188
EPC:CH (1:1)	27.52 $\pm$ 1.46	0.3-0.4	28.88 $\pm$ 1.76	0.115-0.154
EPC:CH:PEG (2:1:0.2)	26.10 $\pm$ 1.13	0.3-0.4	38.40 $\pm$ 2.31	0.087-0.116
EPC:SA (9:1)	29.56 $\pm$ 0.90	0.2-0.3	21.91 $\pm$ 0.58	0.044-0.066
DSPC	32.03 $\pm$ 2.17	0.4-0.5	15.57 $\pm$ 1.21	0.062-0.078
DSPC:CH (2:1)	22.59 $\pm$ 1.13	0.4-0.5	13.12 $\pm$ 2.01	0.052-0.066
DSPC:CH (1:1)	26.01 $\pm$ 1.85	0.1-0.2	36.35 $\pm$ 0.74	0.036-0.073
DSPC:CH:PEG (2:1:0.2)	11.46 $\pm$ 0.81	0.3-0.4	11.49 $\pm$ 0.23	0.034-0.046

Table 6.3. Entrapment and MIC values for LPXB formulations compared to free drug after 18hr incubation at 37°C. Entrapment is expressed as the percentage of drug initially loaded (initial loading 9mg PXB/66 $\mu$ M total lipid). Release was determined as detailed in text and used to calculate effective free drug concentration.

#### 6.4.4. Investigation of the structural distortion of LPS by PXB using SDS-PAGE/immunoblotting techniques

The interaction of PXB with LPS is a primary event in its mode of action against Gram-negative bacteria. PXB acts by binding to acidic groups of the polysaccharide chain and the proximal sugar residues such as 2-keto-3-deoxyoctonate (KDO) (Vaara & Nikaido, 1984). Divalent cations such as Mg<sup>2+</sup> are displaced by binding which results in disordering of adjacent LPS molecules. In addition to antimicrobial activity, PXB may also reduce the generation of inflammatory mediators through distortion of LPS (section 1.2.6.). Several studies have demonstrated binding of PXB to LPS. Morrison and Jacobs (1976) noted that PXB formed a stable molecular complex with the lipid A region of LPS (see schematic structure of LPS, figure 6.5). The complex appeared to involve one molecule of PXB *per*

monomer of LPS, with an increase in the apparent molecular weight of LPS. The acyl chain of PXB is thought to enhance binding through hydrophobic interactions with the lipid A region (Peterson *et al.*, 1985). Polymyxin B nonapeptide which lacks the acyl chain, has a reduced affinity for LPS (Vaara, 1983). Ionic forces also play a role with electrostatic attraction between negatively charged phosphate groups of LPS and the cationic residues of PXB (David *et al.*, 1992). The results of the current study show that PXB binds to the lipid A, changing its migration through the gel. Figure 6.6 shows the appearance of an LPS SDS-PAGE gel after silver staining. Lipid A samples had been incubated with varying concentrations of PXB prior to loading. Lane 7 (LPS only) shows the typical appearance of LPS from S-form (smooth) *P. aeruginosa* (Fomsgaard *et al.*, 1990). Silver staining reveals numerous bands arranged in a ladder-like pattern, reflecting the number of repeating units in the O-specific side chain of LPS (figure 6.5). As the components of LPS are fractionated according to size, the highest molecular weight component is the O-specific side-chain with the core polysaccharide intermediate in weight, followed by the lipid A fraction as the lowest molecular weight component. Lanes 1 to 6 show the appearance of LPS after incubation with PXB. As PXB concentration increases from 5000 to 100000 units/ml, there is a progressive change in migration of LPS through the polyacrylamide chain. The lipid A fraction appears to become more condensed with increasing PXB concentrations, consistent with the formation of a higher molecular weight complex. Figure 6.7 shows the appearance of a similar gel after immunoblotting and probing with pooled human serum from CF patients infected with *P. aeruginosa*. The distortion of LPS was seen again although the lipid A region retained antigenicity, indicating that structural distortion by PXB did not prevent antibody binding. Competitive immunoblotting failed to show any reduction in antibody binding even with high PXB concentrations. This may be due to poor binding of PXB to lipid A which had been fractionated and transferred to nitrocellulose. However, the data from the above experiments appear to indicate that although PXB distorts the lipid A moiety of LPS, it is not sufficient to immunologically mask antibody binding sites. Colistin (polymyxin E) has also been shown to have similar effects on LPS migration in SDS-PAGE gels (Wilton, 1991). LPS would therefore appear to retain its capacity to form immune-complexes after PXB treatment but

numerous studies have shown that the distortion induced by PXB is sufficient to abrogate the endotoxin properties of LPS (Applemelk *et al.*, 1988; Danner *et al.*, 1989; Rifkind, 1967). As discussed in section 1.2.6., binding of LPS to neutrophils results in release of oxygen radicals. As the hydrophobic lipid A region is thought to have a crucial role in binding (Prins *et al.*, 1994; Wilson, 1985), structural distortion of this region may reduce the binding efficiency to endotoxin receptors. It would therefore appear that this property of PXB may be relevant to clinical findings of reduced lung inflammation after polymyxin inhalation treatment (Jensen *et al.*, 1987) particularly as PXB has been shown to possess potent anti-endotoxin properties when given systemically in rats (Rifkind, 1967) and in humans (Endo *et al.*, 1994).

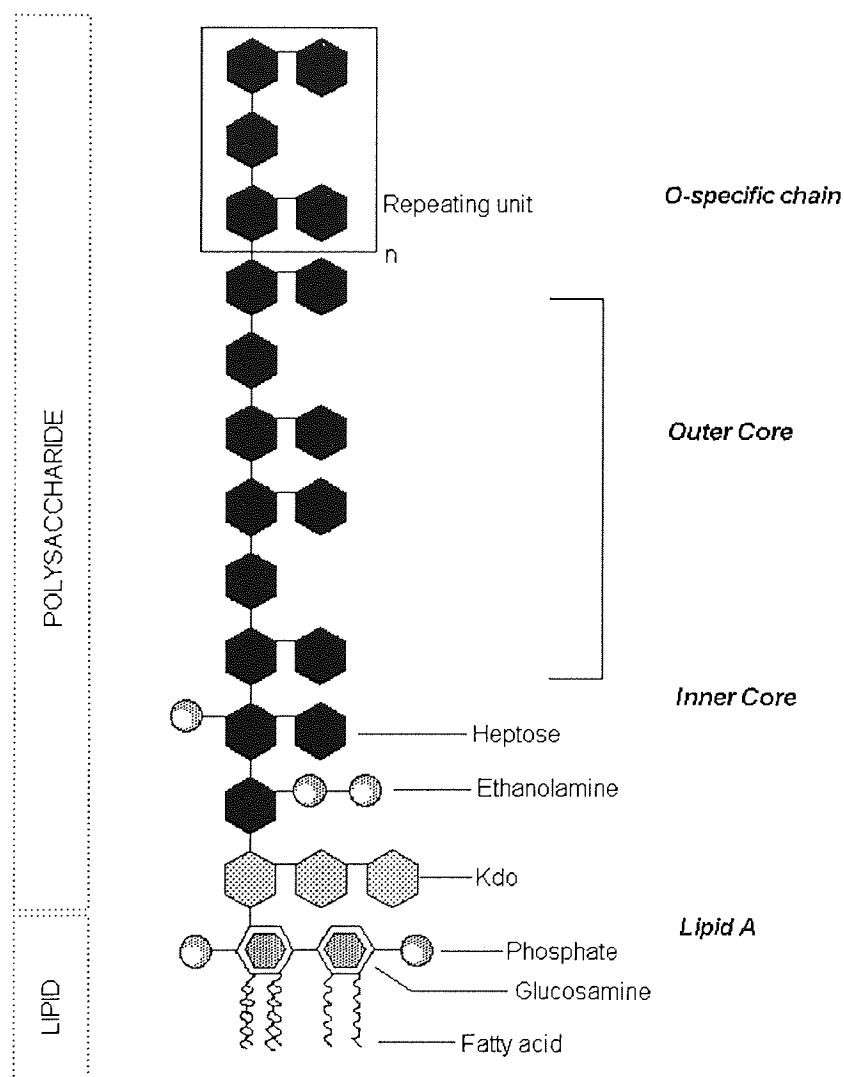


Figure 6.5. Schematic diagram of LPS illustrating main structural features. Adapted from Rietschel & Brade, (1992).



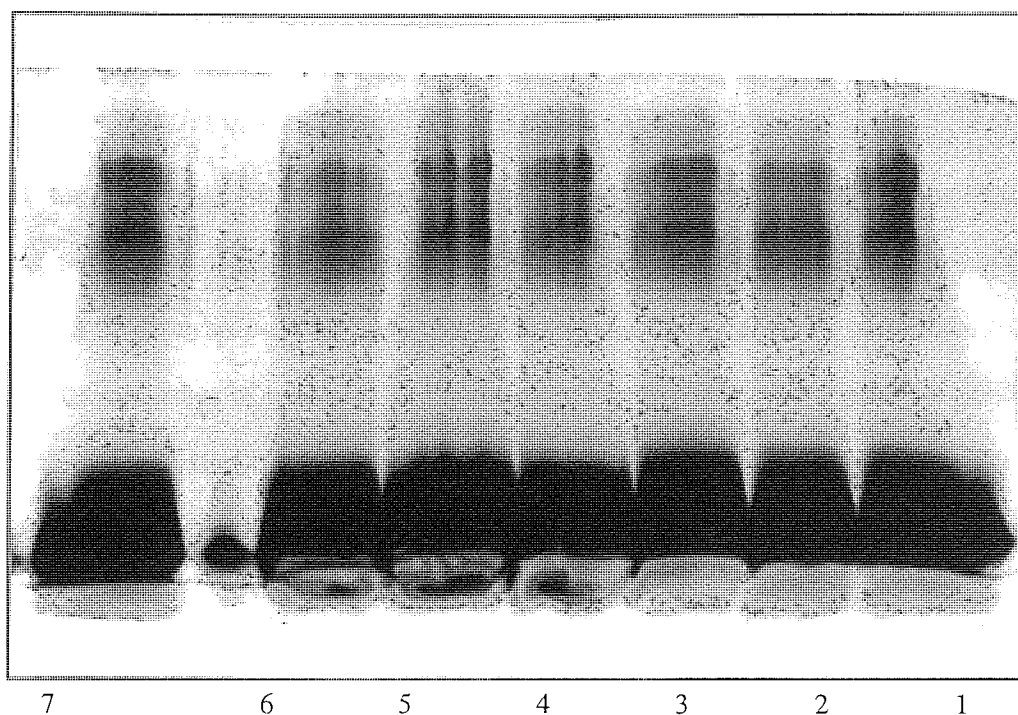


Figure 6.6. Structural distortion of LPS by PXB as visualised by SDS-PAGE. Concentrations of PXB used were 5000 (lane 1), 10000 (lane 2), 25000 (lane 3), 50000 (lane 4), 75000 (lane 5), 100000 (lane 6), 0 (lane 7), units/ml.

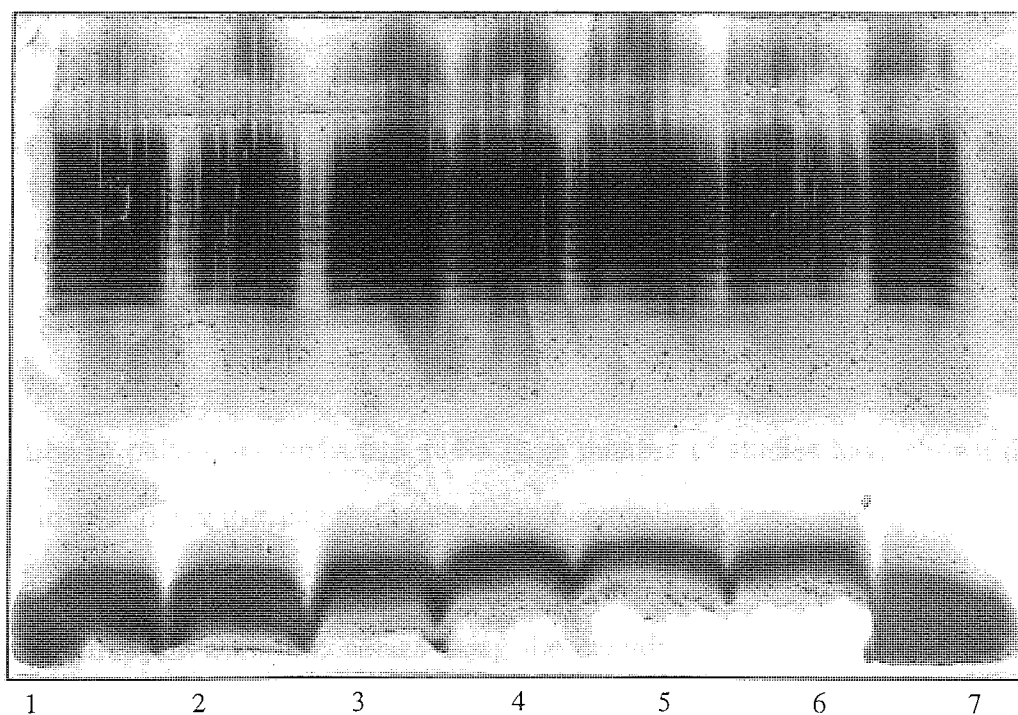


Figure 6.7. Structural distortion of LPS by PXB as visualised by immunoblotting. Concentrations of PXB used were 5000 (lane 1), 10000 (lane 2), 25000 (lane 3), 50000 (lane 4), 75000 (lane 5), 100000 (lane 6), 0 (lane 7), units/ml.

## 7.0 CONCLUDING REMARKS

Although the prospect of gene-therapy appears to have the potential to eliminate the underlying pathophysiological processes in CF, the present management of lung disease in these patients is of paramount importance. Efficient therapy against *P. aeruginosa* is difficult to achieve for a number of reasons. The antibiotics employed may not achieve sufficient lung penetration and resistance is a common problem. The biofilm mode of growth of *P. aeruginosa* often renders it refractory to treatment. As an alternative to aggressive parenteral treatment of infection episodes, prophylactic use of antibiotic aerosols has gained favour in many clinics. However, the inherent practical disadvantages of such an approach are considerable as the patient requires twice daily doses of nebulised antimicrobials. Also, aerosolised antibiotics are quickly absorbed across the pulmonary epithelium and therefore the target organisms are exposed to high concentrations of antibiotics for a limited period. In addition, the effects of long-term accumulation and systemic exposure to agents such as the polymyxins, remains unclear.

In an effort to overcome the difficulties in achieving effective aerosol treatment a drug-delivery approach was adopted. Liposomes, some thirty years since their discovery by Sir Alec Bangham, have now established themselves as a safe and therapeutically useful drug-carrier system. They appear particularly useful for pulmonary delivery given their similarity in composition to pulmonary surfactant and a large number of studies have shown them to be effective in prolonging the lung residence time of aerosolised agents.

PXB was entrapped within liposomes using the dehydration-rehydration vesicle technique. Although this molecule is potentially membrane-perturbing, successful entrapment, with encapsulation efficiencies similar to those of other antimicrobial agents, was achieved through the manipulation of vesicle phospholipid composition. As expected, PXB interacted strongly with anionic phospholipids to destabilise liposomal systems composed of such lipids.

Stable entrapment was achieved with neutral and cationic lipids. Characterisation of these vesicles showed that they possessed the typical size and morphology of DRVs. Zeta potential, DSC and gel adsorption studies indicated that a proportion of entrapped PXB was bilayer-associated. Release studies were conducted in physiologically relevant media and illustrated the role of bilayer composition in determining the efflux profile of PXB. Hydrophobic interaction chromatography was also used to assess surface hydrophilicity/hydrophobicity and the novel application of this technique produced results which were comparable with those reported in two-phase partitioning studies.

Intratracheal instillation in adult rats confirmed the advantages of liposomal PXB over non-entrapped drug. The lung residence time was significantly improved with all liposomal formulations compared to free drug, which was rapidly cleared from the lung. As a result, biodistribution of LPXB was altered relative to free PXB, an effect principally demonstrated by decreased kidney levels with liposomal formulations. Clinically, this may represent a significant advantage in long-term use. The role of phospholipid composition in determining the extent of pulmonary residence was not fully elucidated and the delivery of liposomes composed of unsaturated lipids (*e.g.* DSPC) may further improve lung kinetics and warrants further investigation.

The increased delivery of therapeutic agents to areas of inflammation by long-circulating liposomes, has been established in a number of studies and appears to have particular relevance to CF given the chronic state of lung inflammation. This preliminary study illustrated that a LPXB formulation with a typical 'stealth' composition prolonged the blood levels of PXB relative to free drug. Further studies using animal models of inflammation appear necessary to confirm the therapeutic utility of this route of delivery. Antimicrobial studies demonstrated that PXB retained activity after encapsulation and that the interaction between liposomes and bacterial cells was dependent upon vesicle surface properties. Further work is required to evaluate the *in vivo* antimicrobial efficacy of LPXB in suitable animal infection models.

## 8.0. REFERENCES

- Abra, R.M.**, Hunt, C.A., & Lau, D.T. (1984). Liposome deposition *in vivo* VI: Delivery to the lung. *Journal of Pharmaceutical Sciences*, 73(2): 203-206.
- Afione, S.A.**, Conrad, C.K., & Flotte, T.R. (1995). Gene therapy vectors as drug delivery systems. *Clinical Pharmacokinetics*, 28(3): 181-189.
- Agarwal, A.**, Kandpal, H., Gupta, H.P., Singh, N.P., & Gupta, C.M. (1994). Tuftsin-bearing liposomes as rifampin vehicles in treatment of tuberculosis in mice. *Antimicrobial Agents and Chemotherapy*, 38(3): 588-593.
- Ahmad, I.**, Perkins, W.R., Lupan, D.M., Selsted, M.E., & Janoff, A.S. (1995). Liposomal entrapment of the neutrophil-derived peptide indolicidin endows it with *in vivo* antifungal activity. *Biochimica et Biophysica Acta*, 1237: 109-114.
- Akhtar, S.**, & Juliano, R.L. (1992). Liposome delivery of antisense oligonucleotides: adsorption and efflux characteristics of phosphorothioate oligodeoxynucleotides. *Journal of Controlled Release*, 22: 47-56.
- Aliño, S.F.**, Garcia-Sanz, M., Irruarrizaga, A., Alfaro, J., & Hernandez, J. (1990). High encapsulation efficiencies in sized liposomes produced by extrusion of dehydration-rehydration vesicles. *Journal of Microencapsulation*, 7(4): 497-503.
- Allen, T.M.** (1994a). Long-circulating (sterically stabilized) liposomes for targeted drug delivery. *Trends in Pharmacological Sciences*, 15: 215-220.
- Allen, T.M.** (1994b). The use of glycolipids and hydrophilic polymers in avoiding rapid uptake of liposomes by the mononuclear phagocyte system. *Advanced Drug Delivery Reviews*, 13: 285-309.
- Allen, T.M.**, Austin, G.A., Chonn, A., Lin, L., & Lee, K.C. (1991). Uptake of liposomes by cultured mouse bone marrow macrophages: influence of liposome composition and size. *Biochimica et Biophysica Acta*, 1061: 56-64.
- Allen, T.M.**, & Hansen, C. (1991). Pharmacokinetics of stealth versus conventional liposomes: effect of dose. *Biochimica et Biophysica Acta*, 1068: 133-141.

**Allen, T.M., & Paphadjopoulos, D.** (1993). Sterically stabilized ('Stealth') liposomes: pharmacokinetic and therapeutic advantages. In G. Gregoriadis (Eds.), *Liposome Technology* (pp. 59-72). New York: CRC Press, Inc.

**Allen, T.M., & Cleland, L.G.** (1980). Serum-induced leakage of liposome contents. *Biochimica et Biophysica Acta*, 597: 418-426.

**Allen, T.M., Hansen, C., Martin, F., Redemann, C., & Yau-Young, A.** (1991). Liposomes containing synthetic lipid derivatives of poly(ethylene glycol) show prolonged circulation half-lives in vivo. *Biochimica et Biophysica Acta*, 1066: 29-36.

**Alpar, H.O., & Almeida, A.** (1994). Identification of some of the physico-chemical characteristics of microspheres which influence the induction of immune response following mucosal delivery. *European Journal of Pharmacy and Biopharmaceutics*, 40: 198-202.

**Alpar, H.O., Bason, A.M., Hickman, J.A., Richards, F.M., & Field, W.N.** (1990). Estimation by FACS of the delivery of liposome encapsulated macromolecules into myeloid cells. *International Journal of Pharmaceutics*, 62: 133-141.

**Alpar, H.O., Bamford, J.B., & Walters, V.** (1981). The *in vitro* incorporation and release of hydroxycobalamin from liposomes. *International Journal of Pharmaceutics*, 7: 349-351.

**Alpar, H.O., Xiao, Q.F., & Brown, M.R.W.** (1992). Antimicrobial activities of liposomal tobramycin against *P. aeruginosa*. In *XI International Cystic Fibrosis Congress*. Dublin, Ireland:

**Amselem, A., Gabizon, A., & Barenholz, Y.** (1990). Optimization and upscaling of doxorubicin-containing liposomes for clinical use. *Journal of Pharmaceutical Sciences*, 79(12): 1045-1052.

**Anderson, D.H.** (1938). Cystic fibrosis of the pancreas and its relation to celiac disease. *Am. J. Dis. Child.*, 56: 344-399.

**Anderson, N.P., & Welsh, M.J.** (1992). Regulation by ATP and ADP of CFTR chloride channels that contain mutant nucleotide-binding domains. *Science*, 257: 1701-1704.

**Anwar, H.**, Lambert, P.A., & Brown, M.R.W. (1983). Influence of SDS quality on the electrophoretic mobility of the outer membrane proteins of mucoid and non-mucoid *Pseudomonas aeruginosa*. *Biochimica et Biophysica Acta*, 761: 119-125.

**Aoki, H.**, Tani, T., Hanasawa, K., Endo, Y., Matsuda, K., Yoshioka, T., Numa, K., Araki, H.*et al.* (1992). Treatment of septic shock by extracorporeal elimination of endotoxin using fiber-immobilized polymyxin B. *Artificial Organs*, 16(6): 636.

**App, E.M.**, King, M., Helfesreider, R., Kohler, D., & Matthys, H. (1990). Acute and long-term amiloride inhalation in cystic fibrosis lung disease. *American review of Respiratory Disease*, 141: 605-612.

**Applemelk, B.J.**, Verweij-Van Vught, A.M.J.J., Maaskant, J.J., Schouten, W.F., Thijs, L.G., & Maclaren, O.M. (1988). Comparison of monoclonal antibodies to the deeper core region of gram negative lipopolysaccharide by means of polymyxin B inhibition studies. *Microbial Pathogenesis*, 6: 297-301.

**Aramaki, Y.**, & Tsuchiya, S. (1989). Interactions between aminoglycosides and phospholipids using liposomes: A possible mechanism of nephrotoxicity. *Pharmaceutical Research*, 6(5).

**Arrowsmith, M.**, Hadgraft, J., & Kellaway, I.W. (1983). The *in vitro* release of steroids from liposomes. *International Journal of Pharmaceutics*, 14: 209-221.

**Assil, K.K.**, Frucht-Perry, J., Ziegler, E., Schanzlin, D.J., Schneiderman, T., & Weinreb, R.N. (1991). Tobramycin liposomes: single subconjunctival therapy of pseudomonal keratitis. *Investigative Ophthalmology and Visual Science*, 32(13): 3216-3220.

**Auerbach, H.S.**, Williams, M., Kirkpatrick, J.A., & Colten, H.R. (1985). Alternate-day prednisolone reduces morbidity and improves pulmonary function in cystic fibrosis. *The Lancet*, 28: 686-688.

**Babin, Y.**, D'Amour, J., Pigeon, M., & Pezolet, M. (1987). A study of the structure of polymyxin B-dipalmitoylphosphatidylglycerol complexes by vibrational spectroscopy. *Biochimica et Biophysica Acta*, 903: 78-88.

- Babin, Y., & Pezolet, M.** (1988). Extraction of phosphatidylglycerol from mixed bilayers of phosphatidylcholine and phosphatidylglycerol by polymyxin B. *Biophysical Journal*, 53: 316a.
- Bakker-Woudenberg, I.A.J.M.** (1995). Liposomes in the treatment of parasitic, viral, fungal and bacterial infections. *Journal of Liposome Research*, 5(1): 169-191.
- Bakker-Woudenberg, I.A.J.M., Lokerse, A.F., ten Kate, M.T., Mouton, J.W., Woodle, M.C., & Storm, G.** (1993). Liposomes with prolonged blood circulation and selective localization in *Klebsiella pneumoniae*-infected lung tissue. *The Journal of Infectious Diseases*, 168: 164-171.
- Bakker-Woudenberg, I.A.J.M., Lokerse, A.F., ten Kate, M.T., & Storm, G.** (1992). Enhanced localization of liposomes with prolonged blood circulation time in infected lung tissue. *Biochimica et Biophysica Acta*, 1138: 318-326.
- Bakker-Woudenberg, I.A.J.M., Lokerse, A.F., Roerdink, F.H., & Michel, M.F.** (1985). Free versus liposome entrapped ampicillin in treatment of infection due to *Listeria monocytogenes* in normal and athymic nude mice. *The Journal of Infectious Diseases*, 151: 917-924.
- Bakker-Woudenberg, I.A.J.M., & Lokerse, A.F.** (1991). Liposomes and lipid carriers in the treatment of microbial infections. *Scandinavian Journal of Infectious Diseases*, 74(suppl): 34-41.
- Baltimore, R.S., & Mitchell, M.** (1980). Immunologic investigations of mucoid strains of *Pseudomonas aeruginosa*: comparison of susceptibility to opsonic antibody in mucoid and non-mucoid strains. *The Journal of Infectious Diseases*, 141: 238-247.
- Bangham, A.D., Standish, M.M., & Watkins, J.C.** (1965). Diffusion of univalent ions across the lamellae of swollen phospholipids. *Journal of Molecular Biology*, 13: 238-252.
- Bangham, A.D.** (1993). Liposomes: the Babraham connection. *Chemistry and Physics of Lipids*, 64: 275-285.
- Bangham, A.D., Standish, M.M., & Watkins, J.C.** (1965). Diffusion of univalent ions across the lamellae of swollen phospholipids. *Journal of Molecular Biology*, 13: 238-252.

**Barenholz, Y., & Amselem, S.** (1993). Quality control assays in the development and clinical use of liposome-based formulations. In G. Gregoriadis (Eds.), *Liposome Technology* (pp. 527-616). Boca Raton, Florida: CRC Press, Inc.

**Bartlett, G.R.** (1959). Phosphorus assay in column chromatography. *Journal of Biological Chemistry*, 234: 466-468.

**Bear, C.E., Li, C., Kartner, N., et al,** (1992). Purification and functional reconstitution of the cystic fibrosis transmembrane conductance regulator (CFTR). *Cell*(68): 809-818.

**Belchetz, P.E., Braidman, I.P., Crawley, J.C.W., & Gregoriadis, G.** (1977). Treatment of Gaucher's disease with liposome-entrapped glucocerebroside: B-glucosidase. *Lancet*(ii): 116-117.

**Bennett, D.B., Tyson, E., Mah, S., de Groot, J.S., Hegde, S.G., Terao, S., & Teitelbaum, Z.** (1994a). Sustained delivery of detirelix after pulmonary administration of liposomal formulations. *Journal of Controlled Release*, 32: 27-35.

**Bennett, D.B., Tyson, E., Nerenberg, C.A., Mah, S., de Groot, J.S., & Teitelbaum, Z.** (1994b). Pulmonary delivery of detirelix by intratracheal instillation and aerosol inhalation in the briefly anaesthetized dog. *Pharmaceutical Research*, 11(7): 1048-1055.

**Bensch, K.G., & Dominguez, E.A.M.** (1971). Studies on the pulmonary air-tissue barrier. Part IV: Cytochemical tracing of macromolecules during absorption. *Yale Journal of Biological Medicine*, 43: 236-241.

**Bergers, J.J., ten Hagen, T.L.M., van Etten, E.W.M., & Bakker-Woudenberg, I.A.J.M.** (1995). Liposomes as delivery systems in the treatment and prevention of infectious diseases. *Pharmacy World and Science*, 17(1): 1-11.

**Bermudez, L.E.M., Wu, M., & Young, L.S.** (1987). Intracellular killing of *Mycobacterium avium* complex by rifapentine and liposome-encapsulated amikacin. *Journal of Infectious Diseases*, 156(3): 510-513.

**Betageri, G.V.** (1993). Liposomal encapsulation and stability of dideoxyinosine triphosphate. *Drug Development and Industrial Pharmacy*, 19(5): 531-539.



- Betageri, G.V., & Parsons, D.L.** (1992). Drug encapsulation and release from multilamellar and unilamellar vesicles. *International Journal of Pharmaceutics*, 81: 235-241.
- Beurer, G., Warncke, F., & Galla, H.J.** (1988). Interaction of polymyxin B<sub>1</sub> and polymyxin B<sub>1</sub> nonapeptide with phosphatidic acid monolayer and bilayer membranes. *Chemistry and Physics of Lipids*, 47: 155-163.
- Blume, G., & Cevc, G.** (1993). Molecular mechanism of the lipid vesicle longevity in vivo. *Biochimica et Biophysica Acta*, 1146: 157-168.
- Bonté, F., & Juliano, R.L.** (1986). Interactions of liposomes with serum proteins. *Chemistry and Physics of Lipids*, 40: 359-372.
- Bonté, F., Hsu, M.J., Papp, A., Wu, K., Regen, S.L., & Juliano, R.L.** (1987). Interactions of polymerizable phosphatidylcholine vesicles with blood components: relevance to biocompatibility. *Biochimica et Biophysica Acta*, 900: 1-9.
- Boucher, R.C., & Beall, R.J.** (1989). Summary of drug needs in cystic fibrosis. *Pharmaceutical Research*, 6(6): 525-526.
- Brandl, M.M., Bachmann, D., Drechsler, M., & Bauer, K.H.** (1993). Liposome preparations using high-pressure homogenizers. In G. Gregoriadis (Eds.), *Liposome Technology* (pp. 49-65). New York: CRC Press, Inc.
- Brown, M.R.W., Anwar, H., & Lambert, P.A.** (1984). Evidence that mucoid *P. aeruginosa* in the cystic fibrosis lung grows under iron-restricted conditions. *FEMS Microbiology Letters*, 21: 113-117.
- Brown, M.R.W., Fenton, F.M., & Watkins, W.M.** (1972). Tetracycline-sensitive/polymyxin-resistant *P. aeruginosa*. *The Lancet*, 2: 86.
- Brown Jr., R.A., & Schanker, L.S.** (1983). Absorption of aerosolized drugs from the rat lung. *Drug Metabolism and Disposition*, 11(4): 355-360.
- Brown, R.B., Philips, D., Barker, M.J., Pieczarka, R., Sands, M., & Tees, D.** (1989). Outbreak of nosocomial *Flavobacterium meningosepticum* respiratory infections associated with the use of aerosolised polymyxin B. *American Journal of Infection Control*, 3: 121-125.

- Brownlee, G.**, Bushby, S.R.M., & Short, E. (1952). The chemotherapy and pharmacology of the polymyxins. *British Journal of Pharmacology*, 7: 170-188.
- Buiting, A.M.J.**, van Roojen, N., & Claassen, E. (1992). Liposomes as antigen carriers and adjuvants *in vivo*. *Immunologica Research*, 143(5): 541-548.
- Burton, J.A.**, & Schanker, L.S. (1974). Absorption of antibiotics from the rat lung. *Proceedings of the society for experimental biology and medicine*, 145: 752-756.
- Cajal, Y.**, Alsina, M.A., Busquets, M.A., Cabanes, A., Reig, F., & Garcia-Anton, J.M. (1992). Gentamicin encapsulation in liposomes: factors affecting the efficiency. *Journal of Liposome Research*, 2(1): 11-22.
- Caplen, N.J.**, Alton, E.W.F.M., Middleton, P.G., Dorin, J.R., Stevenson, B.J., Gao, X., Durham, S.R., Jeffery, P.K.*et al.* (1995). Liposome-mediated CFTR gene transfer to the nasal epithelium of patients with cystic fibrosis. *Nature Medicine*, 1(1): 39-46.
- Cerny, F.J.**, Cropp, G.J., & Bye, M.R. (1984). Hospital therapy improves exercise tolerance and lung function in cystic fibrosis. *American Journal of Diseases of Children*, 138: 261-265.
- Cevc, G.** (1993a). Electrostatic characterization of liposomes. *Chemistry and Physics of Lipids*, 64: 163-186.
- Cevc, G.** (1993b). Lipid properties as a basis for membrane modeling and rational liposome design. In G. Gregoriadis (Eds.), *Liposome Technology* (pp. 1-35). Boca Raton, Florida: CRC Press.
- Cevc, G.** (1993c). Novel, ultradeformable lipid vesicles, transferosomes, and their potential as drug carriers. In *Liposomes in drug delivery: the nineties and beyond*, (pp. 20). London
- Chang, H.-C.**, & Flanagan, D.R. (1994). Liposomal entrapment of suramin. *Journal of Pharmaceutical Sciences*, 83(7): 1043-1046.
- Cohen, B.E.** (1975). The permeability of liposomes to non-electrolytes. *Journal of Membrane Biology*, 20: 205-234.

**Cohen, L.F.**, Di Sant' Agnese, P.A., & Friedlander, J. (1980). Cystic fibrosis and pregnancy: a national study. *Lancet*, II: 842-844.

**Colomé, C.**, Alsina, M.A., Busquets, M.A., Haro, I., & Reig, F. (1993). Interaction of aminoglycosides and colistin with model membranes: liposomes and monolayers. *International Journal of Pharmaceutics*, 90: 59-71.

**Crystal, R.** (1994). Results of the first clinical trials. In *19th European Cystic Fibrosis Conference*, (Abstract L1). Paris.

**Cuthbert, A.** (1994). Cystic fibrosis gene update. *Journal of the Royal Society of Medicine*, 87(S21): 2-4.

**Cuthbert, A.W.** (1991). Abnormalities of airway epithelial function and the implications of the discovery of the cystic fibrosis gene. *Thorax*, 46: 124-130.

**Daleke, D.L.**, Hong, K., & Papahadjopoulos, D. (1990). Endocytosis of liposomes by macrophages: binding, acidification and leakage of liposomes monitored by a new fluorescence assay. *Biochimica et Biophysica Acta*, 1024: 352-366.

**Danner, R.L.**, Joiner, K.A., Rubin, M., Patterson, W.H., Johnson, N., Ayers, K.M., & Parrillo, J.E. (1989). Purification, toxicity, and antiendotoxin activity of polymyxin B nonapeptide. *Antimicrobial Agents and Chemotherapy*, 33(9): 1428-1434.

**David, S.A.**, Balasubramanian, K.A., Mathan, V.I., & Balaram, P. (1992). Analysis of the binding of polymyxin B to endotoxic lipid A and core glycolipid using a fluorescent displacement probe. *Biochimica et Biophysica Acta*, 1165: 147-152.

**Davis, P.B.**, Silski, C.L., & Liedtke, C.M. (1992). Amiloride antagonises beta-adrenergic stimulation of cAMP synthesis and Cl secretion in human tracheal epithelial cells. *American Journal of Respiratory Cell Molecular Biology*, 6: 140-145.

**Day, A.J.**, Williams, J., McKeown, C., Bruton, A., & Weller, P.H. (1988). Evaluation of inhaled colomycin in children with cystic fibrosis (C.F.). In *10th International Cystic Fibrosis Congress*, . Sydney, Australia:

**de Marie, S., Janknegt, R., & Bakker-Woudenberg, I.A.J.M.** (1994). Clinical use of liposomal and lipid-complexed amphotericin B. *Journal of Antimicrobial Chemotherapy*, 33: 907-916.

**Debs, R.J., Straubinger, R.M., Brunette, E.N., Lin, J.M., Lin, E.J., Montgomery, B., Friend, D.S., & Papahadjopoulos, D.P.** (1987). Selective enhancement of pentamidine uptake in the lung by aerosolisation and delivery of liposomes. *American review of respiratory disease*, 135: 731-737.

**Demaeyer, P., Akodad, E.M., Gravet, E., Schietecat, P., Van Vooren, J.P., Drowart, A., Yernault, J.C., & Legros, F.J.** (1993). Disposition of liposomal gentamicin following intrabronchial administration in rabbits. *Journal of Microencapsulation*, 10(1): 77-88.

**Desiderio, J.V., & Campbell, S.G.** (1983). Intraphagocytic killing of *Salmonella typhimurium* by liposome-encapsulated cephalothin. *The Journal of Infectious Diseases*, 148: 563-570.

**Di Sant' Agnese, P.A., Darling, R.C., Pevera, G.A., & Shea, G.** (1953). Abnormal electrolyte composition of sweat in cystic fibrosis of the pancreas, its clinical significance and relationship to the disease. *Pediatrics*, 12: 549-563.

**Dickie, K.J., & De Groot, W.J.** (1973). Ventilatory effects of aerosolised kanamycin and polymyxin. *Chest*, 63: 694-697.

**Döring, G., Goldstein, W., Roll, A., Schiotz, P.O., Hoiby, N., & Botzenhart, K.** (1985). Role of *Pseudomonas aeruginosa* exoenzymes in lung infections of patients with cystic fibrosis. *Infection and Immunity*, 49(3): 557-562.

**Dowling, R.D., Zenati, M., Burckart, G.J., Yousem, S.A., Schaper, M., Simmons, R.L., Hardesty, R.L., & Griffith, B.P.** (1990). Aerosolized cyclosporine as single-agent immunotherapy in canine lung allografts. *Surgery*, 108: 198-205.

**Drusano, G.** (1988). Role of pharmacokinetics in the outcome of infections. *Antimicrobial Agents and Chemotherapy*, 32: 289-297.

**Düzgünes, N., Perumal, V.K., Kesavalu, L., Goldstein, J.A., Debs, R.J., & Gangadharum, P.R.J.** (1988). Enhanced effect of liposome encapsulated amikacin on *Mycobacterium avium*

and *Mycobacterium intracellulare* complex infection in beige mice. *Antimicrobial Agents and Chemotherapy*, 32: 1404-1411.

**Eibl, H.** (1981). Phospholipid synthesis. In C. G. Knight (Eds.), *Liposomes: from physical structure to therapeutic applications* (pp. 19-50). Elsevier.

**Eickhoff, T.C., & Finland, M.** (1965). Polymyxin B and colistin: *in vitro* activity against *P. aeruginosa*. *American Journal of Medical Science*, 249: 172-174.

**El Mashak, E.M., & Tocanne, J.F.** (1980). Polymyxin B-Phosphatidylglycerol interactions: A monolayer study. *Biochimica et Biophysica Acta*, 596: 165-179.

**Elborn, J.S. & Shale, D.J.** (1990). Lung injury in cystic fibrosis. *Thorax*, 45: 970-973.

**Elorza, B., Elorza, M.A., Frutos, G., & Chantres, J.R.** (1993). Characterization of 5-fluorouracil loaded liposomes prepared by reverse-phase evaporation or freeze-thawing extrusion methods: study of drug release. .

**Elorza, B., Elorza, M.A., Sainz, M.C., & Chantres, J.R.** (1993). Comparison of particle size and encapsulation parameters of three liposomal preparations. *Journal of Microencapsulation*, 10(2): 237-248.

**Elverdam, I., Larsen, P., & Lund, E.** (1981). Isolation and characterization of three new polymyxins B and E by high performance liquid chromatography. *Journal of Chromatography*, 218: 653-661.

**Endo, S., Inada, K., Kikuchi, M., Yamada, Y., Takakuwa, T., Nakae, H., Inoue, Y., Kasai, T. et al.** (1994). Clinical effects of intramuscular administration of a small dose of polymyxin to patients with endotoxaemia. *Research Communications in Chemical Pathology and Pharmacology*, 83(2): 223-235.

**Enna, S.J., & Schanker, L.S.** (1972). Absorption of saccharides and urea from the rat lung. *American Journal of Physiology*, 222(2): 409-414.

**Eriksson, E.** (1981). Hydrophobic affinity partition of liposomes in aqueous two-phase systems. *Journal of Chromatography*, 205(189-193).

**Eriksson, E., & Albertsson, P.** (1978). The effect of the lipid composition on the partition of liposomes in aqueous two-phase systems. *Biochimica et Biophysica Acta*, 507: 425-432.

**Fick, R.B.** (1989). Pathogenesis of the pseudomonas lung lesion in cystic fibrosis. *Chest*, 96: 158-164.

**Fiel, S.B.** (1993). Clinical management of pulmonary disease in cystic fibrosis. *The Lancet*, 341: 1070-1074.

**Fielding, R.M., & Abra, R.M.** (1992). Factors affecting the release rate of terbutaline from liposome formulations after intratracheal instillation in the guinea pig. *Pharmaceutical Research*, 9(2): 220-223.

**Fielding, R.M.** (1991). Liposomal drug delivery: advantages and limitations from a clinical pharmacokinetic and therapeutic perspective. *Clinical Pharmacokinetics*, 21: 155-164.

**Fifield, F.W., & Kealey, D.** (1983). *Principles and practice of analytical chemistry* (2nd ed.). London: International textbook company limited.

**Fildes, F.J.T., & Oliver, J.E.** (1978). Interaction of cortisol-21-palmitate with liposomes examined by differential scanning calorimetry. *Journal of Pharmacy and Pharmacology*, 30: 337-342.

**Fishman, P., Peyman, G.A., Hendricks, R., & Hui, S.L.** (1989). Liposome-encapsulated 3H-5-FU in rabbits. *International Ophthalmology*, 13: 361-365.

**Folkesson, H.G., Weström, B.R., & Karlsson, B.W.** (1990). Permeability of the respiratory tract to different-sized macromolecules after intratracheal instillation in young and adult rats. *Acta Physiologica Scandinavica*, 139: 347-354.

**Fomsgaard, A., Freudenberg, M.A., & Galanos, C.** (1990). Modification of the silver staining technique to detect lipopolysaccharide in polyacrylamide gels. *Journal of Clinical Microbiology*, 28(12): 2627-2631.

**Forsen, E.A.** (1988). Chemotherapy with anthracycline-loaded liposomes. In G. Gregoriadis (Eds.), *Liposomes as drug carriers Recent trends and progress* (pp. 355-364). Chichester: John Wiley & Sons.

**Frezard, F., Santaella, C., Montisci, M.J., Vierling, P., & Riess, J.G.** (1994). Fluorinated phosphatidylcholine-based liposomes: H<sup>+</sup>/Na<sup>+</sup> permeability, active doxorubicin encapsulation and stability in human serum. *Biochimica et Biophysica Acta*, 1194: 61-68.

**Gabizon, A., & Papahadjopoulos, D.** (1992). The role of surface charge and hydrophilic groups on liposome clearance in vivo. *Biochimica et Biophysica Acta*, 1103: 94-100.

**Gangadharam, P.R.J., Ashtekar, D.A., Ghori, N., Goldstein, J.A., Debs, R.J., & Duzgunes, N.** (1991). Chemotherapeutic potential of free and liposome encapsulated streptomycin against experimental *Mycobacterium avium* complex infections in beige mice. *Journal of Antimicrobial Chemotherapy*, 28: 425-435.

**Gay, B., Cardot, J.-M., Schnell, C., van Hoogevest, P., & Gygax, D.** (1993). Comparative pharmacokinetics of free muramyl tripeptide phosphatidyl ethanolamine (MTP-PE) and liposomal MTP-PE. *Journal of Pharmaceutical Sciences*, 82(10): 997-1001.

**Geddes, M.** (1988). Antimicrobial therapy against *Staphylococcal aureus*, *P. aeruginosa* and *P. cepacia*. *Chest*, 94(2): 140S-143S.

**Gil, J.** (1983). Number and distribution of plasmalemmal vesicles in the lung. *Federation Proceedings*, 42: 2414-2418.

**Gilbert, B.E., Wyde, P.R., & Wilson, S.Z.** (1992). Aerosolized liposomal amphotericin B for treatment of pulmonary and systemic *Cryptococcus neoformans* infections in mice. *Antimicrobial Agents and Chemotherapy*, 36(7): 1466-1471.

**Ginsberg, R.S., Mitlenes, G.M., Lenk, R.P., Jedrusiak, J., Savage, K., & Swenson, C.E.** (1989). The impact of liposome encapsulation of gentamicin on the treatment of extracellular gram negative bacterial infections. In Lopez-Berestein & Fidler (Eds.), *Liposomes in the therapy of infectious diseases and cancer* (pp. 205-214). New York: Alan R. Liss Inc.

**Gonzalez-Rothi, R.J., Straub, L., Cacace, J.L., & Schreier, H.** (1991). Liposomes and pulmonary alveolar macrophages: functional and morphologic interactions. *Experimental Lung Research*, 17: 687-705.

**Govan, J.R.W.** (1988). Alginate biosynthesis and other unusual characteristics associated with pathogenesis of *P. aeruginosa* in cystic fibrosis. In W. Donachie, E. Griffiths, & J. Stephen (Eds.), *Bacterial infections of respiratory and gastrointestinal mucosae* (pp. 67-96). Oxford: IRL Press.

**Govan, J.R.W., & Glass, S.** (1990). The microbiology and therapy of cystic fibrosis lung infections. *Reviews in Medical Microbiology*, 1: 19-28.

**Graham, A.,** Hasani, A., Alton, E.W.F.W., Martin, G.P., Mariott, C., Hodson, M.E., & Clarke, S.W.G. (1993). No added benefit from nebulised amiloride in patients with cystic fibrosis. *European Respiratory Journal*, 6(9): 1243-1248.

**Greco, M.,** Fox, J.D., Riley, D.J., & Poiani, G.J. (1994). Biodistribution of poly(ethylene glycol)-conjugated liposomes following intratracheal instillation in rats. In *Liposome Research Days Conference. Liposomes: the next generation*, (C15). Vancouver, Canada.

**Green, S.T.,** Nathwani, D., Gourlay, Y., McMearium, J., Goldberg, D.J., & Kennedy, D.H. (1992). Nebulised colistin for AIDS-associated *P. aeruginosa* pneumonia. *International Journal of STD and AIDS*, 3: 130-131.

**Gregoriadis, G. & Florence, A.T.** (1993a). Efficient entrapment of solutes on microfluidized small dehydration-rehydration liposomes. In G. Gregoriadis (Eds.), *Liposome Technology* (pp. 37-48). New York: CRC Press, Inc.

**Gregoriadis, G.** (1993). Liposomes, a tale of drug targeting. *Journal of Drug Targeting*, 1: 3-6.

**Gregoriadis, G.** (1988). Fate of injected liposomes: observations on entrapped solute retention, vesicle clearance and tissue distribution *in vivo*. In G. Gregoriadis (Eds.), *Liposomes as drug carriers recent trends and progress* (pp. 3-18). Chichester: John Wiley & Sons.

**Gregoriadis, G.** (1990). Immunological adjuvants: a role for liposomes. *Immunology Today*, 11(3): 89-97.

**Gregoriadis, G.** (1994). Liposomes and anti-ageing creams: the facts beneath the face. *The Biochemist*, Feb/Mar.

**Gregoriadis, G., & Allison, A.C.** (1974). Entrapment of proteins in liposomes prevents allergic reactions in pre-immunised mice. *FEBS Letters*, 45: 71-74.

**Gregoriadis, G., & Florence, A.T.** (1993b). Liposomes in drug delivery Clinical, Diagnostic and Ophthalmic potential. *Drugs*, 45(1): 15-28.



- Gregoriadis, G., & Ryman, B.** (1972). Lysosomal localisation of B-fructofuranosidase-containing liposomes injected into rats. Some implications in the treatment of genetic disorders. *Biochemical and Biophysical Research Communications*, 129: 123-133.
- Gregoriadis, G., McCormack, B., Wang, Z., & Lively, R.** (1993). Polysialic acids: potential in drug delivery. *FEBS Letters*, 315(3): 271-276.
- Gross, E., & Ehrenberg, B.** (1989). The partition and distribution of porphyrins in liposomal membranes. A spectroscopic study. *Biochimica et Biophysica Acta*, 983: 118-122.
- Gruner, S.M., Lenk, R.P., Janoff, A.S., & Ostro, M.J.** (1985). Novel multilayered vesicles: comparison of physical characteristics of multilamellar liposomes and stable plurilamellar vesicles. *Biochemistry*, 24: 2833-2842.
- Gupta, P.K.** (1990). Drug targeting in cancer chemotherapy: a clinical perspective. *Journal of Pharmaceutical Sciences*, 79(11): 949-962.
- Gupta, R., & Jentoft, N.** (1992). The structure of tracheobronchial mucins from cystic fibrosis and control patients. *Journal of Biological Chemistry*, 267: 3160-3167.
- Halliday, N.P.** (1967). *Clinical Trials journal*, 4: 771.
- Hartmann, W., Galla, H.J., & Sackmann, E.** (1978). Polymyxin binding to charged lipid membranes: an example of co-operative lipid-protein interaction. *Biochimica et Biophysica Acta*, 510: 124-139.
- Hernandez-Borrell, J., Pons, M., Juarez, J.C., & Estelrich, J.** (1990). The action of Triton X-100 and sodium dodecyl sulphate on lipid layers. Effect on monolayers and liposomes. *Journal of Microencapsulation*, 7(2): 255-259.
- Higgins, C.F., & Trezise, E.** (1992). Cystic fibrosis mice have arrived. *Human Molecular Genetics*, 1: 459-460.
- Higuchi, T.** (1961). Rates of release of medicaments from ointment bases containing drugs in suspension. *Journal of Pharmaceutical Sciences*, 50: 874-875.
- Hjertén, S.** (1973). Some general aspects of hydrophobic interaction chromatography. *Journal of Chromatography*, 87: 325-331.

- Hodson, M.E.**, Penketh, A.R.L., & Batten, J.C. (1981). Aerosol carbenicillin and gentamicin treatment of *P. aeruginosa* infections in patients with cystic fibrosis. *The Lancet*, Nov 21: 1137-1139.
- Høiby, N.** (1991). Early and repeated treatment of pseudomonas infection. In S. P. Conway & J. M. Littlewood (Ed.), *One day symposium update in the management of cystic fibrosis*. Wakefield, UK:
- Høiby, N.**, & Koch, C. (1990). Cystic fibrosis: *Pseudomonas aeruginosa* infection in cystic fibrosis and its management. *Thorax*, 45: 881-884.
- Høiby, N.**, Fris, B., Jensen, K., Koch, C., Moller, N.E., Storing, S., & Szaff, M. (1982). Antimicrobial chemotherapy in cystic fibrosis patients. *Acta Paediatrica Scandinavia*, 301(suppl.): 75-100.
- Holder, I.A.** (1988). Pseudomonas immunotherapy. *Serodiagnosis and Immunotherapy*, 2: 7-16.
- Hope, M.J.**, Nayar, R., Mayer, L.D., & Cullis, P.R. (1993). Reduction of liposome size and preparation of unilamellar vesicles by extrusion techniques. In G. Gregoriadis (Eds.), *Liposome Technology* (pp. 123-139). CRC Press, Inc.
- Hsuchen, C.-C.**, & Feingold, D.S. (1973). The mechanism of polymyxin B action and selectivity toward biologic membranes. *Biochemistry*, 12(11): 2105-2111.
- Hubbard, R.C.**, McElvaney, N.F., Birrer, P., & al., e. (1992). A preliminary study of aerosolised recombinant human deoxyribose in the sputum of cystic fibrosis. *The New England Journal of Medicine*, 326: 812-815.
- Hunt, C.A.** (1982). Liposomes disposition in vivo V. Liposome stability in plasma and implications for drug carrier function. *Biochimica et Biophysica Acta*, 719: 450-463.
- Illum, L.**, Hunneyball, I.M., & Davis, S.S. (1986). The effect of hydrophilic coatings on the uptake of colloidal particles by the liver and peritoneal macrophages. *International Journal of Pharmaceutics*, 29: 53-65.
- Imai, M.**, Inoue, K., & Nojima, S. (1975). Effect of polymyxin B on liposomal membranes derived from *Escherichia coli* lipids. *Biochimica et Biophysica Acta*, 375: 130-137.

- Inoue, K.** (1974). Permeability properties of liposomes prepared from dipalmitoyllecithin, dimyristoyllecithin, egg lecthin, rat liver lecthin and beef brain sphingomyelin. *Biochimica et Biophysica Acta*, 339: 390-402.
- Isele, U., van Hoogevest, P., Hilfiker, R., Capraro, H.-G., Schieweck, K., & Leuenberger, H.** (1994). Large-scale production of liposomes containing monomeric phthalocyanine by controlled dilution of organic solvents. *Journal of Pharmaceutical Sciences*, 83(11): 1608-1616.
- Janoff, A.S., Minchey, S.R., Perkins, W.R., Boni, L.T., Seltzer, S.T., Adams, D.F., & Blau, M.** (1991). Interdigitation-fusion vesicles: a new approach for selective opacification of the RES. *Investigational Radiology*(26): S167-S168.
- Jensen, T., Pederson, S.S., Garne, S., Heilamn, C., Hoiby, N., & Koch, C.** (1987). Colistin inhalation therapy in cystic fibrosis patients with chronic *Pseudomonas aeruginosa* lung infection. *Journal of Antimicrobial Chemotherapy*, 19: 831-838.
- Jones, M.N., & Nicholas, A.R.** (1991). The effect of blood serum on the size and stability of phospholipid liposomes. *Biochimica et Biophysica Acta*, 1065: 145-152.
- Jones, M.N., Kaszuba, M., Reboiras, M.D., Lyle, I.G., Hill, K.J., Song, Y.-H., Wilmot, S.W., & Creeth, J.E.** (1994). The targeting of phospholipid liposomes to bacteria. *Biochimica et Biophysica Acta*, 1196: 57-64.
- Jones, N.C., & Osborn, M.J.** (1977). Interaction of *Salmonella typhimurium* with phospholipid vesicles. Incorporation of exogenous lipids into intact cells. *Journal of Biological Chemistry*, 252: 7398-7404.
- Jones, M.N.** (1994). Carbohydrate-mediated liposomal targeting and drug delivery. *Advanced Drug Delivery Reviews*, 13: 215-250.
- Joris, J.M. & van Saene, H.K.F.** (1985). Influence of faeces on the activity of antimicrobial agents used for decontamination of the alimentary canal. *Scandinavian Journal of Infectious Diseases*, 17: 295-300.
- Juliano, R.L., & Stamp, D.** (1975). The effect of particle size and charge on the clearance rates of liposomes and liposome encapsulated drugs. *Biochemical and Biophysical Research Communications*, 63(3): 651-658.

- Jurima-Romet, M.,** Barber, R.F., Demeester, J., & Shek, P.N. (1990). Distribution studies of liposome-encapsulated glutathione administered to the lung. *International Journal of Pharmaceutics*, 63: 227-235.
- Jurima-Romet, M.,** Barber, R.F., & Shek, P.N. (1992). Liposomes and bronchoalveolar lavage fluid: release of vesicle-entrapped glutathione. *International Journal of Pharmaceutics*, 88: 201-210.
- Jurima-Romet, M.,** & Shek, P.N. (1991). Lung uptake of liposome-entrapped glutathione after intratracheal administration. *Journal of Pharmacy and Pharmacology*, 43: 6-10.
- Karlik, S.,** Florio, E., & Grant, C.W. (1991). Comparative evaluation of two membrane-based liposomal MRI contrast agents. *Magnetic Resonance in Medicine*, 19: 56-66.
- Karlowsky, J.A.,** & Zhanel, G.G. (1992). Concepts on the use of liposomal antimicrobial agents: applications for aminoglycosides. *Clinical Infectious Diseases*, 15: 654-667.
- Kayes, J.B.** (1988). Disperse systems. In M. E. Aulton (Eds.), *Pharmaceutics-The science of dosage form design* (pp. 81-118). London: Churchill Livingstone.
- Kedar, E.,** Rutkowski, Y., Braun, E., Emanuel, N., & Barenholz, Y. (1994). Delivery of cytokines by liposomes. I. Preparation and characterization of interleukin-2 encapsulated in long-circulating sterically stabilized liposomes. *Journal of Immunotherapy*, 16: 47-59.
- Keenan, R.J.,** Duncan, A.J., Yousem, S.A., Zenati, M., Schaper, M., Dowling, R.D., Alarie, Y., Burckart, G.J.*et al.* (1992). Improved immunosuppression with aerosolized cyclosporine in experimental pulmonary transplantation. *Transplantation*, 53(1): 20-25.
- Kharazmi, A.,** Fomsgaard, A., Conrad, R.S., Galanos, C., & Hoiby, N. (1991). Relationship between chemical composition and biological function of *Pseudomonas aeruginosa* lipopolysaccharide: effect on human neutrophil chemotaxis and oxidative burst. *Journal of Leukocyte Biology*, 49: 15-20.
- King, R.J.,** & Clements, J.A. (1972). Surface active materials from dog lung. 1. Method of isolation. *American Journal of Physiology*, 223: 707-714.

- Kirby, C.,** Clarke, J., & Gregoriadis, G. (1980). Effect of cholesterol content of small unilamellar liposomes on their stability *in vivo* and *in vitro*. *Biochemical Journal*, 186: 591-598.
- Kirby, C.,** & Gregoriadis, G. (1984). dehydration-rehydration vesicles: a simple method for high yield drug entrapment in liposomes. *Biotechnology*, 2: 979-983.
- Kirikae, T.,** Schade, F.U., Zahringer, U., Kirikae, F., Brade, H., Kusumoto, S., Kusama, T., & Rietschel, E.T. (1994). The significance of the hydrophilic backbone and the hydrophobic fatty acid regions of lipid A for macrophage binding and cytokine induction. *FEMS Immunology and Medical Microbiology*, 8(1): 13-26.
- Knowles, M.R.,** Church, N.L., Waltner, W.E., & al, e. (1990). A pilot study of aerosolised amiloride for the treatment of lung disease in cystic fibrosis. *New England Journal of Medicine*, 322: 1189-1194.
- Ko, Y.T.,** Ludescher, R.D., Frost, D.J., & Wasserman, B.P. (1994). Use of cilofungin as a direct fluorescent probe for monitoring antifungal drug-membrane interactions. *Antimicrobial Agents and Chemotherapy*, 38: 1378-1385.
- Koch, C.,** & Hoiby, N. (1993). Pathogenesis of cystic fibrosis. *The Lancet*, 341: 1065-1069.
- Koch, C.,** Bisgaard, H., Lanng, S., & Hoiby, N. (1993). Cyclosporin and course of chronic *P. aeruginosa* lung infection. In *18th European Cystic Fibrosis Conference*, (pp. 90). Madrid.
- Koch-Weser, J.,** Sidel, V.W., federman, E.B., Kanareh, P., Finer, D.C., & Eaton, A.E. (1970). Adverse effects of sodium colistimethate. Manifestations and specific reaction rates during 317 courses. *Annals of Internal Medicine*, 72: 857-868.
- Koike, M.,** Iida, K., & Matsuo, T. (1969). Electron microscopic studies on the mode of action of polymyxin. *Journal of Bacteriology*, 97(1): 448-452.
- Konstan, M.W.,** Hilliard, K.A., Norvell, T.M., & Berger, M. (1994). Bronchoalveolar lavage findings in cystic fibrosis patients with stable, clinically mild lung disease suggest ongoing infection and inflammation. *American Journal of Respiratory and Critical Care Medicine*, 150: 448-454.

- Konstan, M.W.**, Hoppel, C.L., Chai, B., & Davis, P.B. (1991). Ibuprofen in children with cystic fibrosis: pharmacokinetics and adverse effects. *Journal of Pediatrics*, 118(6): 956-964.
- Kubesch, P.**, Boggs, J., Luciano, L., Maass, G., & Tummler, B. (1987). Interaction of polymyxin B nonapeptide with anionic phospholipids. *Biochemistry*, 26: 2139-2149.
- Kubesch, P.**, Dork, T., Wulbrand, U., Kalin, N., Neumann, T., Wulf, B., Geerlings, H., Wiebbrody, H. *et al.* (1993). Genetic determinants of airways' colonisation with *Pseudomonas aeruginosa* in cystic fibrosis. *Lancet*, 336: 1081-1084.
- Kucers, A.** & Bennett, N. (1987). Polymyxin related antibiotics. In *The use of antibiotics* (pp. 899-911). Heinemann Medical Books.
- Kulkarni, S.B.**, Betageri, G.V., & Singh, M. (1995). Factors affecting microencapsulation of drugs in liposomes. *Journal of Microencapsulation*, 12(3): 229-246.
- Kunin, C.M.** (1967). A guide to use of antibiotics in patients with renal disease. *Annals of Internal Medicine*, 67(1): 151-158.
- Kunin, C.M.** & Bugg, A. (1971). Binding of polymyxin antibiotics to tissues: The major determinant of distribution and persistence in the body. *The Journal of Infectious Diseases*, 124(4): 394-400.
- Kyung-Dall, L.**, Shlomo, N., & Papahadjopoulos, D. (1993). Quantitative analysis of liposome-cell interactions in vitro: rate constants of binding and endocytosis with suspension and adherent J774 cells and human monocytes. *Biochemistry*, 32: 889-899.
- Laemmli, E.K.** (1970). Cleavage of structural proteins during the assembly of the head of bacteriophage T4. *Nature*, 227: 680-685.
- Lagacé, J.**, Dubreuil, M., & Montplaisir, S. (1991). Liposome-encapsulated antibiotics: preparation, drug release and antimicrobial activity against *Pseudomonas aeruginosa*. *Journal of Microencapsulation*, 8(1): 53-61.
- Lam, J.**, Chan, R., Lam, K., & Costerton, J.R.W. (1980). Production of mucoid microcolonies by *P. aeruginosa* within infected lungs in cystic fibrosis. *Infection and Immunity*, 28: 546-556.

- Lasch, J., & Schubert, R.** (1993). The interaction of detergents with liposomal membranes. In G. Gregoriadis (Eds.), *Liposome Technology* (pp. 233-260). Boca Raton, Florida: CRC Press.
- Lasic, D.D., Woodle, M.C., Martin, F.J., & Valentincic, T.** (1991). Phase behavior of 'stealth-lipid'-lecithin mixtures. *Periodicum Biologorum*, 93(2): 287-290.
- Lasic, D.D., Frederik, P.M., Stuart, M.C.A., Barenholz, Y., & McIntosh, T.J.** (1992). Gelation of liposome interior - A novel method for drug encapsulation. *FEBS Letters*, 312(2): 255-258.
- Law, S.L., Jang, T.F., Chang, P., & Lin, C.H.** (1994). Release characteristics of mitoxantrone-containing liposomes. *International Journal of Pharmaceutics*, 103: 81-85.
- Lawrence, S.M., Alpar, H.O., McAllister, S.M., & Brown, M.R.W.** (1993). Liposomal (MLV) polymyxin B: physicochemical characterization and effect of surface charge on drug association. *Journal of Drug Targeting*, 1: 303-310.
- Lidgate, D.M., Felgner, P.L., Fleitman, J.S., Whatley, J., & Fu, R.C.-C.** (1988). *In vitro* and *in vivo* studies evaluating a liposome system for drug solubilisation. *Pharmaceutical Research*, 5: 759.
- Lindsay, C.A., & Bosso, J.A.** (1993). Optimisation of antibiotic therapy in cystic fibrosis patients. *Clinical Pharmacokinetics*, 24(6): 496-506.
- Lindsay, S.** (1987). *High performance liquid chromatography*. Chichester: John Wiley & Sons.
- Littlewood, J.M., Miller, M.G., Ghoneim, A.T., & Ramsden, C.H.** (1985). Nebulised colomycin for early pseudomonas colonisation in cystic fibrosis. *The Lancet*: 865.
- Lowry, O.H., Roseborough, N.J., Farr, A.L., & Randall, R.J.** (1951). Protein measurement with the Folin phenol reagent. *Journal of Biological Chemistry*, 193: 265-275.
- Madden, B.P., Hodson, M.E., Tsang, V., et al.** (1992). Intermediate results of heart lung transplantation for CF. *Lancet*, 339: 1583-1587.

- Maddison, J.** (1994). Nebulized colistin causes chest tightness in adults with cystic fibrosis. *Respiratory Medicine*, 88(2): 145-147.
- Makino, K.,** Yamada, T., Kimura, M., Oka, T., Ohsima, H., & Kondo, T. (1991). Temperature- and ionic strength-induced conformational changes in the lipid head group region of liposomes as suggested by the zeta potential data. *Biophysical Chemistry*, 41: 175-183.
- Martin, F.J.** (1990). Pharmaceutical manufacturing of liposomes. In P. Tyle (Eds.), *Specialized drug delivery systems: Manufacturing and production technology* (pp. 267-316). New York: Marcel Dekker Inc.
- Maruyama, K.,** Okuizumi, S., Ishida, O., Yamauchi, H., Kikuchi, H., & Iwatsuru, M. (1994). Phosphatidyl polyglycerols prolong liposome circulation *in vivo*. *International Journal of Pharmaceutics*, 111: 103-107.
- Maskell, J.P.** (1991). The resolution of bacteroides lipopolysaccharides by polyacrylamide gel electrophoresis. *Journal of Medical Microbiology*, 34: 253-257.
- Mayer, L.D.,** Hope, M.J., & Cullis, P.R. (1986). Vesicles of variable sizes produced by a rapid extrusion procedure. *Biochimica et Biophysica Acta*, 858: 161-168.
- McFayden, P.** (1986). Electrophoretic mobility and zeta potential of colloidal particles. *International Laboratory*, 9: 32-42.
- Meadows, G.G. &** Pierson, H.F. (1988). Liposomes as a carrier for tyrosine phenol-lyase. In G. Gregoriadis (Eds.), *Liposomes as drug carriers Recent trends and progress* (461-472). Chichester: John Wiley & Sons.
- Meisner, D.,** Pringle, J., & Mezei, M. (1989). Liposomal pulmonary drug delivery I. *In vivo* disposition of atropine base in solution and liposomal form following endotracheal instillation to the rabbit lung. *Journal of Microencapsulation*, 6(3): 379-387.
- Meisner, D.** (1993). Liposomes as a pulmonary drug delivery system. In A. Rolland (Eds.), *Pharmaceutical particulate carriers. Therapeutic applications* (31-63). New York: Marcel Dekker, Inc.



- Meyer, E.C.**, Dominguez, E.A.M., & Bensch, K.G. (1969). Pulmonary lymphatic and blood absorption of albumin from alveoli. *Laboratory Investigation*, 20: 1-8.
- Meyer, K.C.**, Lewandoski, J.R., Zimmerman, J.R., Nunley, D., Calhoun, W.J., & Dopico, G.A. (1991). Human neutrophil elastase and elastase/alpha<sub>1</sub>-antiprotease complex in cystic fibrosis. *American Reviews in Respiratory Disease*, 144: 580-585.
- Mezei, M.** (1988). Liposomes in the topical application of drugs: a review. In G. Gregoriadis (Eds.), *Liposomes as drug carriers Recent trends and progress* (pp. 663-677). Chichester: John Wiley & Sons.
- Mihalko, P.J.**, Schreier, H., & Abra, R.M. (1988). Liposomes: a pulmonary perspective. In G. Gregoriadis (Eds.), *Liposomes as drug carriers* London: John Wiley & Sons Ltd.
- Milward, F.W.**, Nicoletti, P., & Hoffman, E. (1984). Effectiveness of various therapeutic regimens for bovine brucellosis. *American Journal of Veterinary Reviews*, 45: 1825-1828.
- Moore, R.A.**, Bates, N.C., & Hancock, R.E.W. (1986). Interaction of polycationic antibiotics with *Pseudomonas aeruginosa* lipopolysaccharide and lipid A studied by using dansyl-polymyxin. *Antimicrobial Agents and Chemotherapy*, 29(3): 496-500.
- Morrison, D.C.**, & Jacobs, D.M. (1976). Binding of polymyxin B to the lipid A portion of bacterial lipopolysaccharides. *Immunochemistry*, 13(13): 813-818.
- Mozes, N.**, & Rouxhet, P.G. (1987). Methods for measuring hydrophobicity of microorganisms. *Journal of Microbiological Methods*, 6: 99-112.
- Müller, R.H.** (1991). *Colloidal carriers for controlled drug delivery and targeting. Modification, characterisation and in vivo distribution*. Boca Raton, Ann Arbor, Boston: CRC Press, Inc.
- Mushayakarara, E.** & Levin, I.W. (1984). Interaction of polymyxin B with dipalmitoylphosphatidylcholine monolayers. *Biochimica et Biophysica Acta*, 816: 585-595.
- Myers, M.A.**, Thomas, D.A., Straub, L., Soucy, D.W., Niven, R.W., Kaltenbach, M., Hood, C.I., Schreier, H. *et al.* (1993). Pulmonary effects of chronic exposure to liposome aerosols in mice. *Experimental Lung Research*, 19: 1-19.

- Nacucchio, M.C.**, Gatto Bellora, M.J., Sordelli, D.O., & D'Aquino, M. (1988). Enhanced liposome-mediated antibacterial activity of piperacillin and gentamicin against Gram-negative bacilli *in vitro*. *Journal of Microencapsulation*, 5: 303-309.
- Nacucchio, M.C.**, Gatto, G.J., Bellora, M.J., Sordelli, D.O., & D'Aquino, M. (1985). Enhanced liposome-mediated activity of piperacillin against staphylococci. *Antimicrobial Agents and Chemotherapy*, 27: 137-.
- Nayar, R.**, Hope, M.J., & Cullis, P.R. (1989). Generation of large unilamellar vesicles from long-chain saturated phosphatidylcholines by extrusion technique. *Biochimica et Biophysica Acta*, 986: 200-206.
- Needham, D.**, McIntosh, T.J., & Lasic, D.D. (1992). Repulsive interactions and mechanical stability of polymer-grafted lipid membranes. *Biochimica et Biophysica Acta*, 1108: 40-48.
- New, R.R.C.** (1990). *Liposomes - a practical approach*. Oxford: IRL Press.
- Nicholas, A.R.**, Jones, M.N., & Smith, C. (1994). Permeability characteristics of sterically stabilized polyethylene glycol (PEG5000) phospholipid liposomes. In *Liposome research days conference - Liposomes: the next generation*, (A21). Vancouver, Canada:
- Nicholov, R.**, Khoury, A.E., Bruce, A.W., & DiCosmo, F. (1993). Interaction of ciprofloxacin loaded liposomes with *Pseudomonas aeruginosa* cells. *Cells and Materials*, 3(3): 321-326.
- Niederman, M.S.**, ferranti, R.D., Zielger, A., Merrill, W.W., & Reynolds, H.Y. (1984). Respiratory infection complicating long term tracheostomy. *Chest*, 85: 39-44.
- Nightingale, S.D.**, Saletan, S.L., Swenson, C.E., Lawrence, A.J., Watson, D.A., Pilkiewicz, F.G., Silverman, E.G., & Cal, S.X. (1993). Liposome-encapsulated gentamicin treatment of *Mycobacterium avium-Mycobacterium intracellulare* complex bacteremia in AIDS patients. *Antimicrobial Agents and Chemotherapy*, 37(9): 1869-1872.
- Niven, R.W.**, & Schreier, H. (1990). Nebulization of liposomes. I. Effects of lipid composition. *Pharmaceutical Research*, 7(11): 1127-1133.

- Oja, C.D.**, Semple, S.C., Chonn, A., & Cullis, P.R. (1994). Effect of dose on liposome clearance: RES saturation revisited. In *Liposome Research Days Conference Liposomes: the next generation*, (pp. B9). Vancouver, Canada.
- Olson, F.**, Hunt, C.A., Szoka, F.C., Vail, W.J., & Papahadjopoulos, D. (1979). Preparation of liposomes of defined size by extrusion through polycarbonate membranes. *Biochimica et Biophysica Acta*, 557: 9-23.
- Omri, A.**, Beaulac, C., Bouhajib, M., Montplaisir, S., Sharkawi, M., & Lagace, J. (1994). Pulmonary retention of free and liposome-encapsulated tobramycin after intratracheal administration in uninfected rats and rats infected with *Pseudomonas aeruginosa*. *Antimicrobial Agents and Chemotherapy*, 38(5): 1090-1095.
- Onur, M.A.**, Kirby, C.J., Isimer, A., Beksac, S., Basci, N., Pamir, R., Coskun, T., & Tumer, A. (1992). Effect of liposomal encapsulation of chloramphenicol on its transfer across the human placenta in a dual *in vitro* perfusion system. *International Journal of Pharmaceutics*, 88: 313-317.
- Ostro, M.J.** & Cullis, P.R. (1989). Use of liposomes as injectable drug delivery systems. *American Journal of Hospital Pharmacy*, 46: 1576-1587.
- Pache, W.**, Chapman, D., & Hillaby, R. (1972). Interaction of antibiotics with membranes: polymyxin B and gramicidin S. *Biochimica et Biophysica Acta*, 255: 358-364.
- Pederson, M.** & Stafanger, G. (1983). Bronchopulmonary symptoms in primary ciliary dyskinesia, a study of 27 patients. *European Journal of Respiratory Disease*, 64(suppl.127): S118-S128.
- Perez-Soler, R.**, Khokhar, A.R., & Lopez-Berestein, G. (1988). Development of lipophilic cisplatin analogs encapsulated in liposomes. In G. Gregoriadis (Eds.), *Liposomes as drug carriers Recent trends and progress* (pp. 401-417). Chichester: John Wiley & Sons.
- Perkins, W.R.**, Minchey, S.R., Ahl, P.L., & Janoff, A.S. (1993). The determination of liposome captured volume. *Chemistry and Physics of Lipids*, 64: 197-217.
- Peterson, A.A.**, Hancock, R.E.W., & McGroarty, E.J. (1985). Binding of polycationic antibiotics and polyamines to lipopolysaccharides of *P. aeruginosa*. *Journal of Bacteriology*, 164: 1256-1261.

- Pirson, P.**, Steiger, R.F., Trouet, A., Gillet, J., & Herman, F. (1980). Primaquine liposomes in the chemotherapy of experimental murine malaria. *Annals of Tropical Medicine and Parasitology*, 74: 383-391.
- Plotowski, M.C.**, Bajolet-Laudinat, O., & Puchelle, E. (1993). Cellular and molecular mechanisms of bacterial adhesion to respiratory mucosa. *European Respiratory journal*, 6: 903-916.
- Poyner, E.A.**, Alpar, H.O., & Brown, M.R.W. (1993). Preparation, properties and the effects of free and liposomal tobramycin on siderophore production by *Pseudomonas aeruginosa*. *Journal of Antimicrobial Chemotherapy*, 34: 43-52.
- Prins, J.M.**, van Deventer, S.J.H., Kuijper, E.J., & Speelman, P. (1994). Clinical relevance of antibiotic-induced endotoxin release. *Antimicrobial Agents and Chemotherapy*, 38(6): 1211-1218.
- Proffitt, R.T.**, Grayson, J.B., Chiang, S.-M., Coulter, D.M., Satorius, A.L., & Petersen, E.A. (1993). Biodistribution and therapeutic efficacy of liposomal amikacin. In *Liposomes research days conference - Liposomes: the next generation*, (A18). Vancouver, Canada:
- Quinton, P.M.** (1990). Cystic fibrosis: a disease of electrolyte transport. *FASEB Journal*, 4: 2709-2717.
- Raheja, R.K.**, Kaur, C., Singh, A., & Bhatia, I.S. (1973). *Journal of Lipid Research*, 1(1): 53-59.
- Ramsey, B.W.**, Dorkin, H.L., Eisenberg, J.D., Gibson, R.L., Harwood, I.R., Kravitz, R.M., Schidlow, D.V., Wilmott, R.W.*et al.* (1993). Efficacy of aerosolized tobramycin in patients with cystic fibrosis. *The New England Journal of Medicine*, 328: 1740-1746.
- Ravaoarino, M.**, Toma, E., Agbaba, O., & Morisset, R. (1993). Efficient entrapment of amikacin and teicoplanin in liposomes. *Journal of Drug Targeting*, 1: 191-195.
- Riaz, M.**, Weiner, N., & Martin, F. (1989). Liposomal disperse systems. In H. A. Liebermann, M. M. Reiger, & G. S. Banker (Eds.), *Pharmaceutical dosage forms: disperse systems* (pp. 567-602). Marcel Dekker Inc.

- Rich, D.P.**, Anderson, M.P., Gregory, R.J., & al, e. (1990). Expression of cystic fibrosis transmembrane conductance regulator corrects defective chloride channel regulation in cystic fibrosis airway epithelial cells. *Nature*(347): 358-363.
- Rietschel, E.T.**, & Brade, H. (1992). Bacterial endotoxins. *Scientific American*(August): 26-33.
- Rifkind, D.** (1967). Prevention by polymyxin B of endotoxin lethality in mice. *Journal of Bacteriology*, 93(4): 1463-1464.
- Riordan, J.R.**, Rommens, J.M., Kerem, B.-S., Alon, N., Rozmahel, R., Grzelczak, Z., Zielenski, J., Lok, S.*et al.* (1989). Identification of the cystic fibrosis gene: cloning and characterization of complementary DNA. *Science*, 245: 1066-1072.
- Rivera, M.**, & Nicotra, M.B. (1982). *Pseudomonas aeruginosa* mucoid strain. *American Reviews of Respiratory Disease*, 126: 833-836.
- Rojanasakul, Y.**, Wang, L.-Y., Bhat, M., Glover, D.D., Malanga, C.J., & Ma, J.K.H. (1992). The transport barrier of epithelia: a comparative study on membrane permeability and charge selectivity in the rabbit. *Pharmaceutical Research*, 9(8): 1029-1034.
- Rommens, J.M.**, Iannuzzi, M.C., Kerem, B.-S., Drumm, M.L., Melmer, G., Dean, M., Rozmahel, R., Cole, J.L. *et al.* (1989). Identification of the cystic fibrosis gene: chromosome walking and jumping. *Science*, 245: 1059-1065.
- Rouse, M.S.**, Tallan, B.M., Steckelberg, J.M., Henry, N.K., & Wilson, W.R. (1992). Efficacy of cilofungin therapy administered by continuous intravenous infusion for experimental disseminated candidiasis in rabbits. *Antimicrobial Agents and Chemotherapy*, 36: 56-58.
- Sabath, L.D.** (1984). Biochemical and physiological basis for susceptibility and resistance of *P. aeruginosa* to antimicrobial agents. *Reviews of Infectious Diseases*, 6: 643-656.
- Saiman, L.**, Cacalano, G., Gruenert, D., & Prince, A. (1992). Comparison of the adherence of *Pseudomonas aeruginosa* to respiratory epithelial cells from cystic fibrosis patients and healthy subjects. *Infection and Immunity*, 60: 2808-2814.

- Sajjan, U.S.,** Reisman, J., Doig, P., Irvin, R.T., Forstner, G., & Forstner, J. (1992). Binding of nonmucoid *Pseudomonas aeruginosa* to normal human intestinal mucin and respiratory mucin from patients with cystic fibrosis. *Journal of Clinical Investigation*, 89: 657-665.
- Santis, G.,** & Geddes, D. (1994). Recent advances in cystic fibrosis. *Postgraduate Medical Journal*, 70(822): 247-251.
- Sastrasinh, M.,** C.Knauss, T., M.Weinberg, J., & D.Humes, H. (1982). Identification of the aminoglycoside binding site in rat renal brush border membranes. *The Journal of Pharmacology and Experimental Therapeutics*, 222(2): 350-358.
- Sato, T.,** & Sunamoto, J. (1992). Recent aspects in the use of liposomes in biotechnology and medicine. *Progress in lipid research*, 31(4): 345-372.
- Schindler, M.,** & Osborn, M.J. (1979). Interaction of divalent cations and polymyxin B with lipopolysaccharide. *Biochemistry*, 18(20): 4425-4430.
- Schindler, P.R.G.** & Teuber, M. (1975). Action of polymyxin B on bacterial membranes: morphological changes in the cytoplasm and in the outer membrane of *Salmonella typhimurium* and *Escherichia coli*. *Antimicrobial Agents and Chemotherapy*, 8(1): 95-104.
- Schneeberger, E.E.** (1978). Structural basis for some permeability properties of the air-blood barrier. *Federal Proceedings*, 37: 2471-2478.
- Schreier, H.,** Gonzalez-Rothi, R.J., & Stecenko, A.A. (1993). Pulmonary delivery of liposomes. *Journal of Controlled Release*, 24: 209-223.
- Schreier, H.,** McNicol, K.J., Bennett, D.B., Teitelbaum, Z., & Derendorf, H. (1994a). Pharmacokinetics of deterlix following intratracheal instillation and aerosol inhalation in the unanesthetized awake sheep. *Pharmaceutical Research*, 11(7): 1056-1059.
- Schreier, H.** (1992). Liposome aerosols. *Journal of liposome research*, 2(2): 145-184.
- Schreier, H.,** McNicol, K.J., Ausborn, M., Soucy, D.W., Derendorf, H., Stecenko, A.A., & Gonzalez-Rothi, R.J. (1992). Pulmonary delivery of amikacin liposomes and acute liposome toxicity in the sheep. *International Journal of Pharmaceutics*, 87: 183-193.

- Schreier, H.**, Mobley, W.C., Concessio, N., Hickey, A.J., & Niven, R.W. (1994b). Formulation and *in vitro* performance of liposome powder aerosols. *STP Pharma Sciences*, 4(1): 38-44.
- Schroder, G.**, Brandenburg, K., & Seydel, U. (1992). Polymyxin B induces transient permeability fluctuations in asymmetric planar lipopolysaccharide/phospholipid bilayers. *Biochemistry*, 31(3): 631-638.
- Schroit, A.J.**, Madsen, J., & Nayar, R. (1986). Liposome-cell interactions: *in vitro* discrimination of uptake mechanism and *in vivo* targeting strategies to mononuclear phagocytes. *Chemistry and Physics of Lipids*, 40: 373-393.
- Schwendener, R.A.**, Wuthrich, R., Duewell, S., Wehrli, E., & von Schulthess, G.K. (1990). A pharmacokinetic and MRI study of unilamellar gadolinium-, manganese-, and iron-DTPA-stearate liposomes as organ-specific contrast agents. *Investigative Radiology*, 25: 922-932.
- Sekeri-Pataryas, K.H.**, Vakirtzi-Lemonias, C., Pataryas, H.A., & Legakis, J.N. (1985). Liposomes as carriers of <sup>14</sup>C-labelled penicillin and <sup>125</sup>I-labelled albumin through the cell wall of *Pseudomonas aeruginosa*. *International Journal of Biological Macromolecules*, 7(7): 379-381.
- Seltzer, S.E.**, Gregoriadis, G., & Dick, R. (1988). Evaluation of the dehydration-rehydration method for the production of contrast-carrying liposomes. *Investigative Radiology*, 23: 131-138.
- Senior, J.**, Delgado, C., Fisher, D., Tilcock, C., & Gregoriadis, G. (1991). Influence of surface hydrophilicity of liposomes on their interaction with plasma protein and clearance from the circulation: studies with poly(ethylene glycol)-coated vesicles. *Biochimica et Biophysica Acta*, 1062: 77-82.
- Senior, J.H.** (1987). Fate and behavior of liposomes *in vivo*: a review of controlling factors. *CRC Critical Reviews in Therapeutic Drug Carrier Systems*, 3(2): 123-193.
- Senior, J.H.**, Trimble, K.R., & Maskiewicz, R. (1991). Interaction of positively-charged liposomes with blood: implications for their application *in vivo*. *Biochimica et Biophysica Acta*, 1070: 173-179.

- Shak, S.**, Capon, D.J., Hellmiss, R., Marsters, S.A., & Baker, C.L. (1990). Recombinant human DNase 1 reduces the viscosity of cystic fibrosis sputum. *Proc. Natl. Acad. Sci. USA*, 87: 9188-9192.
- Shale, D.J.** (1991). Management of cystic fibrosis in different countries. *Thorax*, 46: 382.
- Sharpe, P.T.** (1985). The partition of charged liposomes in aqueous two-phase systems. *Molecular and Cellular Biochemistry*, 69: 151-159.
- Shaw, D.J.** (1980). *Introduction to colloid and surface chemistry* (3rd ed.). London: Butterworths.
- Simionescu, D.** & Simionescu, M. (1983). Differentiated distribution of the cell-surface charge on the alveolar-capillary unit. *Microvascular Research*, 25: 85-100.
- Six, H.R.**, Gilbert, B.E., Wyde, P.R., Wilson, S.Z., & Knight, V. (1989). Liposomes as carriers of enviroxime for use in aerosol therapy of rhinovirus infections. In G. Lopez-berestein & I. Fidler (Eds.), *Liposomes in the therapy of infectious diseases and cancer* (pp. 229-238). New York: Alan R. Liss Inc.
- Smith, R.M.**, Traber, L.D., Traber, D.L., & Spragg, R.G. (1989). Pulmonary deposition and clearance of aerosolized  $\alpha_1$ -proteinase inhibitor administered to dogs and to sheep. *Journal of Clinical Investigation*, 84: 1145-1154.
- Smith, P.K.**, Krohn, R.I., Hermanson, G.T., Mallia, A.K., Gartner, F.H., Provenzano, M.D., Fujimoto, E.T., Goeke, N.M. *et al.* (1985). Measurement of proteins using bicinchoninic acid. *Analytical Biochemistry*(150): 76-85.
- Smyth, C.J.**, Jonsson, P., Olsson, E., Soderlind, O., Rosengreen, J., Hjerten, S., & Wadstrom, T. (1978). Differences in hydrophobic surface characteristics of porcine enteropathogenic *Escherichia coli* with or without K88 antigen as revealed by hydrophobic interaction chromatography. *Infection and Immunity*, 22(2): 462-472.
- Sone, S.** (1989). Human monocyte activation to the tumoricidal state by liposome-encapsulated muramyl tripeptide and its therapeutic implication. In Lopez-Berestein & Fidler (Eds.), *Liposomes in the therapy of infectious diseases and cancer* (pp. 125-134). New York: Alan R. Liss, Inc.



**Sordelli, D.O.**, Macri, C.N., Maillie, A.J., & Cerquetti, M.C. (1994). A preliminary study on the effect of anti-inflammatory treatment in cystic fibrosis patients with *Pseudomonas aeruginosa* lung infection. *International Journal of Immunopathology and Pharmacology*, 7(2): 109-117.

**Stableforth, D.E.** (1994). New respiratory therapies in cystic fibrosis. *Journal of the Royal Society of Medicine*, 87(S21): 11-16.

**Stead, R.J.**, Hodson, M.E., & Batten, J.C. (1987). Inhaled ceftazidime compared with gentamicin and carbenicillin in older patients with cystic fibrosis infected with *Pseudomonas aeruginosa*. *British Journal of Diseases of the Chest*, 81: 272-279.

**Stepkowski, S.S.**, Goto, S., Ito, T., Reynolds, K., Didlake, R., Kim, E.K., & Kahan, B.D. (1989). Prolongation of heterotropic heart allograft survival by local delivery of continuous low-dose cyclosporine therapy. *Transplantation*, 47(1): 17-23.

**Stevenson, M.**, Baillie, A.J., & Richards, R.M.E. (1983). Enhanced activity of streptomycin and chloramphenicol against intracellular *Escherichia coli* in the J774 macrophage cell line mediated by liposome delivery. *Antimicrobial Agents and Chemotherapy*, 24(5): 742-749.

**Stevenson, M.**, Baillie, A.J., & Richards, R.M.E. (1984). Quantification of uptake of liposomal carboxyfluorescein by professional phagocytes in-vitro. A flow microfluorimetric study in the J774 murine macrophage cell line. *Journal of Pharmacy and Pharmacology*, 36: 824-830.

**Stewart, J.C.M.** (1980). Colorimetric determination of phospholipids with ammonium ferrothiocyanate. *Analytical Biochemistry*, 104: 10-14.

**Storm, D.R.**, Rosenthal, K.S., & Swanson, P.E. (1977). Polymyxin and related antibiotics. *Annual Reviews in Biochemistry*, 46: 723-763.

**Stuhne-Sekalec, L.**, & Stanacev, N. (1991). Liposomes as cyclosporin A carriers: the influence of ordering of hydrocarbon chains of phosphatidylglycerol liposomes on the association with and topography of cyclosporin A. *Journal of Microencapsulation*, 8(3): 283-294.

**Sunamoto, J.**, Goto, M., Iida, T., Hara, K., Saito, A., & Tomonaga, A. (1984). Unexpected tissue distribution of liposomes coated with amylopectin derivatives and successful use in the

- treatment of experimental Legionaire's disease. In G. Gregoriadis, G. Poste, J. Senior, & A. Trouet (Eds.), *Receptor mediated targeting of drugs* (pp. 359-379). New York: Plenum Press.
- Suntres, Z.E.,** Hepworth, S.R., & Shek, P.N. (1993). Pulmonary uptake of liposome-associated  $\alpha$ -tocopherol following intratracheal instillation in rats. *Journal of Pharmacy and Pharmacology*, 45: 514-520.
- Suntres, Z.E.,** & Shek, P.N. (1994). Incorporation of  $\alpha$ -tocopherol in liposomes promotes the retention of liposome-encapsulated glutathione in the rat lung. *Journal of Pharmacy and Pharmacology*, 46: 23-28.
- Suter, S.** (1994). New perspectives in understanding and management of the respiratory disease in cystic fibrosis. *European Journal of Pediatrics*, 153: 144-150.
- Szaff, M.,** Hoiby, N., & Flensburg, E.W. (1983). Frequent antibiotic therapy improves survival of cystic fibrosis patients with chronic *Pseudomonas aeruginosa* infection. *Acta Paediatrica Scandinavia*, 72: 651-657.
- Szoka, F.,** & Papahadjopoulos, D. (1980). Comparative properties and methods of preparation of lipid vesicles (liposomes). *Annual Reviews in Biophysics and Bioengineering*, 9: 467-508.
- Szoka, F.,** & Papahadjopoulos, D. (1978). Procedure for preparation of liposomes with large internal aqueous space and high capture by reverse-phase evaporation. *Proc. Natl. Acad. Sci. USA*, 75(9): 4194-4198.
- Talmadge, K.W.,** & Siebert, C.J. (1989). Efficient endotoxin removal with a new sanitizable affinity column: affi-prep polymyxin. *Journal of Chromatography*, 476: 175-185.
- Talsma, H.,** & Crommelin, D.J.A. (1992). Liposomes as drug delivery systems, Part I: preparation. *Pharmaceutical Technology*(October): 96-106.
- Talsma, H.,** van Steenberg, M.J., Borchert, J.C.H., & Crommelin, D.J.A. (1994). A novel technique for the one-step preparation of liposomes and nonionic surfactant vesicles without the use of organic solvents. Liposome formation in a continuous gas stream: The 'Bubble' method. *Journal of Pharmaceutical Sciences*, 83(3): 276-280.

- Taniguchi, K.**, Yamazawa, N., Itakura, K., Morisaki, K., & Hayashi, S. (1987). Partition characteristics and retention of anti-inflammatory steroids in liposomal ophthalmic preparations. *Chem. Pharm. Bull.*, 35(3): 1214-1222.
- Taussig, L.M.**, Lobeck, C.C., Di Sant' Agnese, P.A., Ackermann, D.R., & Kattwinkes, J. (1972). Fertility in males with cystic fibrosis. *New England Journal of Medicine*, 279: 65-68.
- Taylor, K.M.G.**, Taylor, G., Kellaway, I.W., & Stevens, J. (1989). The influence of liposomal encapsulation on sodium cromoglycate pharmacokinetics in man. *Pharmaceutical Research*, 6(7): 633-636.
- Taylor, K.M.G.**, Taylor, G., Kellaway, I.W., & Stevens, J. (1990). Drug entrapment and release from multilamellar and reverse-phase evaporation vesicles. *International Journal of Pharmaceutics*, 58: 49-55.
- Taylor, K.M.G.**, & Farr, S.J. (1993). Preparation of liposomes for pulmonary drug delivery. In G. Gregoriadis (Eds.), *Liposome Technology* (pp. 177-195). Boca Raton: CRC Press, Inc.
- Taylor, K.M.G.**, & Newton, J.M. (1992). Liposomes for controlled delivery of drugs to the lung. *Thorax*, 47: 257-259.
- Taylor, R.B.**, Richards, R.M.E., Low, A.S., & Hardie, L. (1994). Chemical stability of polymyxin B in aqueous solution. *International Journal of Pharmaceutics*, 102: 201-206.
- Teuber, M.**, & Miller, I.R. (1977). Selective binding of polymyxin B to negatively charged lipid monolayers. *Biochimica et Biophysica Acta*, 467: 280-289.
- Thomas, D.A.**, Myers, M.A., Wichert, B., Schreier, H., & Gonzalez-Rothi, R.J. (1991). Acute effects of liposome aerosol inhalation on pulmonary function in healthy human volunteers. *Chest*, 99: 1268-1270.
- Tilcock, C.**, Senior, J., Delgado, C., Fisher, D., & Gregoriadis, G. (1993). Partitioning of liposomes in aqueous two-phase systems. In G. Gregoriadis (Eds.), *Liposome Technology* (pp. 291-314). Boca Raton, Florida: CRC Press, Inc.
- Tomioka, H.**, Saito, H., Sato, K., & Yoneyama, T. (1991). Therapeutic efficacy of liposome-encapsulated kanamycin against *Mycobacterium intracellulare* infection induced in mice. *American Reviews in Respiratory Disease*, 144: 575-579.

- Tomlinson, S.**, Taylor, P.W., & Luzio, J.P. (1989). Transfer of phospholipid and protein into the envelope of Gram-negative bacteria by liposome fusion. *Biochemistry*, 28: 8303-8311.
- Torchilin, V.P.**, Berdichevsky, V.R., Barsukov, A.A., & Smirnov, V.N. (1980). Coating liposomes with protein decreases their capture with macrophages. *FEBS Letters*, 111(1): 184-188.
- Torchilin, V.P.**, Trubetskoy, V.S., Milshteyn, A.M., Canillo, J., Wolf, G.L., Papisov, M.I., Bogdanov, A.A., Narula, J.*et al.* (1994). Targeted delivery of diagnostic agents by surface-modified liposomes. *Journal of Controlled Release*, 28: 45-58.
- Torchillin, V.P.** (1985). Liposomes as targetable drug carriers. *CRC Critical Reviews in Therapeutic Drug Carrier Systems*, 2(1): 65-115.
- Towbin, H.**, Staehelin, T., & Gordon, J. (1979). Electrophoretic transfer of proteins from polyacrylamide gels to nitrocellulose sheets. *Proc. Natl. Acad. Sci. USA*, 76: 4350-4354.
- Trexler, P.C.**, Spiers, A.S.D., & Gaya, H. (1975). Plastic isolators for treatment of acute leukaemia patients under 'germ-free' conditions. *British Medical Journal*, 4: 549.
- Tsai, C.-M.**, & Frasch, C.E. (1982). A sensitive silver stain for detecting lipopolysaccharides in polyacrylamide gels. *Analytical Biochemistry*, 119: 115-119.
- Vaara, M.**, & Viljanen, P. (1985). Binding of polymyxin B nonapeptide to Gram-negative bacteria. *Antimicrobial Agents and Chemotherapy*, 27(4): 548-554.
- Vaara, M.** (1983). Polymyxin B nonapeptide complexes with lipopolysaccharide. *FEMS Microbiology Letters*, 18: 117-121.
- Vaara, M.**, & Nikaido, H. (1984). Molecular organisation of bacterial outer membrane. In E. T. Rietschel (Eds.), *Handbook of Endotoxin, Vol 1: Chemistry of endotoxin* Amsterdam: Elsevier Science Publishers.
- Valerius, N.H.**, Koch, C., & Hoiby, N. (1991). Prevention of chronic *Pseudomonas aeruginosa* colonisation in cystic fibrosis by early treatment. *The Lancet*, 338: 725-726.
- van Golde, L.M.G.**, Batenburg, J.J., & Robertson, B. (1988). The pulmonary surfactant system: biochemical aspects and functional significance. *Physiology Reviews*, 68: 374-455.

- Van Wye, J., Collins, M., Bayler, M. et al.** (1990). Pseudomonas hyperimmune globulin passive immunotherapy for pulmonary exacerbations in cystic fibrosis. *Pediatric Pulmonology*, 9: 7-18.
- Vazquez, C., Municio, M., Corera, M., Gaztelurrutia, L., Sojo, A., & Vitoria, J.C.** (1993). Early treatment of *Pseudomonas aeruginosa* colonization in cystic fibrosis. *Acta Paediatrica*, 82: 308-309.
- Vladimirsky, M.A., & Ladigina, G.A.** (1982). Antibacterial activity of liposome-entrapped streptomycin in mice infected with *Mycobacterium tuberculosis*. *Biomedicine*, 36: 375-377.
- Waldrep, J.C., Scherer, P.W., Keyhani, K., & Knight, V.** (1993). Cyclosporin A liposome aerosol: particle size and calculated respiratory deposition. *International Journal of Pharmaceutics*, 97: 205-212.
- Waldrep, J.C., Keyhani, K., Black, M., & Knight, V.** (1994). Operating characteristics of 18 different continuous-flow jet nebulisers with beclomethasone dipropionate liposome aerosol. *Chest*, 105: 106-110.
- Wall, D.A.** (1995). Pulmonary absorption of peptides and proteins. *Drug Delivery*, 2: 1-20.
- Westphal, O., & Jann, K.** (1965). Bacterial lipopolysaccharides: extraction with phenol-water and further applications of the procedure. In *Methods in Carbohydrate Chemistry* (pp. 83-91). New York: Academic Press.
- Whall, T.J.** (1981). High-performance liquid chromatography of polymyxin B sulfate and colistin sulfate. *Journal of Chromatography*, 208: 118-123.
- White, R., Woodward, S., Leppert, M., O'Connell, P., Hoff, M., Herbst, J., Lalouel, J.-M., Dean, M. et al.** (1985). A closely linked marker for cystic fibrosis. *Nature*, 318: 382-384.
- Wichert, B.V., Gonzalez-Rothi, R.J., Straub, L.E., Wichert, B.M., & Schrier, H.** (1992). Amikacin liposomes: characterization, aerosolization, and in vitro activity against *Mycobacterium*
- Williams, N.A., & Weiner, N.D.** (1989). Interactions of small polypeptides with dimyristoylphosphatidylcholine monolayers: effect of size and hydrophobicity. *International Journal of Pharmaceutics*, 50: 261-266.

- Wilson, M.E.** (1985). Effects of bacterial endotoxins on neutrophil function. *Reviews in Infectious Diseases*, 7: 404-418.
- Wilson, J.M., & Collins, F.S.** (1992). More from the modellers. *Nature*, 359: 195-196.
- Wilson, K., & Goulding, K.H.** (1986). *Principles and techniques of practical biochemistry* (3rd ed.). London: Edward Arnold.
- Woodle, M.C.** (1993). Surface-modified liposomes: assessment and characterization for increased stability and prolonged blood circulation. *Chemistry and Physics of Lipids*, 64: 249-262.
- Woodle, M.C., Matthay, K.K., Newman, M.S., Hidayat, J.E., Collins, L.R., Redemann, C., Martin, F.J., & Papahadjopoulos, D.** (1992). Versatility in lipid compositions showing prolonged circulation with sterically stabilized liposomes. *Biochimica et Biophysica Acta*, 1105: 193-200.
- Woodle, M.C., Collins, L.R., Sponsler, E., Kossovsky, N., Papahadjopoulos, D., & Martin, F.J.** (1992). Sterically stabilized liposomes: reduction in electrophoretic mobility but not electrostatic surface potential. *Biophysical Journal*, 61: 902-910.
- Woodle, M.C., & Lasic, D.D.** (1992). Sterically stabilised liposomes. *Biochimica et Biophysica Acta*, 1113: 171-199.
- Young-Ho, S., & Jones, M.N.** (1994). The interaction of positively-charged phospholipid vesicles with bacteria. *Biochemical Society Transactions*, 22: 330S.
- Zach, M.S.** (1991). Pathogenesis and management of lung disease in cystic fibrosis. *Journal of the Royal Society of Medicine*, 84(Suppl.18): 10-17.
- Zalipsky, S., Brandeis, E., Newman, M.S., & Woodle, M.C.** (1994). Long circulating, cationic liposomes containing amino-PEG-phosphatidylethanolamine. *FEBS Letters*(353): 71-74.
- Zaslavsky, Y.B., Borovskaya, A.A., & Rogozhin, S.V.** (1984). Effect of lipid composition on hydrophobic properties of liposomes. *Molecular and Cellular Biochemistry*, 60: 131-136.

**Zenati, M.**, Duncan, A.J., Burckart, G.J., Schaper, M., Yousem, S.A., Griffith, B.P., & Casarotto, D. (1991). Immunosuppression with aerosolized cyclosporine for prevention of lung rejection in a rat model. *European Journal of Cardio-thoracic Surgery*, 5: 266-272.